Agricultural Water Conservation Grants
Texas Water Development Board

Final Project Report

May 10, 2017

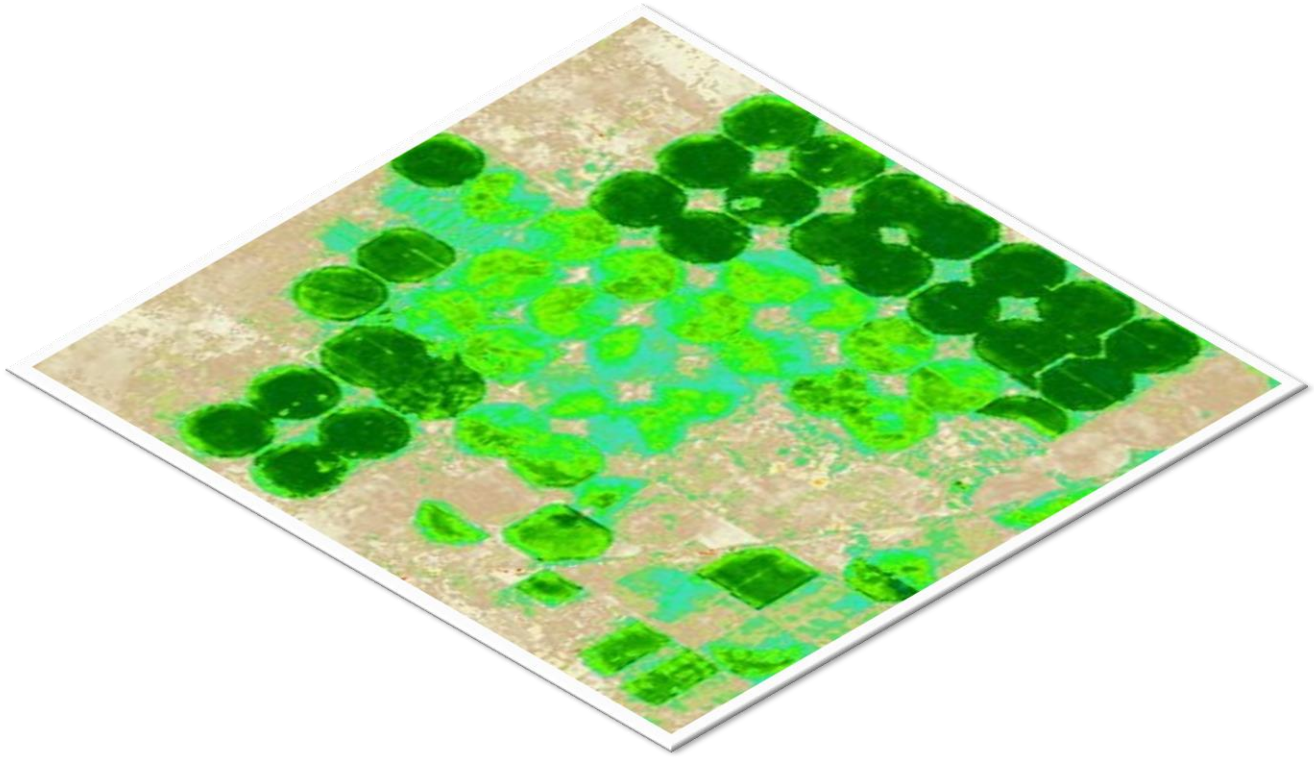

IMPROVING IRRIGATION WATER USE ESTIMATES WITH REMOTE SENSING TECHNOLOGIES: A FEASIBILITY STUDY FOR TEXAS

By Todd Caldwell, Justin Huntington, Bridget Scanlon, Andrew Joros, and Teresa Howard

This page is intentionally blank.

Texas Water Development Board

Contract #1313581612

Improving Irrigation Water Use Estimates with Remote Sensing Technologies: A feasibility study for Texas

By

Todd Caldwell[1], Ph.D.

Justin Huntington[2], Ph.D.

Bridget Scanlon[1], Ph.D.

Andrew Joros[2], M.S.

Teresa Howard[3], M.A.G, G.I.S.P.

[1]University of Texas at Austin, Bureau of Economic Geology, Austin, TX

[2]Desert Research Institute, Division of Hydrologic Sciences, Reno, NV

[3]University of Texas at Austin, Center for Space Research, Austin, TX

TABLE OF CONTENTS

List of Tables

List of Figures

List of Acronyms

ACCA Automatic Cloud Cover Assessment
ALEXI Atmosphere-Land Exchange inverse
ASCE American Society of Civil Engineers
ASTER Advanced Spaceborne Thermal Emission and Reflection Radiometer
AVHRR Advanced Very High Resolution Radiometer
CBERS China-Brazil Earth Resources Satellite
CDL Cropland data layer
CGDD Cumulative growing degree-day
CONUS Conterminous United States
COOP Cooperative Observer Program
Cp Specific heat capacity
CRN Climate Reference Network
disALEXI Disaggregated Atmospheric Land Exchange Inverse Model
DRI Desert Research Institute
DSSAT Decision Support System for Agrotechnology Transfer
EB Energy balance
ET Evapotranspiration
ET_c Evapotranspiration crop
ET_{inst} Evapotranspiration at the instantaneous of satellite overpass time
ET_o Grass reference evapotranspiration
ET_r Reference Evapotranspiration
ET_rF Fraction of Reference Evapotranspiration
ETM+ Enhanced Thematic Mapper
FAO Food and Agriculture Organization
G Ground (i.e. soil) heat flux
GCD Groundwater conservation district
GIS Geographic information system
GOES Geostationary satellite
H Sensible heat flux
HCN Historical Climatology Network
HUC Hydrologic unit code
IWUE Irrigation Water Use Estimate
K_c Crop coefficient
K_{cb} Basal crop coefficient
K_e Soil water evaporation coefficient
K_s Stress coefficient
LDCM Landsat Data Continuity Mission
LCRA Lower Colorado River Authority
LE Latent energy
LST Land-surface temperature
maf Million acre-feet

MAP mean annual precipitation
MBE Mean bias error
METRIC Mapping Evapotranspiration with Internalized Calibration
MODIS Moderate Resolution Imaging Spectroradiometer
MPE Multisensor Precipitation Estimator
NARR North American Regional Reanalysis
NASA National Aeronautics and Space Administration
NASS National Agricultural Statistics Service
NDVI Normalized difference vegetation index
NIWR Net irrigation water requirement
NLDAS North American Land Data Assimilation System
NOAA National Oceanic and Atmospheric Administration
OLI Operational Land Imager
PAI Precipitation accuracy index
PERSIANN Precipitation Estimation from Remotely Sensed Information using Artificial Neural Networks
POD Probability of detection
PPT Precipitation
PRISM Parameter-elevation Regressions on Independent Slopes Model
QA Quality assurance
QC Quality control
r_a Aerodynamic resistance
R_f relative fraction
RMSE Root mean square error
R_n Net long and short wave solar radiation
R_s Solar radiation
R_{so_b} Theoretical clear sky solar radiation
SCAN Soil Climate Analysis Network
SEBAL Surface Energy Balance Algorithm for Land
SEBI Surface Energy Balance Index
SEBS Surface Energy Balance System
SPOT Systeme Probatoire d'Observation de la Terre
S-SEBI Simplified Surface Energy Balance Index
STARFM Spatial and temporal adaptive reflectance fusion model
STATSGO NRCS State Soil Geographic
SWIR Short-wave infrared
T_a Air temperature
TETN TexasET Network
TIR Thermal infrared
TSEB Two-source energy balance model
TSM Two-source model
TSM-DTD Two Source Model Dual Temperature Difference

UofI METDATA University of Idaho Gridded Surface Meteorological Data
USDA United States Department of Agriculture
USGS US Geological Survey
VI Vegetation indices
VIIRS Visible Infrared Imaging Radiometer Suite
VNIR Very near infrared
WRS World Reference System
WSR-88D Weather Surveillance Radar 88 Doppler
WTM West Texas Mesonet
ρa Air density

1 Executive Summary

The Texas climate is characterized by extremes yet agriculture depends on reliable timing and availability of water during the growing season. Plants need water for photosynthesis where it is exchanged with atmospheric carbon to build biomass. As plants and crops grow, water in the root zone is depleted leading to stress and reduced productivity, unless it is replenished. When rainfall is insufficient, irrigation is applied to maintain root zone soil moisture and improve crop yields. In Texas, irrigated agriculture is the largest water-consumer. Most of this applied water is lost to evapotranspiration (*ET*), the combined processes of soil evaporation and plant transpiration – which consumes energy from solar radiation to convert liquid water into vapor. Regardless of its source, the water is returned to the atmosphere and removed from the terrestrial water cycle. An accurate estimate of crop *ET* can be used to estimate net irrigation water requirement (*NIWR*) as the difference between crop *ET* and effective precipitation. When *NIWR* is greater than zero, we assume this water must come from irrigation. We use net *ET* synonymously with *NIWR* herein. Similarly, we can derive *NIWR* from crop models which simulate irrigation based on crops transpiring at or near atmospheric demand. *NIWR,* the amount of water that the crop could transpire in excess of precipitation, is synonymous with irrigation demand, net consumptive use, and precipitation deficit.

Accurate estimates of crop *ET* are needed to improve irrigation demand estimates for water planning at regional and state levels. Remote sensing has the potential to accurately map *ET* at unprecedented resolution and potentially with much less effort as these methods become operational. The state-of-the-science is evolving rapidly but implementing a remotely sensed crop water program state-wide across the climatically diverse State of Texas is not trivial. Our goal is to provide a recommendation on which *ET* algorithms and *NIWR* methods are best suited for an operational, state-wide application, determine what ancillary data are required, and assess the quality and limitations of these methods and data sets. We use a variety of metrics to assess the various components of such calculations including the (1) *ET* algorithms by accuracy tiers and complexity, (2) available weather data from stations and (3) gridded meteorological products. To determine operational feasibility, we implemented a pilot study for 2010 and 2011 on eight counties including Brazos, Cameron, Carson, Dawson, Hale, Medina, Ochiltree, and Wharton. We used both the Mapping evapotranspiration at high resolution with internalized calibration (METRIC) remote sensing algorithm and the ET Demands numerical model to determine annual *NIWR* and compare these results to 2010 and 2011 Irrigation Water Use Estimates (IWUE) – the current methodology used annually at the county-level by the Texas Water Development Board.

There is little doubt that remote sensing could produce state-wide irrigation water use estimates. Several other states are already using such technologies. Idaho, Nevada, and New Mexico are at the forefront of such programs while several programs are operating at the federal level within the U.S. Department of Agriculture (USDA) and the U.S. Geological Survey (USGS). Texas has a multitude of challenges ranging from its sheer size to its diversity of crops and rotations. Furthermore, remotely sensed *ET* requires good satellite images, good meteorological data, good algorithms and a dedicated staff to implement and assess them. Multispectral imagery is needed to produce land surface temperature (*LST*) and optical reflectance maps which derive an instantaneous *ET* map. Reference *ET* (ET_r) from meteorological data at

the image acquisition time is used to spatially scale the evaporative fraction of *ET* (ET_rF) across the image. Temporally, weather data is used to compute 24-hour totals of *ET* cumulated into daily totals between acquisition dates and summed over the growing season. All of the *ET* algorithms we present use this general workflow but differ in the formulation of ET_rF and underlying parameterization of the land and boundary layer. The process involves many steps along the path to a time-integrated estimate of actual *ET* and ultimately *NIWR.*

We found several gridded weather data sets to be accurate but slightly biased in their ability to produce spatially distributed precipitation totals and ET_r. We also found the algorithms to be robust but with varying degrees of accuracy and complexity. Throughout this process and pilot study, we found several notable limitations of these technologies. One of the biggest is the availability of cloud-free imagery where the eastern half of Texas has very low cloud-free probability. A cloud-free pixel is required approximately every month to produce a reasonable estimate of *ET* over the irrigated croplands of interest. The high spatial resolution of Landsat is offset by a longer return period of 8-16 days. Other satellites are more frequent (MODIS) but provide coarser resolutions (1km). Combining such data, fusion, would aid areas of high cloud cover but at increasing complexity to the algorithms. Cloud masks are also evolving quickly which improve the efficacy of detecting and mitigating clouds.

Remotely sensed *ET* is feasible for Texas. With confidence, we believe the algorithms are valid, the results are reproducible and reasonable (possibly biased high), and the data requirements (imagery, gridded data, soil moisture, etc.) can be met. We found crop ET was well reproduced using METRIC; however, when summed over respective crop acreage, the *NIWR* became unrealistically high. This bias results from the use of ET_r that is likely biased and as well as an over-estimation of irrigated acreage. With more concerted effort and time to devote to quality control and assessment (e.g. verifying pixels are irrigated), we have no doubt these numbers can be improved upon, if such a program moves forward. However, it will take commitment from the State to equip and train its staff. Our pilot project laid the groundwork but certainly needs refinement. Experts in the field should be consulted to build the State's capacity. Once in-house capacity (2 or 3 years down the road) is achieved, the annual staff commitment is one senior scientist with a strong remote sensing background and a minimum of two technicians with good computational skills. Remote sensing adds a new tool to quantify field-scale *ET* but it also requires substantial commitment to data processing, quality control, time, skill and effort. There is currently not a turnkey solution to this problem although we predict many of these algorithms are moving to cloud-based computing. Regardless, there is substantial benefit to getting on board with remote sensing sooner than later for the Texas Water Development Board.

2 Introduction and Background

Water resource managers and planners across Texas must balance the current and future water demands from industry, agriculture, and municipal water use with its ephemeral supply, precipitation (PPT). Irrigation is the largest water-consumer in the State, using 7.83 million acre-feet (maf) in 2014 with 82% of that coming from groundwater [*TWDB*, 2014]. Groundwater recharge, though difficult to quantify, is estimated to range from <0.1 to 4.6 in yr^{-1} across Texas where *PPT* ranges from 8.8 in yr^{-1} in the west to 46.4 in yr^{-1} in the east [*Keese et al.*, 2005]. Groundwater storage in the Texas High Plains has decreased by 46 maf since irrigation began in the 1950s with water level declines of ≤4.27 ft yr^{-1} [*Scanlon et al.*, 2010]. Thus, groundwater across much of the irrigated lands in Texas is nonrenewable.

The Texas climate is characterized by extremes and agriculture depends on reliable timing and availability of water. Plants need water for photosynthesis where it is exchanged for atmospheric carbon and used to build biomass. As plants or crops grow, water in the root zone is depleted leading to stress and reduced productivity unless it is replenished. To reduce such risk, irrigation is often used to supplement *PPT* and increase soil moisture storage. Even in regions of higher rainfall, irrigation can increase yields while crop production is likely not possible without it in far-west Texas.

The 2017 Texas State Water Plan [*TWDB*, 2017] projects an 11% decrease in existing water supplies from 15.2 maf in 2020 to 13.6 maf by 2070 while the population is expected to increase by 70%. Water demand from irrigators is also expected to decrease by 18% due to improved efficiencies and conservation practices, reduced groundwater availability and water rights transfers away from agriculture. In particularly, if all irrigation conservation strategies are adopted, then this is expected to increase two-fold from 0.639 maf yr^{-1} in 2010 to 1.33 maf y^{-1} by 2070. These water conservation strategies include the adoption of new technologies like low energy precision application that can allow farmers to grow more with less irrigation. With predicted shortages of water supply, improving estimates of irrigation water use in Texas would be a valuable tool for local and regional water managers. Satellite based measurement of evapotranspiration (*ET*) is just such a technology that could provide farmers and local districts with guidance and knowledge of actual crop water use, and also provide the Texas Water Development Board (TWDB) with more accurate and defensible irrigation water use estimates.

This feasibility study is the first step towards the validation remotely sensed measurement of *ET* to quantify irrigation water use in climatically diverse regions growing a variety of crops across Texas. Satellite technology is the next step to improve such estimates. Therefore, our goal is to assess the feasibility of applying remote sensing to quantify irrigation water use across Texas. Our assessment includes the technical, operational, and economic implementation of these methods through a scientific assessment of the algorithms and time integration methods, limitations and advantages of these algorithms, availability and complexity of the algorithms, ancillary data requirements, computational resources, and technical expertise to implement and maintain such a program.

2.1 Terminology of Evapotranspiration

Evapotranspiration (*ET*) refers to the combined processes of evaporation and plant transpiration – both of which consume solar radiation (energy) which converts liquid water in the biosphere into vapor. This water, whether from rain or irrigation, is returned to the atmosphere and essentially removed from the

terrestrial water cycle. Water loss to ET by crops is directly proportional to their growth and productivity which is all regulated by the stomata on leaf surfaces which open to obtain CO_2 but release water vapor. Reference *ET* (ET_r) is a standardized and reproducible index approximating the climatic demand for water. This flux (units of length [L] per time [t]) is the theoretical *ET* over an extensive surface of well-watered and actively growing reference vegetation, usually alfalfa (ET_r) or grass (ET_o). Crop *ET* (ET_c) is the scaled ET_r according to a time-varying crop coefficient (K_c). None of these are either a direct measures of *ET* nor do they directly equate to irrigation water use.

The net irrigation water requirement (*NIWR*) is the quantity or depth of water required for crop growth in excess of the effective rainfall that infiltrates into the root zone. *NIWR is* calculated as (potential or actual) *ET* minus effective *PPT* and represents the amount of additional water that the crop and bare soil would transpire or evaporate in excess of *PPT* residing in the root zone. *NIWR* is comparable to the terms irrigation demand, consumptive use, and *PPT* deficit. We also use *NIWR* synonymously for the *ET* measured from satellite or potential *ET* from our ET Demands Model (Section 6.2) minus precipitation – this additional quantity coming from irrigation.

Traditionally, *NIWR* requires some knowledge of the spatial and temporal distribution of both weather and vegetation to calculate ET_r and *PPT,* such that:

$$NIWR(t) = K_C(t)\,ET_r(t) - PPT(t) \quad (1)$$

where *t* is time in the unit of choice. As discussed in detail later (Section 4.1), K_C values are crop-specific, varying throughout the growing season. Satellite-based methods determine actual *ET* which differs from a traditional *NIWR* estimate which assumes well-watered conditions and healthy crops. The use of remote sensing is arguably the only way to estimate actual *ET* over large areas. However, remote sensing of *ET* produces an instantaneous snapshot which must be temporally scaled by some ancillary measure of ET_r to quantify weekly, monthly, seasonal or annual *ET*, referred to as *time integration*. Finally, net *ET* equates to water depth resulting from the satellite (actual) *ET* minus any effective *PPT* which is essentially a measure of irrigation water use.

2.2 Current Practices for Net Irrigation Water Requirements

TWDB produces irrigation water use estimates (IWUE) for all 254 counties in Texas annually. The complete methodology is presented at http://www.twdb.texas.gov/conservation/agriculture/irrigation/index.asp. We summarize it briefly here. Beginning in 2003, the total cropped acreage is based on Farm Service Agency (FSA) records of certified irrigated crop acreage aggregated into major crop type by county. This acreage is compared to historical averages and the five-year mean irrigation rate by crop is applied and adjusted per county.

IWUE is calculated based on ET_r and an empirical correction factor based on historical data over the previous 5 years. The annual IWUE estimates are further adjusted and revised based on precipitation, weather data, irrigation water availability, and cropping patterns. This final IWUE is then adjusted based on annual surface water diversion data (TCEQ), estimates of waste water reuse in each county, and revisions provided voluntarily by groundwater conservation districts and other local water authorities. The reported IWUE provide the best known representation of actual irrigation water use in Texas. TWDB

staff are tasked with investigating ways to improve this process and remotely sensed ET has the potential to better quantify irrigation water use.

2.3 Generalized Workflow to Derive Remotely Sensed net *ET*

Remote sensing would improve state-wide irrigation water use estimates. Several states are already using such technologies and many federal agencies are working to operationalize such tools. However, none of these methods are currently there and they all require committed resources to implement at any scale. Several western states (e.g. Idaho, Nevada, and New Mexico) are at the forefront of such programs. In Texas, we have a multitude of challenges from extensive cloud cover in the east to insufficient irrigated acreage maps. High resolution *ET* mapping using Landsat takes 10 paths and nearly 7 rows to completely cover Texas (Figure 2). Derivation of *ET* requires two key components: thermal (and optical) imagery and weather data. Imagery acquired from satellite, aircraft of unmanned aerial systems contains the visual and thermal infrared (*TIR*) bands needed to produce surface temperature and optical reflectance. These data are used to scale the instantaneous ET_r spatially across the *TIR* image – cooler areas have higher *ET* and warmer areas low *ET*. Weather data are next used to compute the instantaneous ET map into daily totals of *ET* as well as between image acquisition dates. All of the *ET* algorithms we present use this general workflow (Figure 3) which ultimately provides the framework the remainder of this report.

The *ET* methods proposed in this study allow improved quantification of crop consumptive water-use, independent of crop type, crop yields, or irrigation metering. Remote sensing of *ET* also has a significant advantage by providing the ability to reconstruct historic water use and change since the mid-1980s, using Landsat 5 and 7 satellites. The launch of Landsat 8 will allow continuity of these techniques into the future (Figure 1). For over 40 years, the Landsat Mission has provided global multispectral data. The Landsat Thematic Mapper (TM) sensor was onboard Landsat 4 and 5 from 1982 to 1993. Images consist of seven spectral bands with a spatial resolution of 30 m for Bands 1 to 5 and 120 m resampled to 30 m pixels for *TIR* Band 6. The Landsat Enhanced Thematic Mapper Plus (ETM+) sensor was only on Landsat 7 beginning in 1999. Images consist of eight spectral bands with a spatial resolution of 60 m for *TIR* Band 6. The Scan Line Corrector on the ETM+ failed on May 31, 2003 which results in about 20% of each image is missing. Beginning in February of 2013, the Landsat 8 Operational Land Imager (OLI) and Thermal Infrared Sensor images consist of nine spectral bands with a spatial resolution of 100 m for *TIR* Bands 10. Landsat 9 is expected to be operational by 2020 and Landsat 10 is already under development – thus its longevity is very likely as our higher spatial resolutions and additional bands.

Landsat 7 and Landsat 8 satellites both travel in sun synchronous orbits at an altitude of 705 kilometers (438 miles) moving from north to south over the sunlit side of the Earth. Each satellite makes a complete orbit every 99 minutes covering the entire globe every 16 days. Their combined orbits are offset to allow 8-day repeat coverage of any Landsat scene area. Along with weather station or spatial weather products, these are the required data (Figure 3). We begin the process by defining the time period and study area which for TWDB would likely be a county or groundwater conservation district (*GCD*). Next, the satellite images are acquired for the study. If needed, multiple images are merged and clipped to the bounding area of interest. For example, a county may not lie completely within one scene. Next, non-croplands, clouds and water bodies are masked. At this point, it is critical to determine if there is enough valid imagery to proceed. Generally, a minimum of one pixel per month over the growing period is required to

interpolate *NIWR*. Each clipped and masked image is processed to calculate various inputs required by the *ET* algorithms (Section 4.1) including spectral reflectance, radiance, vegetation Indices (*VI*), etc. The *ET* algorithm is implemented and a map of the relative fraction of *ET* (ET_rF) is produced. This image is converted to actual *ET* at every cropped pixel in the image by scaling the instantaneous ET_r from corresponding weather data at the time of the overpass to this ET_rF map. The weather data is used to cumulate the actual *ET* in daily, monthly totals by preserving this instantaneous ratio of *ET* between image acquisition dates (section 4.2). The net *ET*, actual *ET* minus *PPT*, equates to the irrigated water use for that pixel, crop, or county (i.e. *NIWR*).

This process (Figure 3) involves many steps along the path to a time integrated estimate of *NIWR*. All weather data (gridded or station-based) must be carefully evaluated to check for inconsistent data, gaps, or generally errors (Section 4.3). Gridded products are generally more robust because they blend ground and satellite observations with models to produce continuous and validated mesoscale weather data. However, they may be less representative of surface conditions under irrigated agriculture and are often biased high in terms of ET_r (Section 5.3). Few of these processes are automated and a trained technician is required to evaluate nearly every step. Our goal is to evaluate this process and estimate its feasibility to provide improved irrigation water use estimates across Texas.

2.4 Water Savings

This technical feasibility study was an appraisal of the current state-of-the-science satellite *ET* and *PPT* methodologies applicable to estimate *NIWR* at a scale such as Texas. Thus, it was a research-based effort and not directly related to any demonstration project with tangible water savings. Our results, if implemented through technology transfer to the State, could be used to evaluate the efficiency of conservation plans and/or programs, and to enhance the value of future water conservation programs. For example, Bonneville Power in Oregon provide farmers rebates of $5.25/acre for using science-based irrigation scheduling. Satellite methods could provide near real-time irrigation scheduling while also providing quantification of actual *ET*.

Regardless, the participants in this study are committed to the development of such techniques to improve agricultural and other water conservation. Furthermore, reliable *ET* and *NIWR* are desperately needed to more accurately assess the state's groundwater supplies (i.e. groundwater availability models). The potential for defensible water rights accounting could greatly aid water rights transfers and compliance agreements. The application of remote sensing techniques to estimate *ET* also has the potential to provide better estimates of K_c for various crops and even native vegetation related to ecosystem services. *ET* is a major consumptive user of water resources across the globe and its quantification along with each component of the water balance is critical to assess water conservation.

2.5 Study Plan and Report Format

This feasibility study identifies remote sensing and modeling technologies capable of estimating *ET* and *PPT* with the end goal of improving *NIWR* across the diverse climate of Texas. We assess current state-of-the-science methods and models to quantify *ET* and *NIWR* including all the applicable data sets required to produce full seasonal estimates. The general goal of this feasibility study is to provide the TWDB with

a review on commonly used approaches, an estimate of the most feasible approaches, and the required level of effort for implementation.

This study provided an initial feasibility report in Year 1 (May 2014), followed by a stakeholders' webinar (October 14, 2015) and culminating in this final report. The initial feasibility study concluded Year 1 with a report and subsequent stakeholder meeting that laid out the implementation design presented here. The workshop resulted plan of course to obtain the eight counties of interest, define the scales, and needs for implementation of the more feasible ET algorithms.

The project was divided into five tasks with two milestones. Tasks 1 through 4 included a comprehensive assessment of the satellite-based *ET* algorithms (Section 5.1), precipitation products and other gridded data sets required by *ET* algorithms (Section 5.4), time integration methods for *ET* algorithms (Section 4.1), and the development and assessment of validation data for net irrigation water requirement. These results were presented in our initial feasibility report (Milestone 1) and a stakeholder workshop (October 14, 2015) with presentation of initial feasibility study. The webinar is currently archived at:

http://www.twdb.texas.gov/conservation/agriculture/doc/10_14_2015_Remote_Sensing_Irrigation_Water_Use_Study.mp4

Following this workshop, we agreed to eight counties: Brazos, Cameron, Carson, Dawson, Hale, Medina, Ochiltree, and Wharton, based on their distribution in different climatic zone, variety of croplands, and each was nearly contained within one Landsat image. The final task (5) involved implementation of highly feasible *ET* algorithms at selected locations, and the production of this final feasibility report. We had planned to implement two *ET* algorithms including METRIC and S-SEBI (see Table 1) but our resources were limited and the image classification using either algorithm would not change the overall feasibility.

The specific goals of the this *ET* feasibility study were to (1) determine which available *ET* and *NIWR* approaches are most feasible under various climates, crops and irrigation technologies across Texas using operational data sets and algorithms, (2) test these methods over specific regions within the State, and (3) determine true feasibility and limitations from demonstration trials. Remotely sensed *ET* and modeled *NIWR* estimates are only as good as the input data, and model assumptions made about *ET* behavior in between satellite image "snap shots", and validation is difficult; however, we address these issues and the requirements to implement such a program at the state-level (Section 7).

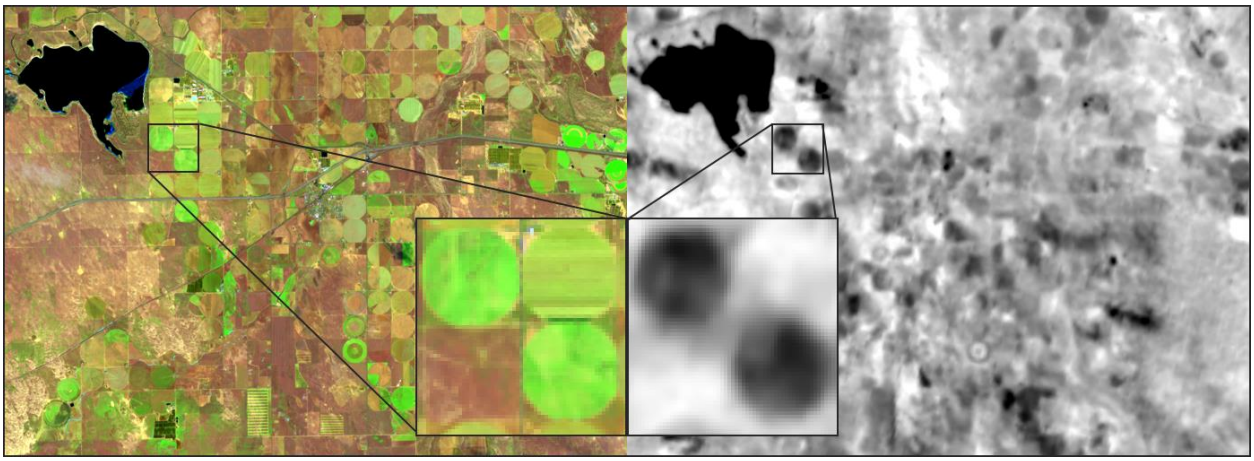

Figure 1. Sample image (Landsat 8) from April 3, 2013 showing agricultural fields near Wiggins, CO. Left is a color composite of shortwave infrared, near-infrared and visible green light and right is the same area as shown by one of the LDCM thermal bands. The inset pair shows three center pivot irrigation fields in greater detail. Darker areas in the thermal band indicate cooler temperatures (and higher *ET*).

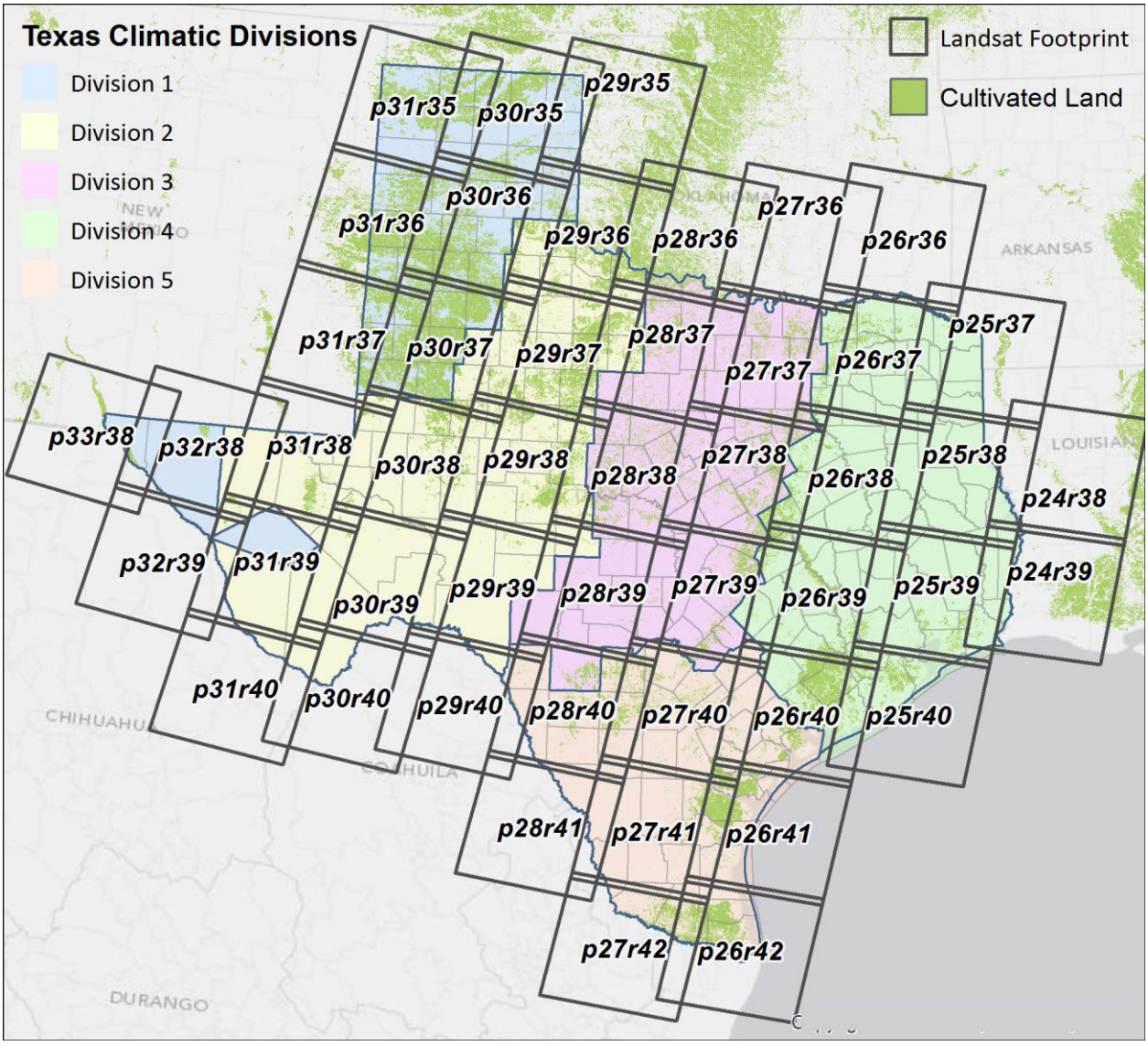

Figure 2. Landsat World Reference System 2 (WRS-2) path and row overlay for Texas in relation to the five climatic regions from the Digital Climatic Atlas of Texas and cultivated land as mapped by the USDA.

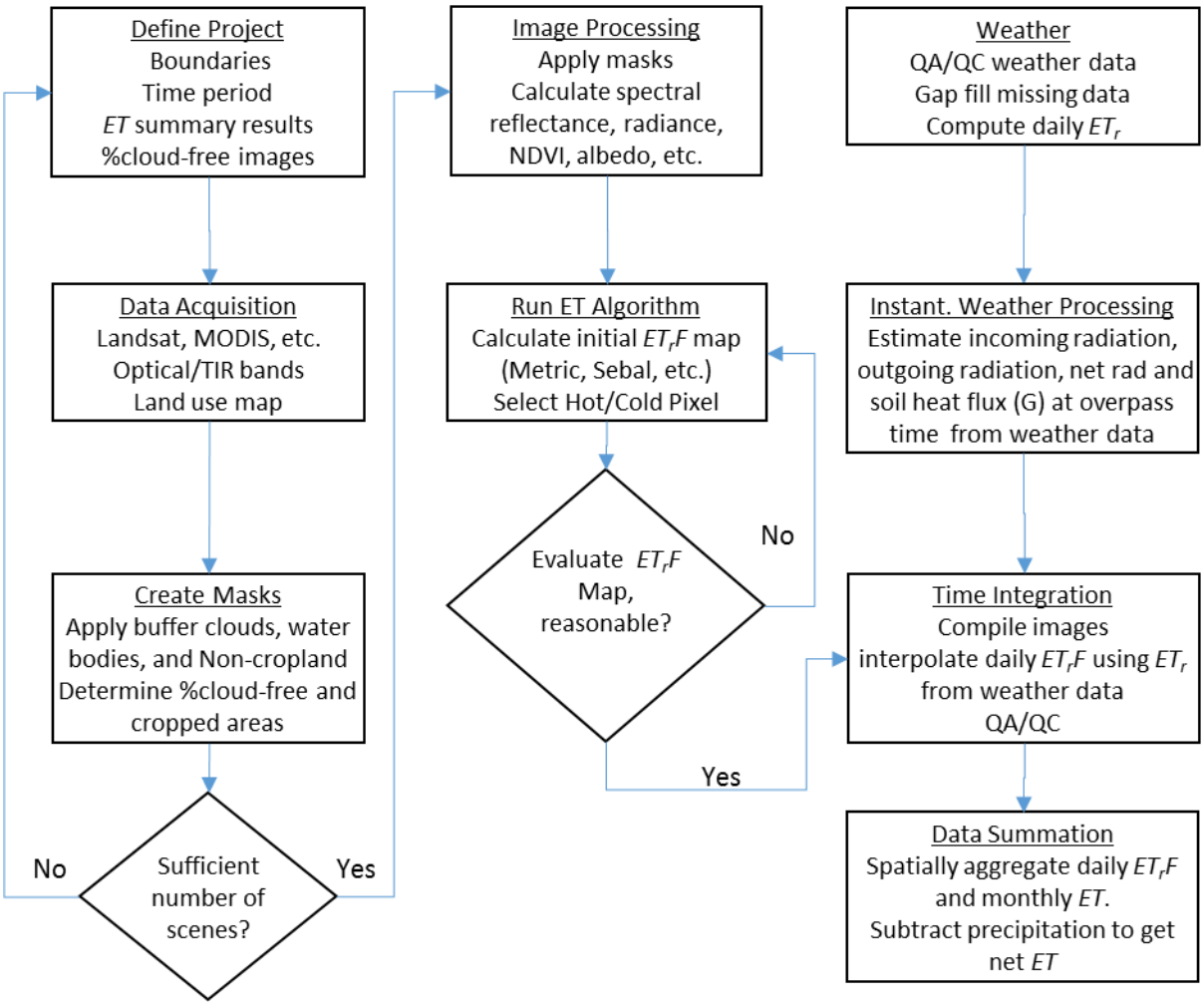

Figure 3. Workflow to produce net *ET* from satellite and weather data.

3 Study Methodology

Our goal is to provide a recommendation on which *ET* algorithms and *NIWR* methods are best suited for operational state-wide application, determine what ancillary data are required, and assess the quality and limitations of these methods and data. Most remote sensing *ET* algorithms require satellite-based thermal and optical images to derive an instantaneous map of *ET.* Imagery is further needed to estimate other model inputs such as the normalized vegetative indices (*NDVI*), albedo, and other requirements such as land cover and land use – both used to estimate roughness height, map crop type, and irrigated agriculture footprints. At the county scale in Texas, Landsat imagery would most commonly be used due to its high *TIR* resolution, its return interval (8 to 16 days depending on Landsat combinations and path overlap areas) and the overall quality in georectification. Landsat is also freely available.

The following section details our assessment of each component we foresee to implement, to estimate net *ET* and *NIWR* across the state using satellite technologies. We further assess a preliminary implementation of an algorithm workflow in sub-regions across the State's varied climatology.

3.1 Regionalizing the State of Texas

Texas has a diverse climatology with strong gradients of increasing temperature from north to south and increasing *PPT* from west to east. To capture this variability in our assessment, we selected two methods to partition the State by (1) mean annual precipitation (*MAP*) and (2) climatic zone. The latest 30-year normals from 1980-2010 from Oregon State's Parameter-elevation Regressions on Independent Slopes Model (PRISM) data were used at 4km resolution. The state-wide mean MAP is 731 ± 307 mm (± one standard deviation), ranging from 207 to 1560 mm. We then contoured MAP at 200 mm bands assigned each monitoring station into one of five categories: <400, 400-600, 600-800, 800-1000 and >1000 mm (Figure 4a).

To capture both the *PPT* and temperature gradients, we also selected five climatic zones reported in the Digital Climatic Atlas of Texas [Narasimhan et al., 2005] based on prior 30 year monthly means (1971-2000) of *PPT*, maximum and minimum temperature, dew point temperature and mean monthly wind speed. In all, 60 data layers were used by *Narasimhan et al.* [2005] to identify unique climatic zones of varying size across Texas. We used ground-based weather stations for validation of data products and categorized each station into one of five zones constrained to county boundaries (Figure 4b).

3.2 Metrics for Feasibility for Remotely Sensed *ET* Algorithms

The feasibility of implementing these remote sensing technologies was comprehensively assessed to in Sections 4 and 5 which include an overview of algorithms and methods. Our feasibility analysis uses the Environmental and Water Resources Institute *ET* committee standards which recognizes four tiers of required accuracy and integrity in remote sensing estimation of *ET*:

Tier 1 (lowest level): Exploratory spatial distribution of water consumption by vegetation with ±30% uncertainty. This level is useful for differentiating irrigated versus non-irrigated land.

Tier 2: Image based products for differentiating the spatial distribution of water consumption where human review is exercised, and where optically or thermally-based algorithms are utilized that have a

generally correct, but limited physical basis. This approach is applicable to annual reporting with minimal computational effort, project-scale water management, or national-level surveys.

Tier 3: Spatial maps of *ET* showing variation over time and space at the monthly time scale and with sufficient accuracy for use in parameterizing or driving hydrologic models, including ground-water recharge and depletion estimation, surface water accounting on streams and stream flow depletion, for general basin-wide water balances, and for developing crop coefficients.

Tier 4 (highest level): For support of water rights, transfers, and litigation. This tier requires a large amount of human oversight and review, and sufficient physics in algorithms to quantify important impacts of vegetation or surface characteristics on the surface energy balance and transformation of energy to latent heat. It should also employ robust means for time-integration that includes adjustment for background evaporation from exposed soil due to *PPT* wetting for the integrated period as opposed to that occurring at the time of the snapshot. This tier of applications must be admissible in courts of law and among the common applications communities. A targeted accuracy might be within 10%.

The algorithm summary (Section 5, Table 5) presents an assessment of the advantages and limitations of each and serves as the basis for our implementation (Section 6) and the feasibility of a program state-wide (Section 7). The overall success of a remotely sensed *ET* program in Texas includes not only the quality and availability of the climate and cloud-free satellite image data, model requirements, assumptions, and accuracy, but also the technical training, staffing costs, and transfer of expertise to TWDB staff.

3.3 Cloud probability

Remotely sensed estimates of *ET* are very sensitive to cloud contamination, especially in the thermal band (Figure 5). Daily MODIS cloud flag images from 2005 to 2012 were used to evaluate the probability of obtaining successive sequences of cloud free images over the course of a growing season. Estimation of probabilities for successfully producing growing season *ET* maps utilized daily cloud masks extracted from the daily MODIS at-surface reflectance (MOD09GA) data for Texas and surrounding states. The MOD09GA data product was retrieved from the online Data Pool, courtesy of the National Aeronautics and Space Administration (NASA) Land Processes Distributed Active Archive Center, USGS/Earth Resources Observation and Science Center, Sioux Falls, South Dakota (https://lpdaac.usgs.gov/data_access/data_pool). This particular MODIS dataset was selected for two reasons. First, the MOD09GA data set contains the State quality assurance (QA) and MOD35_L2 cloud mask data at 1 km spatial resolution. For each pixel, the State QA data specifies status of the cloud state (bit 0-1), cloud shadow (bit 2), and cirrus detected level (bit 8-9). Second, MOD09GA data sets have been projected and geo-located from the raw swath format to a gridded sinusoidal projection and separated into 10° latitude by 10° longitude (at the equator) tiles. This makes it relatively straight-forward to work with the data and to directly compare the cloud masks between different days and years. At each 1 km pixel, if there were multiple images for a day, the pixel that was the most cloud and cloud shadow free, and had the smallest view angle (closest to nadir), and the lowest solar zenith angle, was selected. This process mitigated some of the view angle issues identified, where estimated cloud fraction increased towards the edge of the scan path due to larger effective pixel sizes, oblique views of sides of clouds, and

longer observation paths with thickening of haze effects. However, this phenomenon and tendency to overstate cloudiness toward swath edges may be an issue for the southern states, including Texas. Lastly, we assume our county cloud probabilities at 1km are independent of image resolution.

Growing seasons were computed using the University of Idaho Gridded Surface Meteorological Data (UofI METDATA) 4 km daily minimum and maximum air temperature [*Abatzoglou*, 2013]. UofI METDATA is a combination of gridded 800 m PRISM monthly climate data and 12 km regional-scale reanalysis North America Land Data Assimilation System (NLDAS) hourly forcing data [*Mitchell et al.*, 2004]. The use of UofI METDATA created a spatially and temporally complete and high-resolution gridded daily minimum and maximum temperature dataset temperature dataset to calculate the beginning and end of the growing season.

One km pixels were conservatively flagged as cloudy if the cloud state (bit 0-1) was cloudy or mixed, the cloud shadow state (bit 2) was true, or the cirrus state (bit 8-9) was small, average, or high. Cloud free probabilities were calculated for both a fixed growing season from April 1 - October 31 (day of year 91–304 for non-leap years) as well as for a spatially variable growing season. The UofI METDATA was used to estimate the beginning of the growing season using a cumulative growing degree-day (*CGDD*) approach with a threshold of 300 °C-days from January 1, base temperature of zero, and negative daily average temperatures set to zero. The *CGDD* approach has been widely used as a basis for representing crop development and allows for transferability across regions. The selected threshold of 300°C-days was calibrated based on field observations across the western U.S. for most perennial crops such as alfalfa, and provided a consistent means to identify the primary period when vegetation growth is expected to occur and when seasonal *ET* demands by the atmosphere are highest. The end of the growing season was identified as the first day after the start of the growing season when the minimum air temperature was less than or equal -7°C.

Daily MODIS cloud masks were used to generate binary masks for each year indicating which pixels were cloudy or cloud free during each month of the growing season. At each pixel, if at any time during the growing season the time between cloud free images exceeded a stated threshold, the pixel and year were flagged as “failed” in regard to their capability to produce reliable estimates of growing season *ET* using our definition (here) of reliability. As described previously, in general, reliable estimates of *ET* require a maximum time gap between images of less than 32 days. However, to fully capture rapid changes in vegetation growth associated with green up in spring and harvests of forage, an image every 16 days is valuable. Therefore, separate probabilities were generated for both of these gap thresholds (16 and 32 days) and for both fixed (April 1 – October 31) and variable growing season periods. The probability of a successful retrieval of field scale growing season ET for a MODIS pixel location-year was calculated by dividing the number of successful years by the total number of years (16). Results are presented in Section 5.3.

3.4 Available Monitoring Networks in Texas

Station based climate data have been traditionally used for driving many *ET* algorithms, and are also required to validate gridded estimates of ET_r and *PPT.* We selected readily available national networks and local university networks for our evaluations over an eight year period (2005 to 2012). Our primary

concern are rates and potential biases in gridded estimates of ET_r and *PPT* over the precipitation classes and climatological classes defined previously (Section 3.1). Prior work by Marek et al. [2010] reviewed the existing *ET* networks in Texas and found them to be sparse across Texas and generally lacking in any standardization or quality control on the data. Also, *Moorhead et al.* [2015] found that there is significant high bias (e.g. 2.2 mm d^{-1} for ET_r) in gridded estimates of ET_r when compared to the Texas *ET* networks due to boundary layer conditioning from irrigated agriculture and subsequent reduced *ET* that gridded mesoscale products could not adequately represent. Additionally, most networks utilize either a standard tipping bucket or a weighing gage to quantify *PPT.* All gages are sensitive to wind [*WMO*, 2008] and wetting losses on the containers to evaporation although shielding can decrease these errors. Weighing gages record the weight of a container continuously either by means of a spring mechanism or a balance. The weight is indifferent to rainfall intensity or solid verses liquid *PPT*. Tipping gages tend to under collect due to their small orifice and inefficient tipping under high intensity events. Thus, a weighing gage is considered somewhat more accurate. Our available networks consist of both tipping and weighing gages (Figure 4). The number and regionalized climate classes are presented in Table 1.

West Texas Mesonet (WTM) is operated by Texas Tech University [*Schroeder et al.*, 2005] and initiated in 1999 to provide free real-time weather and agricultural information for residents of the South Plains region of western Texas. The network had 79 surface meteorological stations available over our time period. The networks uses shielded weighing gages for *PPT*. In addition, the WTM collects all the required parameters to calculate ET_r. The WTM was Phase 1 on the now defunct Heart of Texas Network. Daily data were obtained for via http://www.mesonet.ttu.edu/

TexasET Network (TETN) is operated by Texas A&M University beginning in 1994 and includes 49 weather stations located statewide. TETN displays daily weather and ET_r data, heat units, and other data; offers interactive, easy-to-use calculators that allow users to determine the irrigation water requirements of crops and landscapes; and, provides several other tools (e.g., for downloading data and setting up automatic email notifications of customized weather data and irrigation recommendations). TETN collects all the required parameters to calculate ET_r and even provides the value daily. However, due to data availability, data cost, and quality control issues (Section 5.3) (e.g. time required to quality control, gap fill, and make data adjustments, and lack of access to hourly data), these data were excluded from ET_r calculations. Daily *PPT* data from tipping gages was accessed through http://TexasET.tamu.edu

Climate Reference Network (CRN) operated by the National Oceanic and Atmospheric Administration (NOAA) includes comprehensive climate and soil moisture data at 115 stations nation-wide with 8 in Texas. This network is located outside agricultural areas and wind measurements are made at 1.5 m elevation. Soil moisture sensors at depths of 5, 10, 20, 50, and 100 cm in triplicate, as is air temperature and humidity. We accessed hourly data from https://www.ncdc.noaa.gov/crn/

Historical Climatology Network (HCN) is a designated subset of the NOAA Cooperative Observer Program (COOP) Network—the HCN sites having been selected according to their spatial coverage, record length, data completeness, and historical stability [*Menne et al.*, 2009]. The resulting network contains 1,219 COOP stations nationwide with 27 operating in Texas. The daily and monthly data include maximum and minimum temperature, *PPT* amount, snowfall amount, and snow depth and are extensively quality controlled. Most HCN data uses recording *PPT* gage although all stem from COOP networks, they are

considered highly representative. We accessed daily data for Texas at http://cdiac.ornl.gov/ftp/ushcn_daily/

Soil Climate Analysis Network (SCAN): The U.S. Department of Agriculture (USDA) provides comprehensive soil moisture and climate data at 200 stations in 40 states. There are currently 14 SCAN sites operating in Texas; however, only 5 were operating over our study period. This network has a standardized depth profile of soil moisture sensors at 5, 10, 20, 50, and 100 cm along with standard meteorological sensors for calculating ET_r. *PPT* is measured by a tipping bucket gage. Data are freely available at http://www.wcc.nrcs.usda.gov/scan/

Lower Colorado River Authority (LCRA) Hydromet Network consists of 241 tipping bucket *PPT* gages. Some include air temperature and humidity while new additions will include ET_r stations. Historical daily totals for all stations were provided by staff at LCRA and is not readily available. Near real-time data for the past 14 days are available at http://hydromet.lcra.org/

Daily historical data (WTM, TETN, HCN and LCRA) were considered quality controlled and not modified. Hourly data were converted to daily data by first removing any days consisting of less than 20 total hours. The hourly data were summed to daily *PPT*, averaged for solar radiation and wind speed, and the daily maximum and minimum derived for air temperature and humidity. We assessed a total of 401 observational data sets. Most of these data were in the 600-800 (43%), 800-1000 (22%) or 400-600 (21%) mm y^{-1} precipitation classes while fewer stations were found in <400 mm y^{-1} (5%) and >1000 mm y^{-1} precipitation classes (Table 1). For example, WTM has no stations in areas >800 mm y^{-1} while LCRA is predominantly in the 600-800 mm y^{-1} class. Climate class shows similar trends with very little data outside the El Paso area or in east Texas.

3.5 Gridded Meteorological Products

Satellite *ET* is scaled based on available energy (i.e. ET_r) which comes from weather data either an on-ground stations or a gridded products. The source of this water can be either *PPT* or irrigation. However, seepage loses, shallow groundwater, spring discharge, playa lakes may also contribute water available for *ET*. When satellite *ET* exceeds soil moisture storage from *PPT*, the additional water likely comes from irrigation. A good spatially explicit measure of rainfall is required to obtain *NIWR*. As discussed in the prior section, time integration also requires knowledge of any changes to the water or energy balance between satellite passes. In particular, any *PPT* that has fallen between image collection dates must be accounted for to obtain an accurate *NIWR*. Much like *ET* algorithms, many gridded meteorological products at daily and sub-daily time steps exist and are derived from a combination of data sources. With regards to spatial estimates of *NIWR,* telemetered rain gauges are sparse and prone to error; radar estimates of *PPT* are subject to calibration errors and siting issues; and geostationary satellites have lower accuracy. The National Weather Service's River Weather Forecast, for example, produces hourly *PPT* mosaics in the Multisensor Precipitation Estimator (*MPE*) Quantitative *PPT* Estimate Product which combines Doppler radar and gauge data into a distributed *PPT* array at 4 km grid [*Kitzmiller et al.*, 2013]. The Precipitation Estimation from Remotely Sensed Information using Artificial Neural Networks (PERSIANN) system uses neural network function classification/approximation procedures to compute an estimate of rainfall rate at 4 km grids of the infrared brightness temperature image provided by geostationary satellites [*Hsu et*

al., 1997; *Hong et al.*, 2004]. Both of these products continue to evolve as new tools and statistical techniques are evaluated. Recently, other methods use downscaled data from land surface models forcings to develop high-resolution surface meteorological products that include air temperature, humidity, *PPT* and solar radiation needed for *ET* algorithms [*Abatzoglou*, 2013]. This feasibility evaluated six derived *PPT* products of different derivations from gages to satellites (Table 2).

Daymet is a collection of algorithms designed to interpolate and extrapolate daily meteorological observations to produce gridded estimates of weather parameters. Daymet relies on elevation data and discrete observations of maximum and minimum temperature, and *PPT* from ground-based meteorological stations. Output parameters include daily surfaces of minimum and maximum temperature, precipitation, humidity, and radiation produced on a 1 km gridded surface over the conterminous United States (CONUS). The Daymet model is based on Thornton et al. [1997] and maintained by Oak Ridge National Laboratory (http://daymet.ornl.gov).

The latest version of the Parameter-elevation Regressions on Independent Slopes Model (PRISM) climate mapping system combines topography and gage data to produce daily *PPT* and maximum and minimum temperature at 4km resolution [*Daly et al.*, 2008]. The data are produced in near-real time over CONUS by researchers at Oregon State University (http://www.prism.oregonstate.edu/).

Precipitation Estimation from Remotely Sensed Information using Artificial Neural Networks - Cloud Classification System (PERSIANN-CCS) extracts local and regional cloud features from infrared geostationary satellite imagery (GOES) in estimating fine-scale (0.04° or ~3 km every 30 min) rainfall distribution cumulated every 3 hours [*Hong et al.*, 2004]. Data over CONUS was accumulated into daily totals by Hong at the University of Oklahoma. The data are maintained in near-real time by the University of California at Irvine (http://chrs.web.uci.edu/PERSIANN-CCS/).

The Stage IV radar product is produced by the National Centers for Environmental Prediction-Environmental Modeling Center. The process begins by mosaicking rainfall estimates from adjacent WSR-88D radar-only products with a myriad rain gauge networks followed by manual quality control and adjustment by National Weather Service Forecasters. The product is at 5-minute intervals at a 4 km scale available at http://www.emc.ncep.noaa.gov/mmb/ylin/pcpanl/stage4/. Data over CONUS was accumulated into daily totals by Dr. Hong at the University of Oklahoma.

The North American Land Data Assimilation System Project Phase 2 (NLDAS) is a land surface model initiated as a joint collaboration between federal agencies and university partners [*Mitchell et al.*, 2004]. The NLDAS-2 forcings comprise hourly *PPT* and air temperature, specific humidity at 2 m height, downward shortwave and longwave radiation, and wind speed at 10 m height [*Xia et al.*, 2012]. *PPT* is derived from gage data and orographic enhancement using the PRISM algorithm while other data is derived from NCEP North American Regional Reanalysis (NARR) as described by Mesinger et al. [2006]. The data are available in netCDF format at http://disc.sci.gsfc.nasa.gov/hydrology/data-holdings. We also evaluated the downscaled bias corrected 4-km NLDAS-2 product using higher resolution (0.8 km) PRISM data to scale surface meteorological over CONUS from 1979 to 2010 [*Abatzoglou*, 2013].

Gridded data products (Table 2) provide higher spatial coverage than individual stations and generally have a more quality controlled data set. The accuracy of *PPT* is critical to the net *ET* as this value is

subtracted from the total growing season *ET*. These products of varying derivation and complexity will be assessed over Texas and within its five *PPT* bands and climatic zones. The observational data from the last section was used to statistically assess the collocated gridded products. We selected several conventional statistics related to time series analysis, dichotomous statistics related to event detection, and accuracy indices that aggregate these into simple skill scores ranging between 0 and 1. The statistics were calculated for each of the 401 observation locations by extracting the collocated grid cell from each gridded *P* product and comparing the daily time series from 2006-2012 between days of available data (designated as 'n'). Appendix A lists the conventional and dichotomous statistics used in the analysis.

Table 1. Meteorological networks and their precipitation and climate classes used for validation over the years from 2006-2012

		Precipitation Class (mm y^{-1})					Climate Class*				
ID	All	<400	400-600	600-800	800-1000	>1000	1	2	3	4	5
WTM	79	7	59	13	0	0	42	33	1	0	0
TETN	41	8	7	9	10	7	9	3	12	5	12
CRN	8	2	3	0	2	1	1	3	1	1	2
HCN	27	2	7	5	7	6	6	4	6	6	5
SCAN	5	0	4	0	0	1	4	0	0	1	0
LCRA	241	0	3	147	69	22	0	12	192	37	0
Total	401	19	83	174	88	37	62	55	212	50	19

*As defined in by Narasimhan et al. 2005.

Table 2. Gridded precipitation products chosen for validation.

Product	Meteorological Parameters	Spatial resolution (km)	Time step	Time Duration	Derivation
Daymet	Precipitation, daily max/min temperature	1	Daily	1980-pres.	Gage, DEM
PRISM	Parameter-elevation Regressions on Independent Slopes Model	~4	Daily	1981-pres.	Gage, DEM
PERSIANN-CCS	Precipitation	~4	0.5, 3, 6hr	2002-pres.	Satellite
StageIV	Precipitation	4	5 minute	2001-pres.	Radar and gage
NLDAS-12	Precipitation, air temperature, vapor pressure, wind speed (10m), solar radiation, potential *ET*	12	1hr	1979-pres.	Gage and PRISM
NLDAS-4	NLDAS-12 downscaled and biased corrected using PRISM topographic relationships	4	1hr	1979-2012	Gage and PRISM

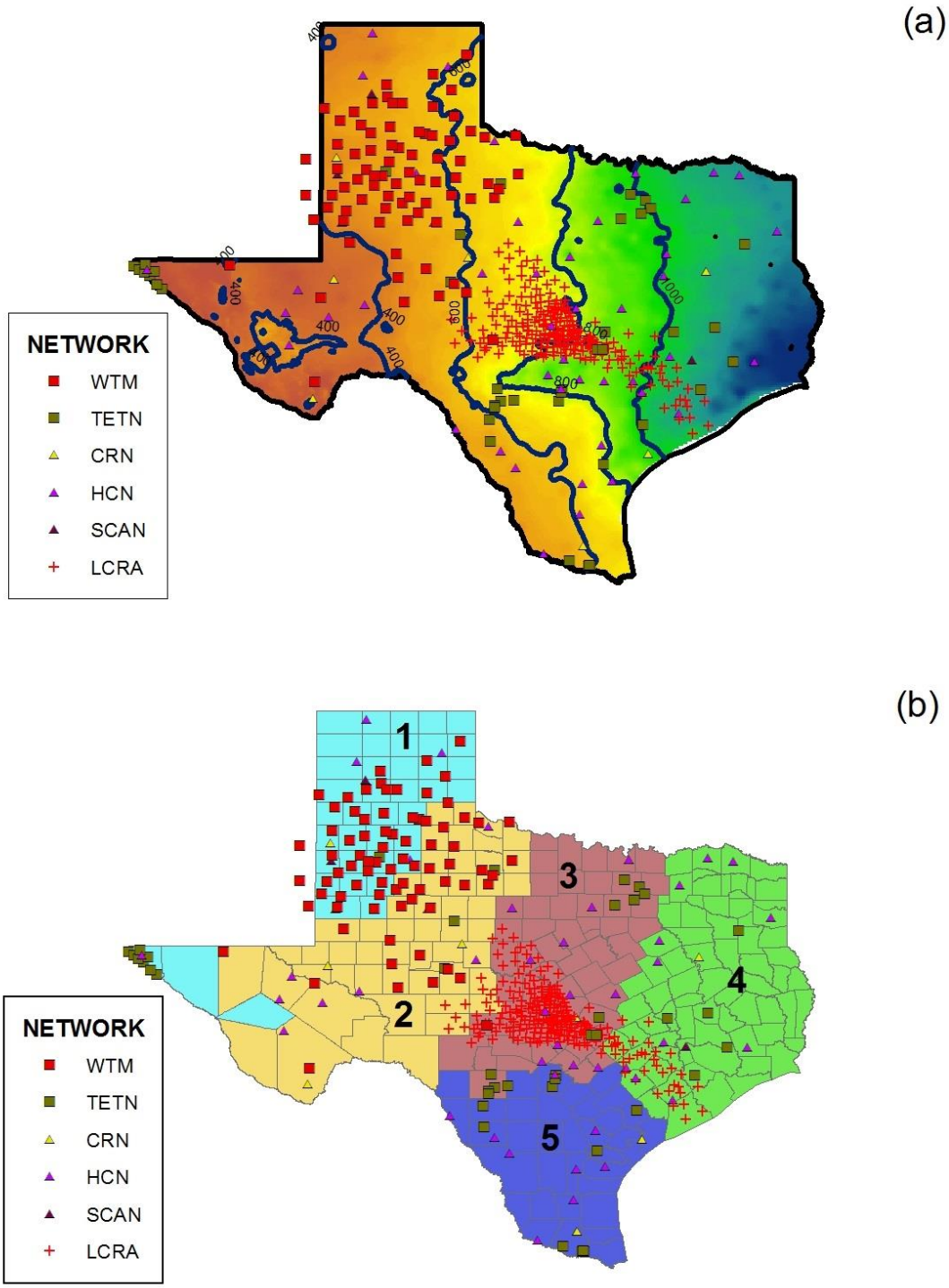

Figure 4. Six monitoring networks in Texas were used for observational data including (1) West Texas Mesonet (WTM) from Texas Tech University, Texas ET Network (TETN) from Texas A&M University, NOAA's Climate reference Network (CRN), USDA's Soil Climate Analysis Network (SCAN), and the Lower Colorado River Authority's (LCRA) Hydromet. Monitoring stations were further categorized based on their (a) mean annual precipitation from 30-year normal from 4 km gridded PRISM (1980-2010), and (b) their 5 climatic zones.

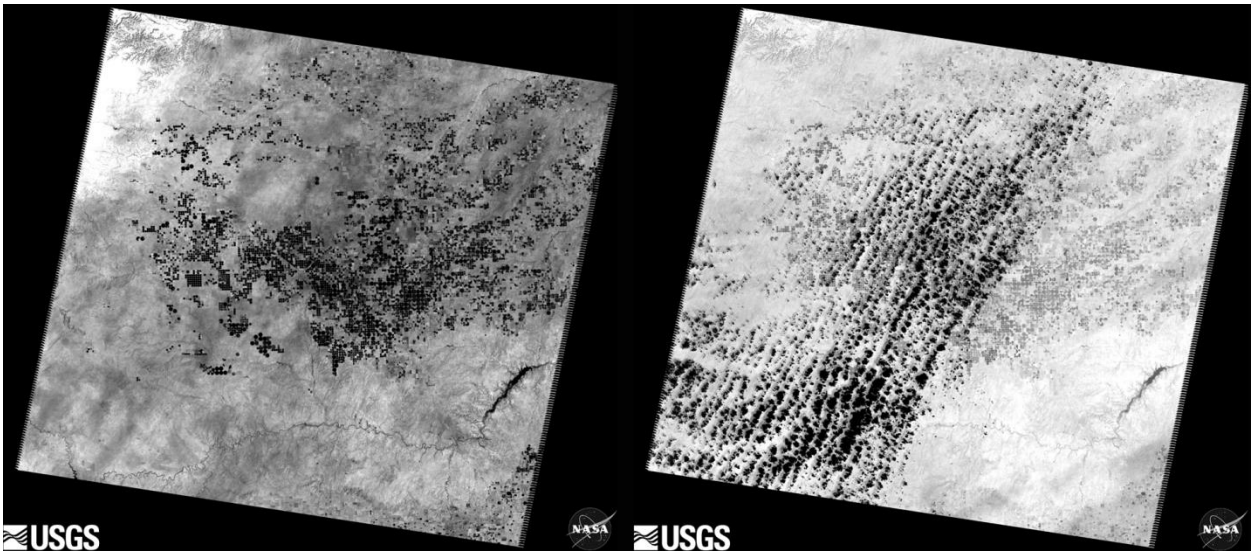

Figure 5. Landsat 5 thermal data for path 31 row 35. Left image shows cloud-free observation from September 4, 2010. Dark pixels are agricultural land and water bodies. The image at right was collected 16 days later on September 20 when cumulus clouds obscure much of the scene. The darkest pixels in this image are clouds. Agricultural land and water bodies appear in a lighter gray tone.

4 Algorithms and Products for Estimating Evapotranspiration

Contrary to uncertainty in Texas weather, its climatology is fairly straightforward: mean annual temperature increases from north to south while *MAP* increases from west to east [*Nielson-Gammon*, 2011]. The climate in Texas is strongly influenced by three large geographical features: the Rocky Mountains, the central plains, and the Gulf of Mexico. These features route and partition the atmospheric transport of cooler air masses from the north and warmer humid air from the south. Regardless of the region, irrigation is utilized across the entire State. In agriculture, *ET* is the major consumptive use (net loss) of soil moisture storage whether it is derived from *PPT* or irrigation. Although irrigation minimizes farmers' risk and can typically increases yield, the volume is often not well documented over a growing season and must be estimated from ancillary data. For the water planner, the variability of *PPT* and applied irrigation make deterministic quantification of irrigation water use challenging at the county and state level. Remote sensing adds a new tool to quantify field-scale *ET* but it also requires substantial commitment to data processing, quality control, time, skill and effort. There is currently not a turnkey solution and many variants exist.

4.1 Satellite-based *ET* algorithms

Traditionally, crop *ET* (ET_C) is estimated by multiplying a weather-based ET_r by a crop coefficient (K_C), determined according to the crop type and growth stage [*Allen et al.*, 1998]; however, the method is limited to an idealized, well-watered (non-water limited) plant in homogeneous terrain and climate. Field-scale measurements of *ET* using micrometeorology, such as Bowen ratio and eddy covariance, provide ET_C, but are site- and time-specific, require many assumptions, corrections, maintenance visits, and may suffer from errors of up to 30% [*Allen et al.*, 2011]. Micrometeorological estimates of ET_C are also difficult to spatially distribute and scale to operational levels required. In contrast, satellite data are ideally suited for deriving spatially continuous fields of *ET* [*Moran and Jackson*, 1991; *Bastiaanssen et al.*, 1998; *Allen et al.*, 2007].

Most remote sensing *ET* methods are based on TIR bands used to derive *LST* for each pixel in a satellite image (Table 3). *LST* is used to estimate various components of the surface energy balance and scale ET_r. There are typically two approaches to estimate *ET* from remotely sensed data based on (1) vegetation indices or (2) *LST* energy balance models. Early satellite-based *ET* models used vegetative indices (*VI*) to derive a K_c and scale ET_r by developing a map of relative fraction of ET_r termed ET_rF [*Heilman et al.*, 1982; *Huete*, 1988]. Such methods utilize surface reflectance in the red and near infrared bands to compute indices such as the Normalized Difference Vegetation Index (*NDVI*) or the enhanced vegetation index. These indices are highly correlated to vegetation vigor (Figure 6) and have been successfully used to estimate ET_rF. The relationship between *VI* and K_c is empirically derived for each crop/vegetation type using local *ET* measurements [*Anderson et al.*, 2012] or can be calibrated with ancillary satellite-based energy balance (*EB*) models [*Tasumi et al.*, 2005; *Tasumi and Allen*, 2007]. However, because *VI* approaches are insensitive to soil wetness and acute plant stress, there is potential for large error in ET_c due to bare soil evaporation and reduced transpiration from water limitations and plant physiological controls. *VI*-only methods tend to overestimate *ET* when stress develops rapidly, and before biomass is able to physically adjust to the water shortage through leaf senescence or leaf drop. *VI* methods tend to

miss reductions in stomatal conductance caused by acute water stress that is not reflected in reductions in biomass. This was verified by a study applying a remotely sensed *EB* model and a *VI* based ET_rF model over a rain-fed corn and soybean production region in Iowa during a prolonged dry-down period [*Gonzalez-Dugo et al.*, 2009].

Energy balance *ET* models use *LST* and other surface characteristics to estimate the latent energy (*LE*) as the residual of the *EB* equation:

$$LE = R_n - G - H \tag{2}$$

where R_n is net long and short wave solar radiation, *G* is ground (i.e. soil) heat flux, and *H* is sensible heat flux to the air (all units of energy or W m^{-2}). Conversion of *LE* to water equivalence (i.e. mm or inches) requires a correction for water density and the latent heat of vaporization, both terms are dependent on temperature.

A variety of *EB* models have been developed that differ in how they distribute *ET*, their overall complexity, and their ancillary data requirements. In general, these models rely on the following expansion of *H* derived from satellite-based *LST*:

$$LE = R_n - G - \frac{\rho_a C_p \left(LST - T_a\right)}{r_a} \tag{3}$$

where ρ_a is air density (kg m^{-3}), C_p is specific heat capacity of the air (J kg^{-1} C^{-1}), T_a is air temperature (C), and r_a is aerodynamic resistance (s m^{-1}). These methods generally assume a linear relationship between the *LST*-T_a calculated at extreme pixels (hot and cold) in each satellite image. The use of end-member pixels assumes *H* is negligible at the cold pixel and all total available energy is partitioned solely to *LE;* conversely at the hot pixel, *LE* is assumed to be near or at zero [*Price*, 1990]. A suite of models exist in this class, see reviews by Gowda et al. [2007] and Anderson et al. [2012]. Many of these algorithms are based on equation (3) but differ with respect to how various components of *H* are derived, how data are used, and how satellite images or "snap shots" of *ET* are integrated in time over daily, monthly or growing season totals. Visual bands, land cover maps and topography are also required to estimate R_n and *G* at each pixel. Together, *H*, *LE*, and ET_rF are estimated and represents *ET* for a given pixel in an image at the moment in time (e.g. 10:00 am for Landsat).

Unfortunately, the spatial resolution of satellite data is negatively correlated with the temporal resolution (i.e. return times) (Table 3). For example, Landsat satellites return every 8-16 days so the snapshot of *ET* must be integrated between return intervals called time integration. Linear or spline interpolation of ET_rF values between image dates is usually accomplished at the per pixel level to estimate daily *ET*, where the instantaneous ET_rF is multiplied by the concurrent weather station (or gridded product) ET_r value. In this approach, it is assumed that per pixel *ET* changes in proportion to the change in daily ET_r at the weather station. In this case, ET_r is used as an index for relative change based on weather conditions, while pixel specific information about the actual *ET* relative to ET_r is represented by interpolated ET_rF values. In the case of riparian and irrigated environments, relying on ET_r to represent a daily index of relative change according to daily weather conditions is fairly robust given that these environments experience advective conditions and are typically energy limited, not water limited. In other words, the coldest pixel within a

scene has an actual *ET* very close to ET_r. This is the foundation of these algorithms: coldest pixel transpiring at or near ET_r and the hottest pixels essentially not transpiring.

The current state-of-the-science algorithms are grouped (A-D) based primarily on their origination algorithm (Table 4). For example, Group A algorithms evolved from the Surface Energy Balance Index (SEBI) originally proposed by *Menenit and Choudhury* [1993]. Although considered potentially a very important need across Texas' diverse climate, few *VI* and *EB* approaches rely on weather station derived ET_r for constraining and computing instantaneous *ET*, and time integrated monthly and annual actual *ET*. We will test the validity and assess the feasibility and implementation of the recommended methods, as discussed in Section 6.

4.2 Time Integration Methods to Quantify Irrigation Water Use

Monthly or seasonal *ET* maps are derived from a series of ET_rF "snap shot" images interpolated between acquisition dates on a pixel by pixel first into a daily total based on ET_r, then cumulating these daily interpolated ET_rF images by the respective *ET* for a given season. The instantaneous ET_{inst} is calculated by dividing by the latent heat of vaporization (λ) at the instant of the satellite image by

$$ET_{inst} = 3,600 \frac{LE}{\lambda \rho_w} \tag{4}$$

where ET_{inst} is now in mm h^{-1} and λ_w is the density of water (~1000 kg m^{-3}) and λ, the latent heat of vaporization, is defined as

$$\lambda = \left[2.501 - 0.00236(LST - 273.15)\right] \times 10^6 \tag{5}$$

The instantaneous ET_rF is computed for every pixel in the image at the time of the satellite overpass as the ratio of ET_{inst} from satellite and ET_r from weather. The daily *ET* (mm d^{-1}) for a 24 hour period (ET_{r24}) and the cumulative ET over some time period from day *m* to *n* as

$$ET_{cum} = \sum_{i=m}^{n} \left(ET_r F_i\right)\left(ET_{r24(i)}\right) \tag{6}$$

Because satellite imagery only provides instantaneous information at the time of acquisition, daily ET_r is used to account for daily variations in atmospheric water demand (i.e. air temperature, humidity, solar radiation, and wind speed). Two major assumptions are 1) ET_rF is constant over the 24-hour period and 2) *ET* is proportional to daily ET_r. These assumptions are generally met for agricultural vegetation due to limited regulation of stomatal conductance, photosynthesis and transpiration [*Mcnaughton and Jarvis*, 1991; *Allen et al.*, 1998; *Tolk and Howell*, 2001; *Hunsaker et al.*, 2003; *Cammalleri et al.*, 2014a].

The interpolation of ET_rF between image dates is not unlike the construction of a traditional K_c curve [*Allen et al.*, 1998], where interpolation is done between discrete values for K_c [Wright, 1982]. Generally one satellite image (ET_{inst}) per month is sufficient to construct an accurate ET_rF function for purposes of interpolating seasonal *ET* [*Allen et al.*, 2007]. However, cloud contamination (thermal sensors do not see through clouds) and *PPT* events between satellite acquisitions decrease the accuracy. Examples of interpolating ET_rF to estimate daily and monthly *ET* are given in Allen et al. [2007] and Singh et al. [2008].

If a specific pixel must be masked out of an image because of cloud cover, then a subsequent image date can be used during the interpolation, however, the ET_rF curve will have reduced accuracy. In addition, substantial time and effort may be required to adjust for 'background' evaporation caused by differences in antecedent *PPT* between two image dates (where one date is used to provide information for cloud filling of the other). During the gap filling, the interpolated values for the clouded and cloud-shadowed areas are adjusted for differences in residual soil moisture between the acquisition dates. This procedure, or a similar one, is required to remove artifacts of precipitation-derived *ET* that are unique to specific image dates, but that may not be representative of the image date represented by the ET_rF from the previous and the following images. Regardless of the remote sensing algorithm, careful consideration of time integration is essential for accurate *ET* estimation of cumulative totals in Texas due to the high potential for both cloudy scenes and discrete *PPT* events between satellite overpasses. Fusing Landsat-derived *ET* images with higher frequency *TIR* images (i.e. MODIS) is also discussed in Section 6.

4.3 Net Irrigation Water Requirement from Numerical Models

Lastly, *NIWR* models have been developed to study historical and future irrigation water demand. Application of these models regionally involves the following considerations: 1) spatial structure and resolution at which water balance variables will be calculated (i.e. gridded or point weather stations); 2) soil classes and characteristics that govern infiltration and water holding capacity; 3) crop characteristics that describe root access to soil moisture and related effects on *ET*; 4) meteorological variables forcing the simulations (i.e. precipitation, temperature, solar radiation, humidity, and wind speed), and ET_r type (i.e. simple temperature base or physically based); 5) model structure and physics such as simulation of energy balance, soil water balance, non-growing season *ET* and *PPT* accumulations, seasonal crop development and harvest for different crop types, and variable growing season lengths; 6) time step for simulating the soil water balance, crop development, and ET_C (i.e. daily or monthly); and 7) calibration objectives such as simulated versus measured green-up and harvest dates, killing frost temperatures, or ET_C.

Among available models, there are several types that generally satisfy these criteria:

1. Reference *ET*, dual crop coefficient, daily soil water balance, ET_C models outlined by the American Society of Civil Engineers (ASCE) and Food and Agriculture Organization (FAO) of the United Nations, FAO Irrigation and Drainage Paper 56 [*Allen et al.*, 1998; *ASCE-EWRI*, 2005]
2. Full crop simulation and growth models that consider the water, nitrogen, and carbon balances, such as the Decision Support System for Agrotechnology Transfer (*DSSAT*) [*Jones et al.*, 2003], or Cupid soil-plant-atmosphere model [*Norman*, 1979].
3. Agro-economic models [*McCarl and Spreen*, 1980; *McCarl et al.*, 1999] are used primarily to forecast future scenarios and optimize commodity prices but such models could forecast irrigation water demand but are generally not applicable here.

Our implementation of the ET Demands Models (Type 1 above) is described in Section 6.2. The following Section 5 include the study methodology, followed by our implementation and feasibility assessment.

Table 3. Satellites products available for *ET* estimations.

		Spatial resolution			
	Return interval	TIR	SWIR	VNIR	Product Availability
Thermal sensor satellites					
Landsat 5	16 days	120 m	30 m		1985 – 2011
Landsat 7	16 days	60 m	30 m		1999 to present *
Landsat 8 (LDM)	16 days	100 m	30 m		May 2013
ASTER	16 days	90 m	15 m		1999 to present (sporadic)
AVHRR	12 hours	1100 m	1100 m		1992 – present
Spectroradiometer satellites					
GOES 1-7	15 min	4 km	1/4 km		1975 – 1999
GOES 8+	15 min	4 km	1/4 km		1994 – present
MODIS	12 hours	1 km	250 m		1999 – present
VIIRS	12 hours	375 m	375 m	750 m	2012 – present
Other multispectral satellites					
SPOT 1-4	4 days		20 m		1986 to 2012
SPOT 5-6	On demand		10 m		2002 to present
CBERS 1 & 2 CCD	26 days		20 m		1999 to early 2010
Ikonos	On demand		4 m		1999 to present
RapidEye	On demand		6.5 m		2008 to present (constellation)
Quickbird	On demand		2.44		2002 to present
GeoEye-1	On demand		0.5		2008 to present

*Data gaps present in Landsat 7 ETM+ data following scan line failure on May 31, 2003.

TIR, thermal infrared; SWIR, short-wave infrared; VNIR, very near infrared

ASTER, Advanced Spaceborne Thermal Emission and Reflection Radiometer; AVHRR, Advanced Very High Resolution Radiometer; CBERS, China-Brazil Earth Resources Satellite; GOES, Geostationary Operational Environmental Satellite; MODIS, Moderate Resolution Imaging Spectroradiometer; SPOT, Systeme Probatoire d'Observation de la Terre; VIRIS, Visible Infrared Imaging Radiometer Suite; VIIRS, Visible Infrared Imaging Radiometer Suite;

Table 4. Energy balance (Groups A, B, and C) and fusion-based (Group D) *ET* models to be evaluated.

ET Algorithm		Name
Group A	SEBI	Surface Energy Balance Index [*Menenti and Choudhury*, 1993]
	SEBS	Surface Energy Balance System [*Su*, 2002]
	S-SEBI	Simplified SEBI [*Roerink et al.*, 2000]
Group B	TSM	Two Source Model [*Norman et al.*, 1995]
	TSM-DTD	Two Source Model Dual Temperature Difference [*Norman et al.*, 2000]
	ALEXI	Atmospheric Land Exchange Inverse Model [*Anderson et al.*, 1997; *Anderson et al.*, 2007a; b]
Group C	SEBAL	Surface Energy Balance Algorithm for Land [*Bastiaanssen et al.*, 1998; *Bastiaanssen et al.*, 2005]
	METRIC	Mapping *ET* with Internalized Calibration [*Allen et al.*, 2007; *Allen et al.*, 2013]
Group D	STARFM	Spatial Temporal Adaptive Reflectance Fusion Model [*Gao et al.*, 2006]
	DisALEXI	Disaggregated Atmospheric Land Exchange Inverse Model [*Kustas et al.*, 2003; *Norman et al.*, 2003]

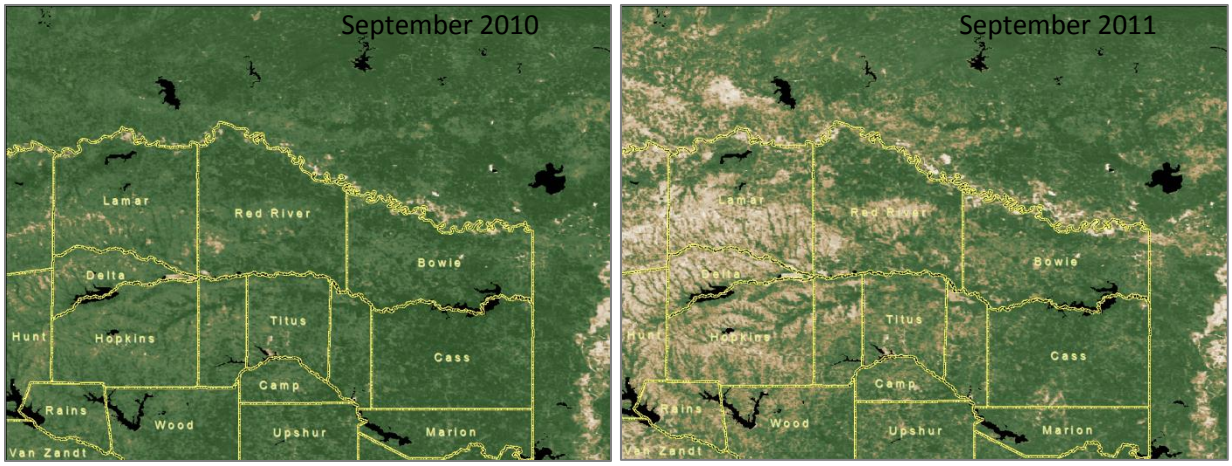

Figure 6. Normalized Difference Vegetation Index for northeast Texas during a wet (September 30, 2010) and a dry year (September 30, 2011).

5 Assessment of *ET* Algorithms and Data Requirements

Currently, there is no operational *ET* algorithm nor is there any turnkey solution to temporally integrate between satellite overpasses. The process to obtain *ET* from remotely sensed data is convoluted and currently requires a knowledgeable expert to both acquire the necessary data, process the images, integrate the data over the growing season and quality control the results. First, we present background data on the *ET* algorithms from the literature. Next, we evaluate the probability of cloud-free image acquisition and gridded data sets over Texas. Lastly, we present a summary of these finding and their operational readiness.

5.1 Residual Energy Balance Methods for *ET*

The combination of thermal and optical remote sensing is the most robust approach estimate the spatial and temporal variability of *ET* at an operational level [*Gowda et al.*, 2007]. The two most common approaches use either the land surface energy balance or reflectance-based crop coefficients [*Gowda et al.*, 2008]. Energy based methods rely on estimates of *LST* to derive *ET* as the residual of the energy balance (Eq. 2). Reflectance approaches commonly use red and near-infrared reflectance to compute vegetation indices such as *NDVI* which is used to scale ET_r from meteorological stations. Either method requires high quality satellite imagery that is cloud free.

Reflectance based *ET* models have some advantages over energy balance in that *VI* is easily computed, *VI* responds more slowly to surface moisture conditions, and the algorithms are simpler. However, *VI*-based models are less accurate particularly under water stressed or bare soil conditions, and meaningful results are difficult to obtain under heterogeneous land cover. In addition, VI-based *ET* models give little indication of *ET* during pre-plant, emergence, or senescence periods [*Anderson et al.*, 2012]. In other words, *VI*-based *ET* models do not correlate directly with actual rates of *ET*. For example, *VI* is indifferent to over–watered fields (i.e. flooded) or bare soil evaporation (i.e. pre-emergent fields). As such, we ruled out the use of *ET* models, and instead focus primarily on *EB* models. However, *VI*-based models are useful to determine irrigated acreage and for non-growing season applications when *LST* differences between are minimal (i.e. *EB* methods would not work).

The use of *EB* algorithms to produce *ET* maps is the most robust approach due to reliance on both optical and thermal imagery data. We group these algorithms according to the origination algorithm (Table 2). Group A algorithms evolved from the Surface Energy Balance Index (SEBI) originally proposed by Menenit and Choudhury [1993]. SEBI produces a location dependent ET_r and T_s range to account for spatial variability of *ET* due to albedo and aerodynamic roughness by implementing a crop water stress index and contrast between wet (cool) and dry (hot) areas to derived the ET_rR scaled between 0 and total available energy - which is assumed constant over the day. Expanding on SEBI, Su [2002] developed Surface Energy Balance System (SEBS) which includes estimation of atmospheric turbulent fluxes and ET_rR using satellite earth observation data, in combination with meteorological information at other scales. SEBS includes a set of tools for the determination of the land surface physical parameters, such as albedo, emissivity, temperature, vegetation coverage, etc., from spectral reflectance and radiance; an extended model for the determination of the roughness length for heat transfer; and a new formulation for the determination of the ET_rR on the basis of energy balance at limiting cases. Its main limitation is the requirement of

aerodynamic roughness height from vegetation indices which can saturate at higher vegetation densities and the relationships are dependent on vegetation type. It also requires daily estimates of on-ground ET_r. To overcome some of the limitation of SEBS, Roerink et al. [2000] simplified this method (S-SEBI) by considering constant atmospheric conditions to derive estimates of *ET* by determining a reflectance dependent maximum temperature for dry conditions and a reflectance dependent minimum temperature for wet conditions.

Group B is based on the two-source model (TSM) where energy fluxes are partitioned between soil and vegetation. The difference between the thermodynamic temperatures of soil and vegetation contribute differently to the measured *LST* in proportion to the fraction of radiometer view. Their respective aerodynamic temperatures and resistance to turbulent transfer are independently modeled resulting in a two-source energy balance model [*Norman et al.*, 1995] or TSEB. More recently, the TSEB has evolved into a time-differential temperature Atmosphere-Land Exchange inverse (ALEXI) model that relates diurnal *LST* from geostationary satellites which operate regionally at coarser spatial scale [*Anderson et al.*, 2007b]. Currently, ALEXI is running at daily time steps over the U.S. using the GOES satellite at ~10km resolution. TSEB requires a surface-atmospheric boundary layer system and a vegetation/soil resistance model, a time-coupled atmospheric boundary layer model; all of which requires significant initial parameterization of boundary conditions and daily interpretation of multiple images.

Group C is also based originally on SEBS. The Surface Energy Balance Algorithm for Land (SEBAL) algorithm estimates the spatial variation of hydro-meteorological parameters empirically, requires only field information on short wave atmospheric transmittance, *LST* and vegetation height [*Bastiaanssen et al.*, 1998]. Furthermore, it calculates the fluxes largely independently from land cover and can handle *TIR* images at resolutions between a few meters to a few kilometers. For SEBAL, *H* is estimated from a linear bulk aerodynamic resistance model between *LST* and T_a which can only be estimated from a wet (H = 0) and dry pixel (LE = 0). This method eliminates the need for accurate *LST* and T_a measurements. Spawning from SEBAL, Mapping Evapotranspiration with Internalized Calibration (METRIC) is internally calibrated using ground-based ET_r to establish and maintain *EB* at the wet and dry pixels [*Allen et al.*, 2007]. The calibration is done for each image using an hourly estimate of ET_r from weather data at the image collection time. The use of ET_r for the extrapolation of instantaneous *ET* from periods of 24 hours and longer compensates for regional advection effects by not tying the *ET* to available energy (i.e. Rn - G), since *ET* can exceed daily available energy in many arid or semi-arid locations due to the oasis effect.

Cloud-free images at high spatial resolution (i.e. Landsat) throughout the growing season are the basis and limitation to all of the above algorithms. In contrast, Group D takes advantage of the high spatial resolution from Landsat imagery coupled to the increased temporal data from other imaging satellites to composite maps at higher spatial and temporal resolutions. Spatial and temporal adaptive reflectance fusion model (STARFM) blends 16-day Landsat ETM+ data at 30m with daily MODIS surface reflectance at 500m to produce synthetic *LST* daily at ETM+ resolution [*Gao et al.*, 2006]. Higher spatial resolution can be also obtained by disaggregating the *TIR* geostationary GOES image to Landsat using disALEXI [*Norman et al.*, 2003; *Anderson et al.*, 2011].

In general, Group B and C are the current state-of-the-science and robustly tested under many environmental conditions while sensor fusion (Group D) is perhaps the future-of-the-science. SEBS was

applied to 15 Landsat images evaluated against lysimeter data at Bushland, TX and found to have an *RMSE* of 0.11 mm h^{-1} (20.8%) when locally derived *G* was used [*Gowda et al.*, 2013]. Many of these algorithms were assessed during the Bushland Evapotranspiration and Agricultural Remote sensing EXperiment 2008 Southern High Plains in the Texas Panhandle [*Evett et al.*, 2012]. Instantaneous *ET* from aircraft imagery using SEBAL had a mean bias error (*MBE*) and root mean square error (*RMSE*) of 0.13 and 0.15 mm h^{-1} (23.8 and 28.2%), respectively, with hot and cold pixel selection accounting for 20% of the variability in *ET* from lysimeter data [*Paul et al.*, 2013]. STARFM fusion using DisALEXI maps had an accuracy of 0.9 mm d^{-1} under more humid conditions in Mead, NE and but failed to capture *ET* spikes immediately following afternoon irrigation in Bushland, TX, resulting in errors of 1.5 mm d^{-1} [*Cammalleri et al.*, 2014b]. Thus, the spatial extent of irrigated fields is missed; however, rainfall likely occurs at a spatial scale large enough for MODIS to capture. Allen et al [2011] further summarizes instantaneous error from remote energy balance errors of 10-20% and VI models at 15-40%.

From 46 published studies using SEBAL, METRIC, SEBS, TSEB, and ALEXI (among other), *Karimi and Bastiaanssen* [2015] found seasonal *ET* had high accuracy (95 ± 5.0%) while accuracy of rainfall data from satellites was slightly lower (82 ± 15%) and land use /land cover was 85 ±7%. Thus, the *ET* algorithms are fairly robust while satellite *PPT* and land use are more error prone. We address *PPT* in Section 5.4; however, we are limited to the CDL for annual land use and land cover (discussed further in our pilot study, Section 6.4) and it is not perfect.

Table 5 presents our opinion of the feasibility of these *ET* algorithms for Texas. Group A, based upon SEBS, have evolved but are complex in that they require many parameters and are more sensitive to input bias (i.e. surface temperature and weather data), and are not commonly used in operations, reducing their feasibility. Group B distinguishes between bare soil evaporation and ET_C but it also requires significant boundary condition parameterization; it is complex and lacks spatial resolution unless the use of research code (like DisALEXI) is applied. Group C improves field scale accuracy levels; however, the increase in accuracy adds complexity and is subject to cloud-free data availability. Both SEBAL and METRIC are open source codes published in the literature, are widely used, and can be easily adapted by the end-user. METRIC is particularly suited to advective conditions and there is potential access to the full suite of METRIC algorithms and developers. Lastly, Group D may prove to be the highly feasible, but these are currently research algorithms and the sources codes are not available or easily implemented. Thus, they are also considered non-operational at this point.

5.2 Numerical Modeling of NIWR using ET Demands

Remotely sensed methods require cloud-free images hampering their use in some areas of Texas (Section 5.3). While full crop simulation and growth models have many research advantages, and are largely physically based, the American Society of Civil Engineers and FAO-56 irrigation water demand methodology are possibly well suited for operational application at local and regional scales. This methodology is currently being used in Arizona, California, Colorado, Idaho, Kansas, Nebraska, Nevada, New Mexico, and by the Bureau of Reclamation for the Lower Colorado River Accounting System and ET Toolbox models [*Jensen*, 1998; *Brower*, 2008]. The University of Idaho, Nevada Division of Water Resources, and Desert Research Institute (DRI) have recently modified and enhanced the ASCE and FAO-56 ET_r and dual crop coefficient approach, and have made state wide applications of the modified model,

named the ET Demands Model [*Allen et al.*, 2005; *Allen and Robison*, 2009; *Huntington and Allen*, 2010; *Huntington et al.*, 2015]

Actual *ET* for multiple crop types is estimated in the ET Demands model at each grid cell or weather station following the FAO-56 dual crop coefficient approach as

$$ET = \left(K_s K_{cb} + K_e\right) ET_r \tag{7}$$

where the stress coefficient (K_s), the basal crop coefficient (K_{cb}), and soil water evaporation (K_e) are dimensionless ranging from 0 to 1. Daily K_{cb} values over a season, commonly referred as a crop coefficient curve, represent impacts on *ET* from changes in vegetation phenology, which can vary from year to year depending on the start, duration, and termination of the growing season, all of which are dependent on temperature conditions. A daily soil water balance over the simulated effective root zone is required and computed in ET Demands to calculate K_s.

The soil and root zone water balance in ET Demands is based on a two stage drying procedure following the work of Allen et al. [*1998; 2005*]. Research has shown that the relatively simple two-stage drying soil water balance model is fairly robust in simulating bare soil evaporation when compared to more physically based models like HYDRUS [*Allen*, 2011]. Soil attributes are obtained from the Natural Resources Conservation Service State Soil Geographic (STATSGO) database. STATSGO is a spatial soils geographic information system (*GIS*) database and contains attributes of the physical character of soils needed for estimating soil water holding and infiltration parameters in the ET Demands Model's dual soil and root zone water balance and runoff modules. Specifically, STATSGO attributes are used to estimate the spatial distribution of total evaporable water and readily evaporable water used in the soil water balance, and total available water and readily available water used in the root zone water balance. These parameters affect the estimation of irrigation scheduling, evaporation losses from soil, deep percolation below root zones, antecedent soil moisture condition, and runoff. For a full description on the background of soil and root zone water balance parameters see Allen et al. [1998; 2005].

For this work, basal crop coefficient (K_{cb}) curves from Allen and Robison [2009] were adopted. Rather than a linear interpolation approach for estimating the K_{cb} between specified time intervals and growth points three different methods are utilized based on thermal heat units, to simulate the effect of air and soil temperature on vegetation development, start, duration, and termination of yearly growing season and non-growing seasons. The three methods to define the advancement of the K_{cb} curve utilized in ET Demands are (1) normalized *CGDD* from planting or greenup to effective full cover, with this ratio extended until termination, (2) percent time from planting to effective full cover, with this ratio extended until termination, and (3) percent time from planting to effective full cover and then number of days after full cover to termination. These K_{cb} development approaches allow for time interpolation and shape of crop specific K_{cb} curves to be a function of *CGDD* and temperature dependent planting or greenup estimates rather than specified and constant calendar dates.

5.3 Cloud-free potential in Texas

First, we reviewed 47 full scene areas (Figure 7) of Landsat 5 Thematic Mapper (TM) images of Texas from January 2005 to November 2011. The raw image counts per climate division and annual statics for each

scene are fully presented in Appendix B. Cloud-free counts increase from east to west along the *PPT* gradient as proximity to the Gulf Coast increases (Figure 7). Repeat storm system can intersect re-visit opportunities, leading to long stretches of low cloud-free image availability. The year 2007 was a particularly challenging year due to above average rainfall across most of the state. Landsat 5 data collection was also lower than average during that year. Both factors combined to greatly reduce cloud-free image collection. In contrast, cloud-free observations increased during 2011, a year of record drought.

Next, eight Landsat 5 scenes were compared with overall availability during the same time (Table 6). These scenes intersect areas with the most agricultural activity, complete county containment within scene extent, and metering programs. In coastal areas, less than 20% of total TM observations are sufficiently cloud-free for consideration. Of images rated as having 10% or less cloud cover with the Automatic Cloud Cover Assessment (ACCA) algorithm, only 41 to 54% meet the cloud-free criteria. In the Texas High Plains, cloud-free observations are available at least 40% and a higher percentage of images rated by the ACCA algorithm as having < 10% cloud cover are actually cloud-free.

The analysis of cloud-free status by climate division further reinforces the feasibility of using Landsat observations for western agricultural areas. During the 7 year analysis period, 601 clear images were collected over Climate Division 1 in Far West Texas and the Texas Panhandle, an area that requires twelve scenes for complete coverage. Climate Divisions 2, 3, and 4 had 990, 552, and 289 cloud-free scenes. In contrast, 289 clear images were collected during the same period in Climate Division 5, South Texas. Climate Division 5 requires nine complete scenes with fragments of three additional scenes for complete coverage. The use of Landsat observations in the coastal plains and East Texas is more problematic but worth investigating. Increased collection capacity with the launch of the Landsat 8 satellite in 2013 and continued tasking of Landsat 7 will increase observation opportunity for the state.

Lastly, we estimated probabilities of success in producing reliable growing season *ET* are displayed separately in Figures 8 and 9 for 1, 2, and 4 Landsat satellites for each combination of growing season length estimate and maximum gap threshold. We first calculated the probabilities for the fixed growing season with one satellite and 16 day (Figure 8a) or a two satellite 8 day (Figure 8b) return time over a fixed growing season. Second, we relaxed the constraints using a variable growing season based on crop and a 32 day clear sky view with a single satellite 16 day (Figure 9a) and two satellite 8 day (Figure (9b) return interval. As expected, the likelihood of successfully producing full growing season *ET* maps increases when there are more satellites and is greatest in regions where the climate is drier. The western portion of Texas has much higher probabilities, especially if only one Landsat is available. Probabilities followed somewhat similar trends for the two methods for estimating growing season length (fixed vs. variables). However, using the more likely estimate of growing season based on air temperature tended to reduce probabilities of success where actual growing seasons extend beyond April – October. In general, with only a single Landsat satellite having revisit time of 16 days, only small portions of west Texas had even 30 to 60% chance of successful production of growing season ET in any particular year (Figures 8a and 9a), when at least one clear look every 32 days is required. The rest of Texas generally had probabilities of success well below 20% for any one year. With two satellites (i.e. combined use of Landsat 5 and 7, or Landsat 7 and 8), probabilities of success increased to about 80-90% for west Texas and 40-50% over the panhandle. The

lowest potential for satellite retrievals are clearly south Texas where probabilities seldom exceed 10%. Of course, the constraints could be further relaxed at the expense of accuracy and quality in the growing season *ET.* Likewise, Group D algorithms using sensor fusion may be required in the lower probability areas.

5.4 Gridded data sets

5.4.1 Precipitation

To obtain accurate estimates of *NIWR* from remotely sensed *ET,* we need accurate *PPT* to determine the fraction of total *ET* not obtained from irrigation. We assessed 6 gridded *PPT* products against 423 on-ground stations from 6 networks operating in Texas (Figure 4). Several observational data sets were hourly (CRN, SCAN and WTM). These data were screened to assure over 20 hours per day were available then hourly *PPT* was totaled for each day. Other networks (HCN, LCRA and TETN) were included directly as daily totals. Of our available networks in Texas over the 2006 to 2012 period, CRN provides nearly 100% daily data while HCN, LCRA and SCAN are generally >80% (Table 7). TETN and WTM are generally less reliable with annual days of data near 60%. Regardless, coverage over Texas is sparse and we chose to not exclude any network despite data gaps. We also focus on daily totals over longer cumulative periods (weeks, months or growing season) to avoid introducing more uncertainties in assessing the gridded products.

The statistics defined in Appendix A can be summarized more efficiently here by three measures: root mean square error (*RMSE*), probability of detection (*POD*), and precipitation accuracy index (*PAI*). *RMSE* (mm d^{-1}) is a quadratic scoring rule which measures the average magnitude of the error giving a relatively high weight to bigger errors. POD is a dichotomous statistics that represents the fraction of observed days with rain detected by the model ranging from perfect prediction (1) to poor (0) prediction. *PAI* is combines normalized conventional (*RMSE*, *MBE*, and R^2) and dichotomous (*POD* and false alarm ratio) into a single skill estimate, also ranging from perfect (1) to poor (0). Given our period of record, we assessed daily *PPT* totals from Daymet, forcing data for NLDAS at 12 km (NLDAS-12) and downscaled, bias corrected NLDAS data at 4 km (NLDAS-4), PRISM, satellite-based PERSIANN-CSS and radar-based Stage IV.

State-wide, *RMSE* values ranged from 0.009 to 6.5 mm d^{-1}, while Daymet had the lower mean *RMSE* (0.327 mm d^{-1}) and Stage IV the largest (0.491 mm d^{-1}) across all observational data sets (Table 8). The range (one standard deviation) was similar for all 6 products near 0.45 mm d^{-1}. Since *RMSE* is implicitly lower in regions of lower precipitation, values in west Texas (Climate Zone 1 and 2) should be lower (than more mesic areas of east Texas (Zones 3 and 4). However, all 6 products have the highest RMSE in Climate Zone 2 and similar skills across the others (Table 9). Precipitation bands based on 30-year normal of PRISM data also indicate lower RMSE values in the west (<200 mm y^{-1}), highest values for 200-400 mm y^{-1} (Table 9). Both Daymet and NLDAS-12 show the lowest RMSE values for either Climate Division or *PPT* Band (Figure 10).

Ability to detect events, based on *POD*, was highest for NLDAS-12 (0.643) and lowest for Stage IV (0.315) (Table 8). Generally, with a fewer number of events in west Texas, *POD* translates to lower *POD* scores (~0.4) since a single miss would carry much more weight (Table 10). Stage IV, again, has particularly low skill at *POD*, while NLDAS-12 is >0.5 across all Climate Divisions and *PPT* Bands. The combined score, *PAI*, was highest for Daymet (0.650) and lowest for Stage IV (0.478) (Table 8) which is also observable across

the network map (Figure 11). When further summarized within each network, it is clear the CRN corresponds best to all products while HCN clearly favors Daymet (Figure 12). Of note, Daymet (and PRISM) likely uses both CRN and HCN in its algorithm, while LCRA data could be considered more independent. Thus, we can see Daymet, NLDAS-12 perform well across all networks, while SCAN and TETN generally have the lower *PAI* for all products.

The ease of implementation, skill in both conventional and dichotomous statistics, and state-wide representativeness indicate Daymet and NLDAS-12 are superior *PPT* product. Radar and satellite products were very difficult to work with due to their binary structure, verse netCDF and higher errors [*Serrat-Capdevila et al.*, 2013].

5.4.2 Reference Evapotranspiration

Accurate reference *ET* (ET_r) estimates that are representative of well-watered conditions are needed for both satellite based estimates of *ET* maps as well as time integration between images. Weather stations located in irrigated regions are ideal to capture local effects of well-watered vegetation and the associated micro-climate that results. However, stations are generally not in well-watered areas, and the data quality can be poor [*Marek et al.*, 2010]. The sensors, ideally at 2m elevation, must include air temperature and humidity, wind speed and solar radiation to calculate ET_r. Gridded NLDAS forcing data at 4km or 12km could potentially also be used if they are representative or are bias corrected. Of our available monitoring networks in Texas, only two contain the required data readily available to calculate ET_r: WTM and SCAN. TETN's historical data only includes daily minimum humidity and wind speed at 4am (although more data is available for purchase). We used station data for the period 2002-2012 from these networks. Of the 79 WTM stations, 51 had acceptable data, and of the 7 SCAN stations available, only two had acceptable data. Appendix C summarizes the stations used, and reasons for exclusion.

Daily data were first assess for quality control [*Allen*, 2008]. Scripts were written to display all variables, provide options, and correct or omit data for each station. The most common variable needing correction at each station was measured solar radiation (R_s). Appendix C lists corrections made to each station. Measured R_s is commonly under or over measured due to debris on the pyranometer window, non-level base plate, sensor miscalibration or drift, or obstructions. Corrections to measured R_s were made to each station using the theoretical clear sky solar radiation, Rso_b [*ASCE-EWRI*, 2005], where the ratio R_s / R_{so_b} for the top 10 percentile of measured R_s for specified time windows (usually 60 days) was used to scale the respective measured R_s for all days within the time window. These correction procedures were applied as needed for the entire study period of measured R_s, based on visual inspection of R_s and R_{so_b}.

Time series of gridded 4 km and 12 km NLDAS forcing (weather) data was extracted for each station location to compute ET_r and compare NLDAS derived ET_r to acceptable and quality controlled respective weather station derived ET_r. If weather station data were missing for extended periods of time, no comparisons were made for those periods. Small amounts of weather station data we filled based on long term daily means and added variance (Appendix C).

Results of the comparison indicate that ET_r is generally well simulated using NLDAS derived weather data (Tables 11). Ratios of the mean annual NLDAS-4 km estimated ET_r to the measured ET_r from 53 stations were found to range from 0.80 to 1.12, with an average of 0.99, a standard deviation of 0.04, and average

RMSE for annual estimated ET_r of 152 mm y^{-1} (Table 11). Seven day 4 km NLDAS ratios of estimated range from 0.91 to 1.12 with an average of 1.00, a standard deviation of 0.16, and an average *RMSE* for estimated ET_r of 6.5 mm $week^{-1}$. Ratios of the mean annual NLDAS-12 km estimated ET_r to the measured ET_r from 53 stations were found to range from 0.86 to 1.17 with an average of 1.03, a standard deviation of 0.05, and average RMSE for annual estimated ET_r of 175 mm y^{-1} (Table 12). Seven day NLDAS-12 km ratios of estimated to measured ET_r were found to range from 0.90 to1.17 with an average of 1.03, a standard deviation of 0.18, and average RMSE for estimated ET_r of 7.5 mm $week^{-1}$.

In general both the NLDAS products (4 and 12km) seem sufficient for estimating ambient ET_r at multiple time steps in Texas with the 4km product having less error than the 12km product. Figure 13 illustrates scatter plots of daily, monthly, and annual station and 4km NLDAS estimated ET_r for WTM Abernathy (Station Number 1) as an example. While these results are promising, bias correction is required to estimate ET_r that is representative of well-watered conditions. *Moorhead et al.* [2015] found a +2.2 mm d^{-1} bias in NLDAS 12km estimated ET_r when compared to the TETN data. Bias correction of gridded ET_r data was not implemented in this product due to the limited scope of work, but is required for full implementation of irrigation demand model estimates of *NIWR*, and satellite based estimates of *ET*.

5.5 Summary of Each Available Technology and Workshop

The initial feasibility study, completed in Year 1 of the project, concluded with a Stakeholders' Workshop posted on TWDB website (Link). To summarize, there is little doubt that *ET* algorithms are robust; they all vary in the spatial scaling of ET_rF across a given scene, but all are essentially constrained by the atmospheric demand (i.e. ET_r). In a similar feasibility study for Oklahoma (and where ground observations of actual *ET* are plentiful), satellite estimations showed agreement with ground observations with daily *ET* bias <15% and seasonal bias less than 8% [*Khan et al.*, 2010]. The accuracies and tiers presented in Table 5 are valid and would do not pose any limitation for Texas provided sufficient cloud-free imagery exists every 30 days. The advantages and disadvantages of each are presented in Table 5. Group A-C are more applicable at the county-level. Group D which integrates finer-scale Landsat with coarse-scale MODIS to find cloud-free scenes may improve feasibility in more humid regions of Texas but at a significant cost to time and expertise of staff. Regardless, all of these techniques and algorithms are complicated and varying in degrees of pre- and post-processing is required. This, on the other hand, is particularly challenging in more humid areas such as Lower Rio Grande Valley and Coastal Prairie. West Texas and the southern High Plains have much higher probabilities of quality satellite data.

All *ET* algorithms produce a scalable map of ET_rF and each map must be masked for clouds and clipped to known areas of irrigated agriculture then integrated between snapshots using weather data (either station or gridded data) to estimate *ET*. Cloud masks are constantly improving and becoming more operations for both Landsat and MODIS imagery [*Zhu and Woodcock*, 2012; 2014; *Zhu et al.*, 2015]. Perhaps, the more pressing challenge is discerning irrigated from non-irrigated agriculture. NASS georeferenced boundaries are considered proprietary ad no longer released. This is perhaps the largest challenge facing the operational readiness of such a program: in many cases our irrigated lands are not spectrally distinct from dryland agriculture. As we will point out in the following section, our only available resource to mask out native vegetation is currently the NASS CDL. Additionally, the CDL may specify 'cotton' but if ET_c for that pixel exceeds *PPT* we must assume that pixel is irrigated. However, even with

its inherent flaws, the CDL is operational with crop-type accuracies ranging from 85-95% and freely provided annually [*Boryan et al.*, 2011]; but it does not distinguish irrigated lands, failed crops or multi-rotational crops accurately.

Weather data are particularly sparse over Texas. Many gridded products, NLDAS and Daymet in particular, produce very high quality *PPT* data. However, these products do not directly represent the more humid microclimates around irrigated agricultural and may bias ET_r slightly higher. *Porter et al.* [2012] found station-based ET_r was most sensitive wind speed and air temperature, thus over-estimating actual *ET*. Ground stations that measure ET_r are particularly deficient in both number and quality in Texas. Furthermore, many of these are associated with non-agricultural environments; so much like the gridded products, ET_r may be biased slightly high. For example, ET_r calculated from NLDAS data sets in Texas was 1-2 mm d^{-1} higher simply due to higher air temperatures and wind speeds [*Moorhead et al.*, 2015]. Relative humidity and air temperature would be the most affected which could be bias-corrected if ET_r was noticeably over-estimated. For now, these products are very operational and recommended for further assessment with possible bias correction. The following section implements the METRIC algorithms and gridded NLDAS weather data to produce annual *NIWR* for 2010 (wet) and 2011 (dry) year across eight counties in Texas. The goal is to fully assess efforts required, from start to finish, to produce annual county estimates.

Table 5. Feasibility assessment of *ET* algorithms for Groups A, B, C, and D.

ET Algorithm		Accuracy	Feasibility	Justification	Complexity
Group A	SEBI	Tier 3	Low	Disadvantages: albedo and aerodynamic roughness, antiquated method	Low
	SEBS	Tier 4	Moderate	Similar limitations to SEBI, also requires daily met data, SEBAL is more current	Moderate
	S-SEBI	Tier 2	High	Simplified version, easy time integration at the expense of accuracy	Low
Group B	TSM	Tier 3	Low	Advantages: separate soil/veg *ET*; disadvantages: no time integration, antiquated method	Moderate
	ALEXI	Tier 3	Low	Advantage: time differential *LST* and robust time integration; disadvantage: course spatial resolution and complexity	High
Group C	SEBAL	Tier 3/4	Moderate	Advantages: no land cover required, high accuracy; disadvantages: no ET at hot cell, complicated algorithms	High
	METRIC	Tier 3/4	High	Advantages: similar to SEBAL but *ET* constrained by soil water balance; disadvantages: complicated algorithms and calibration, but calibration process has been automated of operational application	High
Group D	STARFM DisALEXI	Tier 4	Moderate	Advantages: no cloud issues; disadvantages: complicated, requires significant in-house algorithm development	High

Table 6. Comparison of total Landsat 5 observations during period of January 2005 through November 2011 for select scenes in Texas.

	Calculated with ACCA algorithm			Visual inspection	Percent of total available observations				
Scene Identifier	All available scenes	50% or less	20% or less	10% or less	Cloud-free	50%	20%	10%	Cloud-free	%10 that are cloud-free
p25r39	143	97	64	43	23	67.8%	44.8%	30.1%	16.1%	53.5%
p26r40	137	108	73	54	24	78.8%	53.3%	39.4%	17.5%	44.4%
p26r42	138	110	71	44	18	79.7%	51.4%	31.9%	13.0%	40.9%
p27r42	140	101	78	62	37	72.1%	55.7%	44.3%	26.4%	59.7%
p28r40	141	103	74	62	37	73.0%	52.5%	44.0%	26.2%	59.7%
p29r37	145	102	85	79	51	70.3%	58.6%	54.5%	35.2%	64.6%
p30r36	145	120	102	92	61	82.8%	70.3%	63.4%	42.1%	66.3%
p31r35	143	117	90	75	57	81.8%	62.9%	52.4%	39.9%	76.0%

Table 7. Percentage of daily precipitation data available from existing monitoring networks in Texas.

Network	N	2005	2006	2007	2008	2009	2010	2011	2012
CRN	8	99.9%	99.8%	99.1%	99.3%	99.8%	99.7%	99.7%	99.5%
HCN	49	86.9%	86.1%	84.1%	87.7%	85.8%	83.5%	79.9%	75.9%
LCRA	241	76.7%	83.7%	90.2%	97.8%	99.5%	100.0%	99.9%	100.0%
SCAN	5	32.2%	93.6%	72.9%	78.1%	86.0%	95.9%	82.2%	79.6%
TETN	41	39.1%	43.1%	49.7%	60.5%	72.1%	71.6%	62.7%	60.1%
WTM	79	0.0%	56.5%	58.3%	59.5%	64.2%	67.8%	69.8%	74.4%

Table 8. State-wide performance of 6 gridded *PPT* products against all weather networks.

	Daymet	NLDAS-12	NLDAS-4	PERSIANN	PRISM	Stage IV
RMSE	0.327	0.352	0.351	0.398	0.383	0.491
STD	0.460	0.453	0.453	0.448	0.450	0.433
Min	0.009	0.026	0.030	0.026	0.029	0.034
Max	6.50	6.47	6.47	6.47	6.48	6.41
POD	0.471	0.643	0.532	0.488	0.438	0.315
STD	0.156	0.160	0.164	0.105	0.118	0.043
Min	0.092	0.148	0.075	0.181	0.074	0.059
Max	0.907	0.955	0.888	0.740	0.938	0.667
PAI	0.650	0.616	0.604	0.560	0.570	0.478
STD	0.101	0.075	0.083	0.043	0.055	0.016
Min	0.439	0.466	0.458	0.447	0.448	0.415
Max	0.947	0.860	0.867	0.686	0.915	0.569

Table 9. Root mean square error (mm d^{-1}) for 6 *PPT* products by climate division and annual precipitation band.

Climate Division	Daymet	NLDAS-12	NLDAS-4	PERSIANN	PRISM	Stage IV
1	0.300	0.383	0.384	0.398	0.405	0.487
2	0.443	0.492	0.492	0.518	0.515	0.600
3	0.308	0.305	0.302	0.367	0.344	0.463
4	0.314	0.360	0.359	0.398	0.373	0.491
5	0.345	0.392	0.389	0.414	0.414	0.505
PPT Band (mm y^{-1})						
200	0.177	0.233	0.234	0.250	0.257	0.348
400	0.437	0.512	0.511	0.528	0.531	0.611
600	0.318	0.315	0.313	0.373	0.352	0.468
800	0.290	0.306	0.304	0.362	0.345	0.460
1000	0.309	0.369	0.368	0.403	0.375	0.492

Table 10. Probability of detection for 6 *PPT* products by climate division and annual precipitation band.

Climate Division	Daymet	NLDAS-12	NLDAS-4	PERSIANN	PRISM	Stage IV
1	0.461	0.517	0.416	0.396	0.335	0.320
2	0.479	0.605	0.503	0.472	0.417	0.305
3	0.472	0.690	0.575	0.524	0.461	0.309
4	0.464	0.604	0.486	0.451	0.451	0.355
5	0.485	0.677	0.573	0.493	0.489	0.280
PPT Band (mm y^{-1})						
200	0.396	0.518	0.432	0.428	0.379	0.298
400	0.475	0.560	0.459	0.429	0.371	0.312
600	0.470	0.683	0.569	0.519	0.455	0.306
800	0.482	0.687	0.571	0.518	0.472	0.315
1000	0.480	0.580	0.463	0.428	0.443	0.362

Table 11. Comparison of ET_r between weather station and collocated NLDAS 4km grid cell.

Station Number	Station Name	Start Date	End Date	Number of Days Analyzed out of 2556 Possible	Average Annual Ratio of Estimated ET_r to Measured ET_r	Standard Deviation of Average Annual Ratio of Estimated ET_r to Measured ET_r	Annual RMSE (mm/yr)	Average Monthly Ratio of Estimated ET_r to Measured ET_r	Standard Deviation of Average Monthly Ratio of Estimated ET_r to Measured ET_r	Monthly RMSE (mm/mo)	Average Weekly Ratio of Estimated ET_r to Measured ET_r	Standard Deviation of Weekly Ratio of Estimated ET_r to Measured ET_r	Weely RMSE (mm/wk)	Average Daily Ratio of Estimated ET_r to Measured ET_r	Standard Deviation of Daily Ratio of Estimated ET_r to Measured ET_r	Daily RMSE (mm/d)	Station Annual Average ET_r (mm/yr)	NLDAS Annual Average ET_r (mm/yr)
1	5ENE Abernathy	1/1/2006	12/31/2012	2545	0.97	0.03	120.31	0.96	0.08	17.5	0.97	0.12	5.7	1.06	0.50	1.58	2770	2676
5	1NE Amherst	1/1/2006	12/31/2012	2545	0.98	0.02	68.72	0.98	0.07	13.3	0.99	0.14	5.2	1.08	0.59	1.51	2753	2699
6	2E Andrews	1/1/2006	12/31/2012	2541	1.05	0.02	160.54	1.05	0.06	18.4	1.06	0.12	5.7	1.14	0.63	1.50	2841	2987
7	6SSW Anton	1/1/2006	12/31/2012	2547	1.01	0.03	64.18	1.01	0.08	16.8	1.02	0.14	5.7	1.11	0.61	1.60	2784	2799
8	3NE Aspermont	1/1/2006	12/31/2012	2546	1.01	0.04	96.55	1.00	0.09	17.9	1.01	0.14	6.1	1.09	0.44	1.63	2633	2654
11	2S Brownfield	1/1/2006	12/31/2012	2547	0.93	0.03	204.98	0.92	0.07	21.2	0.93	0.12	6.5	1.01	0.52	1.64	2907	2716
13	2NNE Childress	1/1/2006	12/31/2012	1951	0.90	0.03	262.01	0.89	0.09	26.2	0.91	0.15	7.9	0.99	0.48	2.05	2851	2557
14	2WSW Clarendon	1/1/2006	12/31/2012	2519	1.04	0.04	121.97	1.03	0.08	17.5	1.05	0.16	6.2	1.15	0.55	1.65	2614	2705
16	2N Coyanosa	1/1/2006	12/31/2012	586	0.91	0.05	131.69	0.93	0.07	17.3	0.94	0.14	4.8	1.01	0.41	2.40	3116	2943
18	2NE Dimmitt	1/1/2006	12/31/2012	2550	0.94	0.02	176.93	0.94	0.07	18.8	0.95	0.13	6.2	1.04	0.55	1.61	2830	2664
20	2NNE Floydada	1/1/2006	12/31/2012	2530	0.95	0.03	161.53	0.94	0.07	18.9	0.95	0.12	6.2	1.05	0.56	1.67	2766	2625
21	3WNW Fluvanna	1/1/2006	12/31/2012	2538	0.99	0.02	71.27	0.98	0.06	14.1	0.99	0.13	5.5	1.08	0.54	1.59	2825	2780
22	2NE Friona	1/1/2006	12/31/2012	2520	0.96	0.03	126.45	0.96	0.07	15.4	0.98	0.14	5.5	1.05	0.47	1.58	2786	2682
23	2 ESE Gail	1/1/2006	12/31/2012	2533	1.11	0.02	286.09	1.10	0.07	28.3	1.12	0.14	7.9	1.21	0.56	1.74	2679	2961
24	3W Goodlett	1/1/2006	12/31/2012	2418	0.96	0.04	137.48	0.95	0.08	18.0	0.97	0.16	6.6	1.06	0.52	1.74	2676	2575
25	5SSW Graham	1/1/2006	12/31/2012	2538	0.94	0.03	204.29	0.93	0.07	22.0	0.95	0.13	7.2	1.04	0.56	1.80	2966	2779
26	10WSW Guthrie	1/1/2006	12/31/2012	2508	0.99	0.04	102.12	0.99	0.09	18.1	1.00	0.15	6.3	1.09	0.53	1.74	2740	2710
27	3N Hart	1/1/2006	12/31/2012	2548	1.04	0.04	142.60	1.03	0.10	22.3	1.05	0.15	6.4	1.14	0.63	1.52	2561	2666
28	1NW Haskell	1/1/2006	12/31/2012	1332	1.02	0.04	73.61	1.01	0.09	12.9	1.02	0.16	4.8	1.10	0.44	1.85	2752	2831
29	2NW Hereford	1/1/2006	12/31/2012	2463	0.98	0.04	114.27	0.97	0.09	16.4	0.98	0.14	5.5	1.04	0.41	1.51	2582	2472
31	1SSE Jayton	1/1/2006	12/31/2012	2545	1.01	0.03	77.38	1.00	0.09	17.7	1.01	0.14	5.9	1.09	0.49	1.55	2581	2615
35	2SE Lamesa	1/1/2006	12/31/2012	2546	1.05	0.04	163.18	1.05	0.08	19.9	1.06	0.14	6.0	1.14	0.55	1.54	2630	2768
36	4S Levelland	1/1/2006	12/31/2012	2529	0.99	0.03	95.14	0.98	0.09	19.3	0.99	0.13	6.1	1.07	0.46	1.60	2835	2795
38	3WNW Lubbock-TTU	1/1/2006	12/31/2012	2386	1.02	0.03	96.89	1.02	0.06	13.1	1.03	0.12	4.9	1.13	0.55	1.49	2688	2759
39	1E McLean	1/1/2006	12/31/2012	2472	1.06	0.05	177.43	1.05	0.10	22.3	1.06	0.17	7.0	1.17	0.62	1.67	2542	2700
40	1NE Memphis	1/1/2006	12/31/2012	2537	1.11	0.04	280.72	1.11	0.09	28.8	1.12	0.16	7.8	1.19	0.46	1.68	2325	2588
42	1ENE Morton	1/1/2006	12/31/2012	2547	0.97	0.02	105.76	0.96	0.08	17.1	0.98	0.13	5.8	1.06	0.54	1.57	2865	2774
43	2SSW Muleshoe	1/1/2006	12/31/2012	2506	0.99	0.04	99.18	0.99	0.10	17.4	1.00	0.17	6.0	1.08	0.52	1.66	2639	2594
44	1S Northfield	1/1/2006	12/31/2012	1646	0.99	0.03	62.75	0.98	0.09	14.4	0.99	0.15	5.3	1.09	0.54	1.85	2716	2705
45	4ENE Odell	1/1/2006	12/31/2012	600	0.94	0.04	85.25	0.95	0.08	12.9	0.96	0.15	4.5	1.06	0.52	2.59	2882	2799
47	6S of Olton	1/1/2006	12/31/2012	2546	0.97	0.02	92.58	0.96	0.07	13.8	0.97	0.12	5.1	1.05	0.48	1.48	2744	2662
48	10SW Paducah	1/1/2006	12/31/2012	2528	0.98	0.03	100.67	0.97	0.08	17.6	0.98	0.15	6.5	1.07	0.52	1.76	2815	2760
50	2E Pampa	1/1/2006	12/31/2012	2538	0.95	0.03	132.19	0.95	0.07	15.1	0.96	0.13	5.5	1.05	0.57	1.48	2552	2435
53	3N Plains	1/1/2006	12/31/2012	2500	0.99	0.03	76.93	0.99	0.07	12.4	1.00	0.14	5.2	1.09	0.62	1.53	2837	2810
54	1S Plainview	1/1/2006	12/31/2012	2547	1.05	0.03	161.69	1.05	0.07	18.0	1.06	0.12	5.4	1.15	0.56	1.44	2536	2674
55	1NE Post	1/1/2006	12/31/2012	2538	1.01	0.03	70.84	0.99	0.08	17.7	1.01	0.14	6.3	1.11	0.55	1.71	2763	2777
57	1SE Ralls	1/1/2006	12/31/2012	2548	1.00	0.03	74.65	1.00	0.08	15.2	1.02	0.14	5.6	1.11	0.61	1.56	2717	2720
58	12W Lubbock (Reese)	1/1/2006	12/31/2012	2548	0.97	0.03	134.20	0.97	0.07	17.3	0.98	0.13	5.9	1.07	0.58	1.63	2864	2772
61	1SW Seagraves	1/1/2006	12/31/2012	2384	1.07	0.05	162.39	1.07	0.15	22.0	1.08	0.20	6.5	1.16	0.63	1.69	2687	2815
62	2NNE Seminole	1/1/2006	12/31/2012	2501	1.00	0.02	51.69	0.99	0.07	12.8	1.00	0.11	4.8	1.07	0.51	1.41	2789	2804
63	3NW Seymour	1/1/2006	12/31/2012	1148	1.03	0.07	112.87	1.06	0.10	14.7	1.08	0.16	5.0	1.17	0.50	2.00	2703	2868
64	7ESE Silverton	1/1/2006	12/31/2012	2535	0.92	0.04	247.87	0.92	0.08	26.1	0.94	0.15	8.0	1.06	0.68	1.93	2735	2511
65	2NE Slaton	1/1/2006	12/31/2012	2546	0.97	0.03	107.63	0.97	0.07	16.8	0.99	0.14	6.2	1.09	0.57	1.73	2815	2740
66	3E Snyder	1/1/2006	12/31/2012	2540	0.91	0.04	270.59	0.91	0.06	25.8	0.92	0.12	7.6	0.99	0.46	1.79	2892	2640
67	1W Spur	1/1/2006	12/31/2012	2543	1.12	0.04	297.00	1.11	0.10	31.7	1.11	0.15	8.4	1.19	0.47	1.77	2432	2713
70	8WSW Sundown	1/1/2006	12/31/2012	2541	0.97	0.03	106.22	0.96	0.08	16.5	0.97	0.13	5.7	1.06	0.59	1.55	2885	2808
71	3NNE Tahoka	1/1/2006	12/31/2012	2544	0.94	0.03	191.02	0.93	0.07	21.5	0.95	0.13	6.8	1.04	0.55	1.73	2849	2674
73	2ENE Tulia	1/1/2006	12/31/2012	2547	0.98	0.04	116.15	0.97	0.08	17.3	0.99	0.14	6.1	1.10	0.63	1.65	2722	2652
74	2WSW Turkey	1/1/2006	12/31/2012	2217	0.89	0.05	271.03	0.89	0.09	28.3	0.91	0.16	8.6	1.00	0.50	2.10	2835	2568
76	1E Wall	1/1/2006	12/31/2012	1144	1.00	0.08	92.38	1.03	0.09	14.0	1.05	0.19	5.1	1.13	0.46	1.91	2895	2977
79	6SSW Wolfforth	1/1/2006	12/31/2012	2542	0.94	0.03	201.59	0.93	0.08	23.6	0.95	0.13	7.1	1.03	0.51	1.74	2870	2685
80	SCAN_BUSHLAND	1/1/2006	12/31/2012	1438	0.80	0.10	498.67	0.87	0.41	61.0	0.93	0.69	17.6	1.14	1.59	4.57	3133	2616
81	SCAN_PRAIRIE_VIEW	1/1/2006	12/31/2012	2374	1.00	0.20	397.17	1.01	0.30	52.0	1.04	0.40	14.4	1.18	0.93	2.79	2267	2241
			Average	2320	0.99	0.04	152	0.98	0.09	20.1	1.00	0.16	6.5	1.09	0.56	1.77	2745	2708

Table 12. Comparison of ET_r between weather station and collocated NLDAS 12km grid cell.

Station Number	Station Name	Start Date	End Date	Number of Days Analyzed out of 2556 Possible	Average Annual Ratio of Estimated ET_r to Measured ET_r	Standard Deviation of Average Annual Ratio of Estimated ET_r to Measured ET_r	Annual RMSE (mm/yr)	Average Monthly Ratio of Estimated ET_r to Measured ET_r	Standard Deviation of Average Monthly Ratio of Estimated ET_r to Measured ET_r	Monthly RMSE (mm/mo)	Average Weekly Ratio of Estimated ET_r to Measured ET_r	Standard Deviation of Weekly Ratio of Estimated ET_r to Measured ET_r	Weely RMSE (mm/wk)	Average Daily Ratio of Estimated ET_r to Measured ET_r	Standard Deviation of Daily Ratio of Estimated ET_r to Measured ET_r	Daily RMSE (mm/d)	Station Annual Average ET_r (mm/yr)	NLDAS Annual Average ET_r (mm/yr)
1	5ENE Abernathy	1/1/2006	12/31/2012	2550	1.00	0.04	89	0.99	0.12	24.8	1.00	0.15	6.9	1.08	0.46	1.55	2772	2779
5	1NE Amherst	1/1/2006	12/31/2012	2550	1.02	0.04	116	1.01	0.11	23.6	1.02	0.16	6.6	1.10	0.52	1.51	2754	2803
6	2E Andrews	1/1/2006	12/31/2012	2545	1.05	0.04	165	1.04	0.10	25.0	1.05	0.13	6.8	1.12	0.56	1.48	2843	2974
7	6SSW Anton	1/1/2006	12/31/2012	2552	1.06	0.04	186	1.05	0.12	29.5	1.06	0.17	7.8	1.15	0.56	1.65	2786	2940
8	3NE Aspermont	1/1/2006	12/31/2012	2550	1.07	0.05	207	1.05	0.13	31.3	1.07	0.18	8.2	1.14	0.47	1.67	2636	2812
11	2S Brownfield	1/1/2006	12/31/2012	2552	0.97	0.03	121	0.95	0.10	22.3	0.96	0.14	6.6	1.03	0.47	1.56	2910	2814
13	2NNE Childress	1/1/2006	12/31/2012	1954	0.94	0.04	182	0.92	0.14	27.5	0.94	0.19	7.7	1.01	0.47	1.85	2854	2683
14	2WSW Clarendon	1/1/2006	12/31/2012	2523	1.05	0.05	173	1.04	0.12	26.8	1.05	0.18	7.4	1.13	0.52	1.61	2616	2747
16	2N Coyanosa	1/1/2006	12/31/2012	586	0.93	0.03	97	0.95	0.07	13.8	0.96	0.13	3.7	1.01	0.37	1.92	3116	2965
18	2NE Dimmitt	1/1/2006	12/31/2012	2555	0.98	0.03	100	0.97	0.10	19.5	0.98	0.14	6.1	1.06	0.47	1.50	2832	2787
20	2NNE Floydada	1/1/2006	12/31/2012	2534	1.00	0.04	111	0.98	0.10	22.8	0.99	0.15	6.6	1.08	0.54	1.57	2768	2754
21	3WNW Fluvanna	1/1/2006	12/31/2012	2543	1.03	0.04	133	1.02	0.10	24.3	1.03	0.15	6.8	1.11	0.55	1.54	2828	2906
22	2NE Friona	1/1/2006	12/31/2012	2525	1.02	0.04	120	1.01	0.10	21.3	1.02	0.14	6.1	1.09	0.43	1.50	2788	2833
23	2 ESE Gail	1/1/2006	12/31/2012	2538	1.12	0.04	336	1.11	0.11	37.0	1.12	0.16	9.3	1.20	0.54	1.77	2682	3004
24	3W Goodlett	1/1/2006	12/31/2012	2422	1.01	0.05	111	1.00	0.12	24.7	1.02	0.20	7.2	1.10	0.59	1.64	2680	2745
25	5SSW Graham	1/1/2006	12/31/2012	2543	0.97	0.03	144	0.96	0.10	24.3	0.97	0.16	7.5	1.06	0.56	1.71	2969	2865
26	10WSW Guthrie	1/1/2006	12/31/2012	2511	1.05	0.06	191	1.05	0.12	28.3	1.06	0.17	7.8	1.15	0.57	1.70	2741	2879
27	3N Hart	1/1/2006	12/31/2012	2553	1.10	0.05	291	1.09	0.14	39.7	1.10	0.18	9.8	1.19	0.58	1.78	2562	2827
28	1NW Haskell	1/1/2006	12/31/2012	1334	1.10	0.07	179	1.07	0.11	24.0	1.09	0.18	6.4	1.16	0.45	1.75	2754	2930
29	2NW Hereford	1/1/2006	12/31/2012	2467	1.03	0.04	131	1.02	0.11	22.9	1.03	0.14	6.4	1.10	0.43	1.49	2586	2660
31	1SSE Jayton	1/1/2006	12/31/2012	2549	1.09	0.04	254	1.08	0.13	34.0	1.09	0.18	8.8	1.17	0.53	1.70	2584	2824
35	2SE Lamesa	1/1/2006	12/31/2012	2551	1.11	0.04	287	1.10	0.10	32.4	1.12	0.16	8.2	1.20	0.55	1.62	2632	2906
36	4S Levelland	1/1/2006	12/31/2012	2534	1.01	0.04	99	1.00	0.13	28.4	1.01	0.16	7.6	1.08	0.42	1.63	2837	2870
38	3WNW Lubbock-TTU	1/1/2006	12/31/2012	2391	1.05	0.03	165	1.05	0.09	22.9	1.06	0.14	6.4	1.14	0.50	1.46	2690	2849
39	1E McLean	1/1/2006	12/31/2012	2476	1.09	0.04	227	1.06	0.14	33.2	1.08	0.19	8.8	1.17	0.60	1.74	2545	2744
40	1NE Memphis	1/1/2006	12/31/2012	2541	1.16	0.06	382	1.14	0.13	41.2	1.16	0.19	10.2	1.23	0.52	1.87	2327	2690
42	1ENE Morton	1/1/2006	12/31/2012	2552	1.00	0.03	67	0.99	0.11	23.3	1.00	0.15	6.6	1.07	0.49	1.54	2867	2864
43	2SSW Muleshoe	1/1/2006	12/31/2012	2511	1.02	0.04	118	1.01	0.12	23.2	1.03	0.17	6.7	1.10	0.50	1.60	2641	2695
44	1S Northfield	1/1/2006	12/31/2012	1648	1.02	0.04	89	1.00	0.14	24.1	1.02	0.19	6.6	1.11	0.54	1.79	2718	2793
45	4ENE Odell	1/1/2006	12/31/2012	600	0.95	0.01	65	0.95	0.06	9.2	0.95	0.11	3.2	1.01	0.33	1.64	2882	2779
47	6S of Olton	1/1/2006	12/31/2012	2551	1.03	0.04	120	1.01	0.11	25.3	1.02	0.15	6.9	1.09	0.47	1.51	2746	2815
48	10SW Paducah	1/1/2006	12/31/2012	2532	1.03	0.04	130	1.01	0.12	25.8	1.03	0.18	7.6	1.12	0.56	1.71	2817	2885
50	2E Pampa	1/1/2006	12/31/2012	2542	0.99	0.03	83	0.97	0.10	18.8	0.98	0.15	5.8	1.06	0.52	1.39	2554	2523
53	3N Plains	1/1/2006	12/31/2012	2503	1.03	0.03	108	1.01	0.10	21.3	1.03	0.15	6.4	1.11	0.52	1.52	2838	2908
54	1S Plainview	1/1/2006	12/31/2012	2552	1.11	0.05	294	1.09	0.10	32.7	1.10	0.14	8.2	1.19	0.53	1.57	2538	2807
55	1NE Post	1/1/2006	12/31/2012	2543	1.05	0.04	165	1.03	0.12	29.4	1.05	0.17	8.0	1.14	0.55	1.73	2765	2894
57	1SE Ralls	1/1/2006	12/31/2012	2553	1.04	0.04	134	1.03	0.10	23.7	1.04	0.16	6.7	1.13	0.55	1.52	2719	2814
58	12W Lubbock (Reese)	1/1/2006	12/31/2012	2553	1.00	0.05	128	0.99	0.10	23.0	1.01	0.15	6.7	1.09	0.53	1.57	2866	2861
61	1SW Seagraves	1/1/2006	12/31/2012	2388	1.10	0.05	249	1.11	0.16	31.1	1.11	0.22	8.1	1.19	0.60	1.74	2688	2919
62	2NNE Seminole	1/1/2006	12/31/2012	2505	1.05	0.03	150	1.04	0.09	22.4	1.05	0.14	6.3	1.12	0.52	1.44	2791	2925
63	3NW Seymour	1/1/2006	12/31/2012	1150	1.09	0.04	179	1.09	0.09	20.0	1.11	0.14	5.4	1.17	0.38	1.60	2705	2977
64	7ESE Silverton	1/1/2006	12/31/2012	2539	0.95	0.05	185	0.94	0.12	27.3	0.95	0.17	8.0	1.06	0.61	1.82	2737	2602
65	2NE Slaton	1/1/2006	12/31/2012	2551	1.02	0.04	97	1.00	0.11	23.0	1.02	0.16	6.9	1.11	0.54	1.65	2817	2856
66	3E Snyder	1/1/2006	12/31/2012	2545	0.97	0.04	131	0.96	0.09	20.5	0.97	0.14	6.5	1.04	0.47	1.54	2895	2808
67	1W Spur	1/1/2006	12/31/2012	2547	1.17	0.05	428	1.16	0.13	45.7	1.17	0.18	11.2	1.24	0.51	1.98	2435	2848
70	8WSW Sundown	1/1/2006	12/31/2012	2546	1.01	0.03	77	1.00	0.11	24.3	1.01	0.15	6.9	1.09	0.51	1.56	2887	2924
71	3NNE Tahoka	1/1/2006	12/31/2012	2549	0.96	0.04	140	0.95	0.11	25.3	0.97	0.16	7.3	1.05	0.53	1.68	2852	2749
73	2ENE Tulia	1/1/2006	12/31/2012	2551	1.01	0.05	126	0.99	0.12	24.8	1.01	0.16	7.2	1.11	0.58	1.64	2723	2748
74	2WSW Turkey	1/1/2006	12/31/2012	2221	0.89	0.07	262	0.89	0.13	32.1	0.90	0.19	9.2	0.98	0.47	2.05	2837	2554
76	1E Wall	1/1/2006	12/31/2012	1146	1.07	0.05	152	1.08	0.08	17.4	1.10	0.15	4.9	1.15	0.38	1.55	2897	3101
79	6SSW Wolfforth	1/1/2006	12/31/2012	2547	0.97	0.03	136	0.96	0.11	26.5	0.97	0.16	7.5	1.04	0.47	1.67	2872	2772
80	SCAN_BUSHLAND	1/1/2006	12/31/2012	1439	0.86	0.12	414	0.92	0.41	53.6	0.97	0.68	16.3	1.20	1.59	4.41	3133	2784
81	SCAN_PRAIRIE_VIEW	1/1/2006	12/31/2012	2375	0.98	0.22	444	0.98	0.33	58.0	1.00	0.42	15.5	1.13	0.90	2.96	2267	2200
			Average	2324	1.03	0.05	175	1.02	0.12	27.1	1.03	0.18	7.5	1.11	0.54	1.72	2747	2811

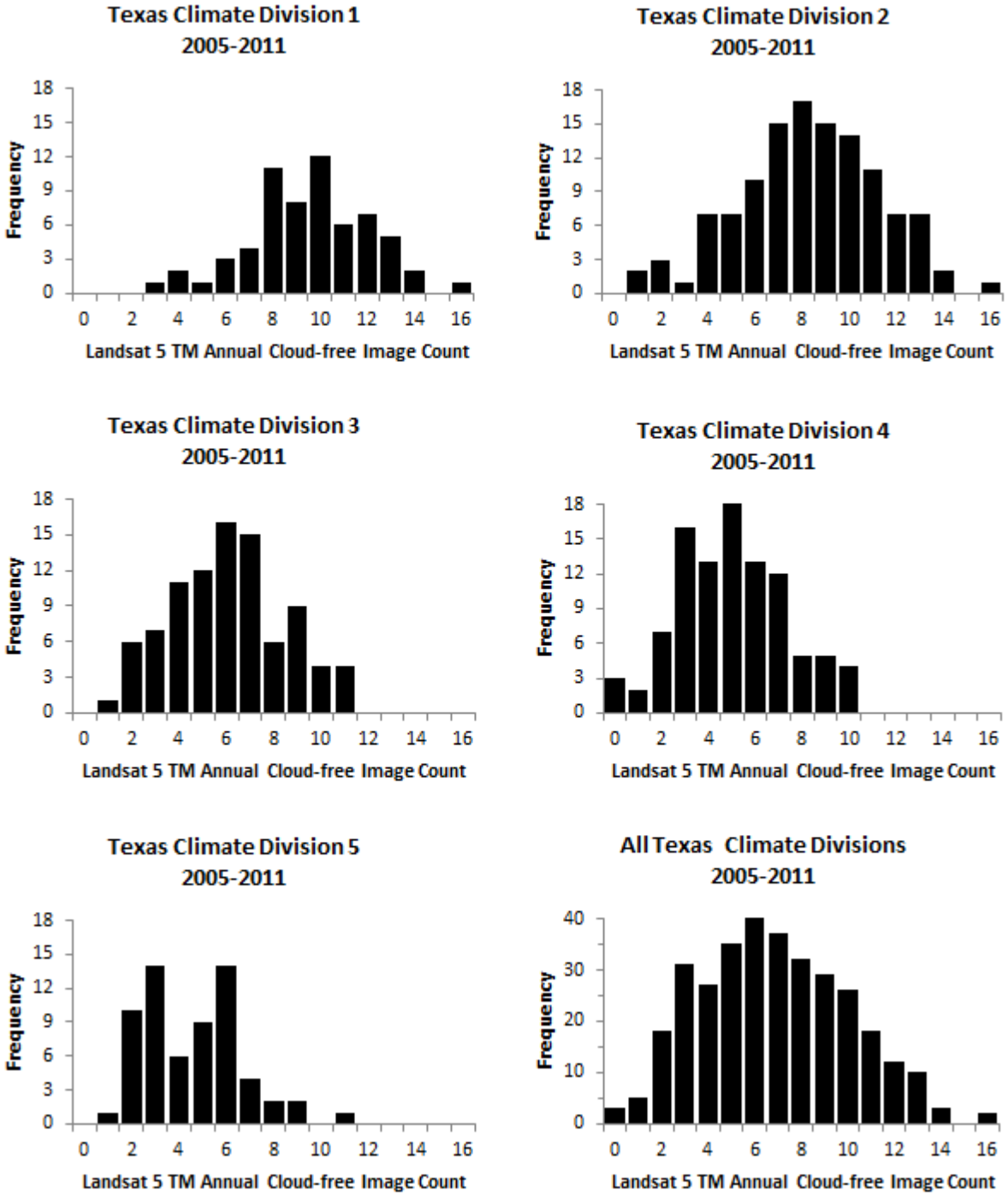

Figure 7. Frequency of cloud-free scenes per year within climate division of the High Plains (1), Edwards Plateau and Rolling Plains (2), North Texas (3), East Texas (4), the Rio Grande and southern Coastal Plain (5), and state-wide.

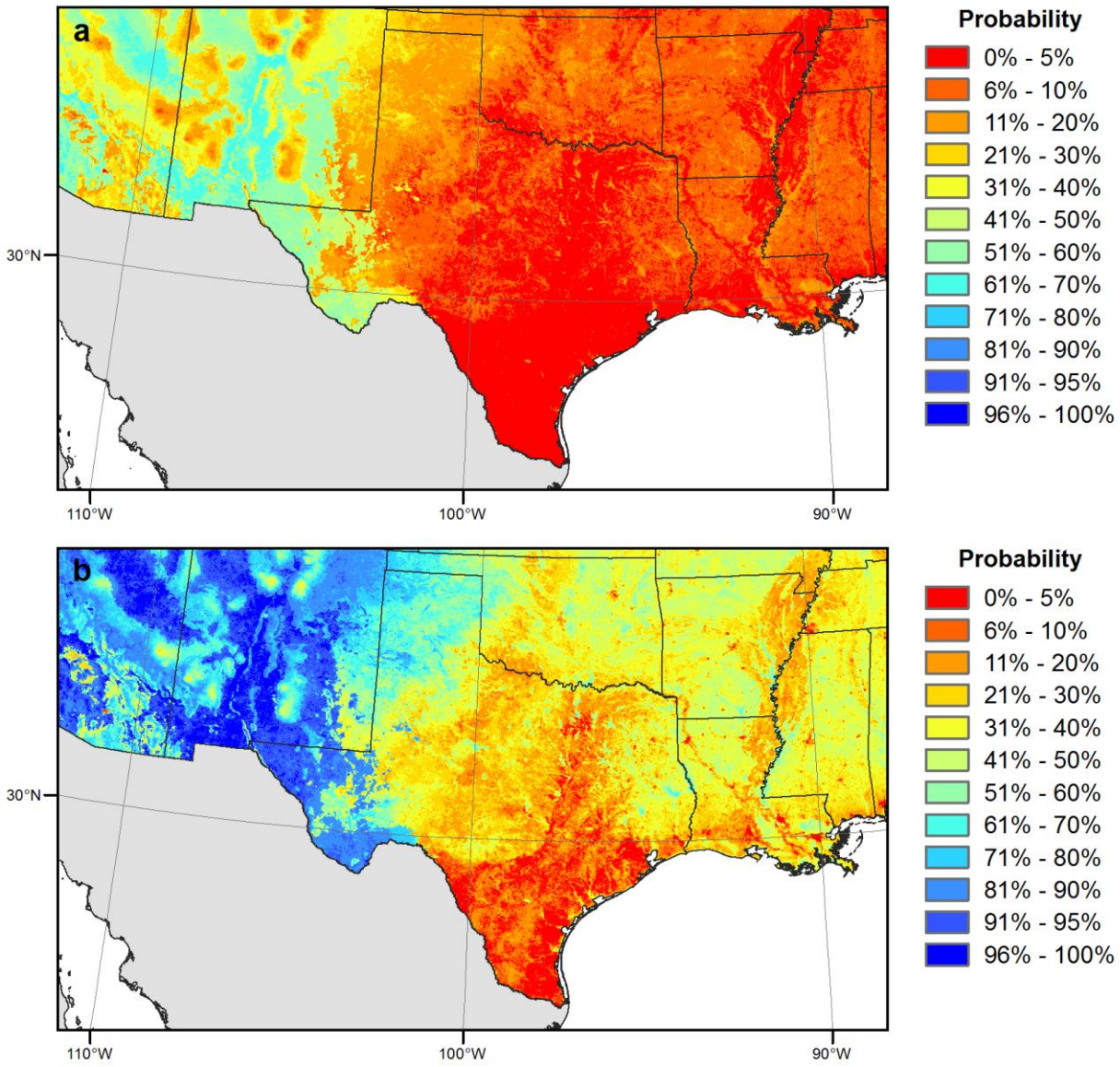

Figure 8. Probability of successful *ET* across Texas for a complete growing season for any particular year based on the requirement of at least one cloud free image every 32 days using (a) 1 satellite with a 16 day return cycle, (b) 2 satellites with an 8 day return cycle, for a fixed growing season from April 1st - October 31st.

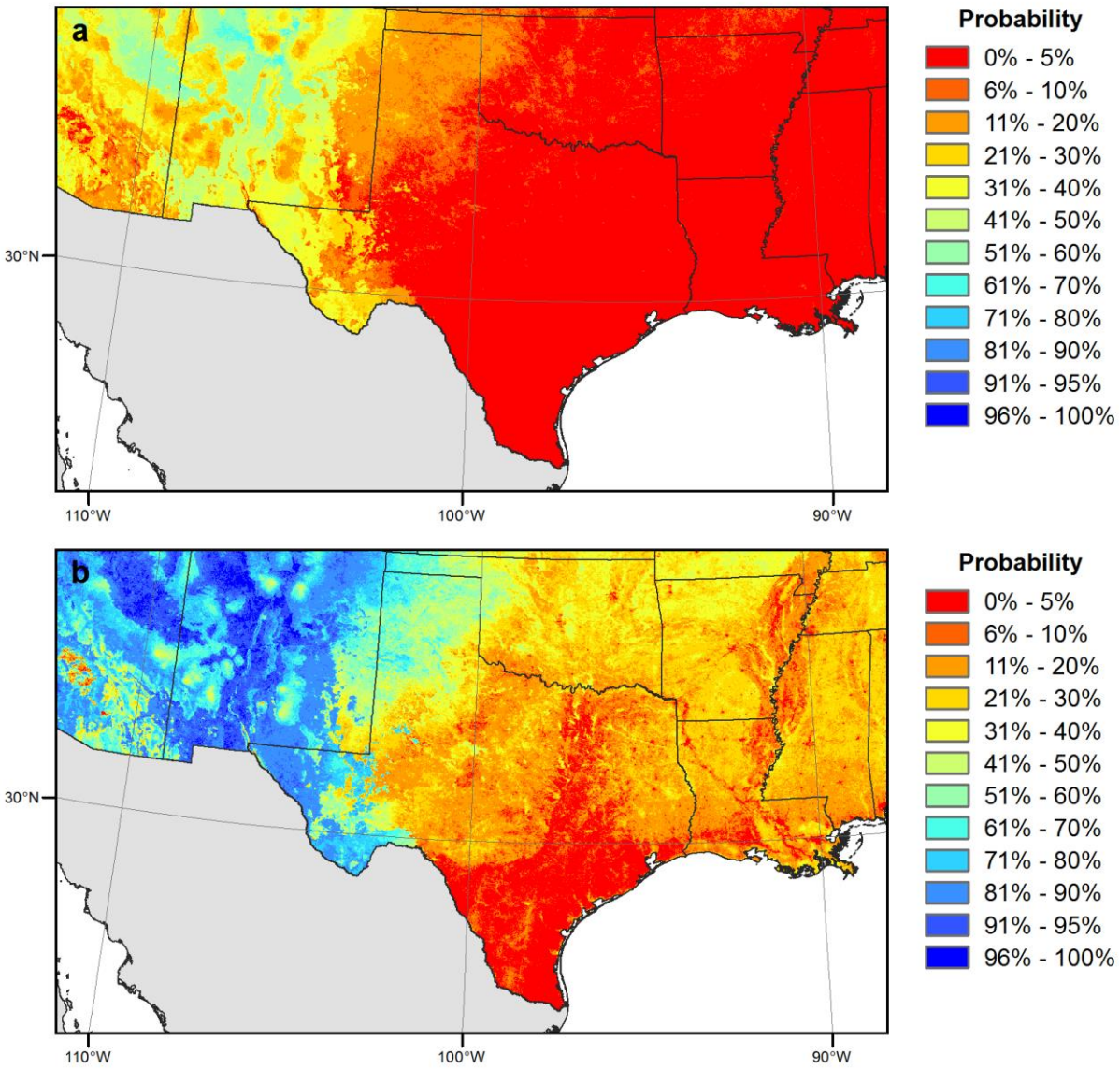

Figure 9. Probability of successful *ET* across Texas for a complete growing season based on the requirement of at least based one cloud free image every 32 days using (a) 1 satellite with a 16 day return cycle, (b) 2 satellites with an 8 day return cycle, for a variable growing season.

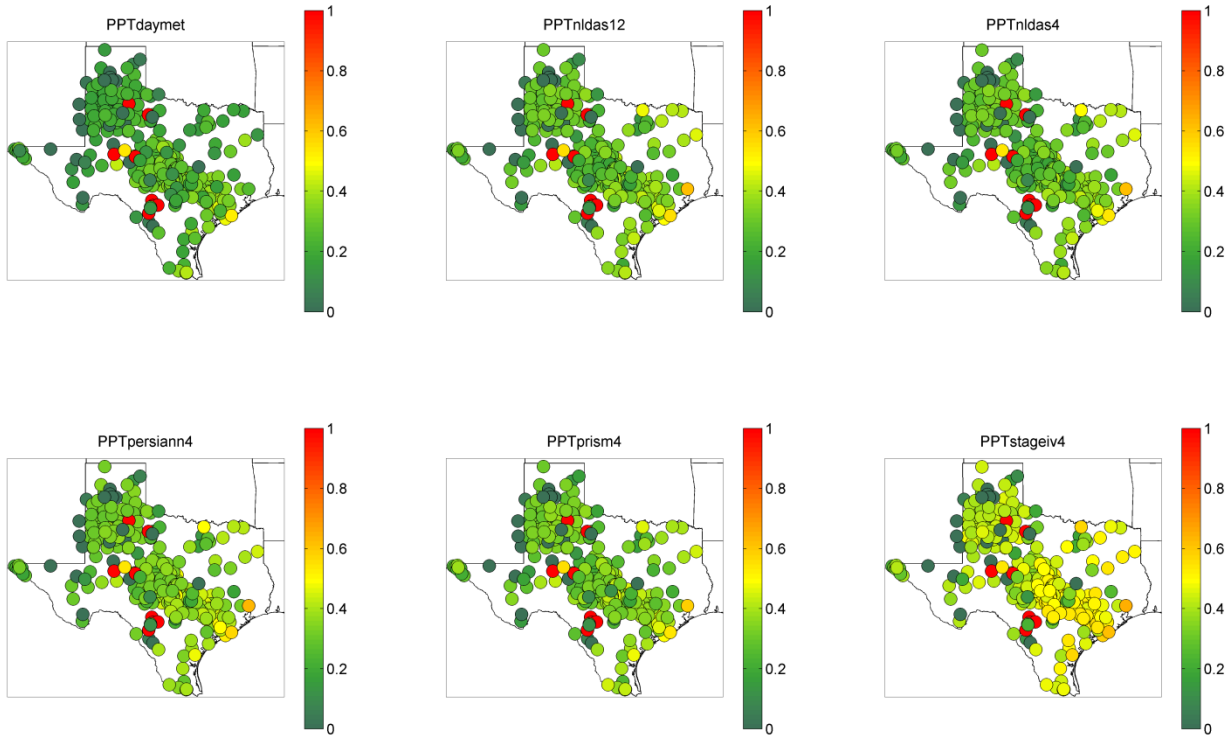

Figure 10. State-wide root mean square error (*RMSE*, mm d^{-1}) for each of 6 *PPT* products.

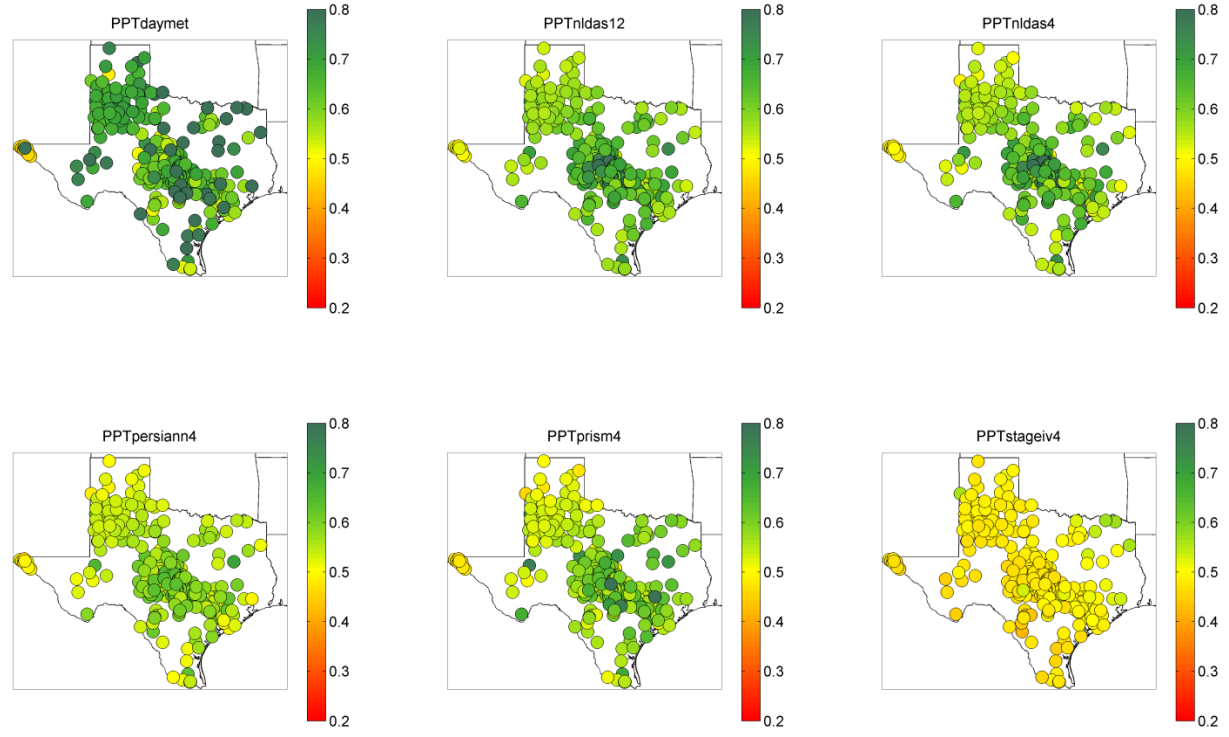

Figure 11. State-wide precipitation accuracy index (*PAI*) for each of 6 *PPT* products.

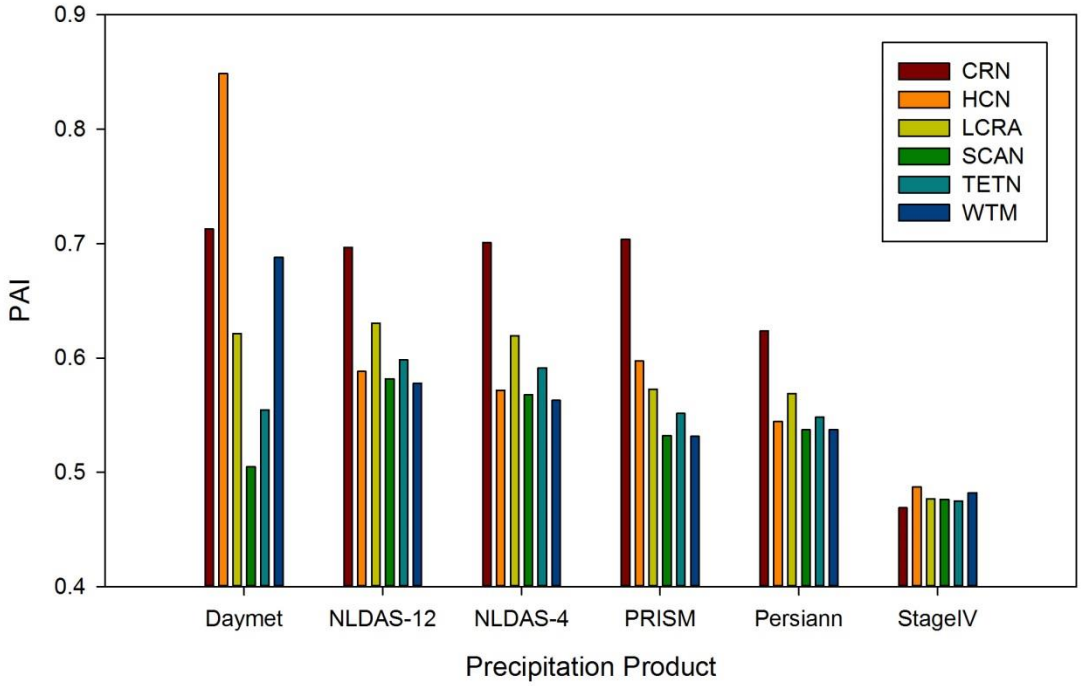

Figure 12. Precipitation accuracy index (*PAI*) by monitoring network for all 6 *PPT* products.

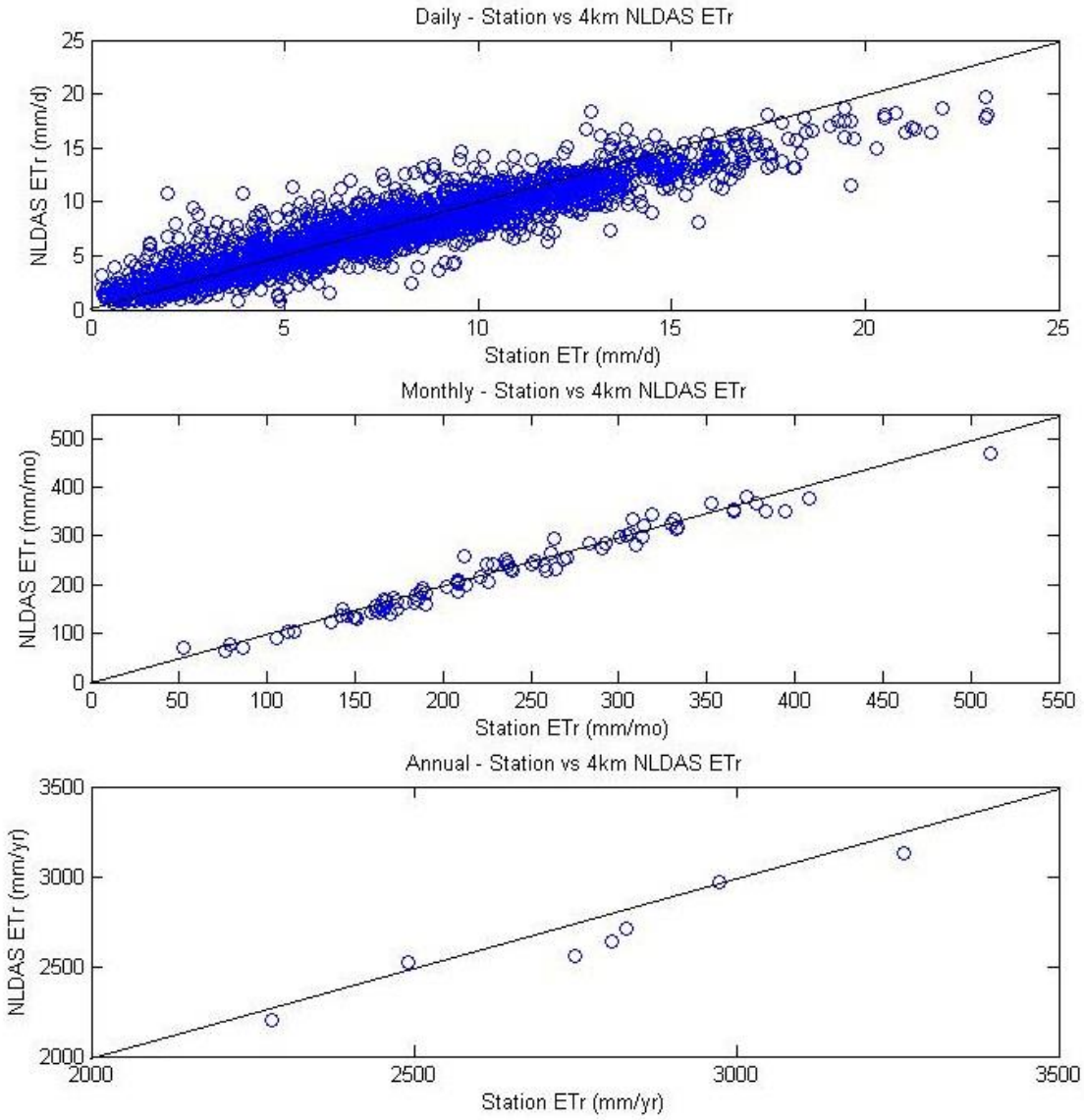

Figure 13. Daily, monthly, and annual ET_r between a 'good' Abernathy monitoring stations and collocated 4km NLDAS forcing data (2006-2012).

6 Feasibility Pilot Study: county ET implementation

A State-wide program requires that irrigation water use be accumulated annually, per county for all the major agriculture regions of Texas which range from humid, cloudy regions of the Coastal Plains to arid west Texas. The feasibility of using remotely sensed *ET* data has some advantages over current IWUE but requires significant data processing, interpretation and overall logistics to implement. To evaluate these logistics of operationalizing such a program for Texas, we designed a pilot study loosely based on the Nevada State Engineer, Division of Water Resources Program developed by DRI co-Investigators. Following our TWDB workshop and discussions with TWDB staff, we chose eight counties (Figure 14) covering a range of agricultural and climatological challenges across Texas. These counties include four in the High Plains (Carson, Dawson, Hale, and Ochiltree) predominantly growing cotton and winter wheat; two counties in the Coastal Plain (Brazos and Wharton) growing corn, cotton and rice; Cameron County in the lower Rio Grande Valley growing cotton and sorghum; and Medina County in the Winter Garden region growing a full mix of crops. For simplicity, these counties are along similar Landsat paths and generally within a single Landsat scene. For each county, we derive an annual METRIC-based *ET* and NIWR estimated for 2010 and 2011 growing seasons with NLDAS-derived ET_r, and *PPT.* Our pilot study years cover two climatically different yet adjacent years; one wet and one dry.

We developed and tested a time integration workflow that relied on ET_rF derived from Landsat into net *ET* totals summarized in section 6.1. Section 6.2 employs the *ET* Demands model to determine the upper limit of potential *NIWR*. The model has heritage traced to FAO-56 ET_c and dual crop coefficient approach, with the source code is also readily available at DRI (Huntington et al., 2015; Huntington and Allen, 2015). Lastly, Section 6.3 presents Irrigation Water Use Estimates (IWUE) from TWDB for these counties and the TWDB Metering Data for specific crops during both years. We provide direct comparisons between our remote sensing, survey and metered data estimates of annual irrigation water use (i.e. *NIWR*).

6.1 Results: actual ET from Remote Sensing for 2010 and 2011

Our preliminary feasibility study results outlined in Section 5 were used to direct this pilot study, implementing a remotely-based irrigation water use estimate in eight counties using both the actual (METRIC) and potential (ET Demands) irrigation water use for two climatically diverse years. Locations were further selected to minimize the total number of scenes required to produce county-wide estimates. A satellite image is instantaneous in time. As a satellite descends along its path, the on-ground times are very similar between adjacent scenes. However, the satellite must complete an entire earth orbit before beginning the next path. Thus, counties contained within the same path (i.e. column) can be processed at essentially the same time step; while a county covering two or more paths (i.e. rows) requires processing steps to sync timing and merge images. This effort is factored into our estimate for state-wide implementation but is beyond the current scope of this pilot study. In-house experience with METRIC at DRI, its broad application among practitioners and researchers along with the adoption by state and federal courts, and the availability of automated software makes METRIC an obvious choice for a Level 3 accuracy *ET* product potentially feasible for Texas.

METRIC was implemented using the processing outlined by *Morton et al.* [2013] and illustrated in Figure 15. Clouds were automatically screened using the F-MASK algorithm [*Zhu and Woodcock*, 2012]. METRIC

was calibrated using a Monte-Carlo approach of 10 different runs in an automated framework and the selection of the hot and cold pixel was varied based on best candidate pixels. The median was computed to produce the ET_rF map for each Landsat scene.

All cropland and *ET* results from our pilot study are presented in Appendix D through H. Pixels within each county were extracted from all available Landsat (5/7) imagery, then masked to exclude non-agricultural areas based on the CDL (see Appendix D). Cloud free pixels were used to derive ET_rF maps of croplands in each scene with the annual means are presented in Appendix E. These maps were scaled to time synchronous ET_r derived from NLDAS and integrated daily and summed to annual *ET* maps (Appendix F). Lastly, the derived annual *ET* estimates, per-pixel cloud free scene counts were computed for each county study area are illustrated in Appendix G.

METRIC *ET* results (Appendix H) illustrate the large variability within each county, between crop types, and amongst years. For example, cotton in Brazos County consumed 39.6 inches of actual *ET* in 2010 and 57.7 inches in 2011. In Dawson County, cotton *ET* consumed 33.8 inches in 2010 and 47.8 inches in 2011. *Borrelli et al.* [1998] presented mean crop consumptive use values for cotton of 26.9 inches the Upper Coast and 36.2 inches in the High Plains. Our values are similar for 2010 which was closer to an average year; however, 2011 was far from average resulting is much higher ET_r resulting from the aridity brought on by drought conditions. This further highlights the need to produce annual data as means are seldom the case.

The annual per county totals are presented in Figure 16 including annual *ET* from METRIC, precipitation from NLDAS, ET_r calculated from NLDAS, and *NIWR*. METRIC *ET* ranged from 40 inches in Hale to nearly 70 inches in Wharton in 2010 and was similar to 2011, except for Brazos County. On the other hand, PPT was much lower in 2011 with only fractions of rainfall in all counties. Drought results in anonymously high ET_r due to increased solar radiation, higher T_a, and lower humidity. In 2010, ET_r ranged between 80 and 100 inches while increasing in 2011 to nearly 120 inches. We derive *NIWR* by subtracting *ET* from precipitation. For 2010, most counties consumed 20 inches with Ochiltree and Wharton higher. By 2011, *NIWR* doubled to nearly 40 inches across all counties. Regardless of drought, 40 inches is a lot of irrigation and perhaps an artifact of NLDAS ET_r, used for time integration between satellite images. Furthermore, when scaled by CDL acreage, the volumes of applied irrigation can quickly exceed 1 maf. Thus, the NIWR is very sensitive to both ET_r and CDL acreage as our results will demonstrate.

Next, we evaluate the per-pixel cloud free Landsat scene counts for each county study area (Appendix G) was used. As previously mentioned, at least one cloud-free scene is required per month to adequately perform time integration of ET_rF. For both years, pilot study counties in the High Plains (Carson, Hale and Ochiltree) and Winter Garden (Medina) satisfy this criteria with ~10 – 24 cloud free scenes per year. Coastal and southern counties (Brazos, Cameron and Wharton) generally do not in 2010 while 2011 produced better results for Brazos County. Given more time and resources, a fusion-based (Group D) algorithm such as STARFM would be preferred but was infeasible without additional software development. For actual implementation, a satellite fusion method should be considered for areas with higher probabilities of cloud cover.

6.2 Results: ET Demands Model

The complete results by county and year are presented in Appendix I. The ET Demand *NIWR* can be considered the upper boundary since the model essentially maintains an equilibrium between root zone soil moisture and atmospheric demand for water through irrigation. Figure 17 compares the annual METRIC net *ET* to the ET-Demands derived *NIWR* across all crops and acreage for both 2010 and 2011. For both years and nearly all counties, METRIC net *ET* from was correlated with ET Demands *NIWR* and consistently greater than METRIC. This is to be expected since ET Demands assumes well-watered, optimal conditions while the reality has more stress and deficit irrigation that Landsat can measure. Interestingly, 2011 has a slope of 1.11 implying that net ET was ~90% of maximum. However, 2010 has a much greater slope (2.15) using less than 50% of the maximum potential *NIWR.* These results indicate the ET Demands model would provide a suitable upper bounds for maximum potential irrigation water while METRIC would provide a more conservative (and likely realistic) actual irrigation water use estimate. For water planning, the ET Demands might suffice and it requires significantly less time and technical expertise, but only reflects optimal conditions, and not the actual *ET* that occurs due to water limitations and crop stress, nor can it account for crop failure.

6.3 Irrigation Water Use Estimates and Metering Data

For further comparison, we extracted the Irrigation Water Use Estimates (IWUE) for 2010 and 2011 for each of our eight selected counties (http://www.twdb.texas.gov/waterplanning/waterusesurvey/estimates/index.asp). The annual irrigation totals are presented in Table 13 and Figure 18. Generally, 2011 used nearly twice the irrigation (1.8 maf) as 2010 (0.9 maf) over these counties. Brazos County had the lowest increase (19%) in 2011 while Cameron, Dawson, and Medina all increased over 100%. Counties were predominantly irrigated from groundwater in the north, and surface water in the south. Cameron, in particular, is solely on surface water irrigation while Wharton has a more even split. The goal of a state-wide remotely sensed *ET* program would be to reproduce IWUE using an *ET* algorithm which relies solely on satellite and meteorological data.

The irrigation metering program in Texas differs from most states' in that participation is voluntary [*Turner et al.*, 2011]. Beginning in 1998, the metering program has evolved to cover 16 groundwater conservation districts (Figure 19). The High Plains are represented by the Panhandle, North Plains, Mesa, Hudspeth and Culberson GCDs – all of which began metering prior to 2005. The Winter Gardens area is represented by Uvalde, Medina and Evergreen (also pre-2005) while the Coastal Plains have active metering in the Lower Neches Valley and Coastal Bend (pre-2005). Metering data obtained from TWDB was pulled from files and reports, and summarized in Table 14. In general, the area weighted cumulative metering data is 50% less than our estimations from METRIC (Figure 20). Direct comparison is difficult: the acreage of metering is small, many of the meters do not contain comparable CDL crops, or the crop is mixed. In particular, alfalfa *NIWR* is much lower at all metering sites (4-41 inches) compared to 34-100 inches from METRIC. Clearly, there is a need for both expansion and standardization of the metering program would benefit water conservation State-wide and validation for crop-specific *ET* estimates from satellite data.

multi-cropping in Medina

6.4 Pilot study results: a county-by-county summary

At the county level, both METRIC and the ET Demands model are producing greater net *ET* and *NIWR* volumes than either the IWUE or metering program data (Figure 21, Table 15). We note that the CDL classified a large amount of acreage with substantial *ET* exceeding *PPT* as Fallow/Idle Crops (Number 61). Data from the FSA (link) compares favorably with the CDL (Table 15) in 2011. The FSA reports total planted acres as 1,780 million compared to 1,766 million (excluding fallow) in the CDL over our eight counties. Conversely in 2010, FSA reports 3,213 million acres verse the CDL total of 1,741 million acres. Unfortunately, the FSA cannot provide spatial reference for their acreage nor can we differentiate irrigated parcels so direct comparisons are not possible between these numbers and our METRIC analysis which uses CDL crop mask to total *NIWR* per county. We do present METRIC results with and without (METRIC*) fallow crops *ET* contribution (Table 15) since it is unclear why there is discrepancy between CDL and FSA data. Regardless, the IWUE were considerably lower than METRIC. In particular for 2011, both METRIC and METRIC* were 300% higher than IWUE. In general, only a few counties were comparable and only in 2010. For example, Wharton had nearly 1,000,000 acres of fallow land in both years resulting in an extremely large METRIC *NIWR*. Since the crop ET values seem reasonable, it must be the scaling to irrigated acreage that causes the NIWR to escalate. Such issues are unavoidable and difficult to reconcile without maps of irrigated lands. Such areas may be abandoned or simply classification errors. For now, we simply present our results with and without (*) CDL fallow idle crop land and provide a complete summary of each county briefly here including annual cropping patterns (see Appendix J).

Brazos County was the lowest irrigator using <45,000 ac-ft in either year, switching from a mix of water sources to solely groundwater in 2011 (Table 13). Total cropped acreage was 24,663 in 2010 increasing to 70,361 acres in 2011 (Appendix H). Of the pilot counties, Brazos also had the lowest agricultural footprint with crops concentrated along its western border (Appendix D). In both years, cotton and corn were the dominant crops (Append J). Brazos County is in the >1000 mm precipitation class and climate zone 4. Our pilot study notes the following:

- Sufficient cloud-free images were available for 2011; very limited for 2010
- METRIC estimates of corn *ET*: 37.2 in (2010) and 61.0 in (2011)
- METRIC estimates cotton *ET*: 39.6 in (2010) and 57.7 in (2011)
- Pecan *ET* was anomalously high: 72.8 in (2010) and 70.2 in (2011) but acreage was very low: 31 ac (2010) and <1 ac (2011)
- *MAP* was 29.5in (2010) and 20.3in (2011)
- All methods produced similar irrigation estimates ranging from 18,000-35,500 ac-ft in 2010 to 42,000-118,000 ac-ft in 2011
- Irrigation doubled from 2010 to 2011

Despite the lack of cloud-free pixel in 2010, METRIC and ET Demands both produced values comparable to TWDB's IWUE.

Cameron County relies solely on surface water from the Rio Grande consuming 255,000 ac-ft in 2010 and 537,217ac-ft in 2011 (Table 13). Cropped acreage dropped from 204,510 ac in 2010 to 156,962 ac in 2011.

The crops were predominantly sorghum and cotton. Cameron County is in the 600-800 mm precipitation class and climate zone 5. We note the following:

- Insufficient in cloud-free imagery for both years; thus actual *ET* was constrained mostly to the time integrated ET_r data
- METRIC estimates for Sorghum *ET*: 48.3 in (2010) and 45.1 in (2011)
- METRIC estimates for cotton *ET*: 44.4in (2010) and 37.2 in (2011)
- Sugarcane *ET* was anomalously high: 60.8in (2010) and 75.5 in (2011) on roughly 6,000 acreages
- *MAP* was 34.8in (2010) and 17.7 in (2011)
- Total irrigation water use from METRIC was comparable to IWUE at 248,000 ac-ft in 2010 and but lower for 2011 at 365,000 ac-ft

Cameron was the only county with higher irrigation water use estimate from IWUE (Figure 21). Despite the 2011 drought, actual *ET* was lower in 2011, but net usage was higher from the lack of offsetting precipitation. Moreover, cloud-free pixels were problematic in both years. Nonetheless, all methods produced highly consistent irrigation water use estimates.

Carson County relies primarily on groundwater for irrigation consuming 60,000 ac-ft in 2010 and 96,000 ac-ft in 2011 (Table 13). Cropped acreage was ~200,000 ac for both years consisting primarily of winter wheat and cotton. Carson County is in the 400-600 mm precipitation class and climate zone 1. We note the following:

- Sufficient in cloud-free imagery for both years
- Clear omission of center-pivot irrigation in the CDL for both years (see appendix E)
- METRIC estimates for winter wheat *ET*: 38.5 in (2010) and 42.1 in (2011)
- METRIC estimates for cotton *ET*: 37.3 in (2010) and 48.1 in (2011)
- Alfalfa *ET* was anomalously high: 63.7 in (2010) and 81.7 in (2011) but on small acreages of 400 and 200, respectively
- *MAP* was 27.5 in (2010) and 8.9 in (2011) – very hard hit by the drought
- Winter wheat irrigation from metering data (Table 14) was 10.9 in (2010) and 37.9 in (2011)
- Cotton irrigation from metering data Is considerably lower at 13.9 in (2010) and 39.0 in (2011)
- Net *ET* from METRIC was considerably higher than IWUE which was 200,000 ac-ft in 2010, reaching 600,000ac-ft in 2011

METRIC net *ET* was several times greater than IWUE irrigation data despite the omission of obvious center-pivot systems in the southeastern corner and center of Carson County. The ET_rF maps (Appendix F) neglect these areas from the METRIC net *ET*. The total cropped acreage in the CDL did not change much between years despite significant drought conditions. Fallow/Idle croplands were actually greater in 2010 (31,648 ac) than in 2011 (21,493 ac). The modest increase in irrigation reported in the IWUE despite the drought suggests a lot of land went fallow. However, METRIC suggests a significant amount of continued irrigation. Metered data are comparable to METRIC net *ET*.

Dawson County relies solely on groundwater consuming 79,000 ac-ft in 2010 and 158,000 ac-ft in 2011 (Table 13). Cropped acreage dropped modestly from 390,800 ac in 2010 to 376,103 ac in 2011. Cotton is

the dominant crop. Dawson County is also in the 400-600 mm precipitation class on the border of climate zones 1 and 2. We note the following:

- Sufficient in cloud-free imagery for both years
- METRIC estimates of *ET* for Cotton: 38.3 in (2010) and 43.2 in (2011)
- *MAP* was 24.5 in (2010) and 4.6 in (2011) – extremely hard hit by the drought
- Cotton irrigation from metering data was considerably higher at 39.5 in (2010), not reported in 2011
- Alfalfa *ET* was anomalously high: 75.1in on 1200 ac in 2010 and 101 in on 400 ac in 2011
- Net *ET* from METRIC was considerably higher than IWUE, which was 478,000 ac-ft in 2010 and reaching 1,370,000 ac-ft in 2011

Unlike Carson County, center pivot systems were included in CDL of cropped acreage. However, the METRIC net *ET* is extremely high. We believe much of this cotton may be rain fed which cannot be omitted without an 'irrigated lands' mask. However, *ET* greatly exceeded rainfall suggesting irrigation (or significant bare soil evaporation) was present plus some bias in ET_r used in time integration.

Hale County relies primarily on groundwater consuming 219,525 ac-ft in 2010 and 389,173 ac-ft in 2011 (Table 13). Cropped acreage increased modestly from 406,698 ac in 2010 to 416,842 ac in 2011. Cotton is the dominant crop and lesser amounts of winter wheat and corn. Hale County is also in the 400-600 mm precipitation class in climate zones 1. We note the following:

- Sufficient in cloud-free imagery for both years
- METRIC estimates for cotton *ET*: 38.0 in (2010) and 48.2 in (2011)
- METRIC estimates for corn *ET*: 49.6 in (2010) and 67.3 in (2011)
- *MAP* was 24.8 in (2010) and 6.4 in (2011) – also hard hit by the drought;
- Cotton irrigation from metering data was 13.3 in (2010) and 18.3 in (2011)
- Corn irrigation from metering data was 16.1 in (2010) and 24.5 in (2011)
- Net *ET* from METRIC was considerably higher than the IWUE for both 2010 and 2011 at 1,350,000 ac-ft in and 1,720,000 ac-ft, respectively.

METRIC net *ET* was nearly an order of magnitude greater than IWUE. The total cropped acreage in the CDL did increased 300,000 ac between years despite significant drought conditions yet CDL Fallow/Idle croplands were insignificant in both years. Again, the 2011 drought resulted in a substantial increase in the estimated irrigation according to the IWUE despite a significant amount of failed crop acres in the county. However, METRIC suggests a significant amount of continued *ET* (i.e. irrigation continued well into the drought).

Medina County relies on both surface and groundwater consuming 49,006 ac-ft in 2010 and 99,120 ac-ft in 2011 (Table 13). Cropped acreage decreased modestly from 114,139 ac in 2010 to 108,675 ac in 2011. Cropping is a mix of corn, sorghum, winter wheat and cotton; however, cotton was predominant in 2011. Medina County is in the ~600 mm precipitation class in climate zone 3 on the border with zone 5. We note the following:

- Sufficient in cloud-free imagery for both years

- METRIC estimates for cotton *ET*: 46.3 in (2010) and 47.5 in (2011)
- METRIC estimates for corn *ET*: 38.7 in (2010) and 52.6 in (2011)
- *MAP* was 30.2 in (2010) and 14.1 in (2011)
- Net *ET* from METRIC was higher than the IWUE for both 2010 and 2011 at 146,000 ac-ft in 2010 and 278,000 ac-ft, respectively

METRIC net *ET* was several times greater than IWUE but within reasonable values. Fallow/Idle croplands were insignificant in both years. Despite the complexity and multi-cropping in Medina, METRIC performed well; the ET Demands models *NIWR* were much higher, as expected.

Ochiltree County relies solely on groundwater consuming 60,484 ac-ft in 2010 and 109,671 ac-ft in 2011 (Table 13). Cropped acreage was 289,040 ac in 2010 and 291,618 ac in 2011. Winter wheat and sorghum were the dominant crops in both years. Ochiltree County is in the 400-600 mm precipitation class in climate zone 1. We found the following:

- Sufficient in cloud-free imagery for both years
- METRIC estimates for winter wheat *ET*: 45.6 in (2010) and 46.6 in (2011)
- METRIC estimates for sorghum *ET*: 47.6 in (2010) and 42.7 in (2011)
- Corn *ET* was anomalously high: 61.0 in (2010) and 73.8 in (2011) on over 2,000ac
- *MAP* was 28.2 in (2010) and 9.4 in (2011)
- Net *ET* from METRIC was significantly higher than the IWUE for both 2010 and 2011 at 452,828 ac-ft in 2010 and 946,951 ac-ft, respectively

METRIC net *ET* was nearly an order of magnitude greater than IWUE. Fallow/Idle croplands were very small in both years of the CDL. Much like the other High Plains counties (Carson, Dawson, and Hale), designating irrigated from rain-fed agriculture might significantly lower irrigation water use estimates. However, the data suggests *ET* greatly exceeding available precipitation.

Wharton County relies on an even split between surface and groundwater consuming 234,000 ac-ft in 2010 and 371,254 ac-ft in 2011 (Table 13). Cropped acreage was 444,626 ac in 2010 to 457,308 ac in 2011. Corn, cotton, and rice were the dominant crops. Wharton County is in the >1000 mm precipitation class in climate zones 4. We found the following:

- Marginal (7-9 scene counts) cloud-free imagery for both years
- METRIC estimates for corn *ET*: 44.5 in (2010) and 47.7 in (2011)
- METRIC estimates for cotton *ET*: 36.2 in (2010) and 42.8 in (2011)
- METRIC estimates for rice *ET*: 52.9 in (2010) and 76.4 in (2011)
- *MAP* was 41.9 in (2010) and 17.5 in (2011)
- Corn irrigation from metering data was 15.9in (2010)
- Cotton irrigation from metering data was 11.2 (2010)
- Rice irrigation from metering data was 21.8 (2010)
- Net *ET* from METRIC was similar to IWUE in 2010 at 254,329 ac-ft; however, 2011 reached 1,450,000 ac-ft

The total cropped acreage in the CDL was similar between years at 450,000 ac; however, fallow/Idle croplands was 209,000 ac in 2010 and 213,000 ac in 2011 – nearly 50% of the total cropped lands. These idle lands also had a significant net *ET* of 207,543 ac-ft in 2010 and 748,498 ac-ft in 2011 – essentially the largest water consumer in both years. Thus, the CDL designation fallow land is questionable. Metering data per crop was higher than with METRIC net *ET* for 2010; no data was available for 2011. The lack of cloud-free image and questionable CDL data make Wharton particularly challenging in our pilot study.

Overall, the pilot study results indicate a good correspondence between crop-specific *ET* from METRIC, metered data and expected values from *Borelli et al [1998].* Note, that the *ET* algorithms do not require crop type, unlike a crop model such as ET Demands. Time integration using gridded data sets such NLDAS to generate ET_r may suffice in many areas of Texas although, METRIC ET and net ET results are likely bias high due to NLDAS ET_r being biased high. Cloud contamination east of the Balcones Escarpment may require some MODIS/Landsat fusion-based algorithm to refine net *ET*. More importantly for upscaling pixels to county estimates, the CDL needs refined beyond simply separating croplands from native vegetation – irrigated lands need to be delineated.

Texas has less dichotomy between rain-fed and irrigated agriculture. The CDL, which uses satellite multi-spectral data, could be locally refined either using additional remotely sensing data or manual mapping of irrigated lands. Regardless, *ET* greatly exceeded *PPT* in much of the High Plains resulting in a METRIC-derived *net ET* that was excessively large often greater than 1 maf per county. Center pivot irrigation is generally easy to identify in arid, irrigated lands of the west. Surprisingly, the CDL missed several center pivots in Carson County but this would only have increased the net *ET* which was already too high.

Counties with substantially lower percentages of agriculture (Brazos, Cameron, Medina, and perhaps Wharton) seemed most comparable to IWUE while regions of predominantly agriculture (Carson, Dawson, Hale and Ochiltree) may simply over-estimate irrigated acreage. Lastly, this pilot study was to assess feasibility highlighting the need for rigorous QA and operator experience which was not possible given our resources for the pilot study. Further refinement is obviously required but beyond the scope of this report. It does allow us a baseline to assess implementation as we will outline in the next sections.

Table 13. Irrigation water use estimates for 2010 and 2011. All volumes are in acre-feet.

County	Year	Irrigation	Irrigation Ground Water	Irrigation Surface Water	Year	Irrigation	Irrigation Ground Water	Irrigation Surface Water
BRAZOS	2010	35,541	31,834	3,707	2011	42,402	38,700	3,702
CAMERON	2010	255,000	0	255,000	2011	537,217	0	537,217
CARSON	2010	60,069	59,823	246	2011	95,956	95,956	0
DAWSON	2010	78,974	78,974	0	2011	158,441	158,441	0
HALE	2010	219,643	219,525	118	2011	389,173	389,019	154
MEDINA	2010	49,006	33,903	15,103	2011	99,120	60,046	39,074
OCHILTREE	2010	60,484	60,484	0	2011	109,671	109,671	0
WHARTON	2010	234,003	118,336	115,667	2011	371,254	181,384	189,870

Table 14. Annual county irrigation estimates based on metering data by crop.

Source	County	Year	N	Crop Acreage	Metered Amount	Metered Units	Meter Irrigation (in)	CDL Crop	Metric net ET (in)
Coastal Bend	Wharton	2010	5	676	3144	inches	4.7	Alfalfa	*NA*
GCD	Wharton	2010	10	1974	9228	inches	4.7	Corn	15.90
	Wharton	2010	2	397	1307	inches	3.3	Cotton	11.20
	Wharton	2010	28	2495	31350	inches	12.6	Aquaculture	2.5
	Wharton	2010	42	7081	131071	inches	18.5	Rice	21.80
		2010	87	12623	176101	inches	14.0	Total	6.47
Mesa GCD	Dawson	2010	2	234	1.29E+08	Gal.	20.2	Alfalfa	50.39
	Dawson	2010	109	11998	3.97E+09	Gal.	12.2	Cotton	39.46
	Dawson	2010	32	3969	1.69E+09	Gal.	15.6	Mixed	36.43
	Dawson	2010	6	598	2.61E+08	Gal.	16.1	Other	29.30
	Dawson	2010	1	120	2.83E+07	Gal.	8.7	Sorghum	26.07
	Dawson	2010	6	720	1.23E+08	Gal.	6.3	Wheat	19.28
		2010	156	17639	6.20E+09	Gal.	12.9	Total	28.47
Mesa GCD	Dawson	2011	4	253	2.81E+08	Gal.	41.0	Alfalfa	101.24
	Dawson	2011	113	12471	7.74E+09	Gal.	22.9	Corn	61.98
	Dawson	2011	3	360	2.21E+08	Gal.	22.6	Mixed	57.10
			120	13084	8.25E+09		23.2	Total	66.97
Panhandle	Carson	2010	9	2813	5.99E+08	Gal.	7.8	Alfalfa	34.41
GCD	Carson	2010	39	8004	2.27E+09	Gal.	10.5	Corn	26.68
	Carson	2010	32	5767	1.14E+09	Gal.	7.2	Cotton	13.93
	Carson	2010	47	17802	3.65E+09	Gal.	7.6	Mixed	NA
	Carson	2010	14	3590	6.84E+08	Gal.	7.0	?	
	Carson	2010	6	2149	3.70E+08	Gal.	6.3	Sorghum	9.46
	Carson	2010	18	4920	1.38E+09	Gal.	10.3	Wheat	10.93
		2010	165	45045	1.01E+10	Gal.	8.2	Total	16.82
Panhandle	Carson	2011	10	3123	4153	ac/ft	16.0	Alfalfa	73.21
GCD	Carson	2011	33	6890	7236	ac/ft	12.6	Corn	60.62
	Carson	2011	52	12173	13665	ac/ft	13.5	Cotton	39.04
	Carson	2011	47	18194	21796	ac/ft	14.4	Mixed	NA
	Carson	2011	7	1784	1507	ac/ft	10.1	Sorghum	28.34
	Carson	2011	17	3948	8532	ac/ft	25.9	Wheat	37.86
		2011	166	46112	56888	ac/ft	14.8	Total	45.13
TAWC	Hale/Floyd	2010	7	1577	9664	Inches	6.1	Alfalfa	39.10
	Hale/Floyd	2010	4	361	5830	Inches	16.1	Corn	24.56
	Hale/Floyd	2010	2	154	731	Inches	4.7	Cotton	13.34
	Hale/Floyd	2010	11	1414	14582	Inches	10.3	Mixed	
		2010	24	3507	30808	Inches	8.8	Total	21.60
TAWC	Hale/Floyd	2011	5	824	15982	Inches	19.4	Alfalfa	74.44
	Hale/Floyd	2011	2	140	3430	Inches	24.5	Corn	60.87
	Hale/Floyd	2011	6	629	11478	Inches	18.3	Cotton	41.87
	Hale/Floyd	2011	13	2012	43407	Inches	21.6	Mixed	NA
		2011	26	3605	74298	Inches	20.6	Total	56.60

Table 15. Annual county-wide irrigation totals (acre feet) based on both FSA and CDL cropped acres with and without (*) fallow/idle land.

County	Year	FSA Planted Acres	FSA Failed Acres	Acres (CDL)	Acres* (CDL)	IWUE (ac-ft)	METRIC ET (ac-ft)	METRIC ET* (ac-ft)	ET Demands
BRAZOS	2010	94,592	-	24,663	20,676	35,541	21,047	18,056	48,066
CAMERON	2010	232,250	802	206,713	192,374	255,000	247,790	215,644	414,963
CARSON	2010	546,156	3,950	204,510	172,862	60,069	199,380	192,041	508,076
DAWSON	2010	567,516	7,483	390,800	383,207	78,974	478,361	467,397	1,161,363
HALE	2010	579,365	28,341	406,698	396,297	219,643	512,061	500,917	1,088,518
MEDINA	2010	160,456	56	114,139	96,483	49,006	146,341	111,856	207,039
OCHILTREE	2010	486,214	2,691	289,040	243,857	60,484	452,828	411,568	654,782
WHARTON	2010	546,680	1,579	444,626	235,379	234,003	254,329	46,788	324,778
SUM		3,213,229	44,901	2,081,190	1,741,134	992,720	2,312,136	1,964,267	4,407,585

County	Year	FSA Planted Acres	FSA Failed Acres	Acres (CDL)	Acres* (CDL)	IWUE (ac-ft)	METRIC ET (ac-ft)	METRIC ET* (ac-ft)	ET Demands
BRAZOS	2011	47,067	264	70,361	69,735	42,402	118,073	115,866	90,666
CAMERON	2011	189,595	8,369	156,962	156,532	537,217	365,727	364,402	408,443
CARSON	2011	231,708	26,164	202,568	181,076	95,956	601,211	554,279	700,503
DAWSON	2011	220,000	301,437	376,103	371,856	158,441	1,369,920	1,344,754	1,773,593
HALE	2011	394,624	165,485	416,842	410,911	389,173	1,502,822	1,486,980	1,510,286
MEDINA	2011	101,821	9,518	108,675	85,274	99,120	278,010	229,110	262,105
OCHILTREE	2011	302,492	10,076	291,618	246,573	109,671	946,957	829,360	867,420
WHARTON	2011	292,805	12,717	457,308	244,270	371,254	1,454,605	706,107	564,545
SUM		1,780,113	534,031	2,080,438	1,766,227	1,803,234	6,637,323	5,630,858	6,177,560

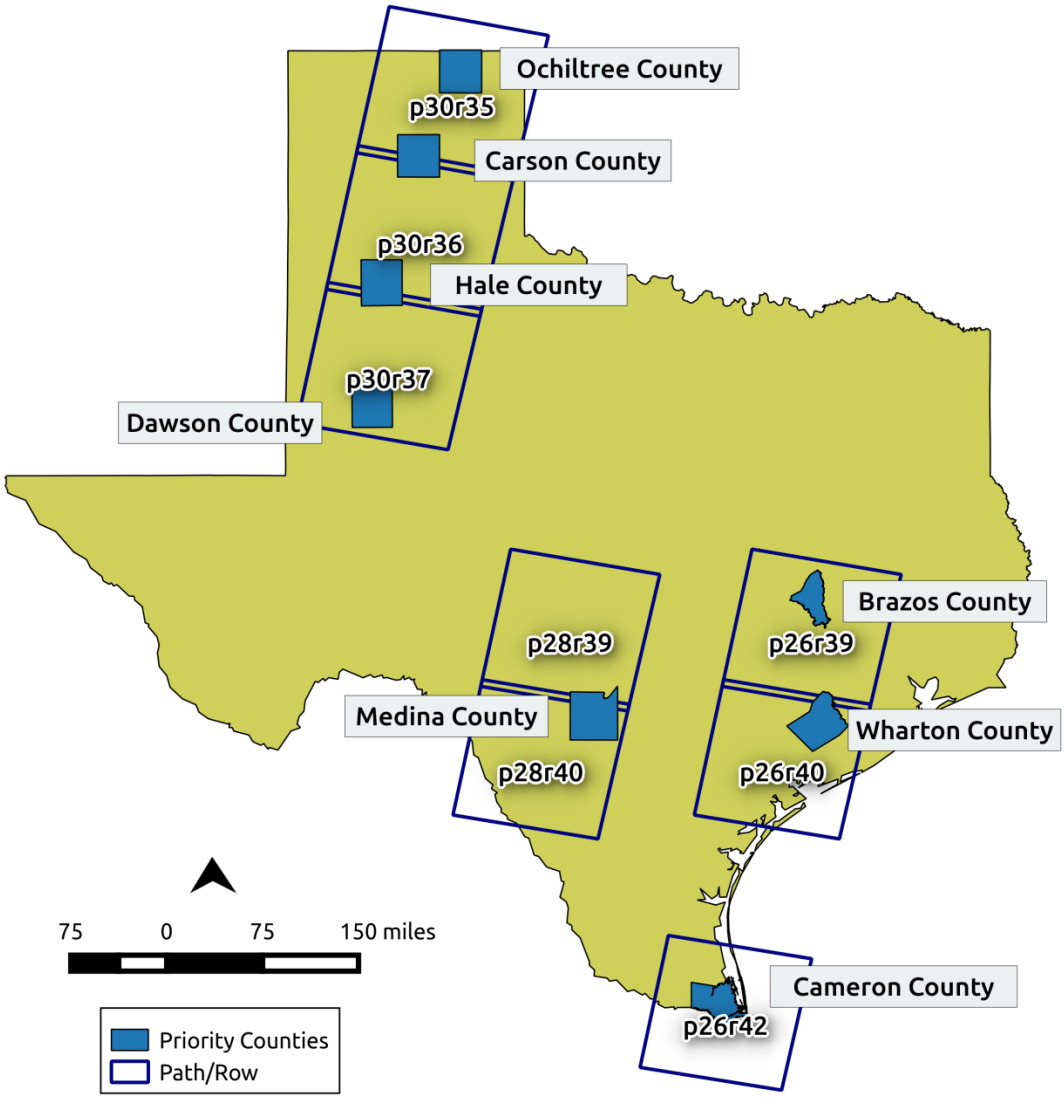

Figure 14. Eight counties selected to maximize different climatologies and inherent challenges to satellite-based *ET* estimates across Texas while minimizing the number of satellite paths.

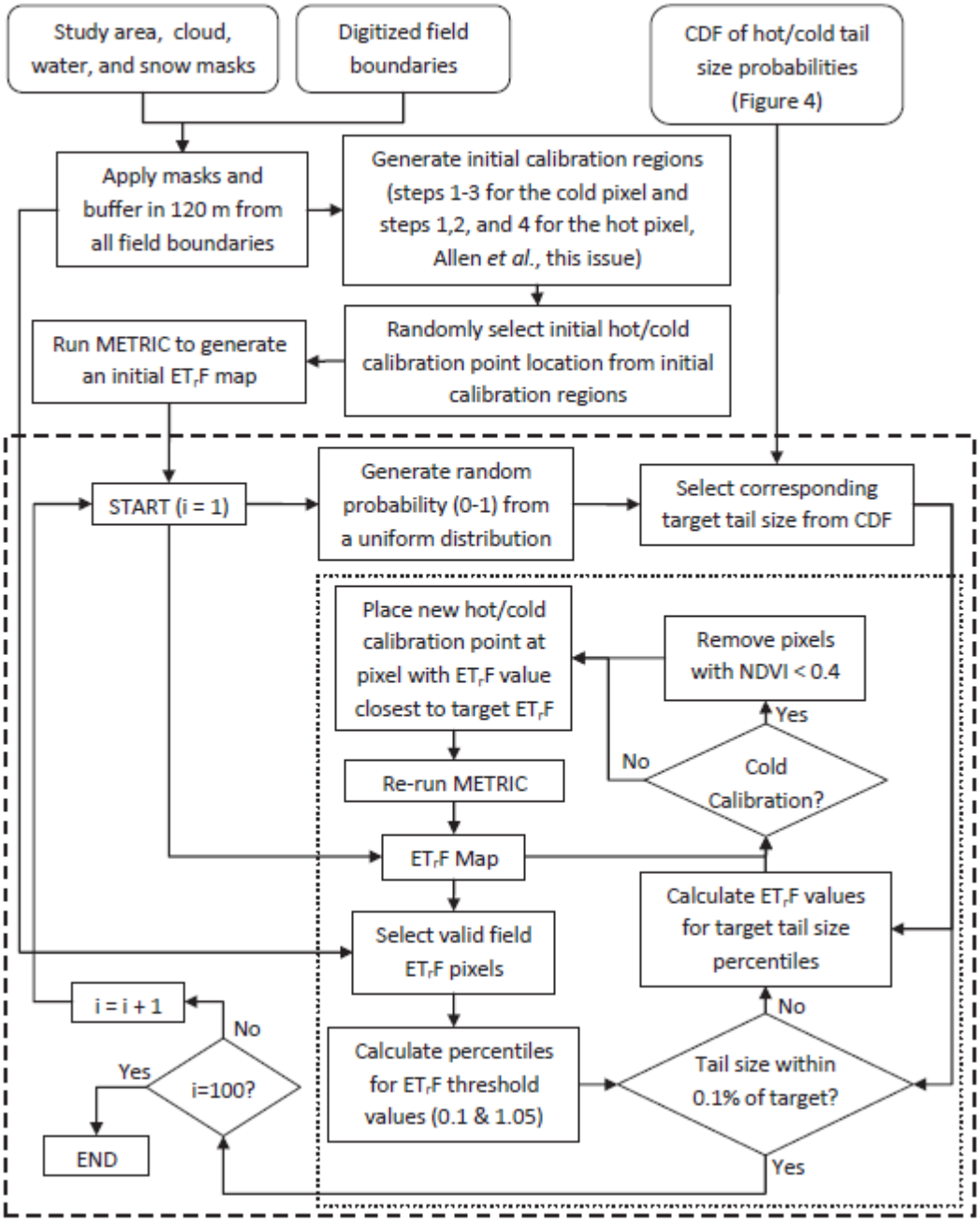

Figure 15. Automated METRIC workflow from Morton et al., (2013). The dashed boxes represent Monte Carlo processes to interactively find the hot and cold calibration pixels that generate the *ETrF* map.

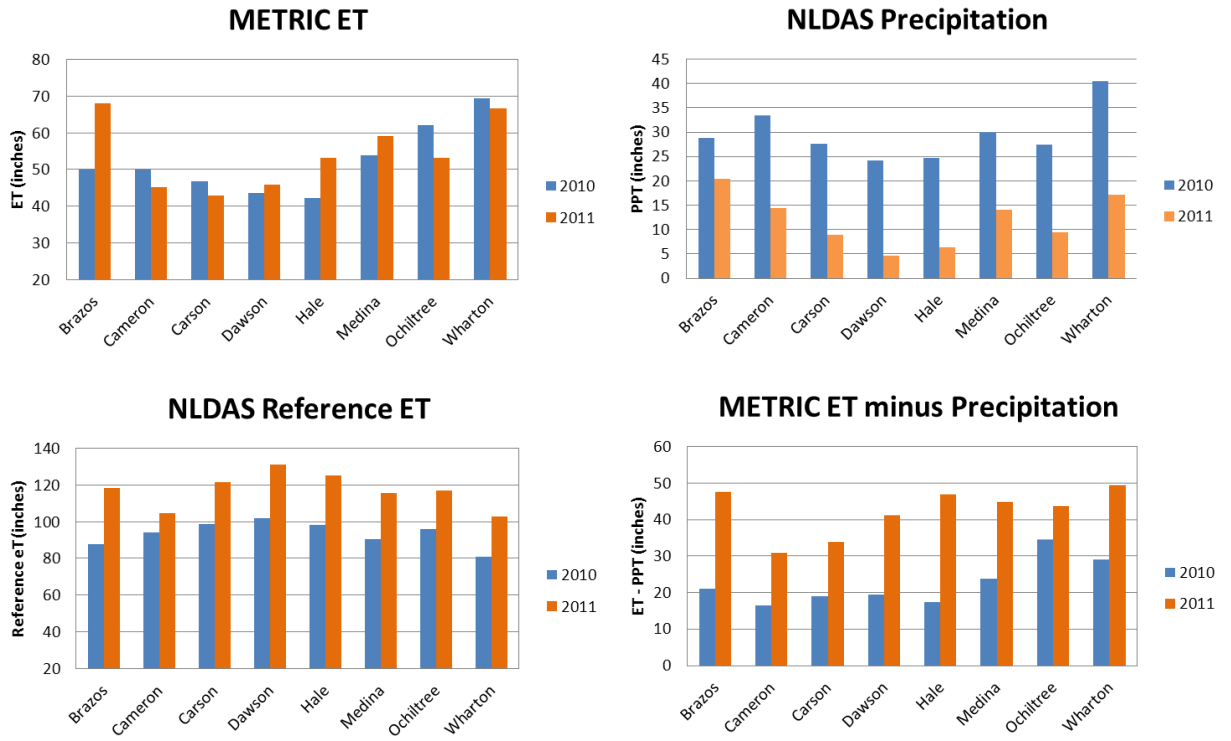

Figure 16. Summary of METRIC annual results per county with *ET* averaged over all croplands, annual precipitation from NLDAS, annual ET_r and annual *NIWR* (*ET-PPT*).

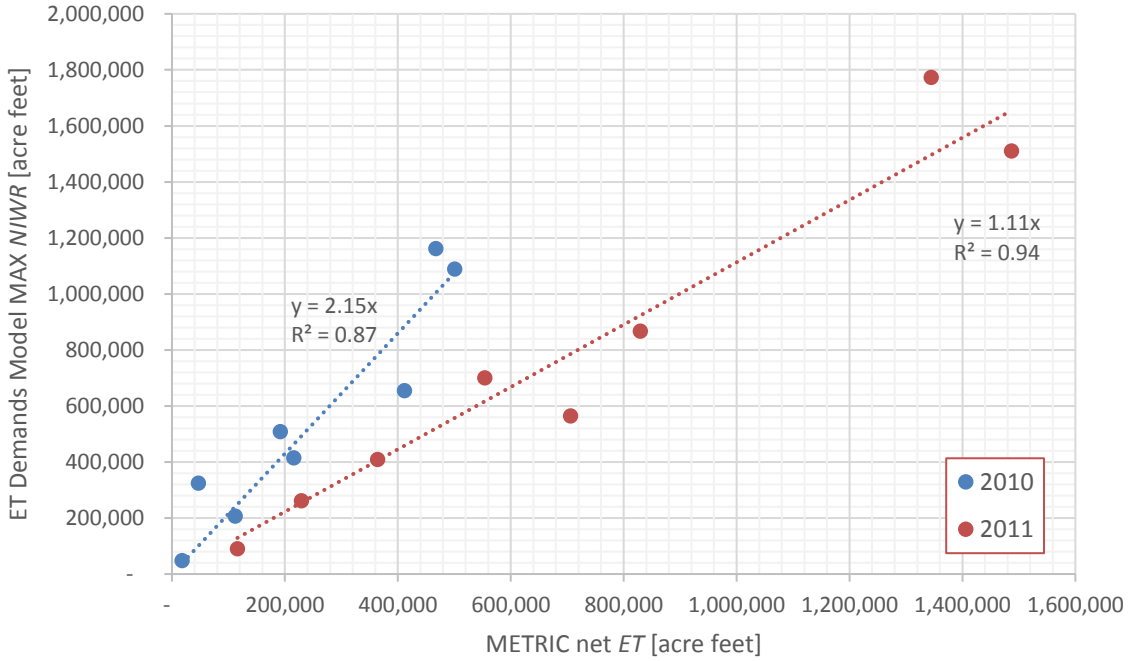

Figure 17. Correlation between net *ET* derived from METRIC and the NIWR form the ET Demands model for 2010 and 2011.

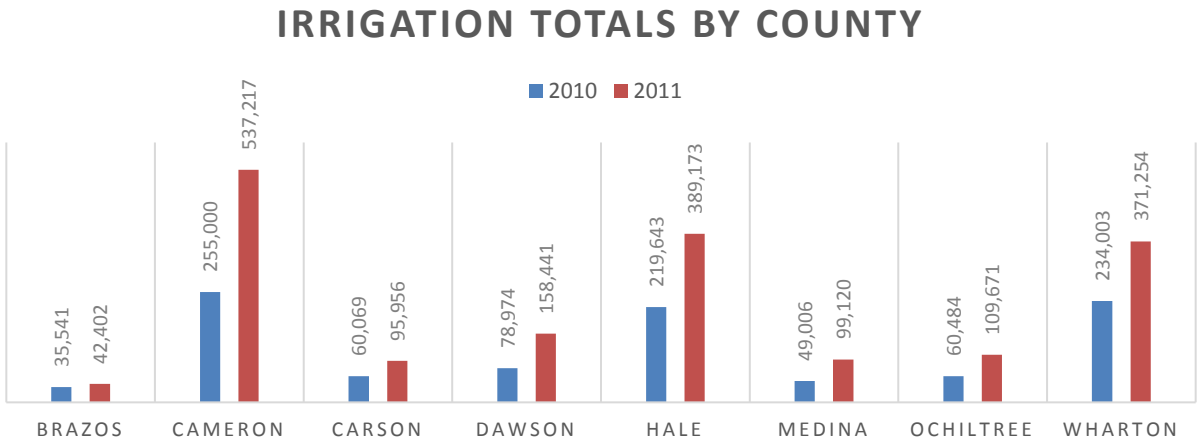

Figure 18. Irrigation Water Use Estimates (acre-feet) for 2010 and 2011.

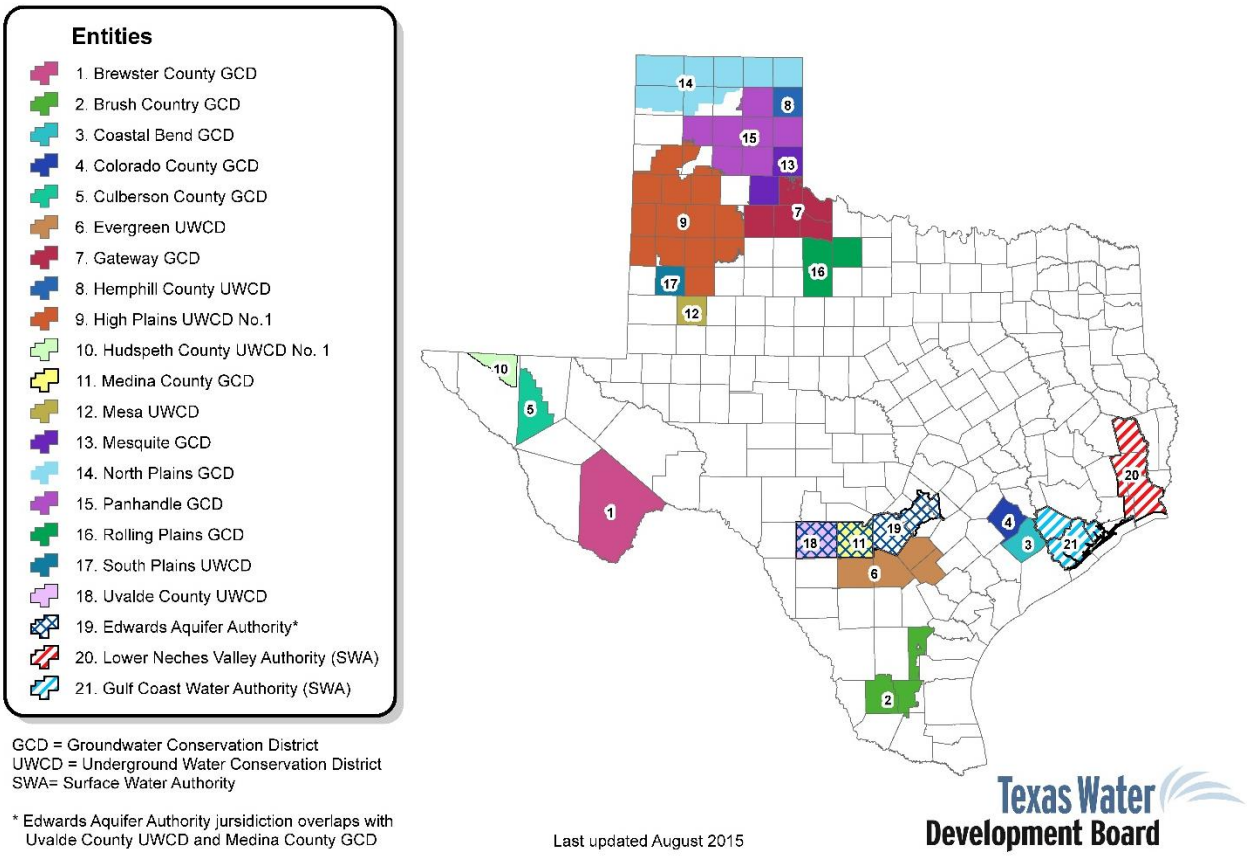

Figure 19. Entities participating in TWDB's Metering Program. The 5 pilot study counties overlap program participants including the Panhandle GCD (Carson), Mesa UWCD (Dawson), High Plains UWCD (Hale), Medina County GCD (Medina, not in 2010-2011), and Coastal Bend GCD (Wharton).

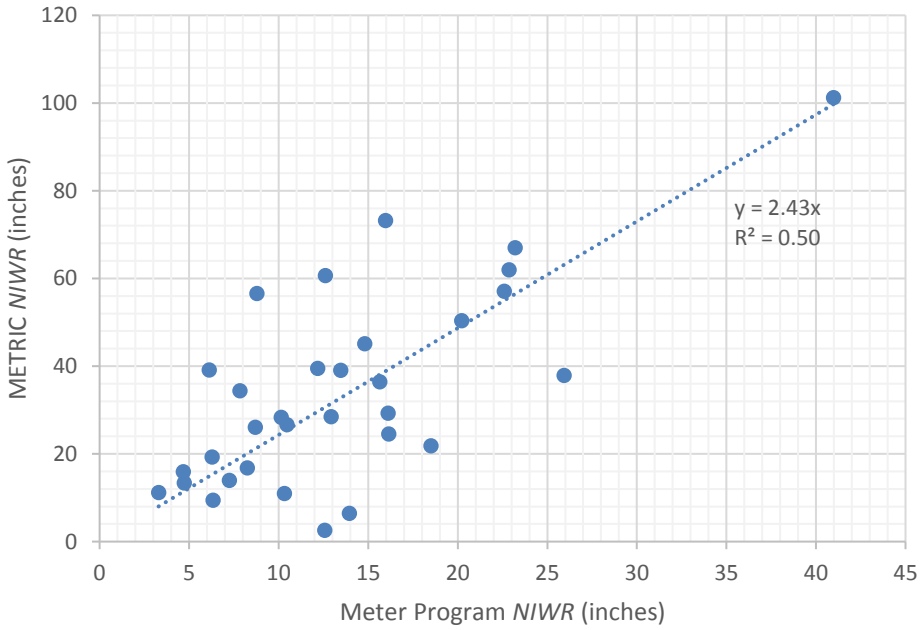

Figure 20. *NIWR* measured by irrigation meters in collocated counties and crops paired with pilot study METRIC *NIWR* results.

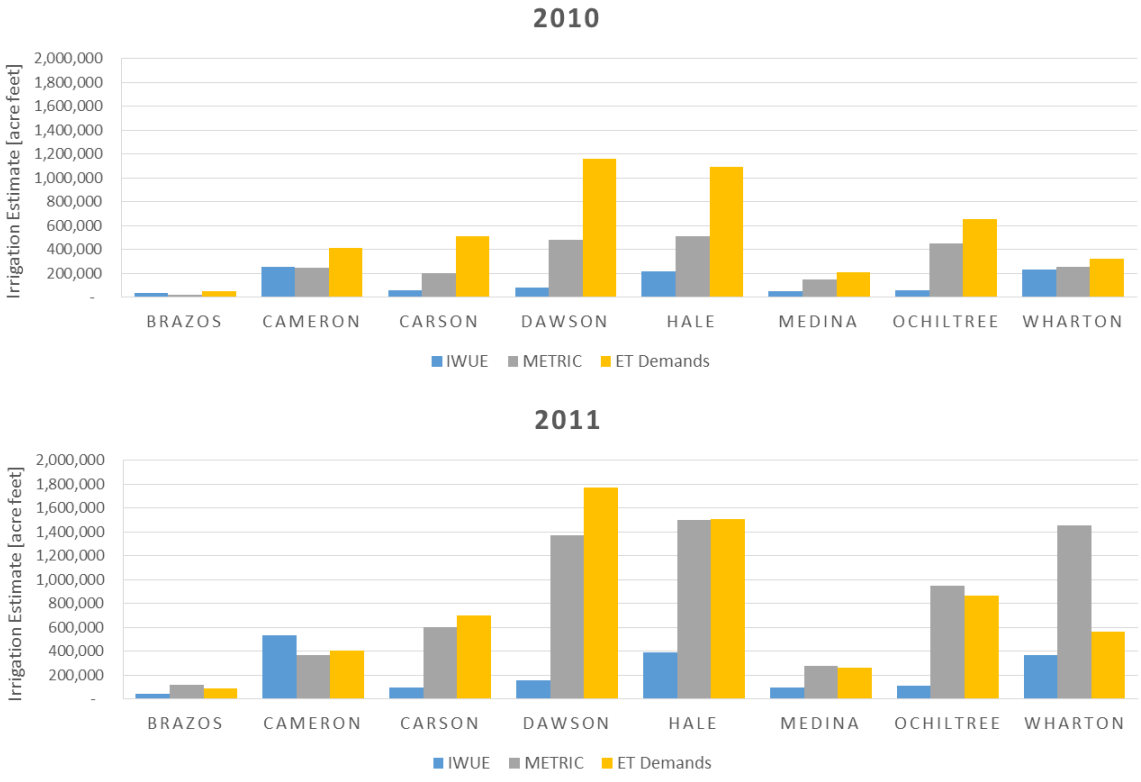

Figure 21. Annual irrigation totals (acre feet) for 2010 and 2011 per county from the TWDB irrigation water use estimates (IWUE), net *ET* from METRIC, and *NIWR* from the ET Demands model.

7 Conclusions

This report illustrates that remotely sensed *ET* *is* feasible for Texas. With confidence, we believe the algorithms are valid, the results are reasonable (but currently biased high), and the data requirements (imagery, gridded data, etc.) can be met. However, it will take commitment from the State, effort from staff and collaboration with researchers to implement. All regions of the State will pose a unique challenge from clouds to crop classification. We assessed many state-of-the-science algorithms and implemented one in our pilot study. Though complicated and challenging, many of these methods are becoming operational, albeit slowly. Furthermore, computations and data storage are moving to cloud-based technologies such as Google Earth-Engine (see EEFlux cloud implementation of METRIC at http://eeflux-training.appspot.com/). This feasibility test not only provides a conclusive document to the Texas Water Development Board, but has also developed the scripts and data methods for technology transfer to staff at the Texas Water Development Board.

Our pilot study produced annual estimates of net *ET* or the Net Irrigation Water Requirement (*NIWR*) using METRIC along with a dual-crop soil water balance model, respectively. Although this was a simple but time consuming effort to logistically assess the process, the actual results are encouraging but not without issues. Eastern counties lacked cloud-free imagery; our mapping of irrigated versus non-irrigated lands is poor, gridded estimates of ET_r and therefore METRIC *ET* and net ET estimates are possibly biased high (we lack ground data for validation), and we do not have much beyond the IWUE to validate *NIWR* against. In this final section, we include a summary of all costs associated with data products and hardware, staff time, and training for implementation, required technical expertise for each method, accuracy and applicability of each technology, and time estimate for full implementation and validation requirements for estimates.

7.1 Expertise, training, and time required for staff implementation

There are several paths for TWDB to implement remotely sensed products into annual per county irrigation water use estimates. Universities or consultants could produce the data with oversight by TWDB. However, as the state water planner agency, it should be done in house by committed staff that understand Texas agriculture and water-use, and can advance with the technologies and drive the operational readiness of the methods. Unfortunately, the technology is not currently quite there. Experts in the field should be consulted to build the State's capacity. Once this capacity (2 or 3 years down the road) is achieved, the annual staff commitment is summarized as the following (based on the workflow in Figure 3). In ID and NV, there is an experiences and well-versed remote sensing profession and 1 or 2 junior level technicians with geographical information system skills and remote sensing backgrounds. We refer to them as 'senior and 'junior'.

The workflow is estimated per image scene assuming Landsat/METRIC type algorithm with Tier 3 accuracy (Table 16). The commitment per year for one scene is a half week (17 hours) for the senior person and nearly a full week (36 hrs) for a junior technician. Texas is large requiring 48 Landsat tiles to completely cover it. We can assume we only need to process 40 of these (rough estimate) totaling 680 and 1440 for senior and junior staff, respectively. That is essentially one senior and two junior staff devoted half time to this effort.

Table 16. Estimate of workforce hours to generate annual net *ET* per Landsat scene area. Based on the workflow presented in Figure 3.

Steps	Task	Description	Senior Person (hr)	Junior Person (hr)
1	Define Project	Identify counties or regions of interest, determine geographical boundaries and time period of interest	4	
2	Acquire Data	Obtain (manually) available imagery: Landsat, MODIS, CDL		4
3	Create Masks	Assess scenes for cloud contamination, ideally using an automated tool, like F-Mask. Process CDL to exclude non-cropped vegetation	1	8
4	Image Processing	Calculate image derivatives required for *ET* algorithm	1	8
5	Run ET Algorithm	Calculate initial ET_rF map and evaluate hot/cold pixels and general distribution of ET_c	4	
6	Weather Data	Extract and process weather data, QA/QC and calculate spatially distributed ET_r and precipitation	1	4
		Estimate overpass times for each scenes and extract needed parameters for ET_rF maps	1	
7	Time Integration	Compile images, interpolate ET_rF maps between satellite acquisitions times	1	8
		QA/QC integration, compare against other data sources or expert knowledge	2	
8	Data Summary	Aggregate daily ET_c estimates and rainfall into defined project boundaries and sum into totals	2	4
		Total labor per processed scene (hr)	17	36
		Number of scenes to analyze (48 over Texas)	~40	
		Total Man-Hours Per Year	680	1440

Computationally, these algorithms require high-level computers, ideally dual-cores with substantial RAM and multiple monitors to aid visualization of the results. The standard Dell business workstation is ~$3000 and would suffice. Systems must have a GIS-based software (e.g. ArcMap, Global Mapper, QGIS) and a

scripting capabilities. Python and many other programming languages are free and often a requirement to implement the algorithms and to automate the more routine processing tasks. Lastly, data storage can be substantial, if all the historical runs are archived, considering the 48 Landsat scenes required to cover Texas and each scene is 300MB of data. Revisit times between satellites are every 8 days but we can assume we only retain 20 images per growing season to produce *ET*. However, each scene had 5 derivatives such as spectral and at-satellite reflectance, radiance, albedo, NDVI, etc. These are generally archived as well. That totals 1.7 TB of data per year in Landsat imagery alone (Table 17).

Table 17. Annual data storage requirements for Landsat imagery.

48	Landsat scenes over Texas
5	Landsat Derivatives Required per scene
20	Images per year likely
5760	Total Images per year
300	Image Size (MB)
1.73	Total (TB) per year

MODIS tiles use a sinusoidal projection covering a much larger area but at a coarser spatial resolution (1km) than Landsat (30m). However, they are also daily data sets. Data storage requirements could double should a fusion-based method be necessary. Along with various gridded and/or weather station data, it would be safe to double the data storage requirement to 3 TB/year. Cloud storage and computing is evolving, and may be an option as EEFlux or similar cloud computing *ET* programs and products develop in the coming years (e.g. ClimateEngine.org).

7.2 Accuracy and applicability of remotely sensed *ET*

Clearly, remote sensing opens many doors into water resource management across Texas. The methods presented herein can derive a physically based and constrained estimate of actual *ET*. Subtracting this value from gridded rainfall totals can provide a value of net *ET* at unprecedented spatial resolution. It can also potentially provide a historical perspective of net *ET* over the past three decades. However, such data are difficult to evaluate directly since little field data exist at the appropriate scale. As presented in Table 5, each class of algorithm can produce a range of accuracy, which generally correlates well with its level of complexity, data requirements, and skills of the practitioner.

Currently, several approaches have been used to validate satellite-based *ET* data in Texas including lysimeters [*Evett et al.*, 2012; *Paul et al.*, 2013], micrometeorological data using eddy covariance or Bowen ratio [*Todd et al.*, 2000; *Heilman et al.*, 2009], as well as sap flow measurements [*Colaizzi et al.*, 2012]. All of these methods are equally complicated, field-intensive, commonly have errors of 20% in energy balance closure [*Wilson et al.*, 2002; *Foken*, 2008]. In addition many field methods have inadequate boundary conditions for irrigated agriculture [*Huntington et al.*, 2011] or simply do not scale accurately

[*Famiglietti and Wood*, 1995]. Allen et al. [2011] provide an estimate of typical *ET* measurement error ranging from 5-15% for lysimeters to 10-20% for remote sensing energy balance algorithms. These errors increase substantially with novice personnel and common equipment malfunctions. Furthermore, there is a general lack of active stations monitoring ET_r and actual *ET* in Texas, challenging the validation of any *ET* product.

7.3 Limitations and recommendations of satellite *ET* technologies in Texas

We summarize the limitations of an irrigation water use estimate from remotely sensed *ET* methods as:

- Clouds
- Operational readiness of the *ET* algorithms
- Robustness of time integration
- Lack of station data in irrigated environments
- Insufficient validation data (e.g. metered data from specific, single cropped fields)
- Irrigated lands are not spectrally distinct from dryland agriculture (e.g. irrigated crop mask)
- Bare soil evaporation or carry-over soil water storage

Clouds are an obvious a hindrance for much of the State. Cloud masks are continually being improved. Some irrigated areas will inevitably be cloudy. Landsat's ~8day return intervals can be augmented (fused) with 1km MODIS (daily) but there is a loss of spatial resolution. Many advanced algorithms can deal with this but they require more expertise to implement. In general, none of the algorithms are operational: ready to use, out-of-the-box solutions. METRIC, which we used in the pilot study, is no exception. The original code is quite archaic but researchers are moving it to more accessible programming languages (Python, C++, Matlab) and even automated platforms (i.e. Google Earth Engine). Committed stakeholders, like TWDB, would move this process forward and we expect more advances in the near future.

Time integration requires reliable weather data and knowledge of soil moisture storage. We found that NLDAS produces excellent rainfall but also reliable ET_r – although biased high. On-ground data will always be a large challenge for a state covering as much territory, climatology, and agricultural practices as Texas. It would be difficult and costly to maintain meteorological station(s) in every county. However, some stations in irrigated agriculture designed to validate ET_r would be very valuable. Net *ET* produced monthly here assumes no change in soil water storage between months. Our results in Wharton and much of the north Texas had significantly greater net *ET* than is likely attributable to irrigation. We suspect soil moisture storage prior to the growing season may be a substantial source of water available for ET later. Thus, more detailed knowledge of soil moisture would reduce this uncertainly. In the western states where such net *ET* programs are operational, irrigation is a requirement for crop growth. They have nearly no rainfall during the growing season, less native vegetation transpiring within satellite scenes, and have fewer clouds. The irrigated agriculture is much more obvious from satellites. For Texas, we have more challenges; some of these limitations are only specific to certain areas (i.e. clouds and weather data) like east Texas, others are ubiquitous.

7.4 Time estimate for full implementation and final thoughts

Through this exercise, our team produced a conclusive feasibility report on the *ET* algorithms, available data sets and costs (hardware, software, and man-hours) to implement a state-wide program. The minimum requirements would be met by one senior scientist with a solid remote sensing background and two junior technician with half-time commitments. The implementation time would take several years to launch and likely require full-time commitments from the assigned staff until the program became more operational.

This feasibility study essentially lays the groundwork to implement a state-wide *ET*, precipitation, and irrigation water-use program including the image processing, *ET* algorithms and fusion methods to quantify irrigated water use regardless of climate, crop type, or available data. Several research areas could be filled by researchers including assistance operationalizing the methodology, automating and validating irrigated land mapping (and CDL), measuring ET_r in representative agricultural areas, and using advanced meteorological methods, such as eddy covariance or scintillometry to measure *ET* for validation. Lastly, the irrigation metering program produced two significant findings related to this research. First, it showed that metered crops water use was consistently lower than net *ET* from satellite imagery. This discrepancy may suggest that satellite *ET* is incorrect – or it may suggest that metering promotes water conservation. Secondly, the metering data per crop shows good correlation with satellite *ET* and with better implementation could also be used to better validate satellite *ET* methods. Ideally, the meters would be geolocated and recorded monthly along with *PPT* and in a standardized format over a single uniform crop type.

In summary, we fully believe the state of Texas has the need and abilities implement remote sensing into their state-wide irrigation water use estimation program. We have the expertise to build such a program at our universities and we have the dedicated staff to implement it at the TWDB.

8 Acknowledgments

We acknowledge the following contributions to this project including Mindy Conyers who supplied irrigation meter data and excellent program oversight (TWDB), as well as Cameron Turner, John Ellis, and Antonio Delgado (TWDB); Andrea Fey and Scott Embler (NOAA) for help with CRN wind speed data; Yang Hong and Xianwu Xue (University of Oklahoma) for access to PERSIANN rainfall data; John Abatzoglou (University of Idaho) for providing downscale daily NLDAS data; Steven Quiring and Balaji Narasimhan (Texas A&M University) for the raw Climate Atlas of Texas Data; Wesley Burgett (Texas Tech University) for mesonet data sets; Bob Huber (Lower Colorado River Authority) for Hydromet rainfall data; Guy Fipps (Texas A&M University) for the Texas PET network data. We also acknowledge discussions with noted ET experts throughout this project including Richard Allen (University of Idaho), Richard Cuenca (Oregon State University), Yang Hong (OU), and Martha Anderson (USDA-ARS). We also acknowledge operational discussions with Adam Sullivan (Nevada State Engineers Office) and Carlos Kelley (university of Idaho).

9 References

Abatzoglou, J. T. (2013), Development of gridded surface meteorological data for ecological applications and modelling, *Int. J. Climatol.*, *33*, 121-131, 10.1002/joc.3413.

Allen, R. G. (2008), Quality assessment of weather data and micrometeorological flux: Impacts on evapotranspiration calculation, *J. Agric. Meteorol.*, *64*, 191-204.

Allen, R. G. (2011), Skin layer evaporation to account for small precipitation events-An enhancement to the FAO-56 evaporation model, *Agr. Water Manage.*, *99*, 8-18, doi 10.1016/j.agwat.2011.08.008.

Allen, R. G., and C. W. Robison (2009), *Evapotranspiration and Consumptive Irrigation Water Requirements for Idaho*, 299 pp., University of Idaho.

Allen, R. G., M. Tasumi, and R. Trezza (2007), Satellite-based energy balance for mapping evapotranspiration with internalized calibration (METRIC) - Model, *J. Irrig. Drain. Eng.*, *133*, 380-394.

Allen, R. G., L. S. Pereira, D. Raes, and M. Smith (1998), *Crop evapotranspiration: Guidlines for computing crop water requirements*, 300 pp., FAO, Rome, Italy.

Allen, R. G., L. S. Pereira, T. A. Howell, and M. E. Jensen (2011), Evapotranspiration information reporting: I. Factors governing measurement accuracy, *Agr. Water Manage.*, *98*, 899-920, 10.1016/j.agwat.2010.12.015.

Allen, R. G., A. J. Clemmens, C. M. Burt, K. Solomon, and T. O'Halloran (2005), Prediction accuracy for projectwide evapotranspiration using crop coefficients and reference evapotranspiration, *J. Irrig. Drain. Eng.*, *131*, 24-36.

Allen, R. G., B. Burnett, W. Kramber, J. Huntington, J. Kjaersgaard, A. Kilic, C. Kelly, and R. Trezza (2013), Automated calibration of the METRIC-Landsat evapotranspiration process, *J. Am. Water Resour. As.*, 1-14, doi 10.1111/jawr.12056.

Anderson, M. C., R. G. Allen, A. Morse, and W. P. Kustas (2012), Use of Landsat thermal imagery in monitoring evapotranspiration and managing water resources, *Remote Sens. Environ.*, *122*, 50-65, doi 10.1016/j.rse.2011.08.025.

Anderson, M. C., J. M. Norman, G. R. Diak, W. P. Kustas, and J. R. Mecikalski (1997), A two-source time-integrated model for estimating surface fluxes using thermal infrared remote sensing, *Remote Sens. Environ.*, *60*, 195-216.

Anderson, M. C., J. M. Norman, J. R. Mecikalski, J. A. Otkin, and W. P. Kustas (2007a), A climatological study of evapotranspiration and moisture stress across the continental United States based on thermal remote sensing: 2. Surface moisture climatology, *J. Geophys. Res - Atmos.*, *112*, Artn D11112, doi 10.1029/2006jd007507.

Anderson, M. C., J. M. Norman, J. R. Mecikalski, J. A. Otkin, and W. P. Kustas (2007b), A climatological study of evapotranspiration and moisture stress across the continental United States based on thermal remote sensing: 1. Model formulation, *J. Geophys. Res - Atmos.*, *112*, Artn D10117, doi 10.1029/2006jd007506.

Anderson, M. C., W. P. Kustas, J. M. Norman, et al. (2011), Mapping daily evapotranspiration at field to continental scales using geostationary and polar orbiting satellite imagery, *Hydrol. Earth Syst. Sc.*, *15*, 223-239, doi 10.5194/hess-15-223-2011.

ASCE-EWRI (2005), *The ASCE Standardized Reference Evapotranspiration Equation*, 216 pp., American Society of Civil Engineers, Reston, VA.

Bastiaanssen, W. G. M., M. Menenti, R. A. Feddes, and A. A. M. Holtslag (1998), A remote sensing surface energy balance algorithm for land (SEBAL) - 1. Formulation, *J. Hydrol.*, *212*, 198-212.

Bastiaanssen, W. G. M., E. J. M. Noordman, H. Pelgrum, G. Davids, B. P. Thoreson, and R. G. Allen (2005), SEBAL model with remotely sensed data to improve water-resources management under actual field conditions, *J. Irrig. Drain. Eng.*, *131*, 85-93.

Borrelli, J., C. B. Fedler, and J. M. Gregory (1998), Mean Crop Consumptive Use and Free-water Evaporation for Texas, Texas Water Development Board, *Rep. 95-483-137*, Austin, TX.

Boryan, C., Z. W. Yang, R. Mueller, and M. Craig (2011), Monitoring US agriculture: the US Department of Agriculture, National Agricultural Statistics Service, Cropland Data Layer Program, *Geocarto International*, *26*, 341-358, 10.1080/10106049.2011.562309.

Brower, A. (2008), *ET Toolbox – Evapotranspiration Toolbox for the Middle Rio Grande, A Water Resources Decision Support Tool*, 195 pp., Bureau of Reclamation, Denver, CO.

Cammalleri, C., M. C. Anderson, and A. P. Kustas (2014a), Upscaling of evapotranspiration fluxes from instantaneous to daytime scales for thermal remote sensing applications, *Hydrol. Earth Syst. Sc.*, *18*, 1885-1894.

Cammalleri, C., M. C. Anderson, F. Gao, C. R. Hain, and W. P. Kustas (2014b), Mapping daily evapotranspiration at field scales over rainfed and irrigated agricultural areas using remote sensing data fusion, *Agric. For. Meteorol.*, *186*, 1-11, doi 10.1016/j.agrformet.2013.11.001.

Colaizzi, P. D., W. P. Kustas, M. C. Anderson, N. Agam, J. A. Tolk, S. R. Evett, T. A. Howell, P. H. Gowda, and S. A. O'Shaughnessy (2012), Two-source energy balance model estimates of evapotranspiration using component and composite surface temperatures, *Adv. Water Resour.*, *50*, 134-151, 10.1016/j.advwatres.2012.06.004.

Daly, C., M. Halbleib, J. I. Smith, W. P. Gibson, M. K. Doggett, G. H. Taylor, J. Curtis, and P. P. Pasteris (2008), Physiographically sensitive mapping of climatological temperature and precipitation across the conterminous United States, *Int. J. Climatol.*, *28*, 2031-2064, doi 10.1002/Joc.1688.

Evett, S. R., W. P. Kustas, P. H. Gowda, M. C. Anderson, J. H. Prueger, and T. A. Howell (2012), Overview of the Bushland Evapotranspiration and Agricultural Remote sensing EXperiment 2008 (BEAREX08): A field experiment evaluating methods for quantifying ET at multiple scales, *Adv. Water Resour.*, *50*, 4-19, doi 10.1016/j.advwatres.2012.03.010.

Famiglietti, J. S., and E. F. Wood (1995), Effects of spatial variability and scale on areally averaged evapotranspiration, *Water Resour. Res.*, *31*, 699-712, doi 10.1029/94wr02820.

Foken, T. (2008), The energy balance closure problem: An overview, *Ecol. Appl.*, *18*, 1351-1367.

Gao, F., J. Masek, M. Schwaller, and F. Hall (2006), On the blending of the Landsat and MODIS surface reflectance: Predicting daily Landsat surface reflectance, *IEEE Trans. Geosci. Remote Sens.*, *44*, 2207-2218, doi 10.1109/TGRS.2006.872081.

Gonzalez-Dugo, M. P., C. M. U. Neale, L. Mateos, W. P. Kustas, J. H. Prueger, M. C. Anderson, and F. Li (2009), A comparison of operational remote sensing-based models for estimating crop evapotranspiration, *Agric. For. Meteorol.*, *149*, 1843-1853, doi 10.1016/j.agrformet.2009.06.012.

Gowda, P. H., J. L. Chavez, P. D. Colaizzi, S. R. Evett, T. A. Howell, and J. A. Tolk (2007), Remote sensing based energy balance algorithms for mapping ET: Current status and future challenges, *Trans. ASABE*, *50*, 1639-1644.

Gowda, P. H., J. L. Chavez, P. D. Colaizzi, S. R. Evett, T. A. Howell, and J. A. Tolk (2008), ET mapping for agricultural water management: present status and challenges, *Irrigation Science*, *26*, 223-237, doi 10.1007/s00271-007-0088-6.

Gowda, P. H., T. A. Howell, G. Paul, P. D. Colaizzi, T. H. Marek, B. Su, and K. S. Copeland (2013), Deriving hourly evapotranspiration rates with SEBS: A lysimetric evaluation, *Vadose Zone J.*, *12*, doi 10.2136/vzj2012.0110.

Heilman, J. L., W. E. Heilman, and D. G. Moore (1982), Evaluating the crop coefficient using spectral reflectance, *Agron. J.*, *74*, 967-971.

Heilman, J. L., K. J. McInnes, J. F. Kjelgaard, M. K. Owens, and S. Schwinning (2009), Energy balance and water use in a subtropical karst woodland on the Edwards Plateau, Texas, *J. Hydrol.*, *373*, 426-435, doi 10.1016/j.jhydrol.2009.05.007.

Hong, Y., K. L. Hsu, S. Sorooshian, and X. G. Gao (2004), Precipitation estimation from remotely sensed imagery using an artificial neural network cloud classification system, *J. Appl. Meteor.*, *43*, 1834-1852, doi 10.1175/jam2173.1.

Hsu, K. L., X. G. Gao, S. Sorooshian, and H. V. Gupta (1997), Precipitation estimation from remotely sensed information using artificial neural networks, *J. Appl. Meteor.*, *36*, 1176-1190.

Huete, A. R. (1988), A soil-adjusted vegetation index (SAVI), *Remote Sens. Environ.*, *25*, 295-309.

Hunsaker, D. J., P. J. Pinter, E. M. Barnes, and B. A. Kimball (2003), Estimating cotton evapotranspiration crop coefficients with a multispectral vegetation index, *Irrigation Science*, *22*, 95-104.

Huntington, J. L., and R. G. Allen (2010), Evapotranspiration and Net Irrigation Water Requirements for Nevada, State of Nevada, Division of Water Resources, *Rep.*, 260 pp, Carson City, NV.

Huntington, J. L., J. Szilagyi, S. W. Tyler, and G. M. Pohll (2011), Evaluating the complementary relationship for estimating evapotranspiration from arid shrublands, *Water Resour. Res.*, *47*, Artn W05533, doi 10.1029/2010wr009874.

Huntington, J. L., S. Gangopadhyay, M. Spears, R. G. Allen, D. King, C. Morton, A. Harrison, D. J. McEvoy, and A. Joros (2015), West-Wide Climate Risk Assessments: Irrigation Demand and Reservoir Evaporation Projections, U.S. Bureau of Reclamation, *Rep. 68-68210-2014-01*, 196 pp.

Jensen, M. E. (1998), Coefficients for Vegetative Evapotranspiration and Open Water Evaporation for the Lower Colorado River Accounting System, Bureau of Reclamation, *Rep.*, Boulder City, NV.

Jones, J. W., G. Hoogenboom, C. H. Porter, et al. (2003), The DSSAT cropping system model, *Eur. J. Agron.*, *18*, 235-265.

Karimi, P., and W. G. M. Bastiaanssen (2015), Spatial evapotranspiration, rainfall and land use data in water accounting - Part 1: Review of the accuracy of the remote sensing data, *Hydrol. Earth Syst. Sc.*, *19*, 507-532, doi 10.5194/hess-19-507-2015.

Keese, K. E., B. R. Scanlon, and R. C. Reedy (2005), Assessing controls on diffuse groundwater recharge using unsaturated flow modeling, *Water Resour. Res.*, *41*, W06010, doi 06010.01029/02004WR003841.

Khan, S. I., Y. Hong, B. Vieux, and W. J. Liu (2010), Development and evaluation of an actual evapotranspiration estimation algorithm using satellite remote sensing and meteorological observational network in Oklahoma, *Int J Remote Sens*, *31*, 3799-3819, Pii 925191365, Doi 10.1080/01431161.2010.483487.

Kitzmiller, D., D. Miller, R. Fulton, and F. Ding (2013), Radar and multisensor precipitation estimation techniques in National Weather Service Hydrologic Operations, *J. Hydrol. Eng.*, *18*, 133-142, doi:10.1061/(ASCE)HE.1943-5584.0000523.

Kustas, W. P., J. M. Norman, M. C. Anderson, and A. N. French (2003), Estimating subpixel surface temperatures and energy fluxes from the vegetation index-radiometric temperature relationship, *Remote Sens. Environ.*, *85*, 429-440.

Marek, T. H., D. O. Porter, P. H. Gowda, T. Howell, and J. Moorhead (2010), Assessment of Texas Evapotranspiration (ET) Networks, Texas Water Development Board, *Rep. 0903580904*, 367 pp, Austin, TX.

McCarl, B. A., and T. H. Spreen (1980), Price endogenous mathematical-programming as a tool for sector analysis, *Am J Agr Econ*, *62*, 87-102.

McCarl, B. A., C. R. Dillon, K. O. Keplinger, and R. L. Williams (1999), Limiting pumping from the Edwards Aquifer: An economic investigation of proposals, water markets, and spring flow guarantees, *Water Resour. Res.*, *35*, 1257-1268.

Mcnaughton, K. G., and P. G. Jarvis (1991), Effects of spatial scale on stomatal control of transpiration, *Agric. For. Meteorol.*, *54*, 279-302.

Menenti, M., and B. J. Choudhury (1993), Parameterization of land surface evapotranspiration using a location dependent potential evapotranspiration and surface temperature range, in *Exchange*

Processes at the Land Surface for a Range of Space and Time Scales, edited by H. J. Bolle, R. A. Feddes and J. D. Kalma, pp. 561-568, IAHS Press, Institute of Hydrology, Wallingford, Oxfordshire.

Menne, M. J., C. N. Williams, and R. S. Vose (2009), The U.S. Historical Climatology Network monthly temperature data, version 2, *B. Am. Meteorol. Soc.*, *90*, 993-1007, doi 10.1175/2008bams2613.1.

Mesinger, F., G. DiMego, E. Kalnay, et al. (2006), North American regional reanalysis, *B. Am. Meteorol. Soc.*, *87*, 343-360, doi 10.1175/BAMS-87-3-343.

Mitchell, K. E., D. Lohmann, P. R. Houser, et al. (2004), The multi-institution North American Land Data Assimilation System (NLDAS): Utilizing multiple GCIP products and partners in a continental distributed hydrological modeling system, *J. Geophys. Res - Atmos.*, *109*, D07S90, doi 10.1029/2003JD003823.

Moorhead, J., P. Gowda, M. Hobbins, G. Senay, G. Paul, T. Marek, and D. Porter (2015), Accuracy assessment of NOAA gridded daily reference evapotranspiration for the Texas High Plains, *J. Am. Water Resour. As.*, *51*, 1262-1271.

Moran, M. S., and R. D. Jackson (1991), Assessing the spatial distribution of evapotranspiration using remotely sensed inputs, *J. Environ. Qual.*, *20*, 725-737.

Morton, C. G., J. L. Huntington, G. M. Pohll, R. G. Allen, K. C. McGwire, and S. D. Bassett (2013), Assessing calibration uncertainty and automation for estimating evapotranspiration from agricultural areas using METRIC, *J. Am. Water Resour. As.*, 1-14, doi 10.1111/jawr.12054.

Narasimhan, B., R. Srinivasan, S. M. Quiring, and J. W. Nielsen-Gammon (2005), Digital Climatic Atlas of Texas, Texas Water Development Board, *Rep. 2005-483-559*, 31 pp, Austin, TX.

Nielson-Gammon, J. W. (2011), The Changing Climate of Texas, in *The Impact of Global Warming on Texas*, edited by J. Schmandt, G. R. North and J. Clarkson, pp. 39-68, University of Texas Press, Austin, TX.

Norman, J. M., W. P. Kustas, and K. S. Humes (1995), Source approach for estimating soil and vegetation energy fluxes in observations of directional radiometric surface temperature, *Agric. For. Meteorol.*, *77*, 263-293.

Norman, J. M., W. P. Kustas, J. H. Prueger, and G. R. Diak (2000), Surface flux estimation using radiometric temperature: A dual temperature-difference method to minimize measurement errors, *Water Resour. Res.*, *36*, 2263-2274.

Norman, J. M., M. C. Anderson, W. P. Kustas, A. N. French, J. Mecikalski, R. Torn, G. R. Diak, T. J. Schmugge, and B. C. W. Tanner (2003), Remote sensing of surface energy fluxes at 10^1-m pixel resolutions, *Water Resour. Res.*, *39*, Artn 1221, doi 10.1029/2002wr001775.

Norman, J. W. (1979), Modeling the complete crop canopy, in *Modification of the Aerial Environment of Plants*, edited by B. J. Barfield and J. F. Gerber, pp. 249-277, American Society of Agricultural Engineers, St. Joseph, Michigan.

Paul, G., P. H. Gowda, P. V. V. Prasad, T. A. Howell, S. A. Staggenborg, and C. M. U. Neale (2013), Lysimetric evaluation of SEBAL using high resolution airborne imagery from BEAREX08, *Adv. Water Resour.*, *59*, 157-168, doi 10.1016/j.advwatres.2013.06.003.

Porter, D., P. Gowda, T. Marek, T. Howell, J. Moorhead, and S. Irmak (2012), Sensitivity of grass- and alfalfa-reference evapotranspiration to weather station sensor accuracy, *Applied Engineering in Agriculture*, *28*, 543-549.

Price, J. C. (1990), Using spatial context in satellite data to infer regional scale evapotranspiration, *IEEE Trans. Geosci. Remote Sens.*, *28*, 940-948, doi 10.1109/36.58983.

Roerink, G. J., Z. Su, and M. Menenti (2000), S-SEBI: A simple remote sensing algorithm to estimate the surface energy balance, *Phys. Chem. Earth Pt. B.*, *25*, 147-157.

Scanlon, B. R., R. C. Reedy, J. B. Gates, and P. H. Gowda (2010), Impact of agroecosystems on groundwater resources in the Central High Plains, USA, *Agriculture Ecosystems & Environment*, *139*, 700-713.

Schroeder, J. L., W. S. Burgett, K. B. Haynie, I. Sonmez, G. D. Skwira, A. L. Doggett, and J. W. Lipe (2005), The West Texas Mesonet: A technical overview, *Journal Of Atmospheric And Oceanic Technology*, *22*, 211-222, doi 10.1175/Jtech-1690.1.

Serrat-Capdevila, A., J. B. Valdes, and E. Z. Stakhiv (2013), Water management applications for satellite precipitation products: Synthesis and recommendations, *J. Am. Water Resour. As.*, *50*, 509-525, doi 10.1111/jawr.12140.

Singh, R. K., A. Irmak, S. Irmak, and D. L. Martin (2008), Application of SEBAL model for mapping evapotranspiration and estimating surface energy fluxes in south-central Nebraska, *J. Irrig. Drain. Eng.*, *134*, 273-285.

Su, Z. (2002), The Surface Energy Balance System (SEBS) for estimation of turbulent heat fluxes, *Hydrol. Earth Syst. Sc.*, *6*, 85-99.

Tasumi, M., and R. G. Allen (2007), Satellite-based ET mapping to assess variation in ET with timing of crop development, *Agr. Water Manage.*, *88*, 54-62, doi 10.1016/j.agwat.2006.08.010.

Tasumi, M., R. G. Allen, R. Trezza, and J. L. Wright (2005), Satellite-based energy balance to assess with in-population variance of crop coefficient curves, *J. Irrig. Drain. Eng.*, *131*, 94-109.

Thornton, P. E., S. W. Running, and M. A. White (1997), Generating surfaces of daily meteorological variables over large regions of complex terrain, *J. Hydrol.*, *190*, 214-251.

Todd, R. W., S. R. Evett, and T. A. Howell (2000), The Bowen ratio-energy balance method for estimating latent heat flux of irrigated alfalfa evaluated in a semi-arid, advective environment, *Agric. For. Meteorol.*, *103*, 335-348.

Tolk, J. A., and T. A. Howell (2001), Measured and simulated evapotranspiration of grain sorghum grown with full and limited irrigation in three high plains soils, *Trans. ASAE*, *44*, 1553-1558.

Turner, C. G., K. McAfee, S. Pandey, and A. Sunley (2011), Irrigation Metering and Water Use Estimates: A Comparative Analysis, 1999-2007, Texas Water Development Board, *Rep. 378*, 137 pp, Austin, TX.

TWDB (2014), 2014 Texas Water Use Summary Estimates, *accessed* 1 November 2014, https://www.twdb.texas.gov/waterplanning/waterusesurvey/estimates/index.asp,

TWDB (2017), Water for Texas 2017 State Water Plan, Texas Water Development Board, *Rep.*, 133 pp, Austin, TX.

Wilson, K., A. Goldstein, E. Falge, et al. (2002), Energy balance closure at FLUXNET sites, *Agric. For. Meteorol.*, *113*, 223-243.

W. M. Organization, WMO (2008), Guide to Meteorological Instruments and Methods of Observation, World Meteorological Organization, Rep. WMO-No.8, 680 pp, Geneva 2, Switzerland

Wright, J. L. (1982), New evapotranspiration crop coefficients, *J. Irr. Drain. Div.*, *108*, 57-74.

Xia, Y. L., M. Ek, H. L. Wei, and J. Meng (2012), Comparative analysis of relationships between NLDAS-2 forcings and model outputs, *Hydrol. Process.*, *26*, 467-474, doi 10.1002/Hyp.8240.

Zhu, Z., and C. E. Woodcock (2012), Object-based cloud and cloud shadow detection in Landsat imagery, *Remote Sens. Environ.*, *118*, 83-94.

Zhu, Z., and C. E. Woodcock (2014), Automated cloud, cloud shadow, and snow detection in multitemporal Landsat data: An algorithm designed specifically for monitoring land cover change, *Remote Sens. Environ.*, *152*, 217-234.

Zhu, Z., S. X. Wang, and C. E. Woodcock (2015), Improvement and expansion of the Fmask algorithm: cloud, cloud shadow, and snow detection for Landsats 4-7, 8, and Sentinel 2 images, *Remote Sens. Environ.*, *159*, 269-277.

CONTENTS

Appendix A: Statistical analysis of gridded precipitation data

1. Conventional Statistics

Mean absolute error (MAE) measures the average magnitude of the errors in a set of forecasts, without considering their direction (or sign). It measures accuracy for continuous variables. The MAE is a linear score which means that all the individual differences are weighted equally in the average.

$$MAE = \frac{1}{n}\int_{i=1}^{n}(S_i - O_i)$$

Where n is the number of corresponding days of gridded or simulated (S) and observed (O) data from gages.

Root mean square error (*RMSE*) is a quadratic scoring rule which measures the average magnitude of the error. Since the errors are squared, *RMSE* gives a relatively high weight to bigger errors. This means the RMSE is most useful when large errors are particularly undesirable.

$$RMSE = \left[\frac{1}{n}\int_{i=1}^{n}(S_i - O_i)^2\right]^{1/2}$$

Both the *MAE* and *RMSE* range from 0 to ∞ and have units equal to their data source. They are negatively-oriented scores: lower values indicate a better prediction.

Percent bias (PBIAS) measures the average tendency of the simulated values to be larger or smaller than their observed ones. The optimal value of PBIAS is 0.0, with low-magnitude values indicating accurate model skill while positive values indicate overestimation and negative values indicate underestimation.

$$PBIAS = \frac{\int_{i=1}^{n}(S_i - O_i)}{\int_{i=1}^{n}(O_i)} * 100$$

Correlation coefficient (R) and coefficient of determination (R^2) are the degree of collinearity between simulated and observed data. Pearson's *R* ranges from -1 to +1 indicating the direction of correlation while a values near 0 indicate poor correlations. Variance is described by R^2 ranging between 0 and 1 with a higher value indicating less variance between the model and the observations. Both *R* and R^2 are more sensitive to outliers but do provide a simple measure of simulated performance.

2. Dichotomous Statistics

Dichotomous statistics determine the probability that an event occurred and whether or not the gridded product forecast that event. For our analysis, we are simply comparing observed and simulated days with rainfall. There are four combinations of dichotomous ('yes' or 'no') predictions:

1. *Hit*: event occurred and was predicted
2. *Miss*: event occurred by not predicted
3. *False alarm*: event predicted by did not occur
4. *Correct negative*: event predicted to not occur and no event occurred

Frequency bias (*FB*) indicates the tendency for a model to under-predict (FB<1) or over-predict (FB>1) events

$$FB = \frac{hits + false\ alarms}{hits + misses}$$

A score of 1 is perfect. The probability of detection (*POD*) measures the fraction of observed days with rain detected by the model as

$$POD = \frac{hits}{hits + misses}$$

which ranges from 0 (poor) to 1 (perfect). The false alarm ratio (FAR) determines the fraction of simulated precipitation days that did not occur as

$$FAR = \frac{false\ alarms}{hits + false\ alarms}$$

3. Accuracy Index

Precipitation has both a length component (how much it rained) as well as an event component (did it rain). The former is determined through conventional statistics and the latter through dichotomous; together these are normalized into an accuracy index [*Ebert et al.*, 2007]. The precipitation accuracy index (*PAI*) consists of five prior variables including normalized *RMSE* and *MBE*, R^2, *POD*, and *FAR*. Normalization is performed by subtracting the minimum value from each and dividing by its range (maximum – minimum). The PAI is calculated as the weighted average of these five by

$$PAI = \frac{1}{5}(1 - nRMSE) + \frac{1}{5}(1 - nMAE) + \frac{1}{5}(R^2) + \frac{1}{5}(POD) + \frac{1}{5}(1 - FAR)$$

The *PAI* ranges from 0 (poor) to 1 (perfect) skill index which includes both conventional and dichotomous performance.

Appendix B: Landsat 5 Thematic Mapper Data

Table B1. Total number of cloud-free observations from January 2005 to November 2011 by climate division.

Scene Identifier	Named Location	Climate Division Primary	Climate Division Secondary	Climate Division Tertiary	Total Count
p24r38	Hemphill	5			47
p24r39	Orange	5			36
p25r37	Texarkana	5			43
p25r38	Nacogdoches	5			30
p25r39	Houston	5			23
p25r40	Freeport	5			23
p26r36	Hugo	5			38
p26r37	Mount Pleasant	5	3		43
p26r38	Corsicana	5	3		37
p26r39	College Station	5			31
p26r40	Victoria	5	4		24
p26r41	Corpus Christi	4			24
p26r42	Brownsville	4			18
p27r36	Denison	3			46
p27r37	Dallas	3	5		44
p27r38	Waco	3	5		42
p27r39	Austin	3	5	4	32
p27r40	San Antonio	4	3		33
p27r41	Freer	4			37
p27r42	McAllen	4			37
p28r36	Wichita Falls	3	2		54
p28r37	Mineral Wells	3	2		53
p28r38	Brownwood	3	2		51
p28r39	Kerrville	3	2		42
p28r40	Eagle Pass	4	3		37
p28r41	Laredo	4			35
p29r35	Allison	1			50
p29r36	Childress	2	1	3	53
p29r37	Abilene	2			51
p29r38	San Angelo	2			46
p29r39	Sonora	2	3		38
p29r40	Del Rio	4	2		44
p30r35	Borger	1			54
p30r36	Amarillo	1	2		61
p30r37	Lubbock	1	2		61
p30r38	Midland	2	1		57
p30r39	Fort Stockton	2			66

p30r40	Big Bend	2		73
p31r35	Dalhart	1		57
p31r36	Muleshoe	1		66
p31r37	Brownfield	1	2	72
p31r38	Pecos	2	1	67
p31r39	Fort Davis	2	1	61
p31r40	Terlingua	2		78
p32r38	Van Horn	1	2	76
p32r39	Candelaria	1	2	84
p33r38	El Paso	1		70

Table B2. Annual counts of cloud-free Landsat 5 Thematic Mapper observations in Texas with summary statistics

Scene Identifier	Total Count	2005 Count	2006 Count	2007 Count	2008 Count	2009 Count	2010 Count	2011 Count	Mean	Min	Max	Median
p24r38	47	3	5	3	10	10	7	9	6	3	10	7
p24r39	36	4	4	1	9	6	7	5	5	1	9	5
p25r37	43	3	7	6	7	6	6	8	6	3	8	6
p25r38	30	0	5	3	8	4	5	5	4	0	8	5
p25r39	23	0	6	1	3	4	4	5	3	0	6	4
p25r40	23	0	5	3	4	5	3	3	3	0	5	3
p26r36	38	8	7	3	2	6	5	7	5	2	8	6
p26r37	43	6	5	5	4	7	6	10	6	4	10	6
p26r38	37	6	6	2	2	10	4	7	5	2	10	6
p26r39	31	5	6	2	3	5	4	6	4	2	6	5
p26r40	24	3	2	4	3	4	5	3	3	2	5	3
p26r41	24	1	2	4	2	4	5	6	3	1	6	4
p26r42	18	2	2	2	3	3	3	3	2	2	3	3
p27r36	46	7	7	6	5	9	4	8	6	4	9	7
p27r37	44	9	5	2	4	9	7	8	6	2	9	7
p27r38	42	9	3	3	7	7	5	8	6	3	9	7
p27r39	32	7	2	3	4	5	5	6	4	2	7	5
p27r40	33	6	3	2	4	6	6	6	4	2	6	6
p27r41	37	6	5	2	4	6	6	8	5	2	8	6
p27r42	37	6	5	3	5	7	6	5	5	3	7	5
p28r36	54	9	8	2	11	9	6	9	7	2	11	9
p28r37	53	6	7	4	8	7	11	10	7	4	11	7
p28r38	51	8	10	4	4	7	7	11	7	4	11	7
p28r39	42	6	5	3	4	6	7	11	6	3	11	6
p28r40	37	6	5	3	3	6	5	9	5	3	9	5
p28r41	35	3	3	3	2	7	6	11	5	2	11	3
p29r35	50	6	7	3	10	7	7	10	7	3	10	7
p29r36	53	7	8	4	10	5	7	12	7	4	12	7
p29r37	51	4	9	3	10	8	6	11	7	3	11	8
p29r38	46	2	8	1	8	6	10	11	6	1	11	8
p29r39	38	4	5	1	7	5	7	9	5	1	9	5
p29r40	44	5	8	2	7	6	7	9	6	2	9	7
p30r35	54	9	9	4	9	6	9	8	7	4	9	9

p30r36	61	10	7	6	12	8	10	8	8	6	12	8
p30r37	61	6	7	4	13	10	11	10	8	4	13	10
p30r38	57	5	8	6	11	12	8	7	8	5	12	8
p30r39	66	8	8	9	11	10	11	9	9	8	11	9
p30r40	73	7	6	9	13	12	13	13	10	6	13	12
p31r35	57	5	11	7	8	9	9	8	8	5	11	8
p31r36	66	7	12	8	10	8	11	10	9	7	12	10
p31r37	72	8	12	8	10	10	12	12	10	8	12	10
p31r38	67	7	12	5	10	9	13	11	9	5	13	10
p31r39	61	5	9	6	8	8	13	12	8	5	13	8
p31r40	78	10	9	9	11	9	14	16	11	9	16	10
p32r38	76	9	12	8	14	10	13	10	10	8	14	10
p32r39	84	13	12	13	16	9	10	11	12	9	16	12
p33r38	70	8	11	3	11	14	10	13	10	3	14	11

Appendix C: Reference ET stations and statistics

Table C1. West Texas Mesonet and SCAN stations used for assessing NLDAS estimated ET_r to weather station computed ET_r.

Station Name	Station	Corrections	Additional Notes
5ENE Abernathy	1	RS	
1NE Amherst	5	RS	
2E Andrews	6	RS RH	Adjusted RH about 5% for a couple years.
6SSW Anton	7	RS	
3NE Aspermont	8	RS	
2S Brownfield	11	RS	
2NNE Childress	13	RS	1 year missing, data needed heavy correction.
2WSW Clarendon	14	RS RH	Filled in ~ 1 month missing temp and RH values with monthly avgs
2N Coyanosa	16	RS MISSING DATA	Only about 1.5 years present.
2NE Dimmitt	18	RS	RS adjusted ~-10% between 2010 and 2011.
2NNE Floydada	20	RS	
3WNW Fluvanna	21	RS	RS adjusted ~-10% in several places.
2NE Friona	22	RS	RS adjusted ~-10% in several places. RS missing ~1.5 month data.
2 ESE Gail	23	RS	
3W Goodlett	24	RS RH	Filled in ~ 2 months missing temp and RH values with monthly avgs in 2 locations
5SSW Graham	25	RS	
10WSW Guthrie	26	RS	
3N Hart	27	RS	
1NW Haskell	28	RS MISSING DATA	Missing 2006-2009, processed anyways.
2NW Hereford	29	RS	Threw out ~3 months of RS data due to sensor malfunction.

1SSE Jayton	31	RS	
2SE Lamesa	35	RS RH	RH adjusted ~5%
4S Levelland	36	RS	
3WNW Lubbock-TTU	38	RS RH	First half of 2006 missing, corrected RH about 10%.
1E McLean	39	RS	Two months of 2009 are missing.
1NE Memphis	40	RS	
1ENE Morton	42	RS	
2SSW Muleshoe	43	RS	
1S Northfield	44	RS MISSING DATA	2006-Early 2008 is missing, corrected anyways.
4ENE Odell	45	RS MISSING DATA	Only about 1.5 years present.
6S of Olton	47	RS	
10SW Paducah	48	RS	RS adjusted ~-10% in several places.
2E Pampa	50	RS	
3N Plains	53	RS	
1S Plainview	54	RS	
1NE Post	55	RS	
1SE Ralls	57	RS	
12W Lubbock (Reese)	58	RS	RS needed to be de-spiked in several locations.
1SW Seagraves	61	RS	First half of 2008 missing.
2NNE Seminole	62	RS	
3NW Seymour	63	RS RH MISSING DATA	2006-Late 2009 is missing, corrected anyways, adjusted RH about 5%.
7ESE Silverton	64	RS RH	Removed bad RH value in one location.
2NE Slaton	65	RS	
3E Snyder	66	RS	

1W Spur	67	RS	Corrected RS +10% in one location.
8WSW Sundown	70	RS	
3NNE Tahoka	71	RS	
2ENE Tulia	73	RS	Didn't de-spike precip because the high value seemed natural.
2WSW Turkey	74	RS	2006 is missing, eliminated about 2 months of bad data from RS
1E Wall	76	RS MISSING DATA	2006-Late 2009 is missing, corrected anyways.
6SSW Wolfforth	79	RS RH	Corrected RH +5%
SCAN_BUSHLAND	1	RS MISSING DATA	Late 2005-2009 is missing.

RS = solar radiation

RH = relative humidity

Appendix D. Croplands for 2010 and 2011 extracted from CDL for pilot study counties.

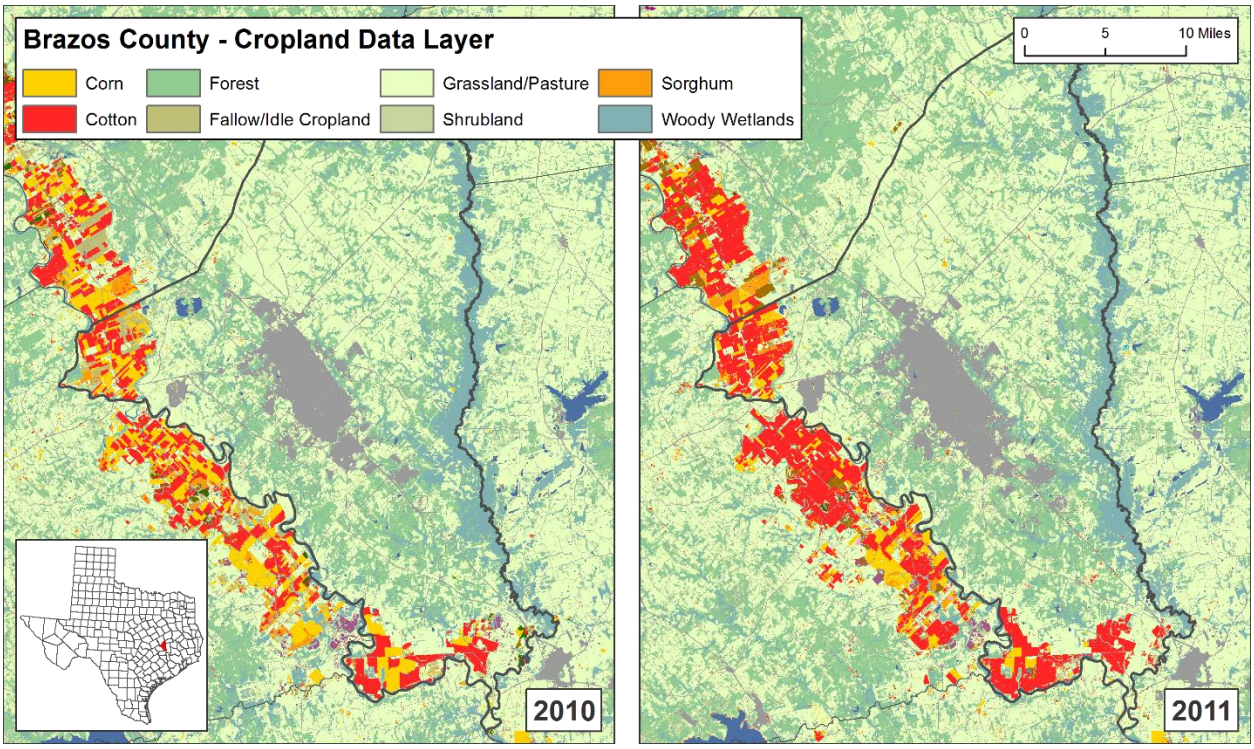

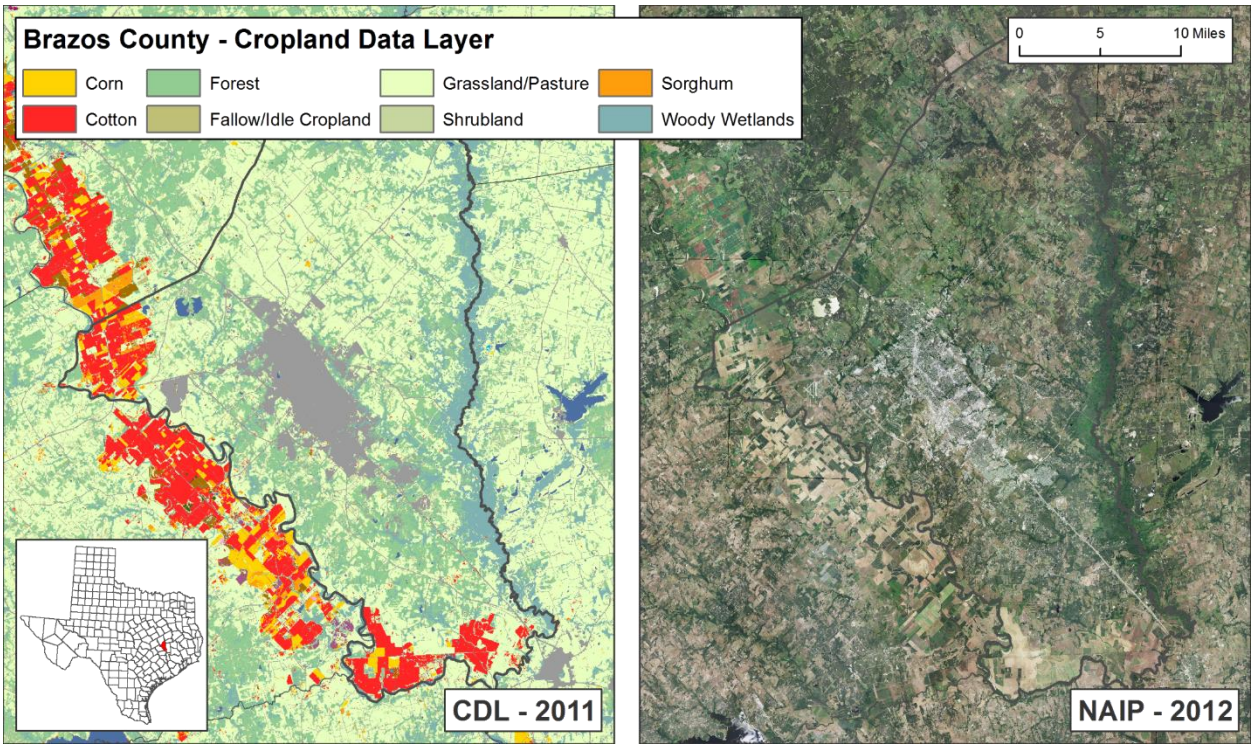

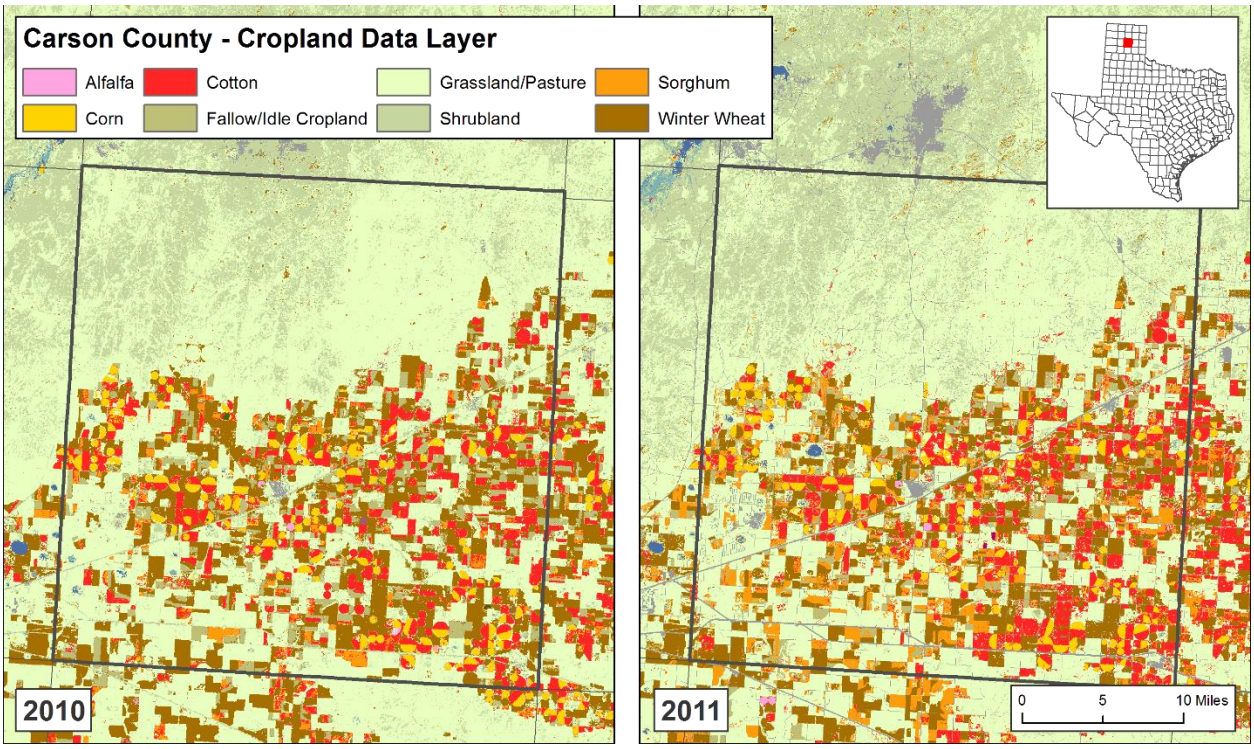
Carson County - Cropland Data Layer
Alfalfa
Cotton
Grassland/Pasture
Sorghum
Corn
Fallow/Idle Cropland
Shrubland
Winter Wheat
2010
2011
0
5
10 Miles

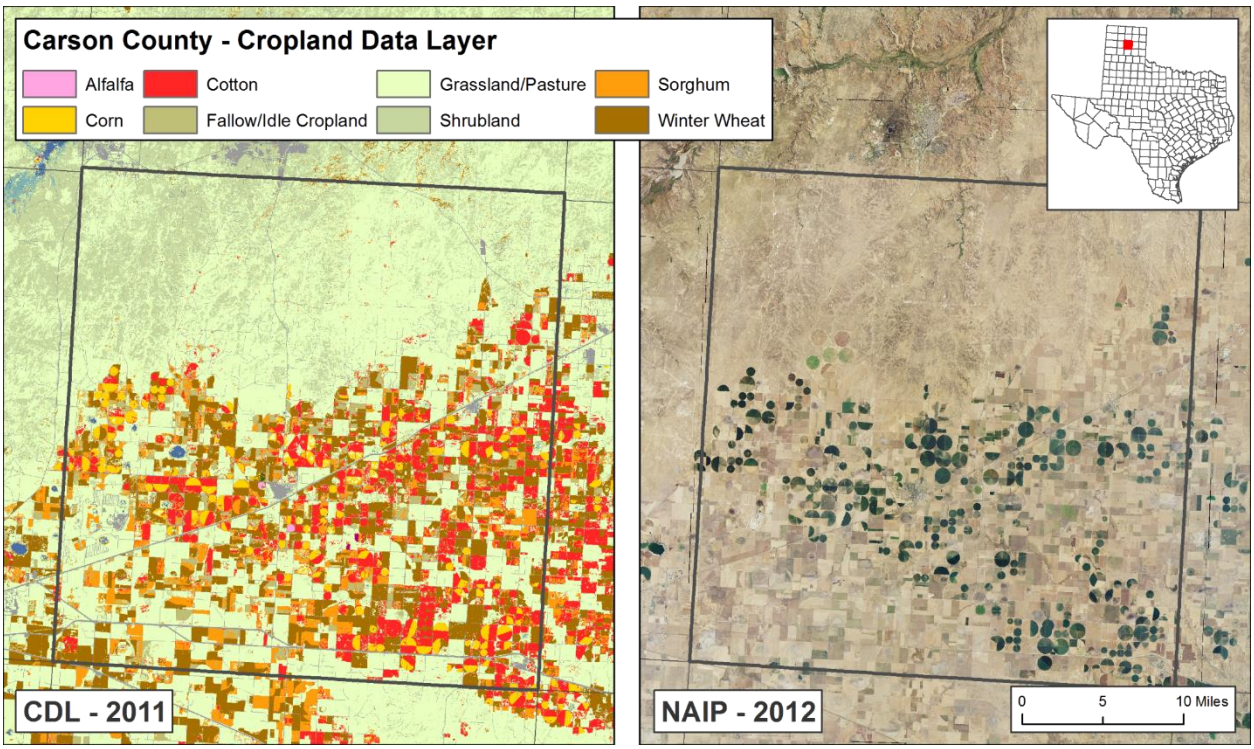
Carson County - Cropland Data Layer
Alfalfa
Cotton
Grassland/Pasture
Sorghum
Corn
Fallow/Idle Cropland
Shrubland
Winter Wheat
CDL - 2011
NAIP - 2012
0
5
10 Miles

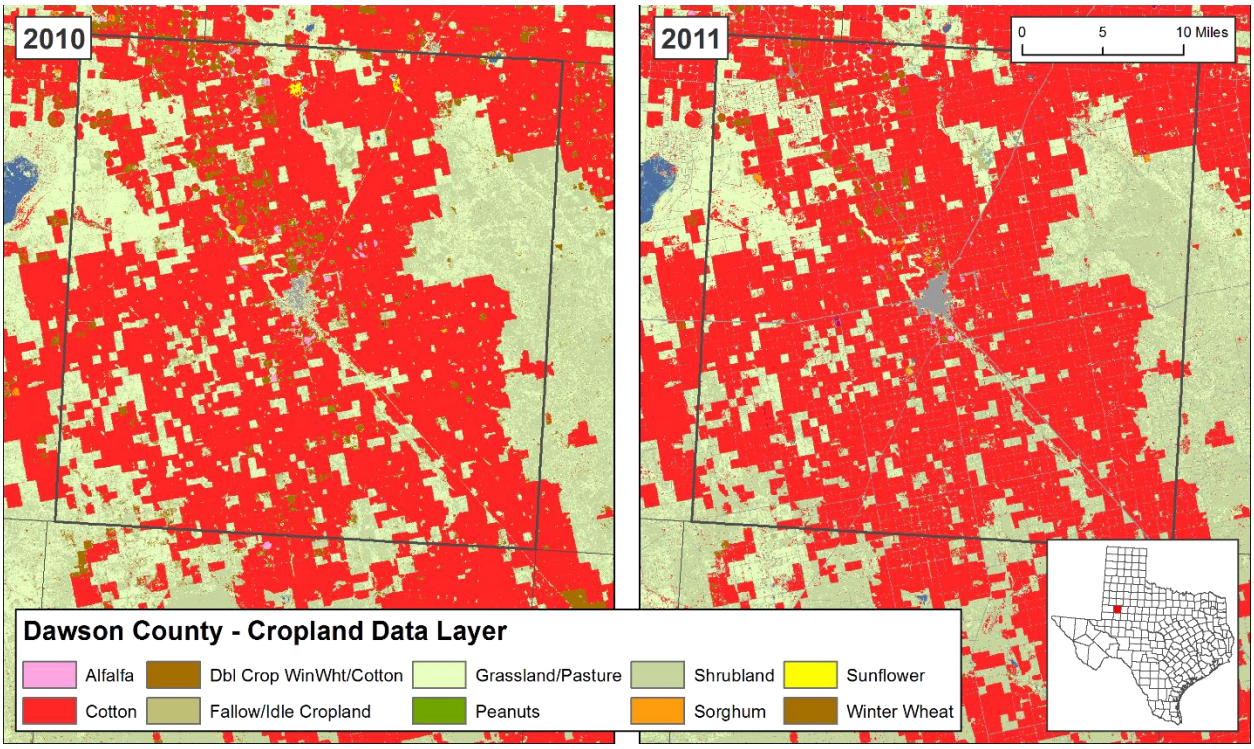
2010
2011
0 5 10 Miles
Dawson County - Cropland Data Layer
Alfalfa
Dbl Crop WinWht/Cotton
Grassland/Pasture
Shrubland
Sunflower
Cotton
Fallow/Idle Cropland
Peanuts
Sorghum
Winter Wheat

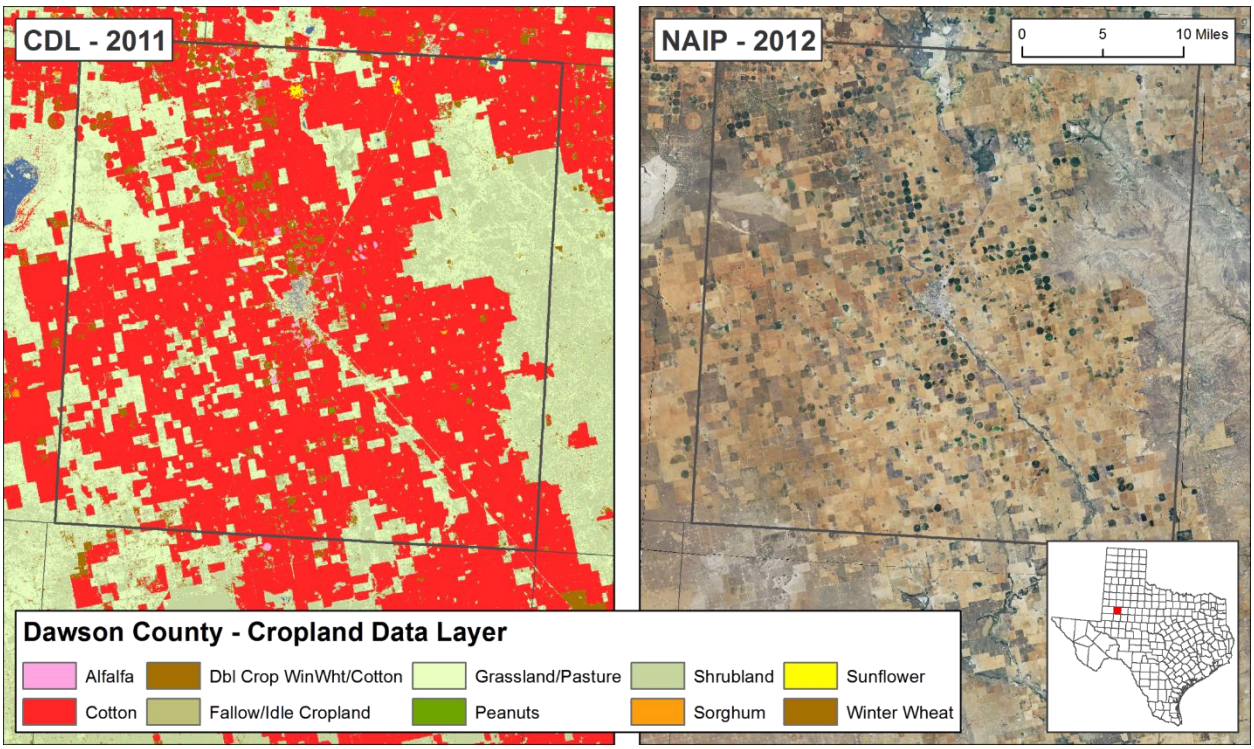
CDL - 2011
NAIP - 2012
0 5 10 Miles
Dawson County - Cropland Data Layer
Alfalfa
Dbl Crop WinWht/Cotton
Grassland/Pasture
Shrubland
Sunflower
Cotton
Fallow/Idle Cropland
Peanuts
Sorghum
Winter Wheat

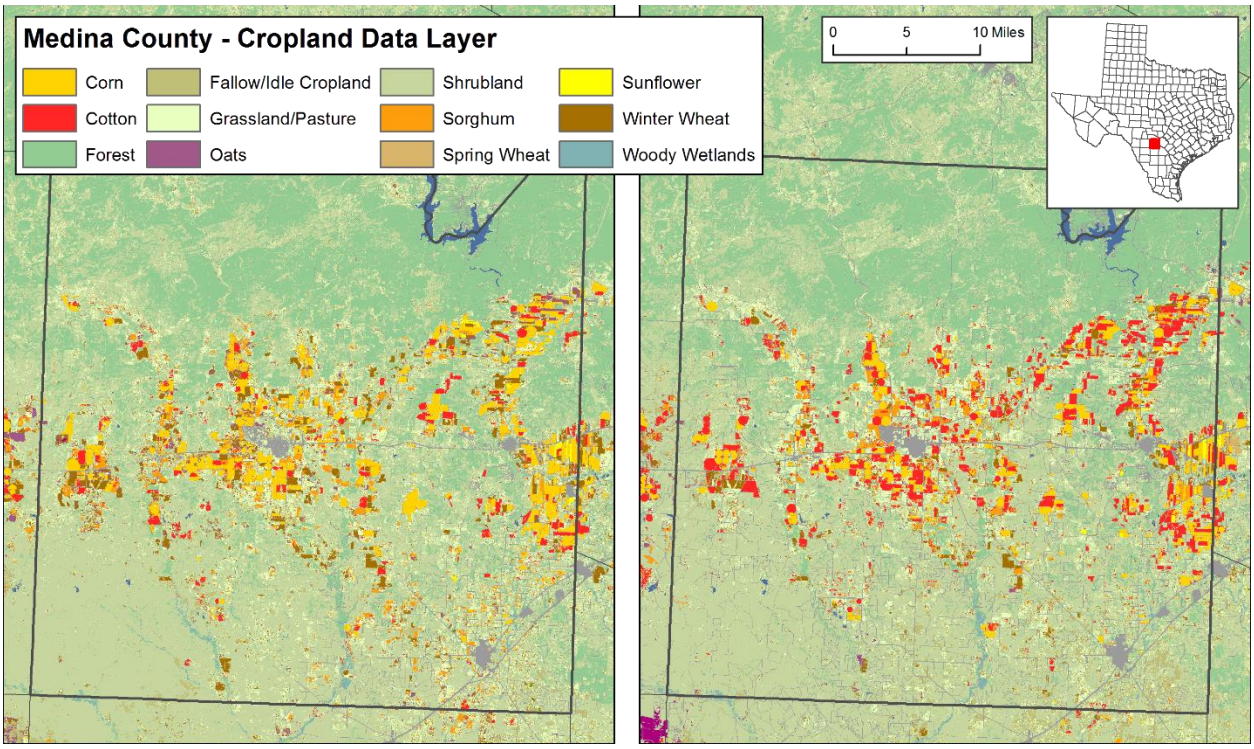
Medina County - Cropland Data Layer
Corn
Cotton
Forest
Fallow/Idle Cropland
Grassland/Pasture
Oats
Shrubland
Sorghum
Spring Wheat
Sunflower
Winter Wheat
Woody Wetlands
0
5
10 Miles

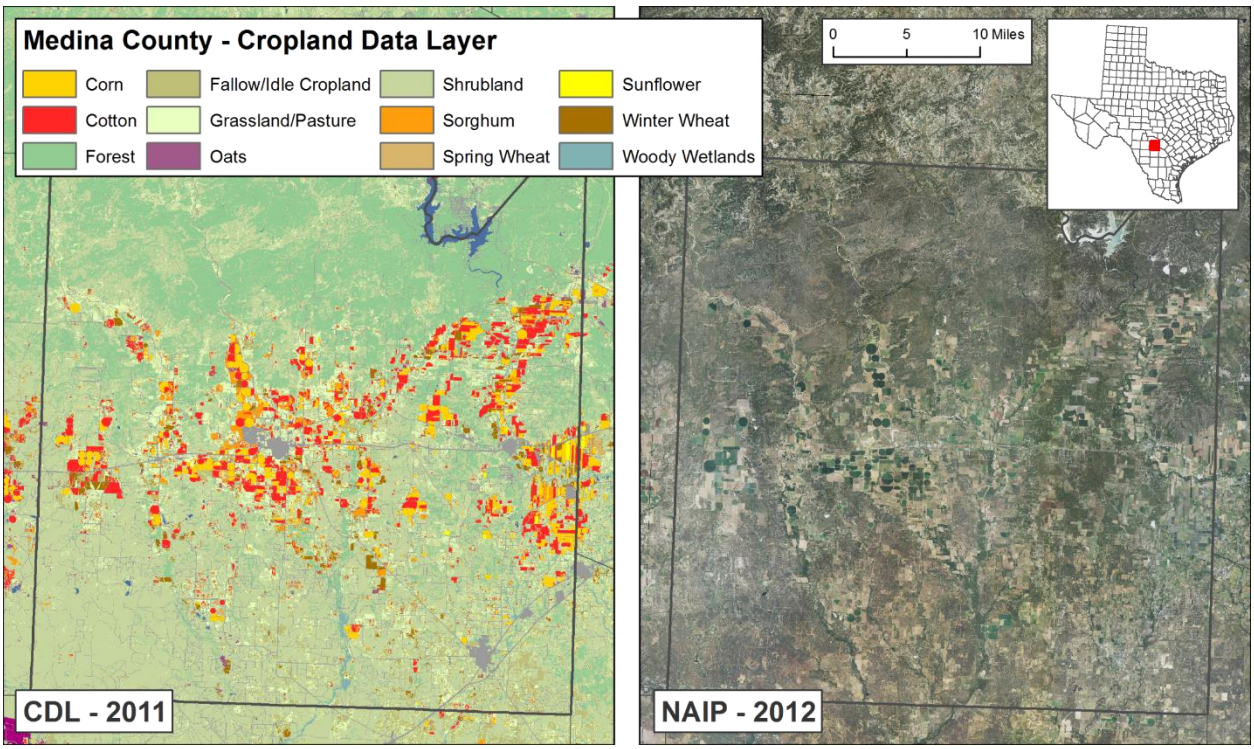
Medina County - Cropland Data Layer
Corn
Cotton
Forest
Fallow/Idle Cropland
Grassland/Pasture
Oats
Shrubland
Sorghum
Spring Wheat
Sunflower
Winter Wheat
Woody Wetlands
0
5
10 Miles
CDL - 2011
NAIP - 2012

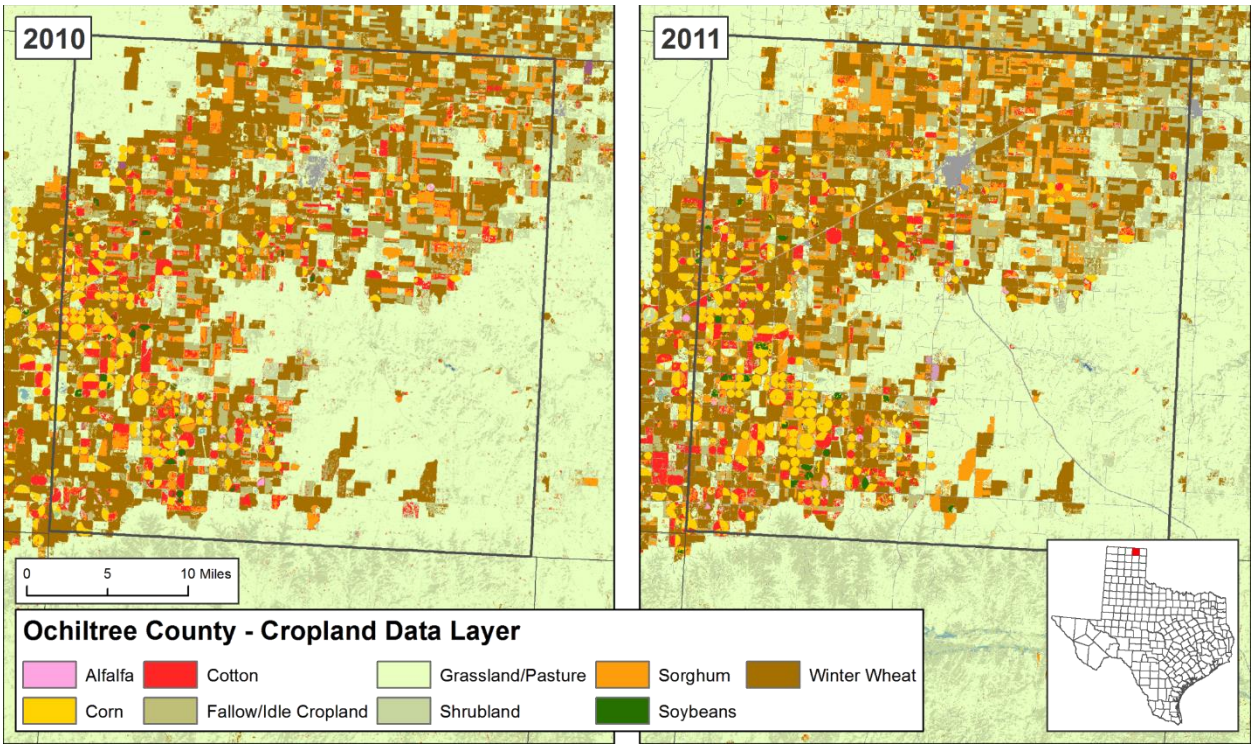
2010
2011
0 5 10 Miles
Ochiltree County - Cropland Data Layer
Alfalfa
Cotton
Grassland/Pasture
Sorghum
Winter Wheat
Corn
Fallow/Idle Cropland
Shrubland
Soybeans

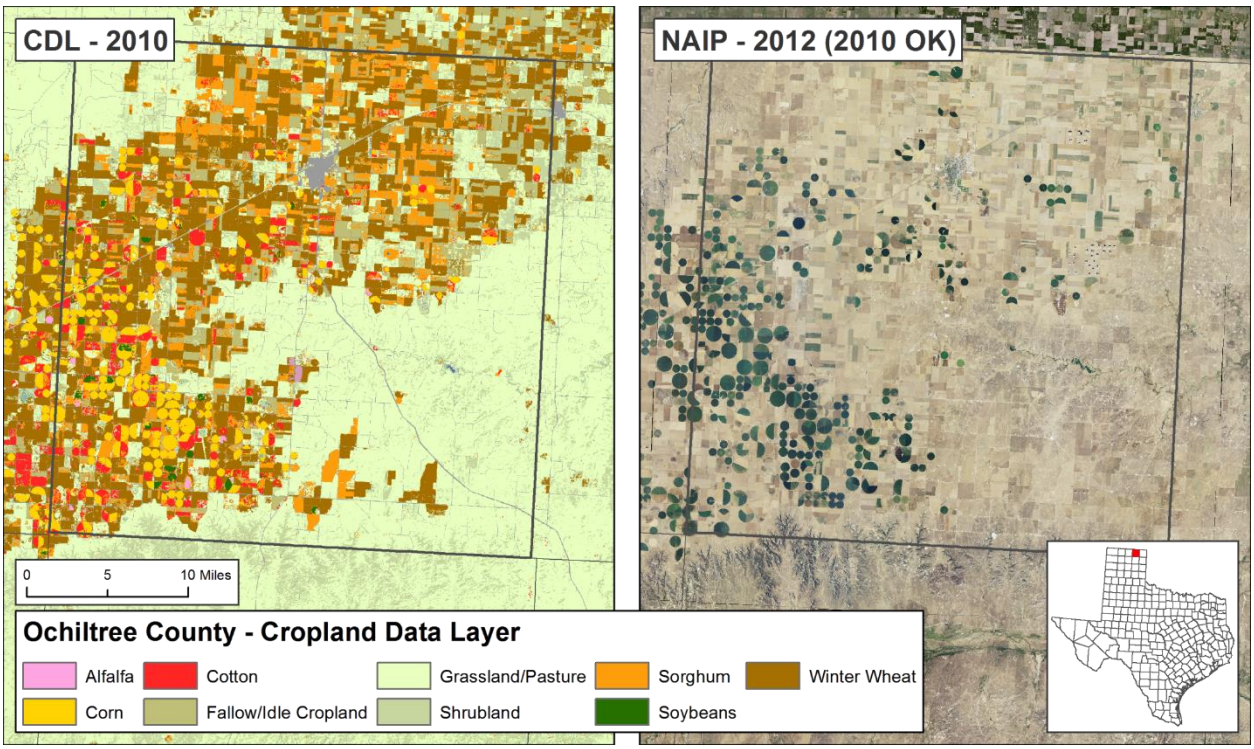
CDL - 2010
NAIP - 2012 (2010 OK)
0 5 10 Miles
Ochiltree County - Cropland Data Layer
Alfalfa
Cotton
Grassland/Pasture
Sorghum
Winter Wheat
Corn
Fallow/Idle Cropland
Shrubland
Soybeans

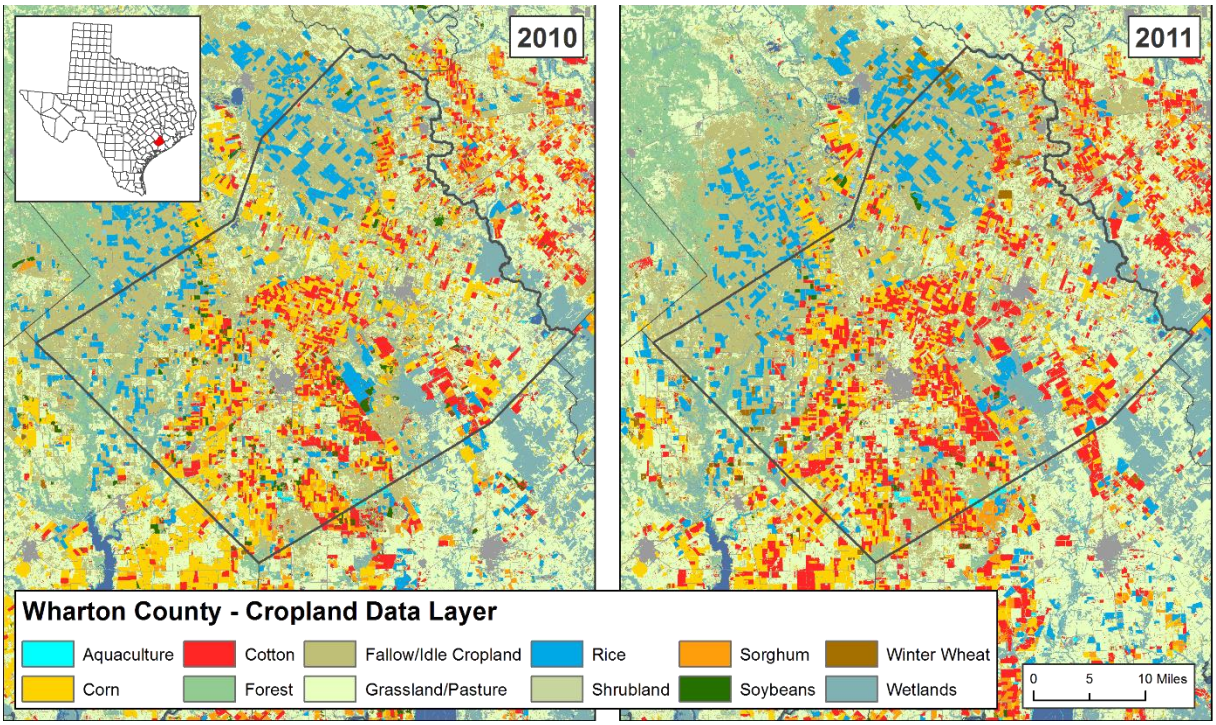
2010
2011
Wharton County - Cropland Data Layer
Aquaculture
Cotton
Fallow/Idle Cropland
Rice
Sorghum
Winter Wheat
Corn
Forest
Grassland/Pasture
Shrubland
Soybeans
Wetlands
0 5 10 Miles

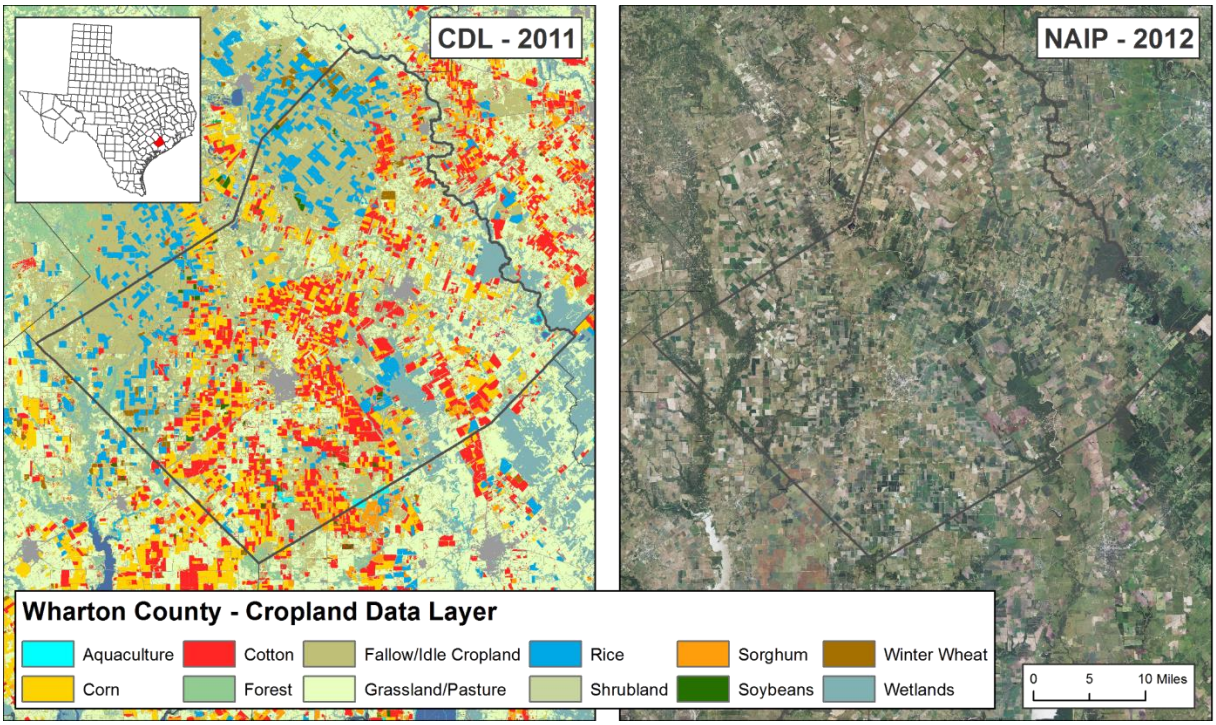
CDL - 2011
NAIP - 2012
Wharton County - Cropland Data Layer
Aquaculture
Cotton
Fallow/Idle Cropland
Rice
Sorghum
Winter Wheat
Corn
Forest
Grassland/Pasture
Shrubland
Soybeans
Wetlands
0 5 10 Miles

Appendix E. METRIC average *ETrF* results for pilot study counties and masked to CDL cropland areas.

Brazos County

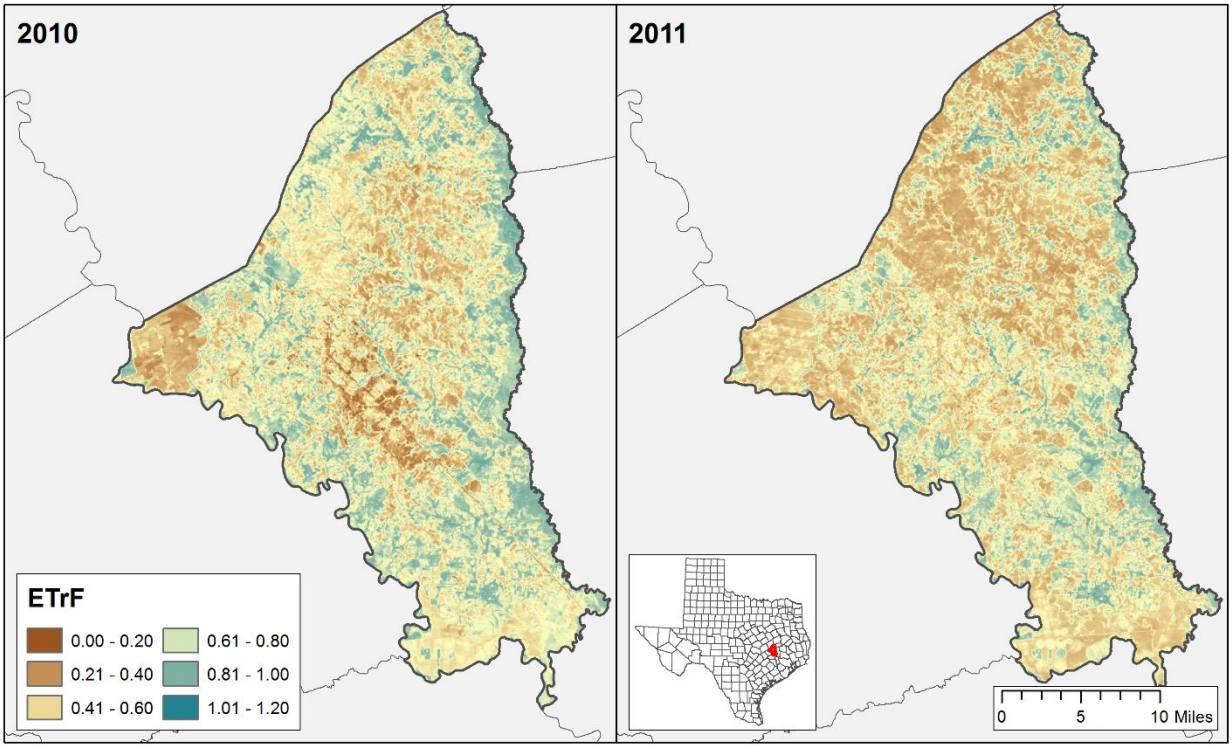

Brazos County

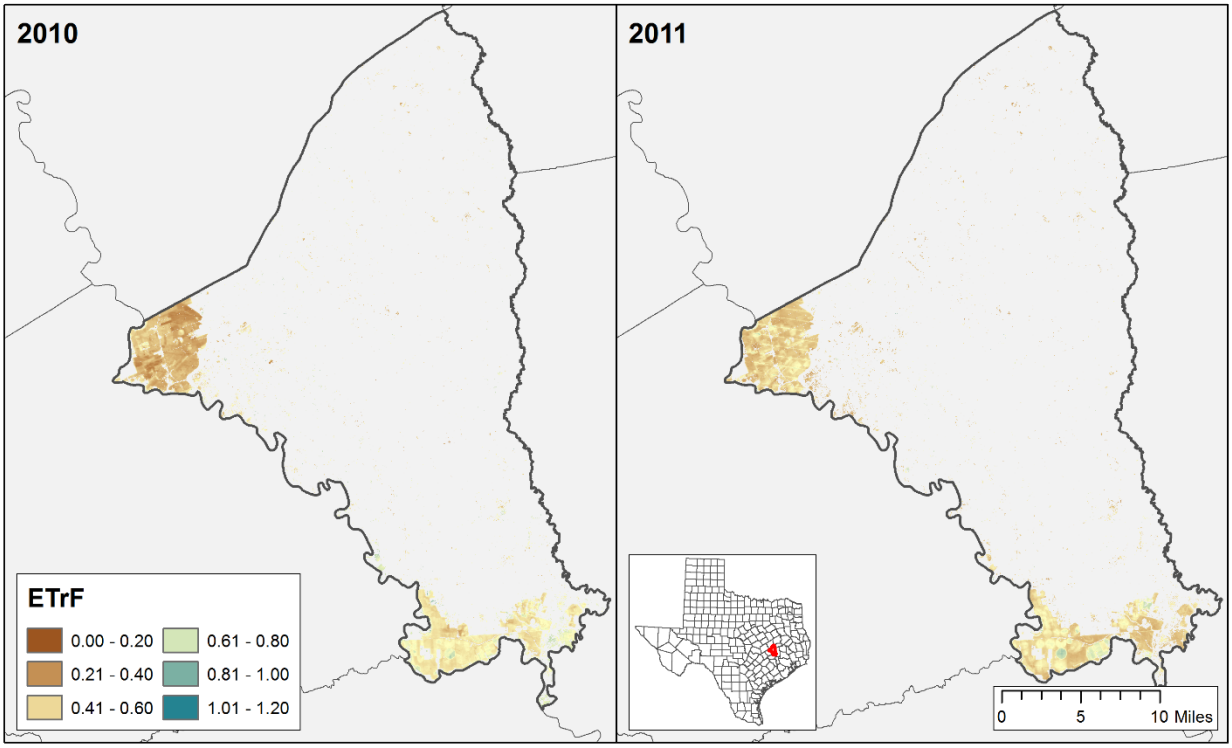

Cameron County

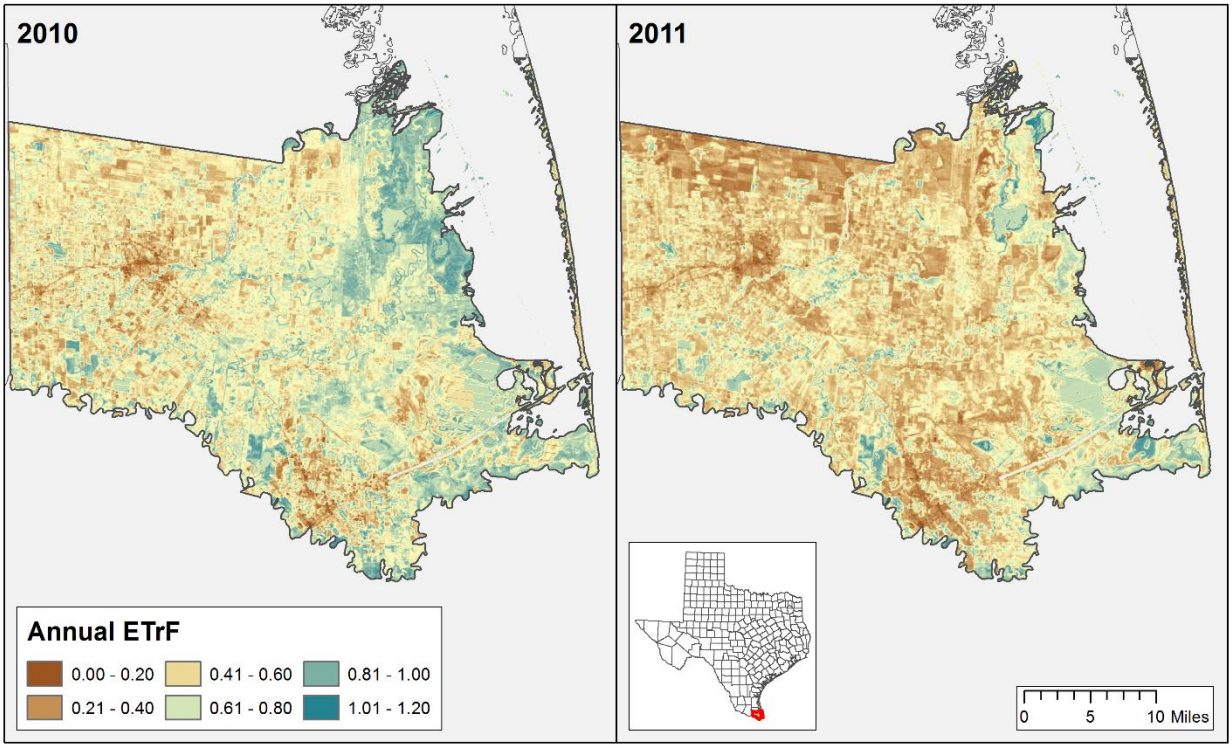

Cameron County

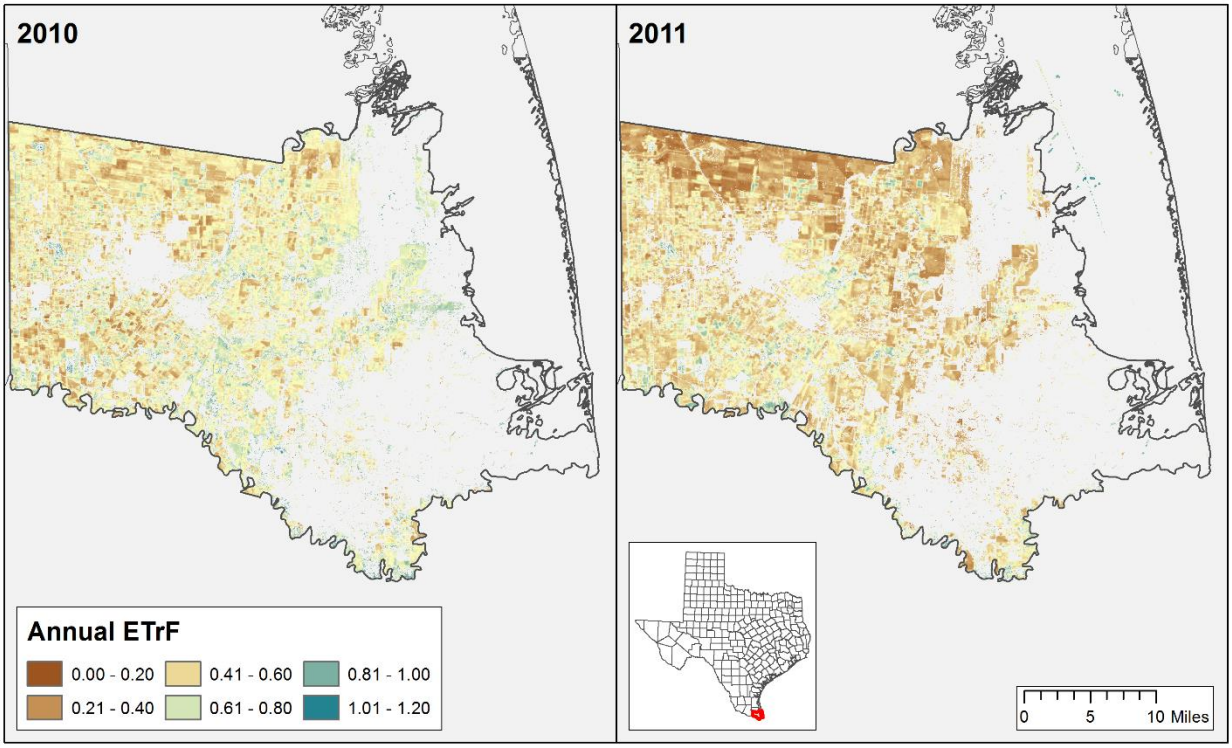

Carson County

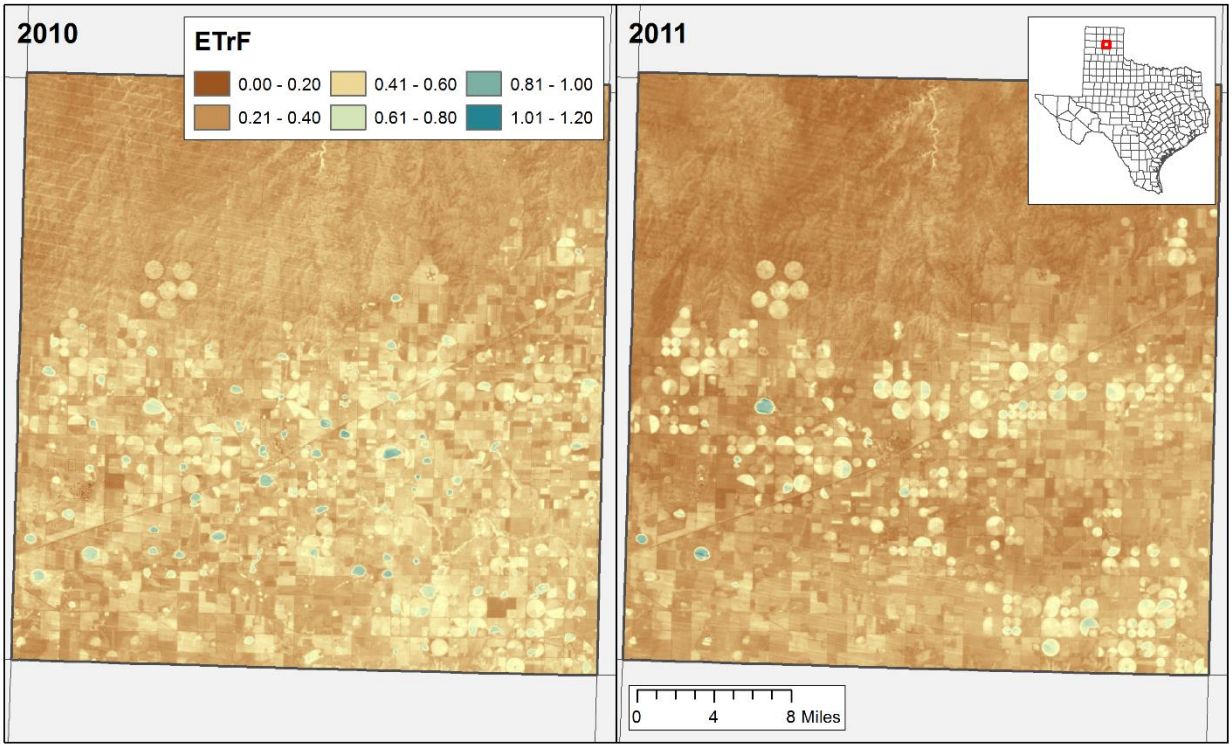

Carson County

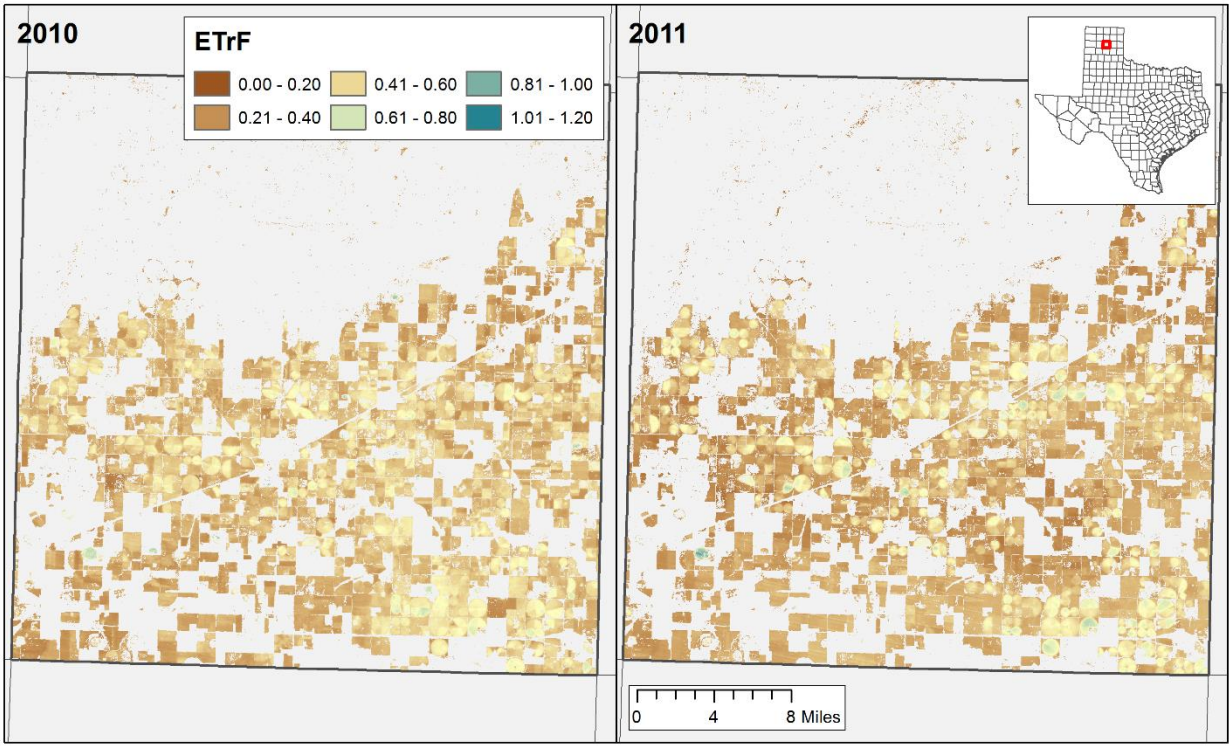

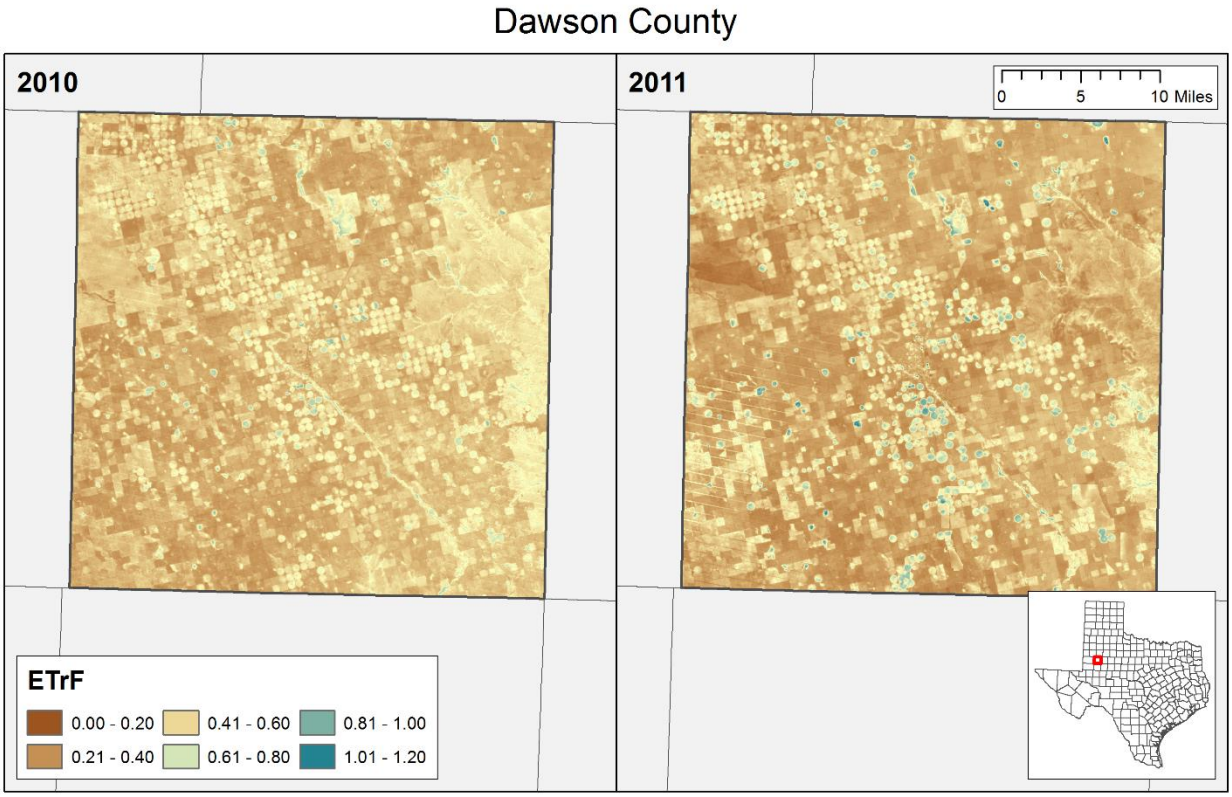
Dawson County
2010
2011
0
5
10 Miles
ETrF
0.00 - 0.20
0.21 - 0.40
0.41 - 0.60
0.61 - 0.80
0.81 - 1.00
1.01 - 1.20

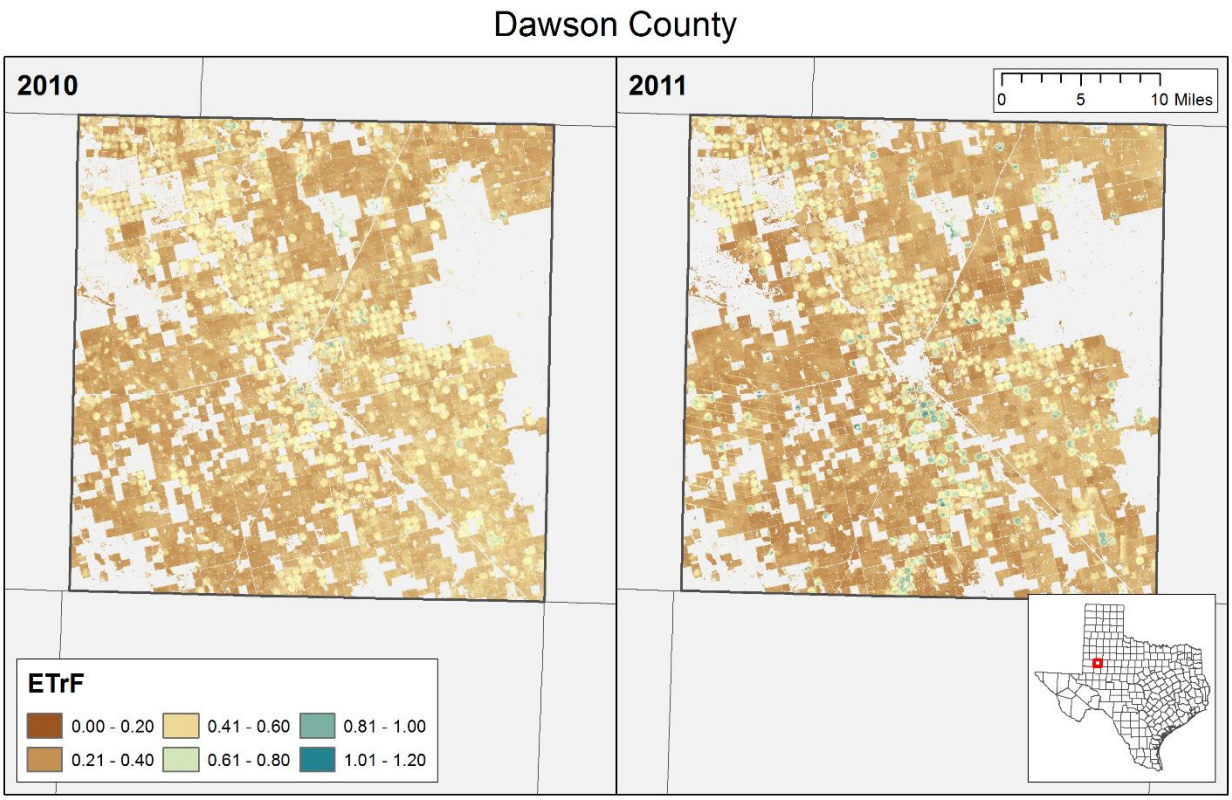
Dawson County
2010
2011
0
5
10 Miles
ETrF
0.00 - 0.20
0.21 - 0.40
0.41 - 0.60
0.61 - 0.80
0.81 - 1.00
1.01 - 1.20

.

Hale County

Hale County

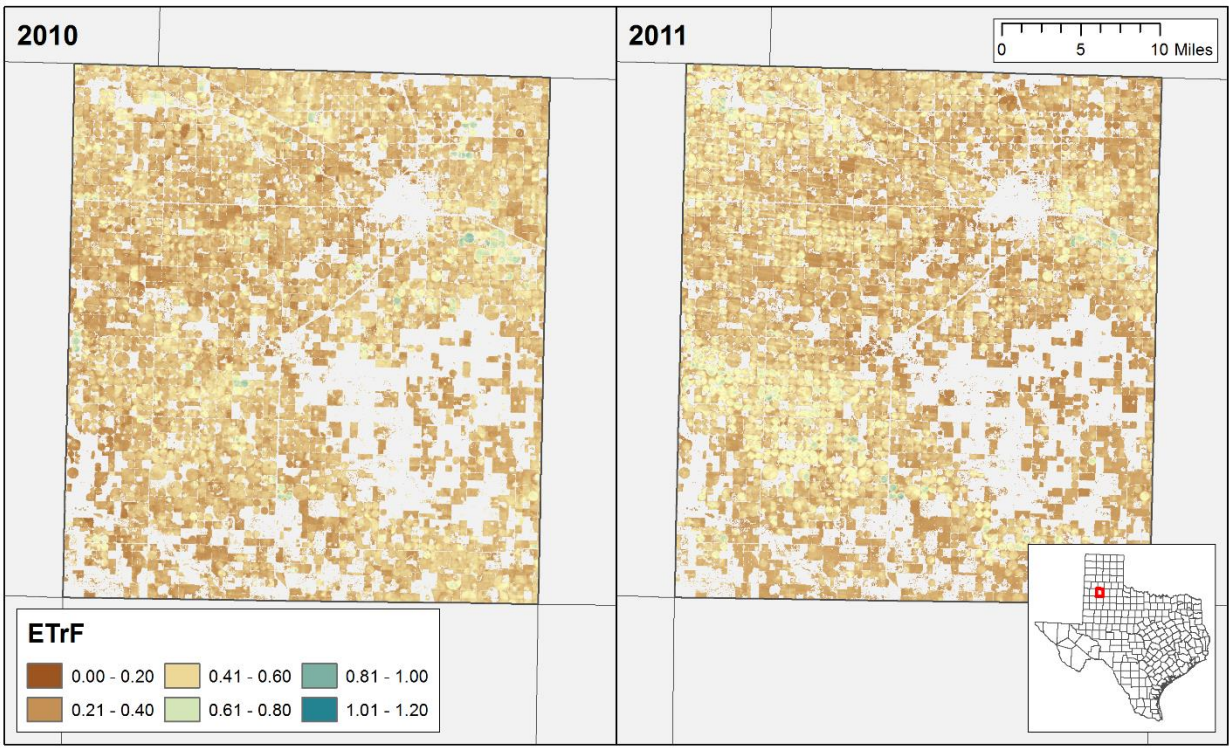

Medina County

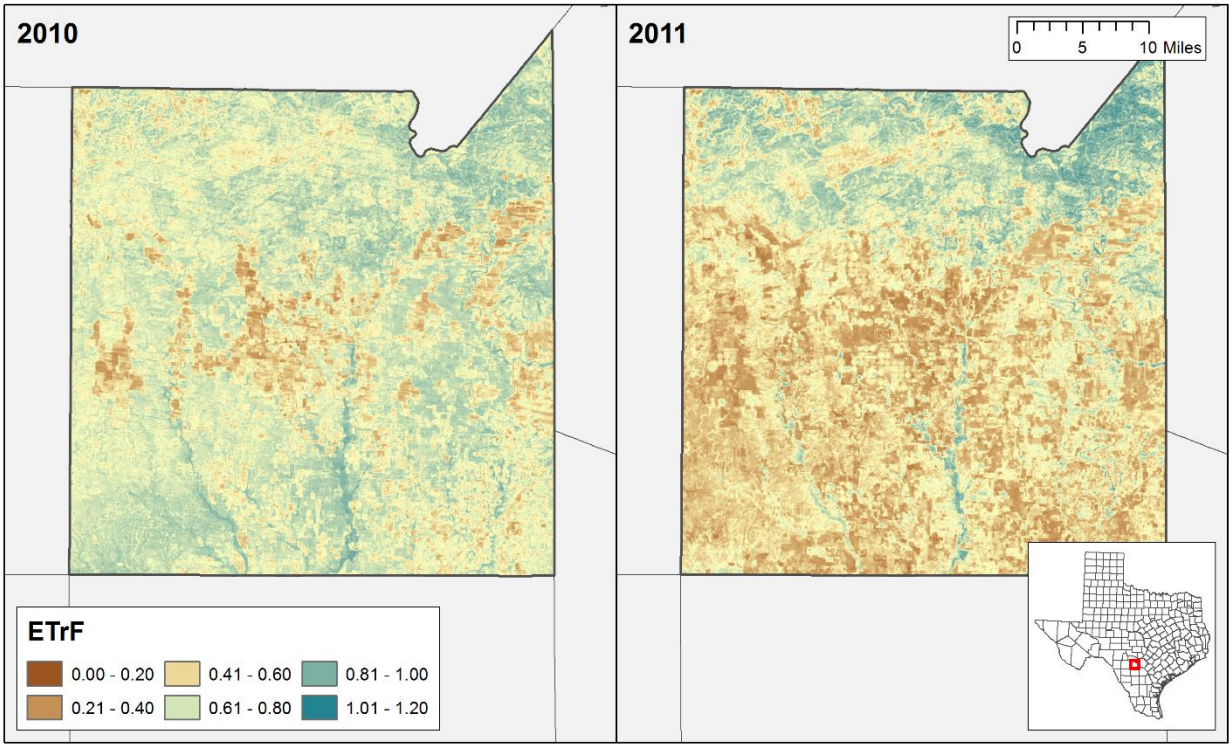

Medina County

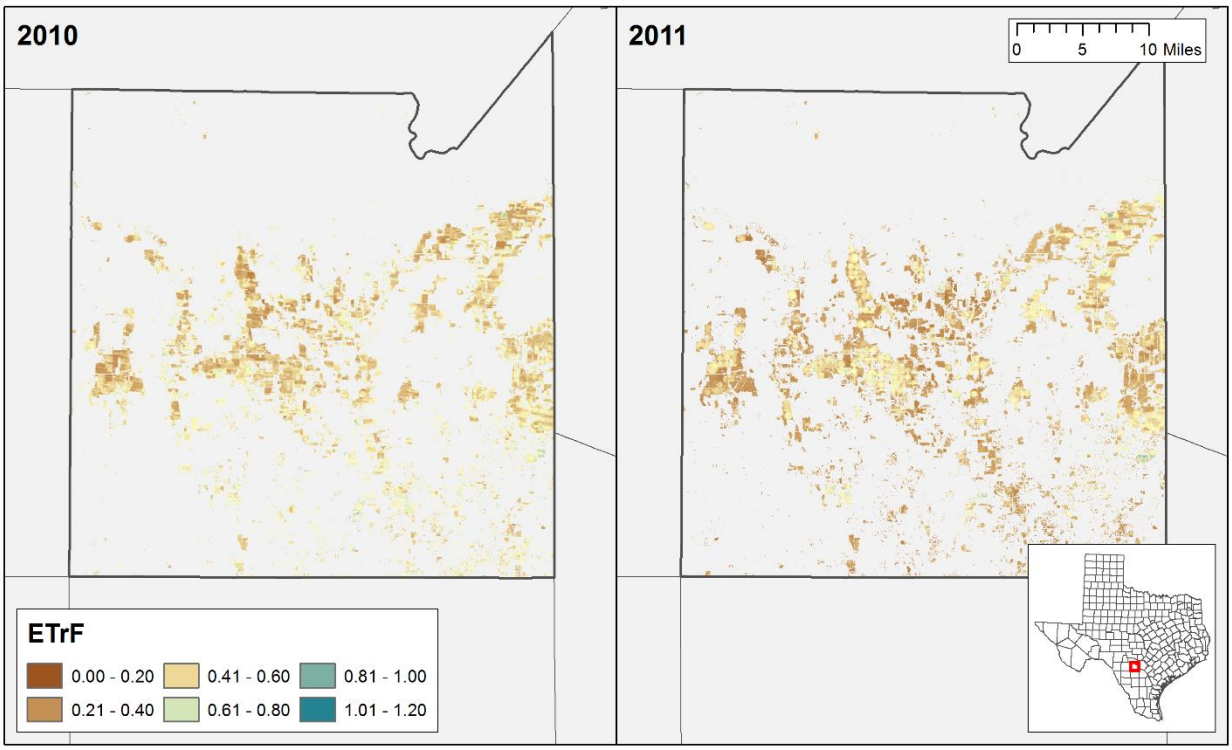

Ochiltree County

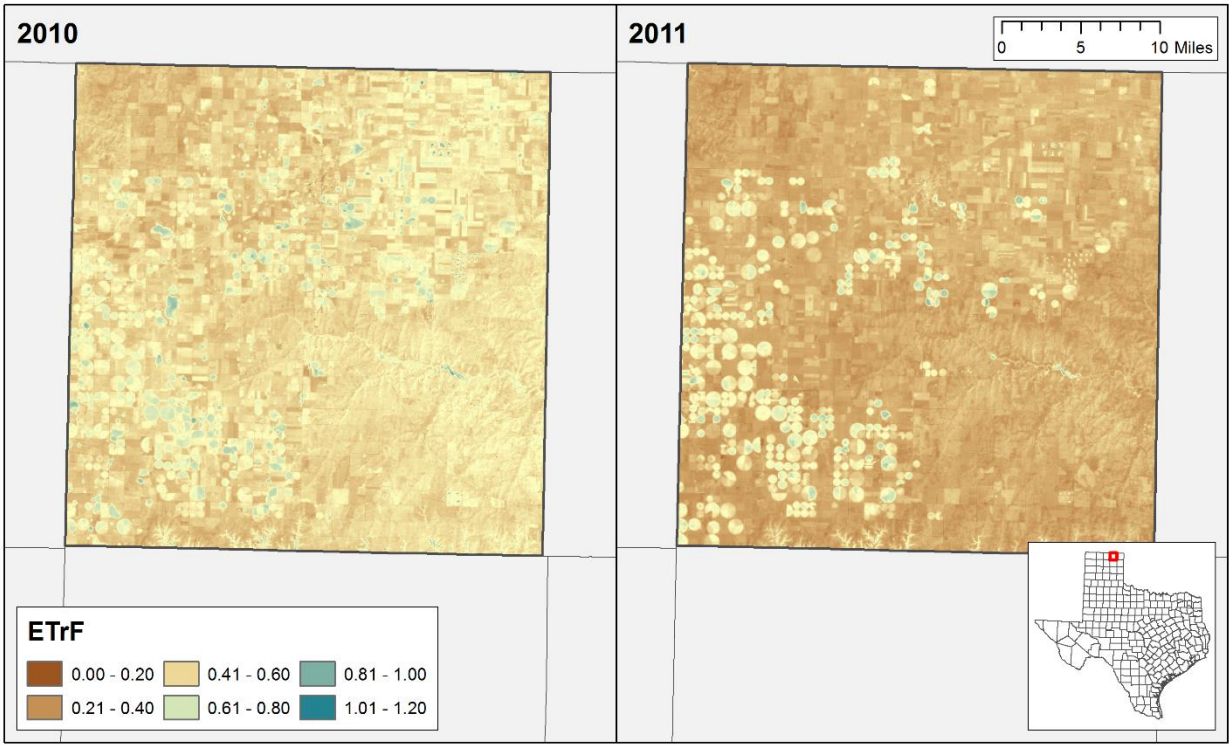

Ochiltree County

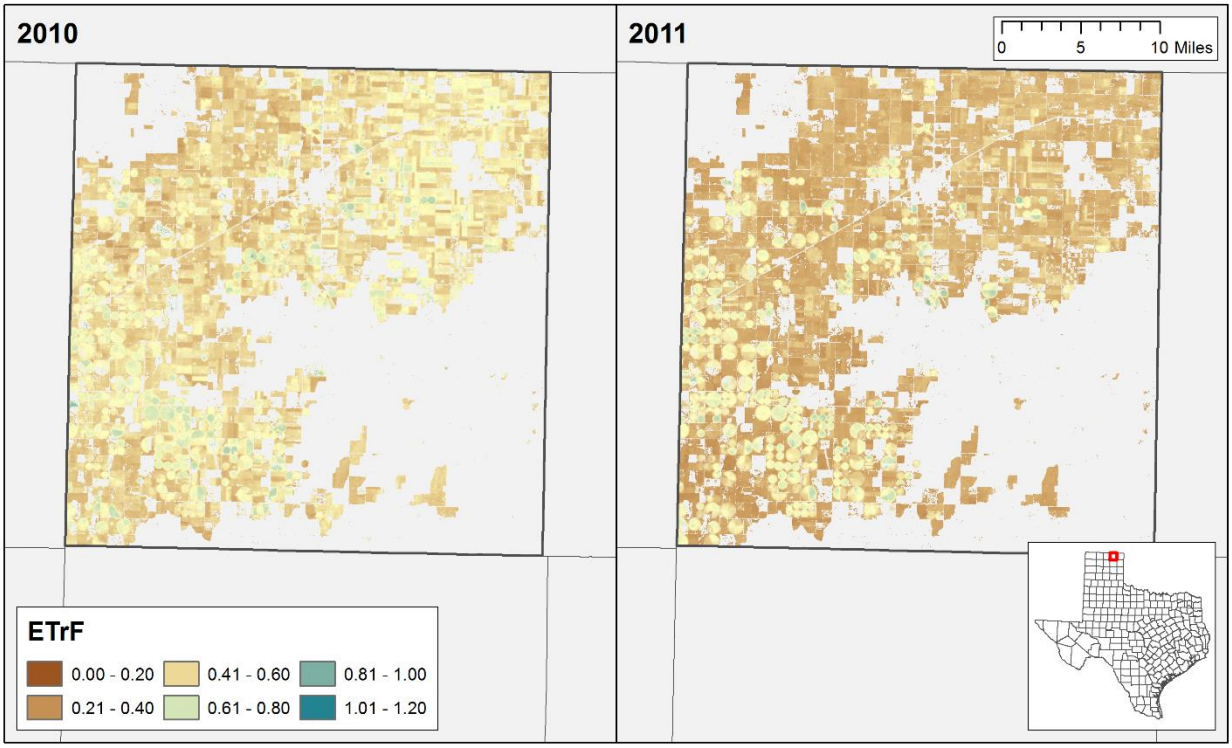

Wharton County

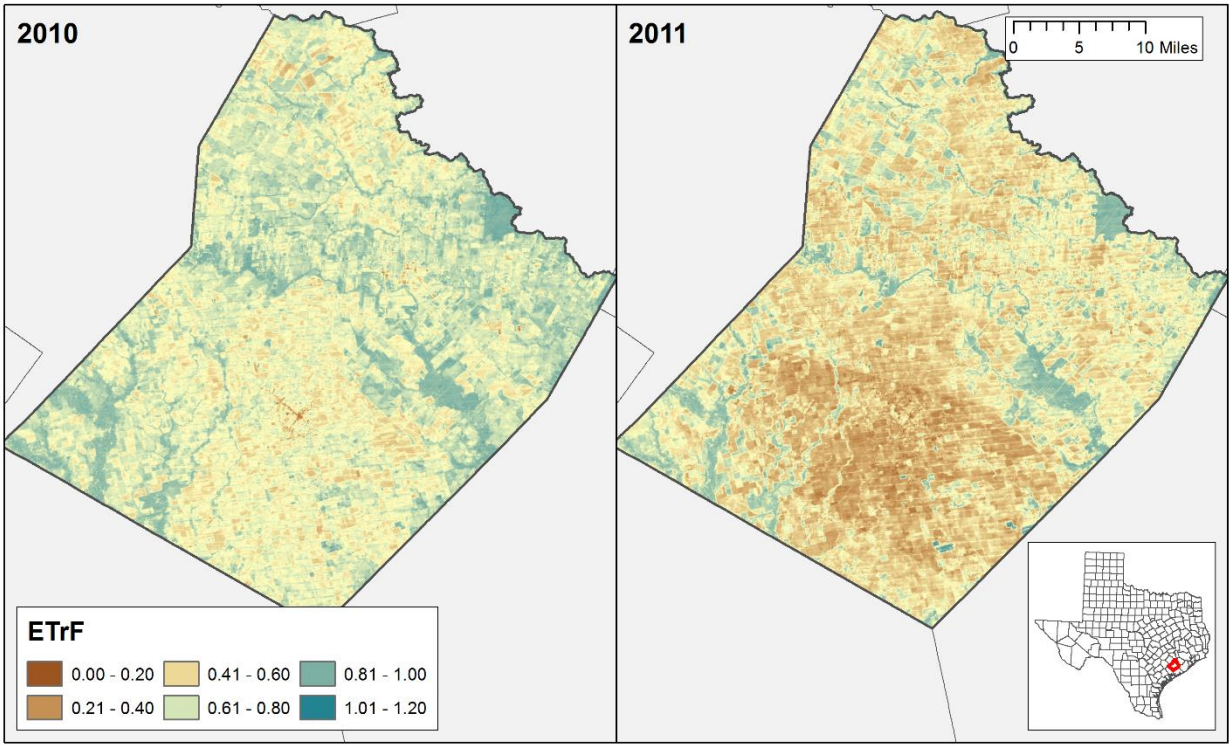

Wharton County

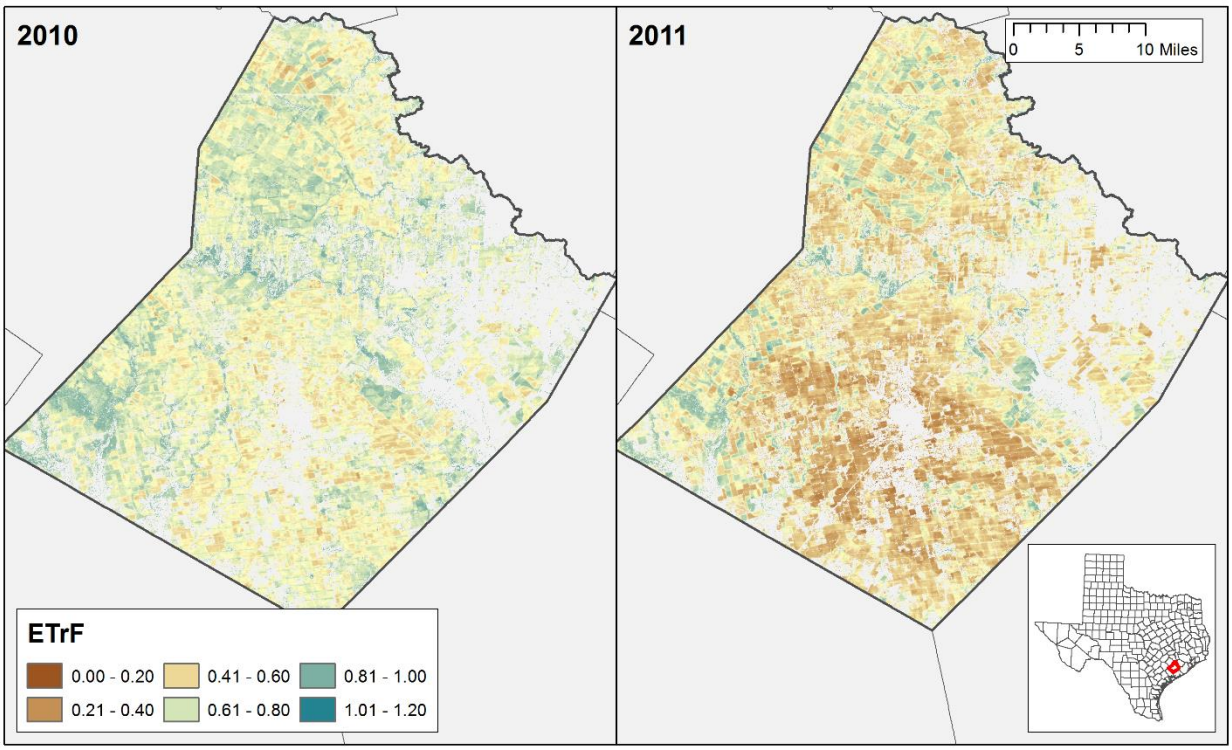

Appendix F. METRIC annual *ET* results for pilot study counties and masked to CDL cropland areas.

Brazos County

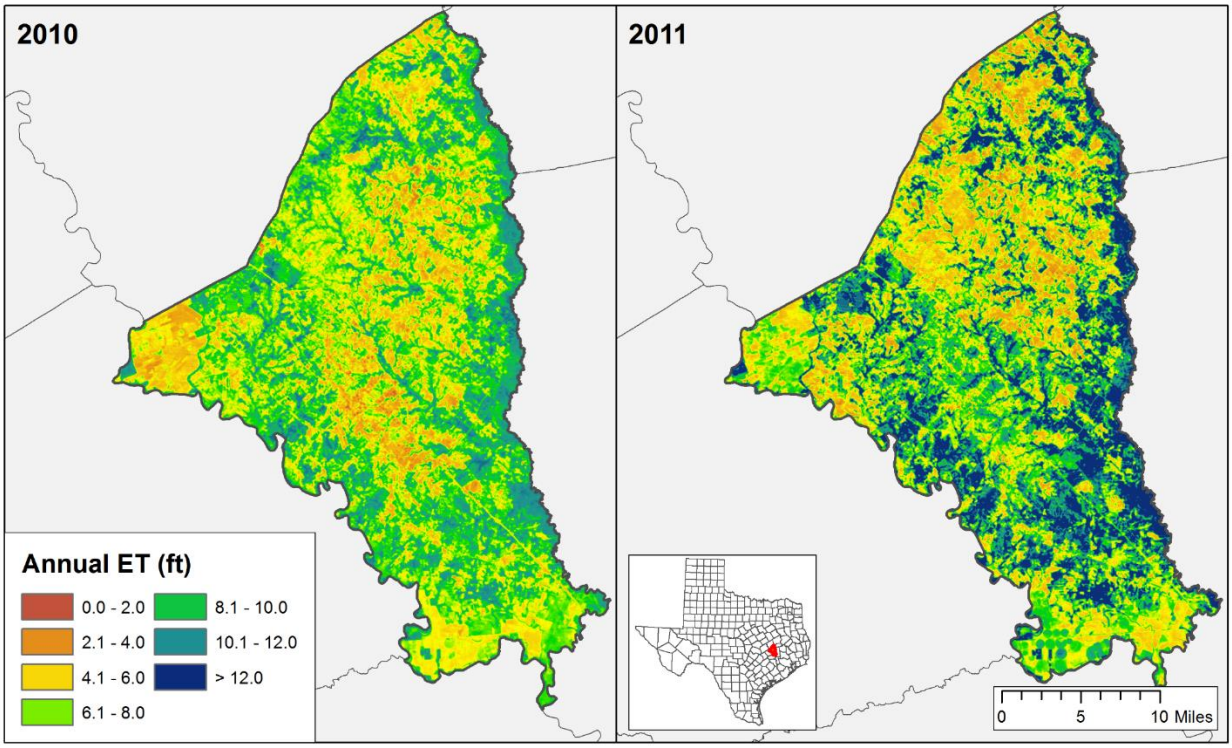

Brazos County

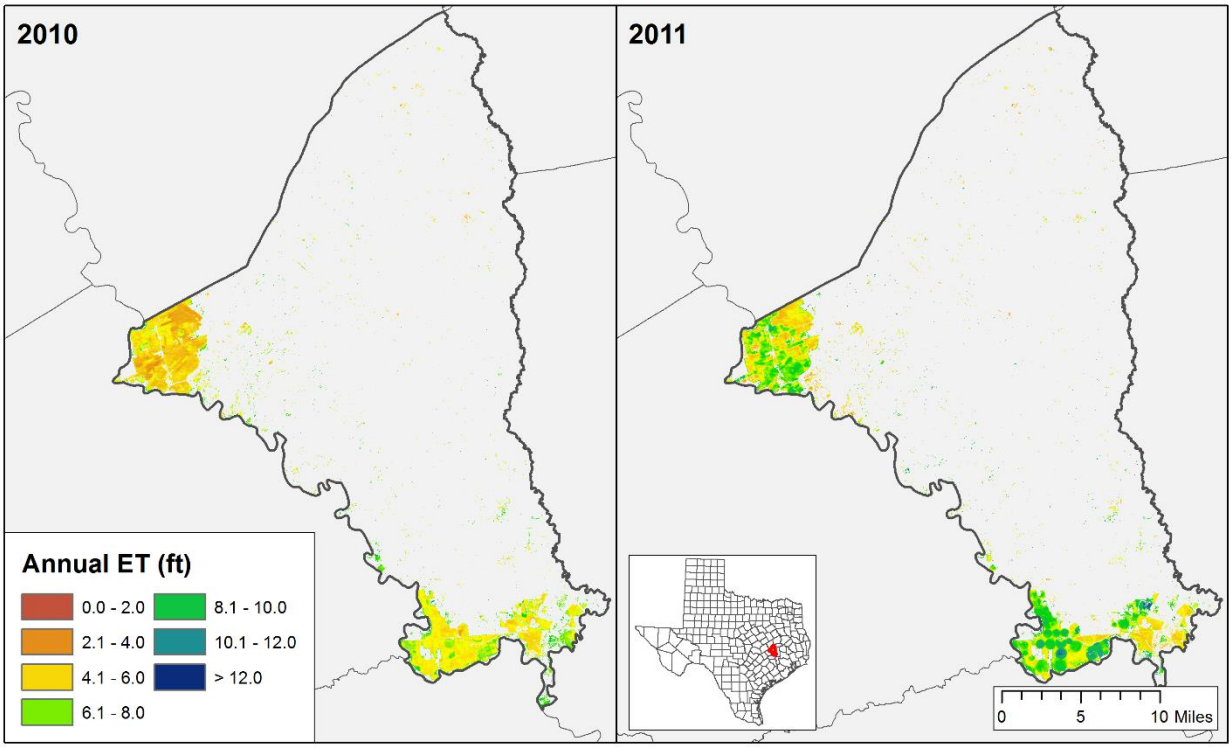

Cameron County

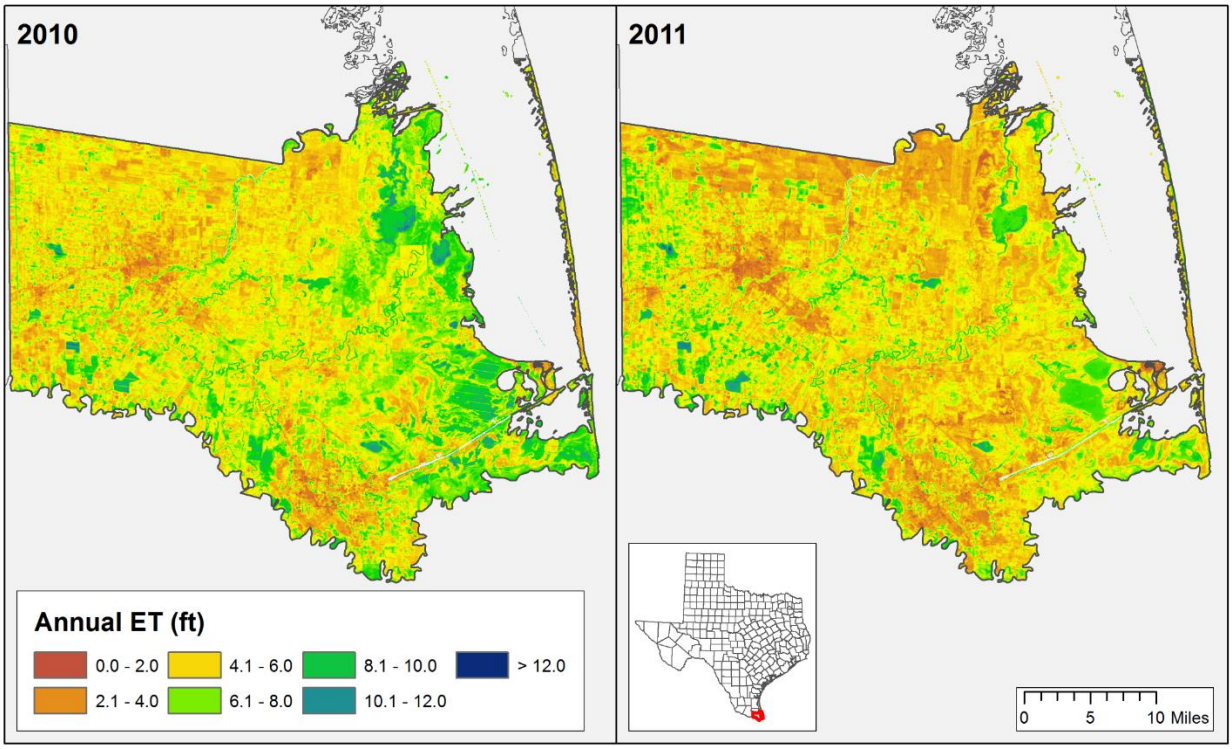

Cameron County

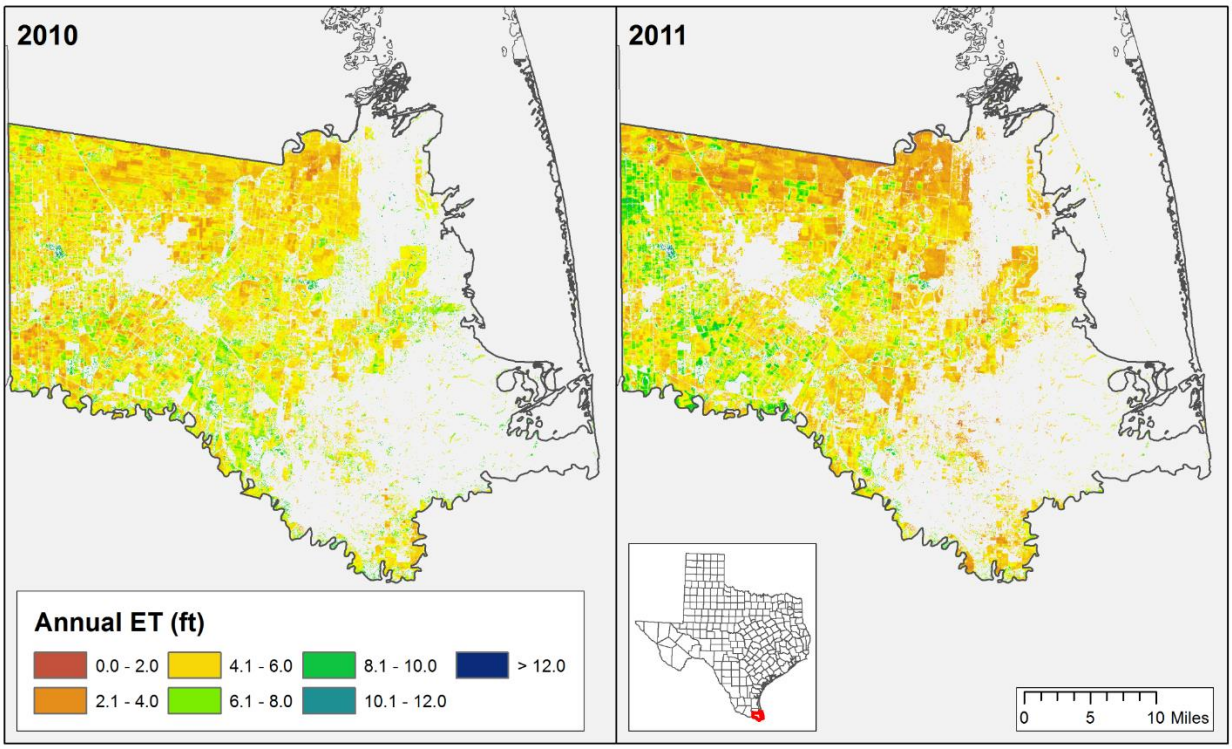

Carson County

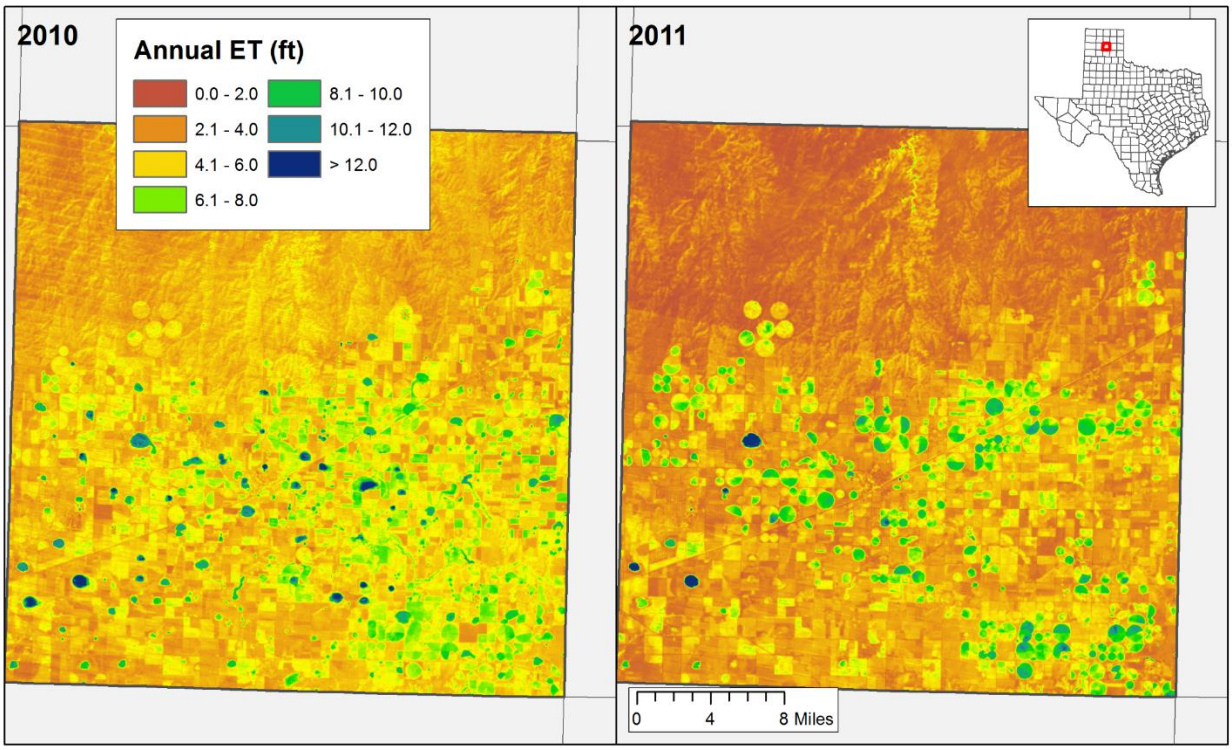

Carson County

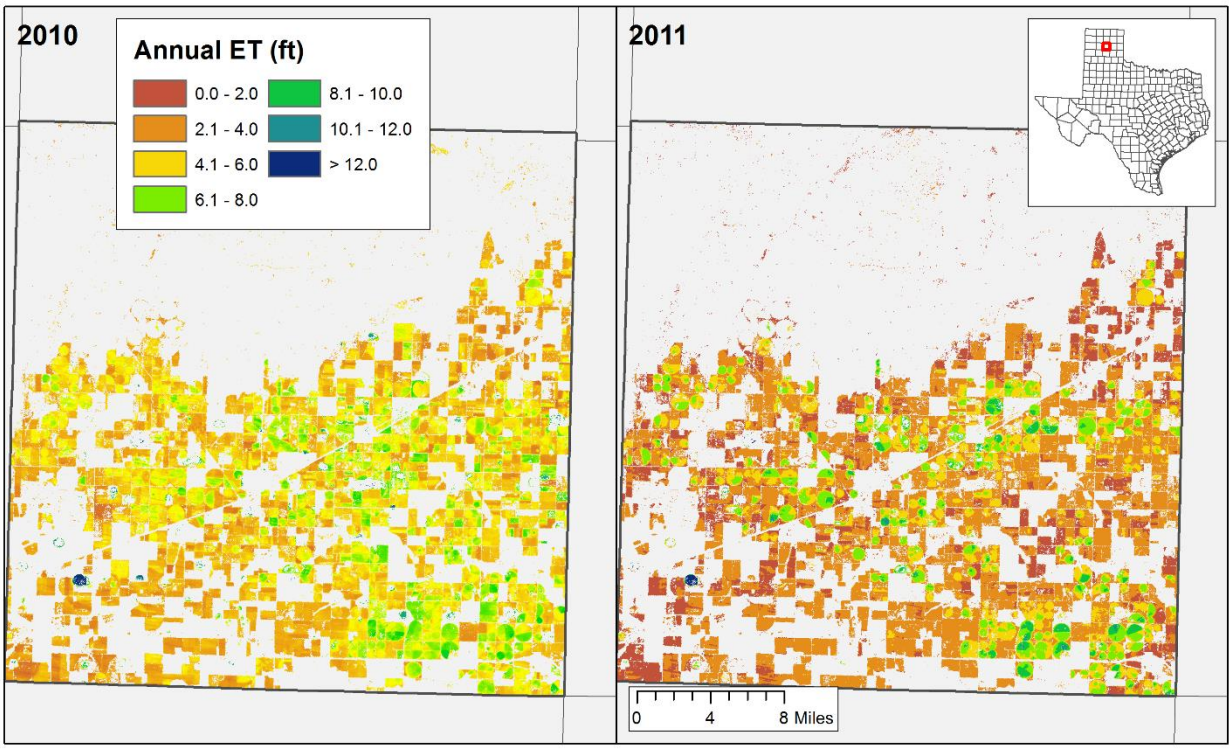

Dawson County

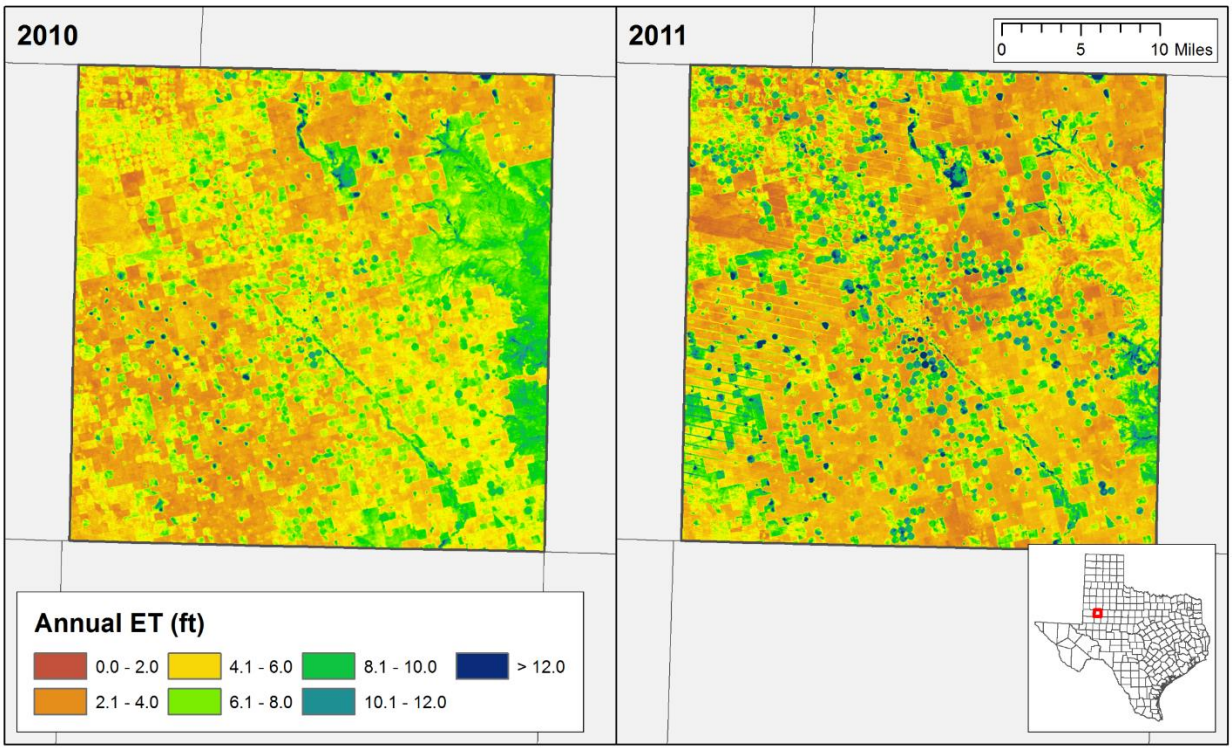

Dawson County

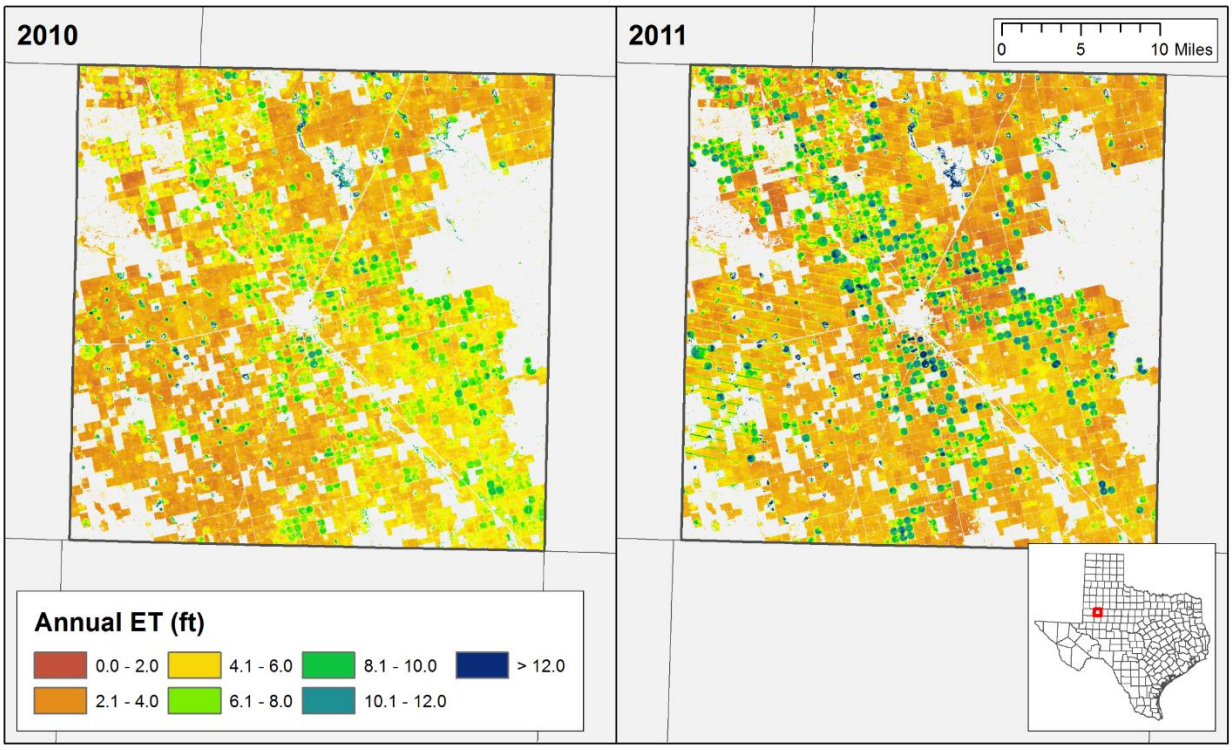

Hale County

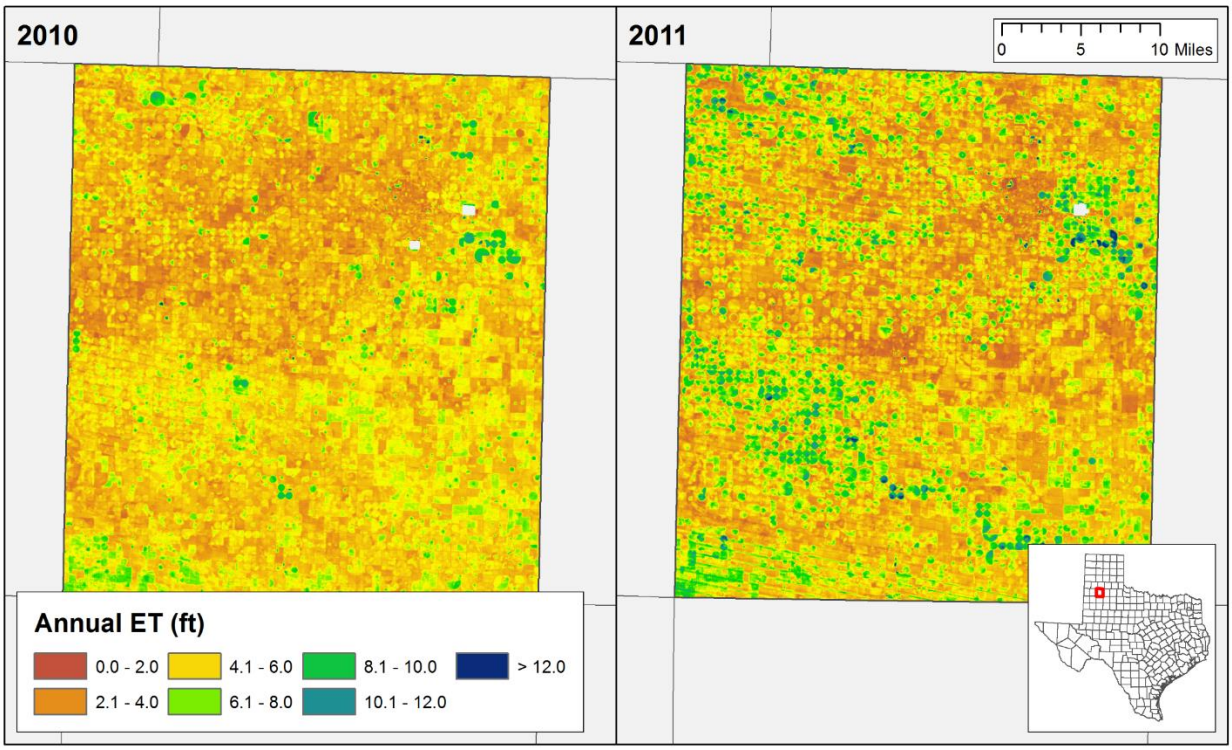

Hale County

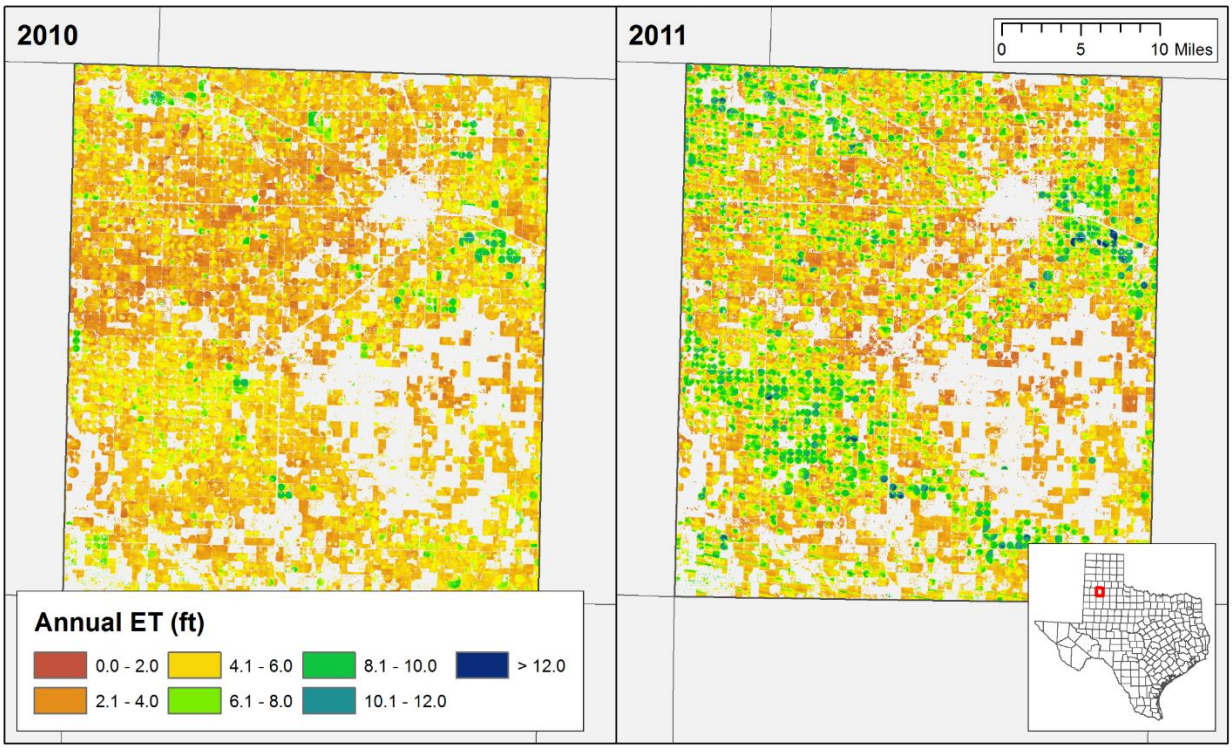

Medina County

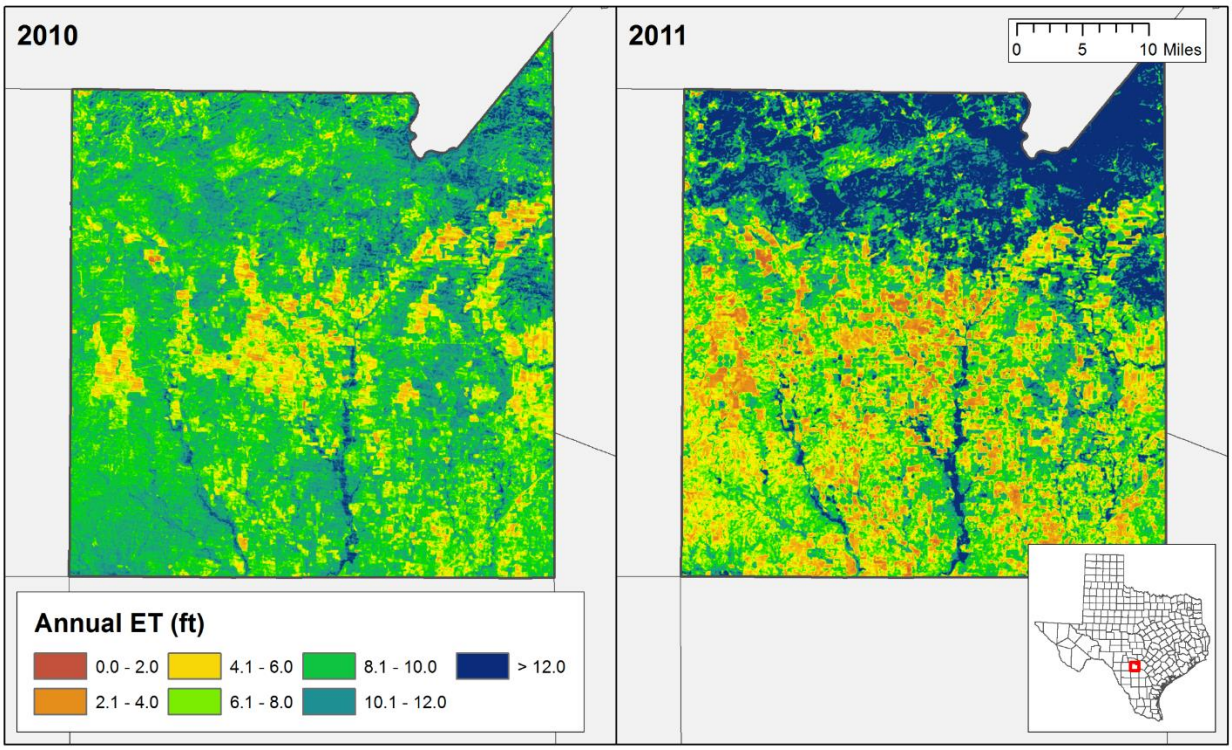

Medina County

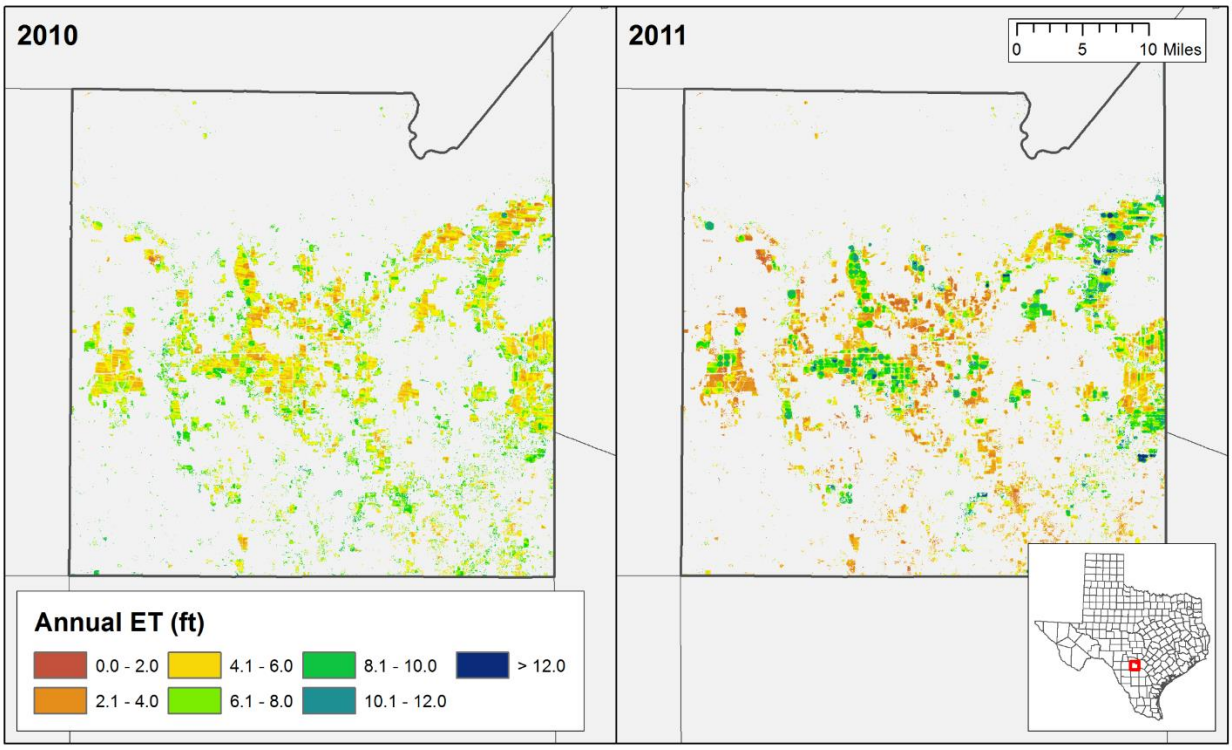

Ochiltree County

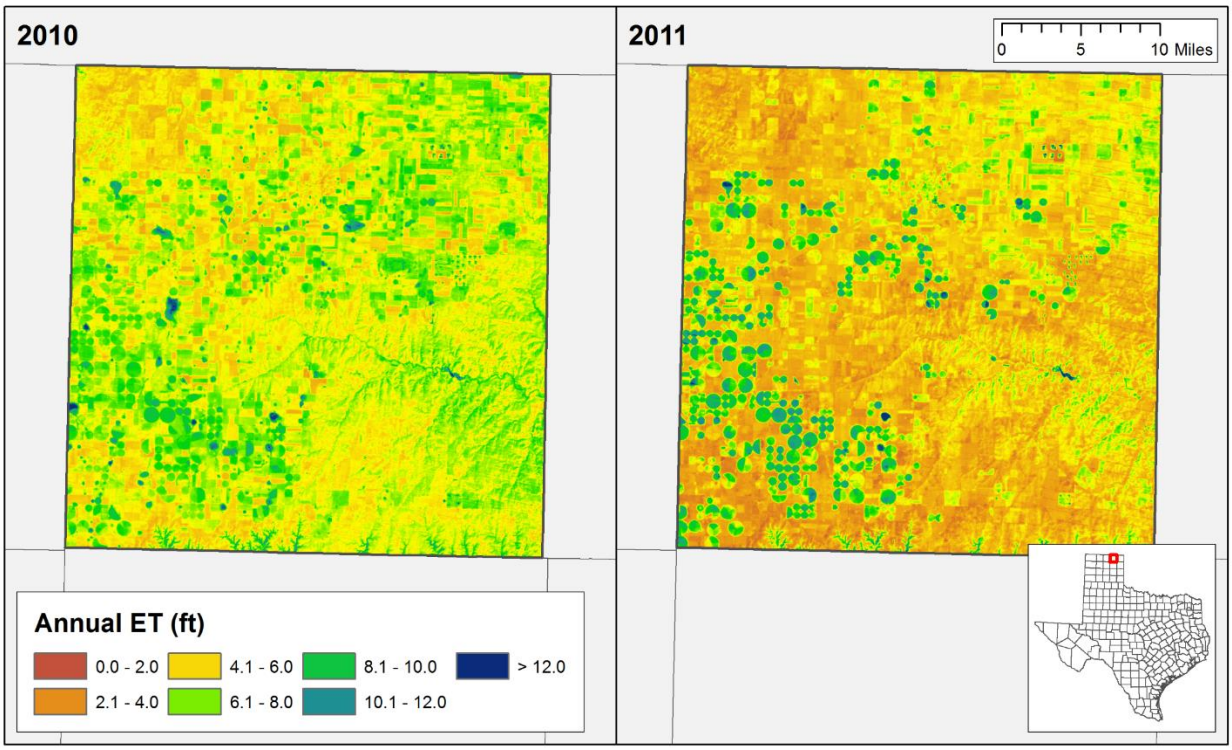

Ochiltree County

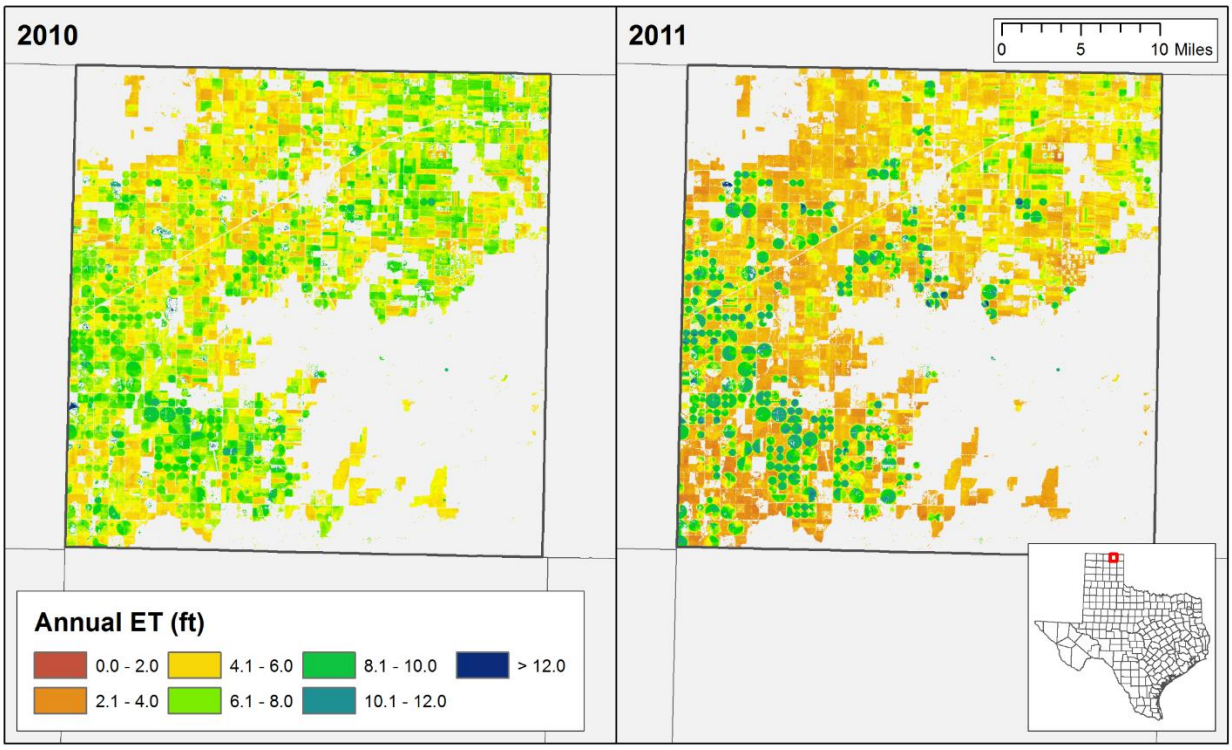

Wharton County

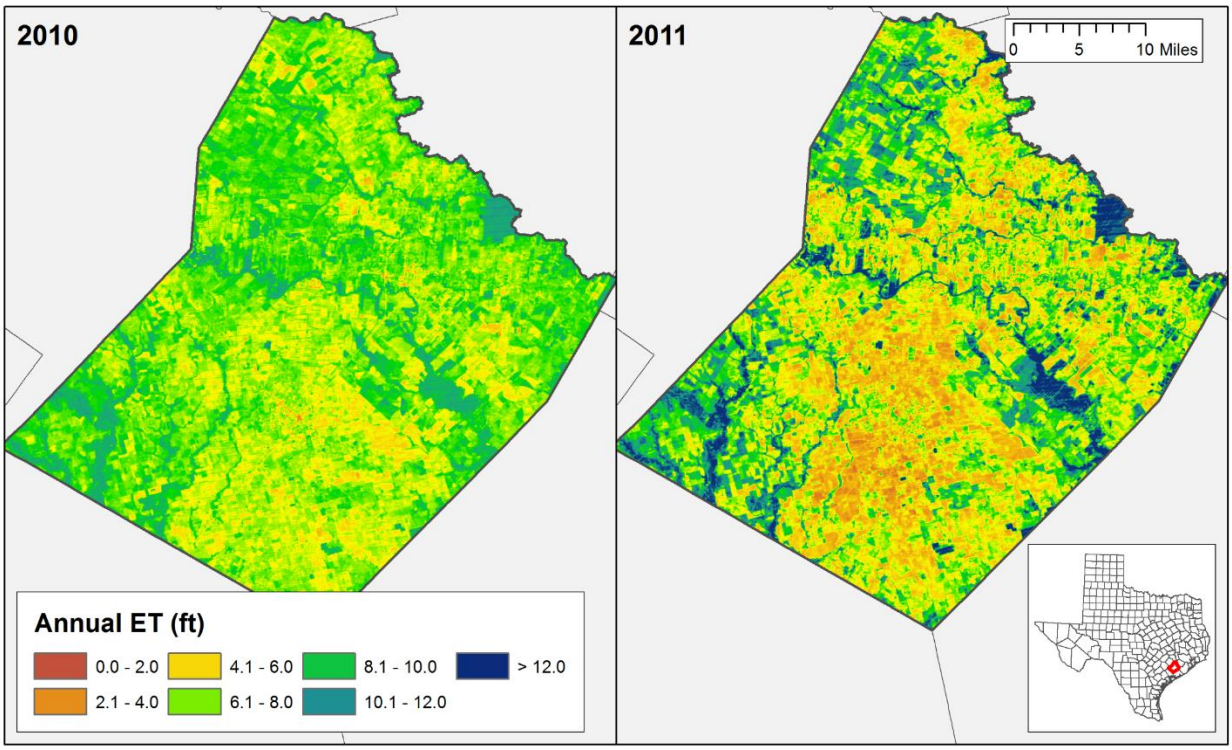

Wharton County

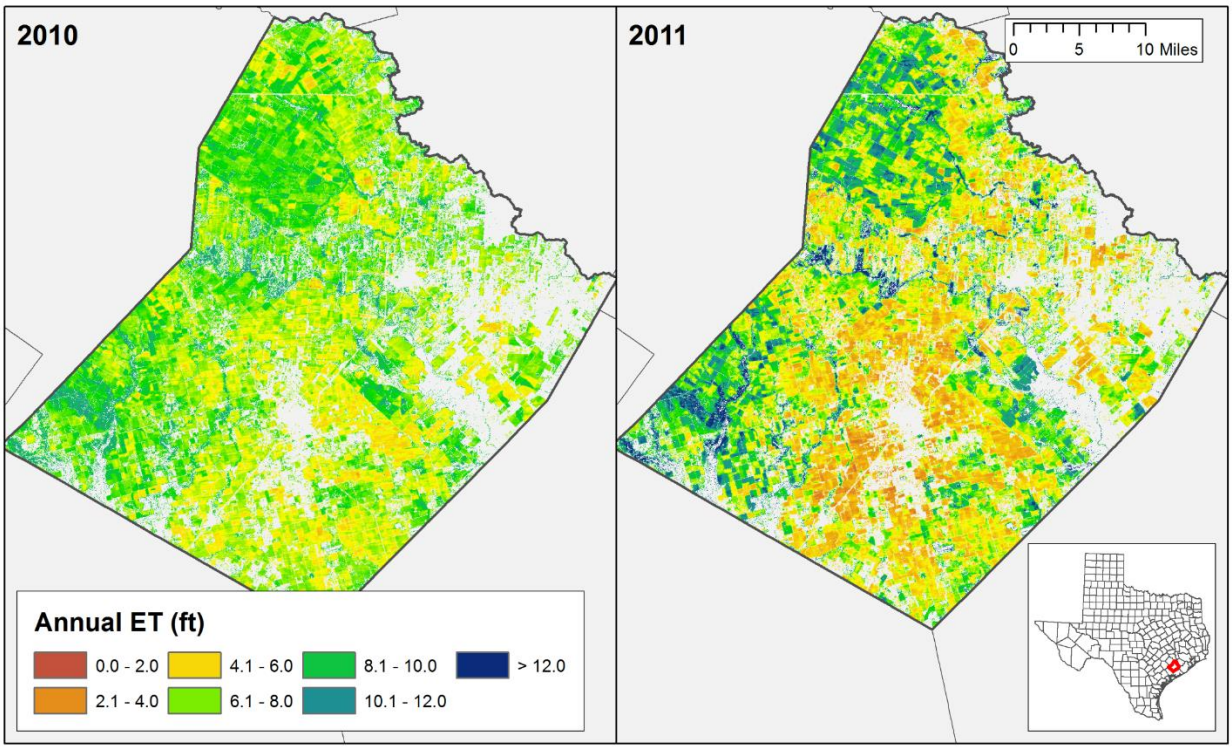

Appendix G. Cloud free Landsat 5/7 scene counts used to develop METRIC annual *ET* totals per county.

Brazos County

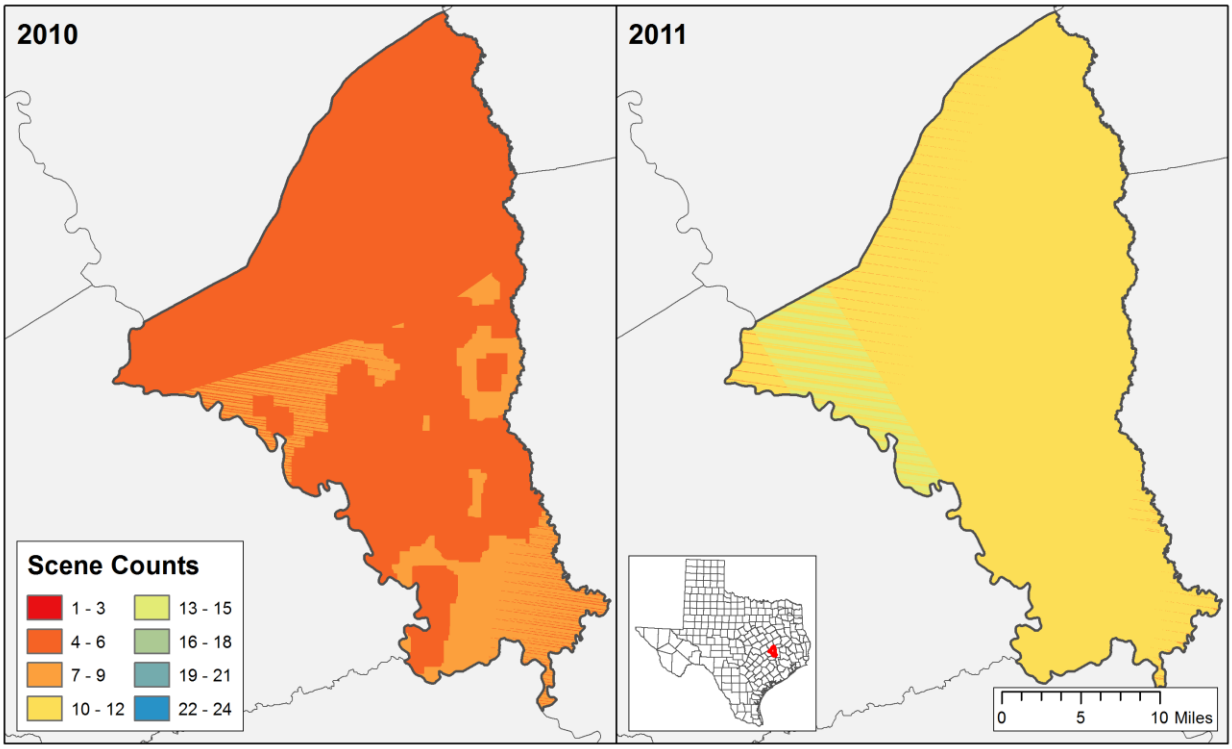

Cameron County

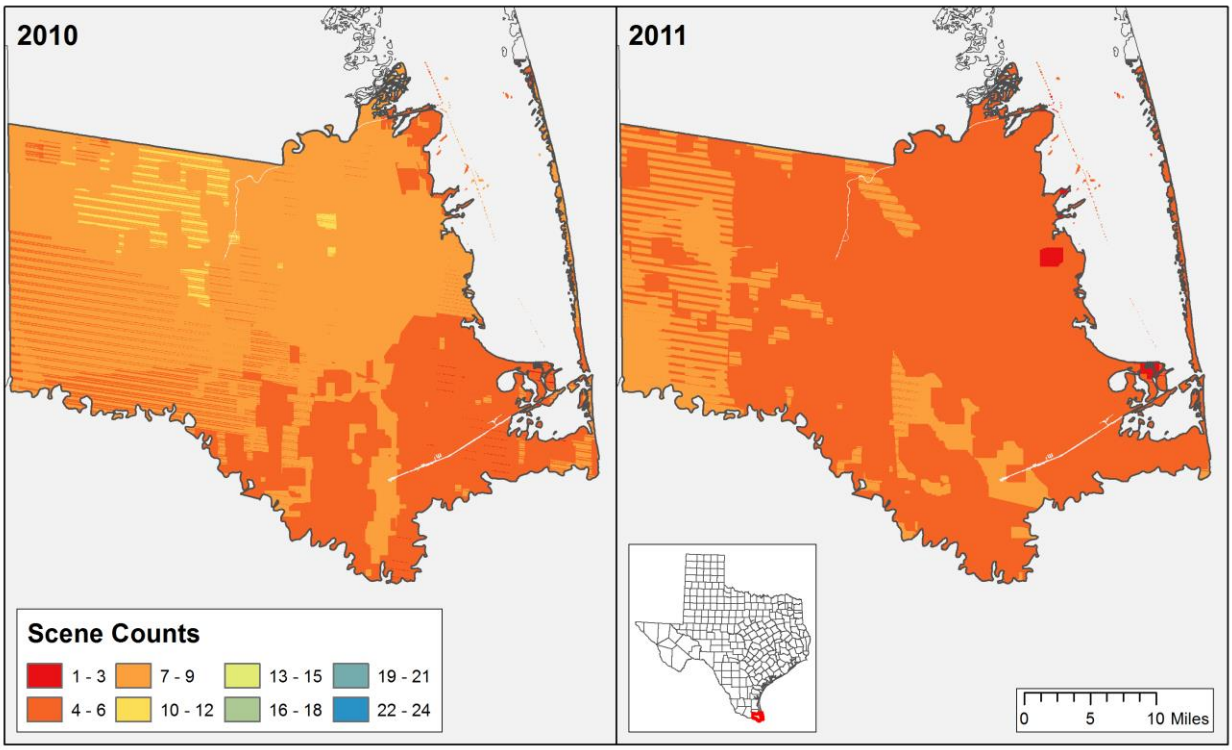

Carson County

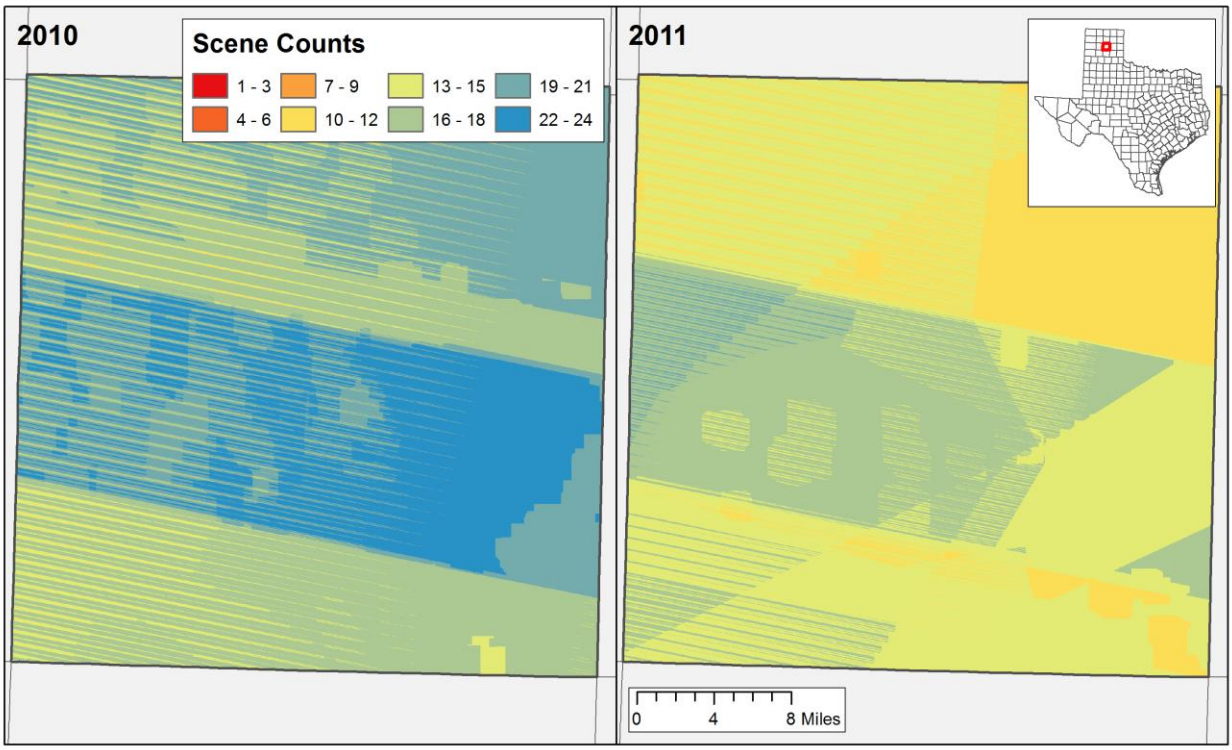

Dawson County

Hale County

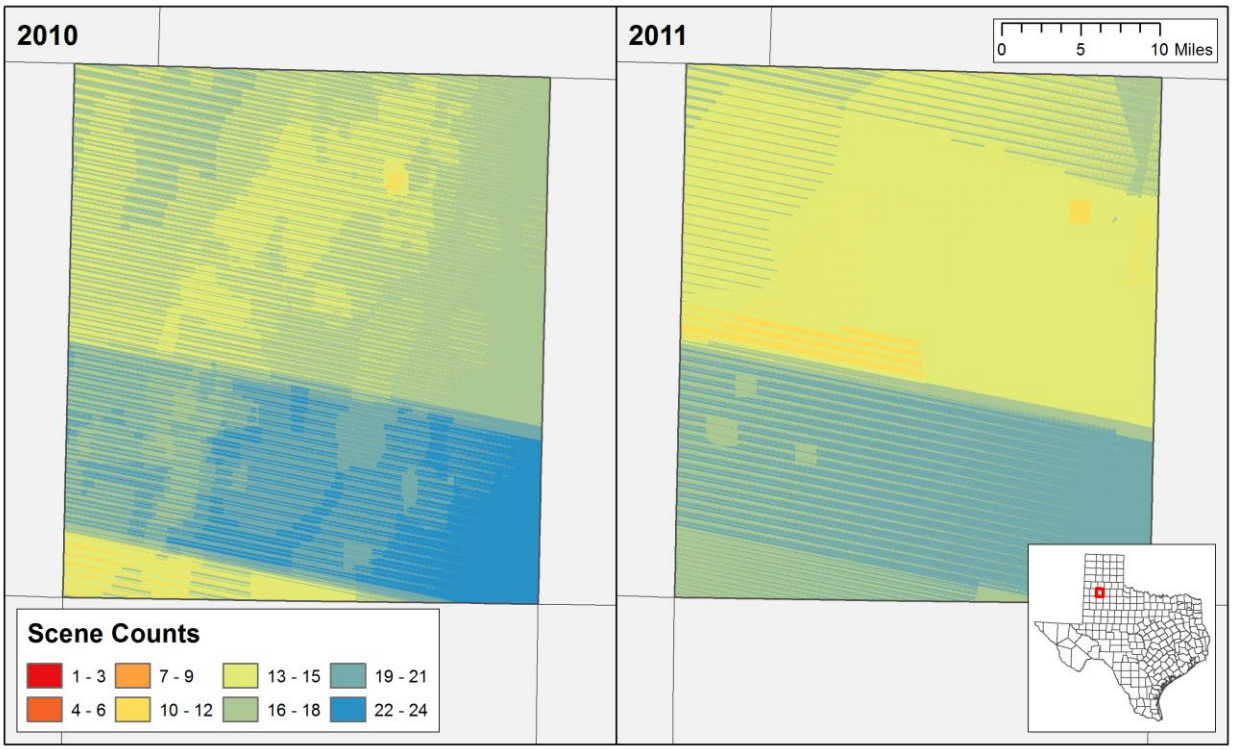

Medina County

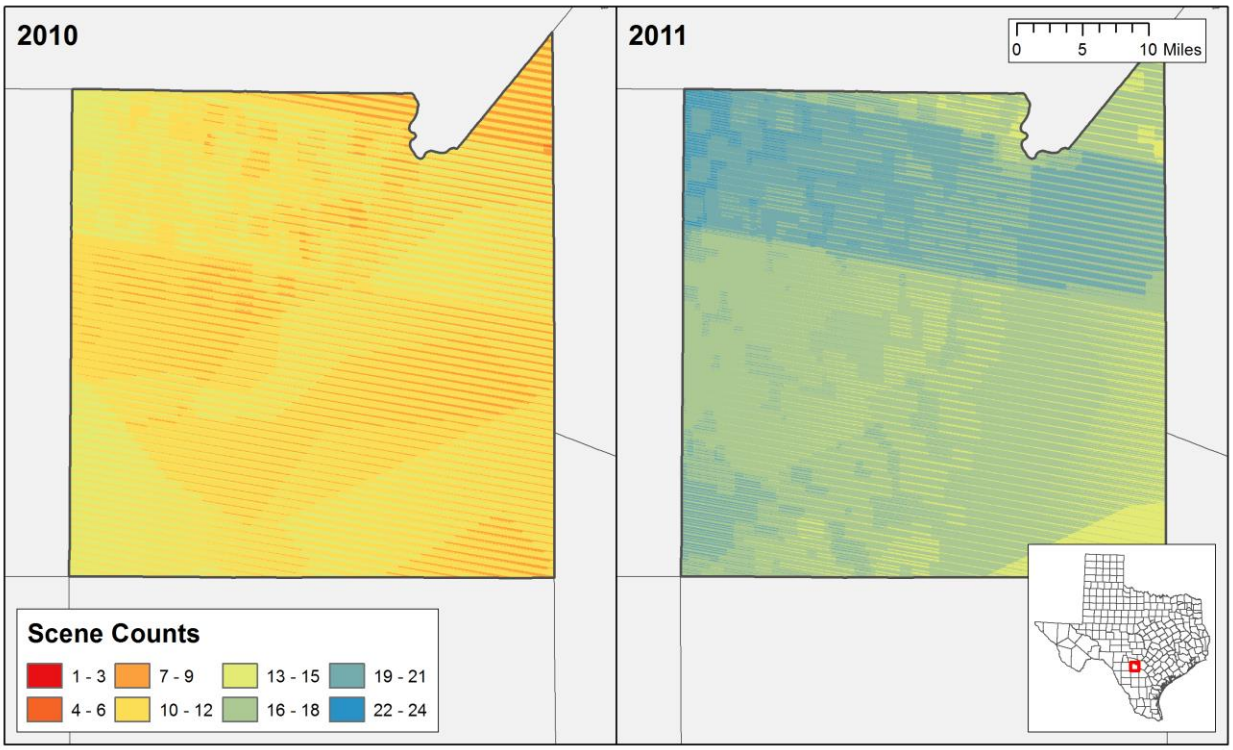

Ochiltree County

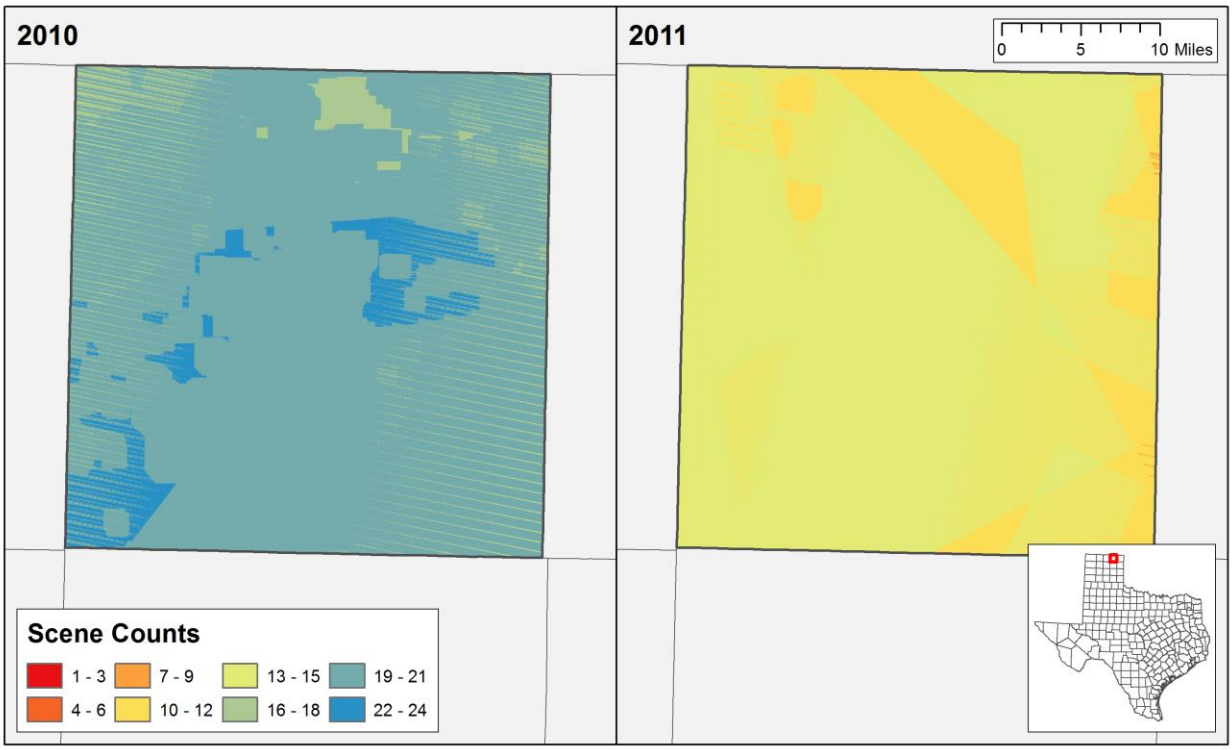

Wharton County

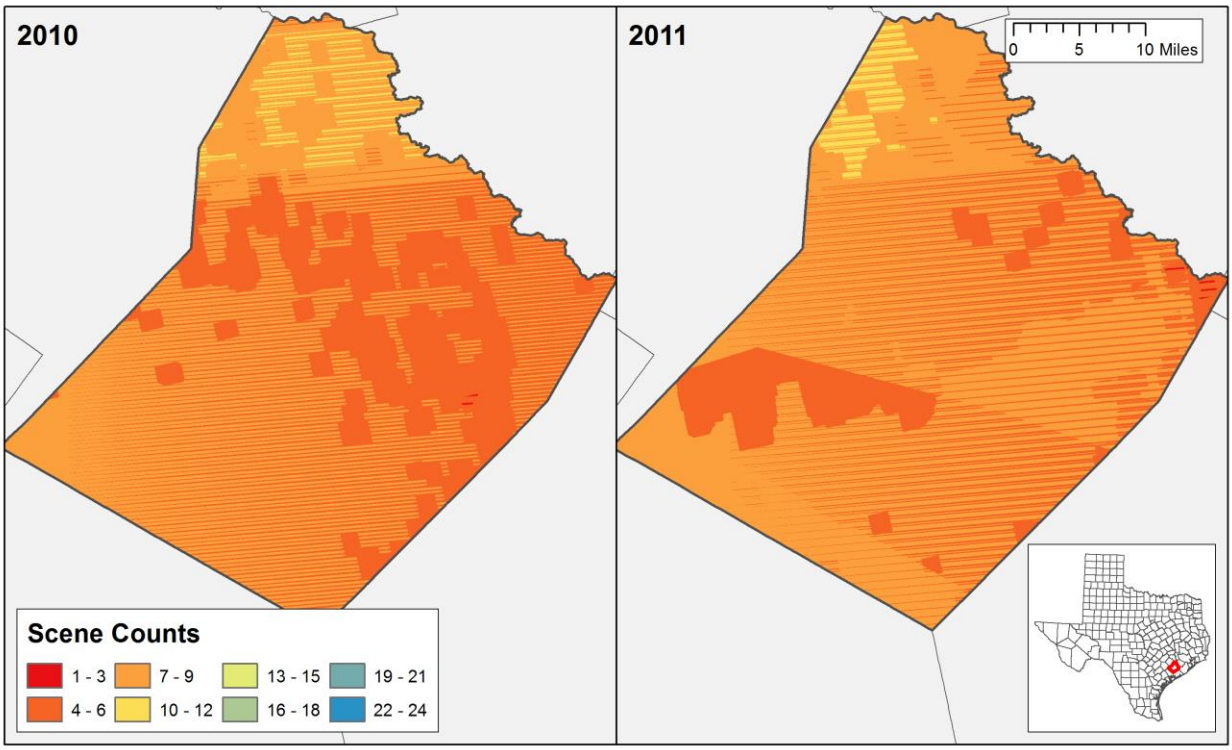

Appendix H. Annual crop water balance summaries from METRIC for each pilot study county. County totals are bolded and means italicized. County totals are shown with and without ‘Fallow or Idle Cropland’.

COUNTY	YEAR	CDL_NUM	CDL_NAME	PIXELS	ACRES	ETr (ft)	ET (ft)	PPT (ft)	ET (ac-ft)	PPT (ac-ft)	NET ET (ac-ft)	ET (in)	PPT (in)	NET ET (in)
Brazos	2010	1	Corn	31,810	7,074	7.54	3.10	2.40	21,906	17,003	4,903	37.2	28.8	8.3
Brazos	2010	2	Cotton	50,996	11,341	7.52	3.30	2.41	37,460	27,305	10,155	39.6	28.9	10.7
Brazos	2010	3	Rice	697	155	7.48	4.70	2.51	728	389	339	56.4	30.1	26.2
Brazos	2010	4	Sorghum	4,356	969	7.60	3.17	2.31	3,073	2,242	831	38.1	27.8	10.3
Brazos	2010	5	Soybeans	1,906	424	7.48	3.35	2.44	1,419	1,036	383	40.2	29.3	10.8
Brazos	2010	6	Sunflower	1	0	7.46	6.07	2.46	1.3	0.5	0.8	72.8	29.5	43.3
Brazos	2010	23	Spring Wheat	4	1	7.44	4.31	2.46	3.8	2.2	1.6	51.7	29.5	22.2
Brazos	2010	24	Winter Wheat	237	53	7.62	3.25	2.38	172	126	46	39.1	28.6	10.5
Brazos	2010	26	Dbl Crop WinWht Soybeans	5	1	7.72	4.65	2.44	5.2	2.7	2.5	55.8	29.3	26.5
Brazos	2010	28	Oats	2,461	547	7.44	4.68	2.47	2,562	1,352	1,210	56.2	29.6	26.5
Brazos	2010	36	Alfalfa	8	2	7.72	3.45	2.45	6.1	4.4	1.8	41.4	29.4	12.0
Brazos	2010	43	Potatoes	8	2	7.44	1.52	2.51	2.7	4.5	(1.8)	18.3	30.1	0.0
Brazos	2010	48	Watermelons	8	2	7.70	1.73	2.54	3.1	4.5	(1.4)	20.8	30.5	0.0
Brazos	2010	57	Herbs	2	0	7.46	3.64	2.53	1.6	1.1	0.5	43.7	30.3	13.4
Brazos	2010	58	Clover Wildflowers	1	0	7.69	4.95	2.63	1.1	0.6	0.5	59.3	31.6	27.7
Brazos	2010	61	Fallow Idle Cropland	17,930	3,988	7.57	3.13	2.38	12,482	9,492	2,990	37.6	28.6	9.0
Brazos	2010	74	Pecans	141	31	7.59	6.07	2.27	190	71	119	72.8	27.2	45.6
Brazos	2010	92	Aquaculture	19	4	7.50	4.76	2.58	20	11	9.2	57.1	31.0	26.1
Brazos	2010	236	Dbl Crop WinWht Sorghum	308	68	7.42	3.28	2.46	225	168	57	39.4	29.5	9.9
			Total		**24,663**				**80,262**	**59,216**	**21,047**	*46.2*	*29.5*	*17.8*
			No fallow/idle		**20,676**				**67,780**	**49,724**	**18,056**			
Brazos	2011	1	Corn	15,565	3,462	10.12	5.08	1.71	17,588	5,926	11,663	61.0	20.5	40.4
Brazos	2011	2	Cotton	84,685	18,833	10.05	4.81	1.70	90,506	32,082	58,424	57.7	20.4	37.2
Brazos	2011	3	Rice	296	66	9.93	7.17	1.67	472	110	362	86.1	20.1	66.0
Brazos	2011	4	Sorghum	5,883	1,308	10.23	4.58	1.74	5,997	2,272	3,725	55.0	20.8	34.2
Brazos	2011	5	Soybeans	284	63	10.14	4.69	1.70	296	108	189	56.3	20.4	35.9
Brazos	2011	23	Spring Wheat	55	12	9.91	4.88	1.69	60	21	39	58.6	20.2	38.3
Brazos	2011	24	Winter Wheat	2,132	474	10.10	5.46	1.72	2,587	814	1,773	65.5	20.6	44.9
Brazos	2011	27	Rye	3	1	10.28	5.29	1.66	3.5	1.1	2.4	63.5	19.9	43.6
Brazos	2011	28	Oats	686	153	10.03	5.05	1.69	770	258	512	60.6	20.3	40.3
Brazos	2011	36	Alfalfa	28	6	10.19	4.64	1.71	29	11	18	55.7	20.5	35.2
Brazos	2011	46	Sweet Potatoes	1	0	10.30	4.25	1.63	0.9	0.4	0.6	51.0	19.6	31.4
Brazos	2011	58	Clover Wildflowers	3	1	10.15	4.83	1.72	3.2	1.1	2.1	58.0	20.6	37.3
Brazos	2011	61	Fallow Idle Cropland	2,812	625	10.02	5.24	1.71	3,279	1,072	2,207	62.9	20.6	42.3
Brazos	2011	74	Pecans	2	0	9.90	5.85	1.68	2.6	0.7	1.9	70.2	20.2	50.0
Brazos	2011	92	Aquaculture	15	3	9.87	7.32	1.68	24	6	19	87.8	20.1	67.7
Brazos	2011	206	Carrots	3	1	10.00	4.90	1.70	3.3	1.1	2.1	58.8	20.4	38.4
Brazos	2011	236	Dbl Crop WinWht Sorghum	4	1	10.20	4.98	1.73	4.4	1.5	2.9	59.8	20.7	39.1
Brazos	2011	238	Dbl Crop WinWht Cotton	54	12	9.90	3.98	1.68	48	20	28	47.8	20.2	27.6
			Total		**70,361**				**269,717**	**151,644**	**118,073**	*62.0*	*20.3*	*41.7*
			No fallow/idle		**69,735**				**266,438**	**150,571**	**115,866**			

COUNTY	YEAR	CDL_NUM	CDL_NAME	PIXELS	ACRES	ETr (ft)	ET (ft)	PPT (ft)	ET (ac-ft)	PPT (ac-ft)	NET ET (ac-ft)	ET (in)	PPT (in)	NET ET (in)
Cameron	2010	1	Corn	72,168	16,050	8.28	4.00	2.76	64,158	44,343	19,815	48.0	33.2	14.8
Cameron	2010	2	Cotton	288,167	64,087	8.04	3.53	2.67	226,201	170,921	55,280	42.4	32.0	10.4
Cameron	2010	3	Rice	133	30	8.45	5.56	2.70	165	80	85	66.8	32.4	34.4
Cameron	2010	4	Sorghum	463,674	103,119	8.00	4.02	2.84	414,683	292,425	122,258	48.3	34.0	14.2
Cameron	2010	5	Soybeans	5,395	1,200	8.14	3.70	2.99	4,442	3,587	855	44.4	35.9	8.5
Cameron	2010	44	Other Crops	464	103	7.92	4.28	2.88	441.8	297.3	144.4	51.4	34.6	16.8
Cameron	2010	45	Sugarcane	28,041	6,236	8.27	5.07	2.77	31,587.8	17,287.3	14,300.5	60.8	33.3	27.5
Cameron	2010	48	Watermelons	2	0	7.69	1.64	3.17	0.7	1.4	(0.7)	19.7	38.1	0.0
Cameron	2010	49	Onions	871	194	8.36	2.89	2.69	560.3	521.1	39.2	34.7	32.3	2.4
Cameron	2010	61	Fallow Idle Cropland	64,479	14,340	8.03	5.23	2.99	75,039	42,893	32,146	62.8	35.9	26.9
Cameron	2010	72	Citrus	3,980	885	8.30	5.11	2.74	4,521.4	2,421.1	2,100.3	61.3	32.8	28.5
Cameron	2010	92	Aquaculture	121	27	7.78	3.73	3.41	100.3	91.7	8.6	44.7	40.9	3.8
Cameron	2010	212	Oranges	175	39	8.41	5.60	2.71	217.9	105.6	112.4	67.2	32.5	34.6
Cameron	2010	239	Dbl Crop Soybeans Cotton	259	58	8.53	5.18	2.79	298.1	160.9	137.2	62.1	33.5	28.6
Cameron	2010	241	Dbl Crop Corn Soybeans	1,561	347	7.81	4.89	3.42	1,698.0	1,188.6	509.4	58.7	41.1	17.6
			Total		**206,713**				**824,114**	**576,325**	**247,790**	*51.5*	*34.8*	*17.9*
			No fallow/idle		**192,374**				**749,075**	**533,431**	**215,644**			
Cameron	2011	1	Corn	33,373	7,422	9.19	4.55	1.15	33,802	8,517	25,285.4	54.7	13.8	40.9
Cameron	2011	2	Cotton	387,933	86,274	8.85	3.10	1.22	267,449	104,984	162,465	37.2	14.6	22.6
Cameron	2011	3	Rice	1	0	9.29	1.15	1.13	0	0	0	*13.7*	*13.5*	*0.2*
Cameron	2011	4	Sorghum	252,188	56,085	8.83	3.76	1.21	210,640	67,981	142,659	*45.1*	*14.5*	*30.5*
Cameron	2011	5	Soybeans	506	113	8.08	2.77	1.40	311	157	154	33.2	16.8	16.5
Cameron	2011	24	Winter Wheat	183	41	9.25	4.36	1.15	178	47	131	52.4	13.8	38.5
Cameron	2011	36	Alfalfa	326	73	9.44	6.19	1.08	449	79	370	74.3	13.0	61.3
Cameron	2011	44	Other Crops	334	74	8.41	3.68	1.30	273	97	176	44.1	15.6	28.5
Cameron	2011	45	Sugarcane	27,552	6,127	9.24	6.29	1.16	38,528	7,088	31,441	75.5	13.9	61.6
Cameron	2011	57	Herbs	99	22	9.02	5.77	1.22	127	27	100	69.2	14.6	54.6
Cameron	2011	61	Fallow Idle Cropland	1,936	431	8.84	4.31	1.23	1,856	531	1,325	51.7	14.8	36.9
Cameron	2011	72	Citrus	1,110	247	8.85	6.65	1.24	1,641.5	305.5	1,335.9	79.8	14.9	64.9
Cameron	2011	212	Oranges	242	54	8.67	6.56	1.28	353	69	284	78.7	15.3	63.4
			Total		**156,962**				**555,608**	**189,881**	**365,727**	*54.7*	*17.7*	*37.1*
			No fallow/idle		**156,532**				**553,752**	**189,350**	**364,402**			

COUNTY	YEAR	CDL_NUM	CDL_NAME	PIXELS	ACRES	ETr (ft)	ET (ft)	PPT (ft)	ET (ac-ft)	PPT (ac-ft)	NET ET (ac-ft)	ET (in)	PPT (in)	NET ET (in)
Carson	2010	1	Corn	76,944	17,112	8.48	4.56	2.34	78,036	39,997	38,040	54.7	28.0	26.7
Carson	2010	2	Cotton	218,513	48,596	8.48	3.44	2.28	167,144	110,746	56,397	41.3	27.3	13.9
Carson	2010	4	Sorghum	53,607	11,922	8.40	3.11	2.32	37,101	27,706	9,395	37.3	27.9	9.5
Carson	2010	5	Soybeans	1,042	232	8.52	4.02	2.35	931	544	387	48.2	28.2	20.1
Carson	2010	6	Sunflower	82	18	8.50	3.60	2.30	66	42	24	43.2	27.6	15.6
Carson	2010	10	Peanuts	75	17	8.46	4.62	2.45	77	41	36	55.5	29.4	26.1
Carson	2010	24	Winter Wheat	422,285	93,914	8.44	3.21	2.30	301,644	216,106	85,538	38.5	27.6	10.9
Carson	2010	26	Dbl Crop WinWht Soybeans	2	0	8.44	3.21	2.16	1	1	0	38.6	25.9	12.7
Carson	2010	27	Rye	3	1	8.45	3.25	2.19	2	1	1	39.1	26.3	12.7
Carson	2010	28	Oats	664	148	8.67	3.33	2.37	492	350	142	40.0	28.5	11.5
Carson	2010	29	Millet	2	0	8.43	4.35	2.19	2	1	1	52.2	26.2	25.9
Carson	2010	33	Safflower	310	69	8.69	3.49	2.33	240	161	80	41.9	28.0	13.8
Carson	2010	36	Alfalfa	2,000	445	8.53	5.30	2.44	2,360	1,084	1,275	63.7	29.2	34.4
Carson	2010	60	Switchgrass	2	0	8.25	2.43	2.12	1	1	0	29.2	25.4	3.8
Carson	2010	61	Fallow Idle Cropland	142,304	31,648	8.44	2.51	2.28	79,511	72,172	7,339	30.1	27.4	2.8
Carson	2010	74	Pecans	46	**10**	**8**	**4**	**2**	**40**	**24**	**17**	*47.1*	*27.7*	*19.4*
Carson	2010	205	Triticale	97	**22**	**9**	**3**	**2**	**71**	**47**	**24**	*39.3*	*26.2*	*13.2*
Carson	2010	225	Dbl Crop WinWht Corn	729	162	8.39	4.84	2.28	784	370	415	58.0	27.4	30.7
Carson	2010	236	Dbl Crop WinWht Sorghum	316	70	8.41	3.61	2.34	254	165	89	43.3	28.1	15.2
Carson	2010	238	Dbl Crop WinWht Cotton	558	124	8.48	3.75	2.29	465	285	181	45.0	27.5	17.5
			Total		**204,510**				**669,222**	**469,843**	**199,380**	*44.3*	*27.5*	*16.8*
			No fallow/idle		**172,862**				**589,711**	**397,671**	**192,041**			
Carson	2011	1	Corn	77,624	17,263	10.38	5.79	0.74	99,953	12,750	87,203	69.5	8.9	60.6
Carson	2011	2	Cotton	243,018	54,046	10.45	4.01	0.76	216,782	40,950	175,832	48.1	9.1	39.0
Carson	2011	4	Sorghum	158,606	35,273	10.29	3.10	0.73	109,189	25,900	83,289	37.1	8.8	28.3
Carson	2011	5	Soybeans	431	96	10.45	5.18	0.70	497	67	430	62.2	8.4	53.8
Carson	2011	10	Peanuts	6	1	10.46	6.81	0.79	9	1	8	81.8	9.5	72.3
Carson	2011	23	Spring Wheat	290	64	10.57	3.88	0.73	250	47	203	46.6	8.7	37.9
Carson	2011	24	Winter Wheat	330,527	73,507	10.37	3.51	0.74	257,936	54,624	203,312	42.1	8.9	33.2
Carson	2011	27	Rye	530	118	10.73	2.56	0.74	302	87	215	30.7	8.8	21.9
Carson	2011	36	Alfalfa	1,101	245	11	7	1	1,667	173	1,494	*81.7*	*8.5*	*73.2*
Carson	2011	61	Fallow Idle Cropland	96,642	21,493	10.30	2.92	0.74	62,749	15,817	46,931	35.0	8.8	26.2
Carson	2011	74	Pecans	26	6	10.23	4.84	0.71	28	4	24	58.0	8.5	49.6
Carson	2011	225	Dbl Crop WinWht Corn	47	10	10.55	6.94	0.75	73	8	65	83.2	9.0	74.3
Carson	2011	236	Dbl Crop WinWht Sorghum	852	189	10.30	5.33	0.76	1,010	145	865	64.0	9.2	54.8
Carson	2011	238	Dbl Crop WinWht Cotton	1,152	256	10.47	6.00	0.77	1,537	197	1,340	72.0	9.2	62.8
			Total		**202,568**				**751,981**	**150,770**	**601,211**	*58.0*	*8.9*	*49.1*
			No fallow/idle		**181,076**				**689,232**	**134,953**	**554,279**			

COUNTY	YEAR	CDL_NUM	CDL_NAME	PIXELS	ACRES	ETr (ft)	ET (ft)	PPT (ft)	ET (ac-ft)	PPT (ac-ft)	NET ET (ac-ft)	ET (in)	PPT (in)	NET ET (in)
Dawson	2010	1	Corn	944	210	8.71	5.34	2.05	1,121	430	690	64.0	24.6	39.5
Dawson	2010	2	Cotton	1,615,170	359,205	8.76	3.19	2.02	1,147,189	725,497	421,691	38.3	24.2	14.1
Dawson	2010	4	Sorghum	6,992	1,555	8.72	4.22	2.05	6,565	3,187	3,378	50.7	24.6	26.1
Dawson	2010	5	Soybeans	17	4	8.69	4.72	2.13	18	8	10	56.7	25.5	31.2
Dawson	2010	6	Sunflower	2,529	562	8.65	3.28	2.23	1,845	1,255	590	39.4	26.8	12.6
Dawson	2010	10	Peanuts	3,253	723	8.73	4.45	2.01	3,217	1,451	1,766	53.4	24.1	29.3
Dawson	2010	24	Winter Wheat	76,073	16,918	8.73	3.67	2.06	62,022	34,841	27,181	44.0	24.7	19.3
Dawson	2010	26	Dbl Crop WinWht Soybeans	16	4	8.65	5.87	1.94	21	7	14	70.4	23.2	47.2
Dawson	2010	27	Rye	159	35	8.76	3.08	2.05	109	73	36	36.9	24.6	12.3
Dawson	2010	28	Oats	238	53	8.72	3.47	2.00	184	106	78	41.6	24.0	17.6
Dawson	2010	29	Millet	117	26	8.69	4.94	1.94	129	50	78	59.3	23.2	36.0
Dawson	2010	33	Safflower	3	1	8.76	3.94	1.94	3	1	1	47.3	23.3	24.0
Dawson	2010	36	Alfalfa	5,687	1,265	8.63	6.26	2.06	7,914	2,603	5,311	75.1	24.7	50.4
Dawson	2010	61	Fallow Idle Cropland	34,143	7,593	8.77	3.47	2.03	26,343	15,380	10,963	41.6	24.3	17.3
Dawson	2010	74	Pecans	21	5	8.77	4.74	2.00	22	9	13	56.9	24.0	32.9
Dawson	2010	205	Triticale	56	12	8.71	4.80	2.05	60	25	34	57.6	24.6	33.1
Dawson	2010	225	Dbl Crop WinWht Corn	35	8	8.68	5.13	2.09	40	16	24	61.5	25.1	36.4
Dawson	2010	236	Dbl Crop WinWht Sorghum	834	185	8.75	4.78	2.09	886	387	499	57.3	25.0	32.3
Dawson	2010	238	Dbl Crop WinWht Cotton	10,952	2,436	8.73	4.55	2.09	11,084	5,081	6,003	54.6	25.0	29.6
			Total		**390,800**				**1,268,770**	**790,409**	**478,361**	*53.0*	*24.5*	*28.5*
			No fallow/idle		**383,207**				**1,242,427**	**775,029**	**467,397**			
Dawson	2011	1	Corn	55	12	11.21	5.53	0.37	68	4	63	66.4	4.4	62.0
Dawson	2011	2	Cotton	1,645,937	366,047	11.19	3.99	0.39	1,458,831	142,483	1,316,349	47.8	4.7	43.2
Dawson	2011	4	Sorghum	2,840	632	11.14	4.52	0.39	2,854	244	2,610	54.2	4.6	49.6
Dawson	2011	24	Winter Wheat	3,707	824	11.12	4.64	0.39	3,826	322	3,504	55.7	4.7	51.0
Dawson	2011	27	Rye	1,011	225	11.15	5.55	0.38	1,248	86	1,162	66.6	4.6	62.0
Dawson	2011	36	Alfalfa	1,785	397	11.10	8.81	0.37	3,496	147	3,349	105.7	4.4	101.2
Dawson	2011	61	Fallow Idle Cropland	19,095	4,247	11.15	6.32	0.39	26,823	1,658	25,165	75.8	4.7	71.1
Dawson	2011	74	Pecans	34	8	11.13	8.34	0.38	63	3	60	100.0	4.5	95.5
Dawson	2011	236	Dbl Crop WinWht Sorghum	1	0	11.31	6.78	0.36	2	0	1	81.4	4.3	77.0
Dawson	2011	238	Dbl Crop WinWht Cotton	16,686	3,711	11.10	5.15	0.39	19,104	1,448	17,656	61.8	4.7	57.1
			Total		**376,103**				**1,516,314**	**146,394**	**1,369,920**	*71.5*	*4.6*	*67.0*
			No fallow/idle		**371,856**				**1,489,491**	**144,737**	**1,344,754**			

COUNTY	YEAR	CDL_NUM	CDL_NAME	PIXELS	ACRES	ETr (ft)	ET (ft)	PPT (ft)	ET (ac-ft)	PPT (ac-ft)	NET ET (ac-ft)	ET (in)	PPT (in)	NET ET (in)
Hale	2010	1	Corn	169,781	37,758	8.44	4.14	2.09	156,163	78,872	77,292	49.6	25.1	24.6
Hale	2010	2	Cotton	1,295,746	288,167	8.43	3.17	2.06	912,765	592,539	320,226	38.0	24.7	13.3
Hale	2010	4	Sorghum	36,815	8,187	8.43	3.37	2.08	27,608	17,014	10,594	40.5	24.9	15.5
Hale	2010	5	Soybeans	188	42	8.44	3.79	2.11	159	88	70	45.5	25.4	20.2
Hale	2010	6	Sunflower	2,734	608	8.47	3.71	2.17	2,256	1,320	936	44.5	26.0	18.5
Hale	2010	10	Peanuts	281	62	8.45	4.12	2.06	257	129	129	49.4	24.7	24.7
Hale	2010	24	Winter Wheat	252,748	56,210	8.44	3.42	2.04	192,397	114,864	77,534	41.1	24.5	16.6
Hale	2010	26	Dbl Crop WinWht Soybeans	24	5	8.44	4.21	2.12	22	11	11	50.5	25.4	25.1
Hale	2010	27	Rye	18	4	8.44	3.44	2.09	14	8	5	41.3	25.1	16.2
Hale	2010	28	Oats	675	150	8.42	3.53	2.04	531	307	224	42.4	24.5	17.9
Hale	2010	29	Millet	48	11	8.49	3.84	2.27	41	24	17	46.1	27.2	18.9
Hale	2010	33	Safflower	57	13	8.42	3.47	2.05	44	26	18	41.6	24.6	17.0
Hale	2010	36	Alfalfa	5,825	1,295	8.45	5.37	2.11	6,956	2,735	4,221	64.4	25.3	39.1
Hale	2010	42	Dry Beans	52	12	8.41	3.11	2.16	36	25	11	37.3	25.9	11.4
Hale	2010	43	Potatoes	2	0	8.44	3.29	1.87	1	1	1	39.4	22.4	17.0
Hale	2010	60	Switchgrass	19	4	8.61	2.12	2.00	9	8	1	25.5	24.0	1.5
Hale	2010	61	Fallow Idle Cropland	46,770	10,401	8.43	3.11	2.04	32,353	21,209	11,144	37.3	24.5	12.9
Hale	2010	74	Pecans	346	77	8.44	4.10	1.97	316	152	164	49.2	23.6	25.6
Hale	2010	205	Triticale	839	187	8.43	4.54	2.11	848	393	455	54.5	25.3	29.3
Hale	2010	225	Dbl Crop WinWht Corn	3,317	738	8.44	5.18	2.03	3,818	1,496	2,322	62.1	24.3	37.8
Hale	2010	236	Dbl Crop WinWht Sorghum	3,445	766	8.45	4.57	2.02	3,501	1,546	1,955	54.8	24.2	30.6
Hale	2010	237	Dbl Crop Barley Corn	19	4	8.46	4.82	1.91	20	8	12	57.9	23.0	34.9
Hale	2010	238	Dbl Crop WinWht Cotton	8,975	1,996	8.46	4.52	2.15	9,013	4,291	4,722	54.2	25.8	28.4
			Total		**406,698**				**1,349,128**	**837,067**	**512,061**	*46.4*	*24.8*	*21.6*
			No fallow/idle		**396,297**				**1,316,775**	**815,858**	**500,917**			
Hale	2011	1	Corn	129,817	28,871	10.69	5.60	0.53	161,804	15,356	146,448	67.3	6.4	60.9
Hale	2011	2	Cotton	1,636,450	363,937	10.68	4.02	0.53	1,461,693	191,862	1,269,831	48.2	6.3	41.9
Hale	2011	4	Sorghum	7,197	1,601	10.68	5.01	0.53	8,014	849	7,165	60.1	6.4	53.7
Hale	2011	5	Soybeans	85	19	10.68	5.46	0.53	103	10	93	65.5	6.4	59.1
Hale	2011	6	Sunflower	11	2	10.67	5.13	0.53	13	1	11	61.6	6.4	55.2
Hale	2011	10	Peanuts	23	5	10.68	5.69	0.54	29	3	26	68.3	6.4	61.8
Hale	2011	24	Winter Wheat	64,470	14,338	10.69	4.15	0.53	59,501	7,651	51,850	49.8	6.4	43.4
Hale	2011	27	Rye	1	0	10.70	7.04	0.53	2	0	1	84.5	6.4	78.1
Hale	2011	28	Oats	341	76	10.67	4.96	0.52	376	39	337	59.5	6.2	53.3
Hale	2011	29	Millet	2	0	10.64	2.91	0.52	1	0	1	34.9	6.2	28.7
Hale	2011	36	Alfalfa	4,396	978	10.71	6.74	0.53	6,586	521	6,065	80.8	6.4	74.4
Hale	2011	43	Potatoes	100	22	10.78	6.56	0.54	146	12	134	78.7	6.5	72.2
Hale	2011	61	Fallow Idle Cropland	26,670	5,931	10.70	3.20	0.53	18,968	3,126	15,842	38.4	6.3	32.1
Hale	2011	74	Pecans	58	13	10.75	5.91	0.54	76	7	69	70.9	6.4	64.5
Hale	2011	205	Triticale	521	116	10.66	4.01	0.52	464	60	404	48.1	6.2	41.8
Hale	2011	225	Dbl Crop WinWht Corn	1,131	252	10.67	7.10	0.53	1,785	133	1,651	85.1	6.4	78.8
Hale	2011	236	Dbl Crop WinWht Sorghum	316	70	10.70	6.39	0.54	449	38	411	76.7	6.5	70.2
Hale	2011	238	Dbl Crop WinWht Cotton	2,748	611	10.70	4.59	0.53	2,804	323	2,481	55.1	6.3	48.7
			Total		**416,842**				**1,722,813**	**219,991**	**1,502,822**	*63.0*	*6.4*	*56.6*
			No fallow/idle		**410,911**				**1,703,846**	**216,866**	**1,486,980**			

COUNTY	YEAR	CDL_NUM	CDL_NAME	PIXELS	ACRES	ETr (ft)	ET (ft)	PPT (ft)	ET (ac-ft)	PPT (ac-ft)	NET ET (ac-ft)	ET (in)	PPT (in)	NET ET (in)
Medina	2010	1	Corn	148912	33,117	7.74	3.22	2.54	106,759	84,195	22,563	38.7	30.5	8.2
Medina	2010	2	Cotton	55467	12,336	7.75	3.86	2.56	47,579	31,623	15,956	46.3	30.8	15.5
Medina	2010	4	Sorghum	87432	19,444	7.76	3.77	2.49	73,232	48,369	24,862	45.2	29.9	15.3
Medina	2010	6	Sunflower	4161	925	7.66	3.11	2.67	2,876	2,472	405	37.3	32.1	5.2
Medina	2010	10	Peanuts	646	144	7.80	4.19	2.42	602	348	253	50.3	29.1	21.2
Medina	2010	12	Sweet Corn	17	4	7.70	3.03	2.45	11	9	2	36.3	29.4	7.0
Medina	2010	21	Barley	7	2	7.76	4.08	2.45	6	4	3	49.0	29.4	19.6
Medina	2010	23	Spring Wheat	1010	225	7.80	3.99	2.44	896	547	349	47.9	29.2	18.6
Medina	2010	24	Winter Wheat	101662	22,609	7.78	4.09	2.48	92,479	56,060	36,419	49.1	29.8	19.3
Medina	2010	27	Rye	359	80	8.02	4.51	2.36	360	188	172	54.1	28.3	25.8
Medina	2010	28	Oats	33297	7,405	7.78	3.93	2.51	29,111	18,567	10,544	47.2	30.1	17.1
Medina	2010	29	Millet	14	3	7.73	3.78	2.60	12	8	4	45.3	31.2	14.1
Medina	2010	33	Safflower	7	2	7.72	3.35	2.66	5	4	1	40.2	31.9	8.3
Medina	2010	36	Alfalfa	12	3	7.80	4.17	2.36	11	6	5	50.0	28.3	21.7
Medina	2010	44	Other Crops	29	6	7.75	3.86	2.43	25	16	9	46.3	29.1	17.2
Medina	2010	53	Peas	1	0	7.72	4.52	2.88	1	1	0	54.2	34.6	19.6
Medina	2010	57	Herbs	1	0	7.74	4.93	2.38	1	1	1	59.2	28.6	30.6
Medina	2010	58	Clover Wildflowers	5	1	7.77	4.93	2.67	5	3	3	59.1	32.0	27.1
Medina	2010	61	Fallow Idle Cropland	79392	17,656	7.78	4.39	2.43	77,437	42,951	34,486	52.6	29.2	23.4
Medina	2010	67	Peaches	54	12	7.59	3.61	2.85	43	34	9	43.4	34.2	9.2
Medina	2010	74	Pecans	313	70	7.76	4.78	2.58	333	180	153	57.4	30.9	26.4
Medina	2010	205	Triticale	184	41	7.80	4.58	2.62	188	107	80	55.0	31.4	23.6
Medina	2010	236	Dbl Crop WinWht Sorghum	32	7	7.87	2.67	2.43	19	17	2	32.0	29.1	2.9
Medina	2010	238	Dbl Crop WinWht Cotton	213	47	7.84	3.66	2.39	173	113	60	43.9	28.7	15.2
Medina	2010	243	Cabbage	2	0	7.83	3.95	2.19	2	1	1	47.4	26.3	21.1
			Total		**114,139**				**432,167**	**285,825**	**146,341**	*47.5*	*30.2*	*17.3*
			No fallow/idle		**96,483**				**354,730**	**242,875**	**111,856**			
Medina	2011	1	Corn	110599	24,597	9.86	4.38	1.20	107,723	29,425	78,298	52.6	14.4	38.2
Medina	2011	2	Cotton	158529	35,256	9.86	3.95	1.20	139,436	42,154	97,282	47.5	14.3	33.1
Medina	2011	4	Sorghum	44321	9,857	9.85	3.14	1.18	30,964	11,615	19,349	37.7	14.1	23.6
Medina	2011	6	Sunflower	3768	838	9.88	3.46	1.22	2,900	1,021	1,880	41.5	14.6	26.9
Medina	2011	10	Peanuts	7	2	9.82	6.06	1.16	9	2	8	72.7	14.0	58.8
Medina	2011	23	Spring Wheat	4751	1,057	9.88	4.17	1.15	4,403	1,215	3,189	50.0	13.8	36.2
Medina	2011	24	Winter Wheat	47065	10,467	9.88	3.30	1.18	34,561	12,401	22,161	39.6	14.2	25.4
Medina	2011	27	Rye	203	45	9.89	3.16	1.08	143	49	94	37.9	13.0	24.9
Medina	2011	28	Oats	12801	2,847	9.85	3.34	1.18	9,507	3,371	6,136	40.1	14.2	25.9
Medina	2011	36	Alfalfa	2	0	9.79	4.54	1.23	2	1	1	54.5	14.8	39.8
Medina	2011	42	Dry Beans	73	16	9.85	4.97	1.17	81	19	62	59.7	14.0	45.7
Medina	2011	44	Other Crops	2	0	9.86	3.36	1.17	1	1	1	40.3	14.0	26.3
Medina	2011	47	Misc Vegs & Fruits	90	20	9.82	3.83	1.16	77	23	53	46.0	13.9	32.0
Medina	2011	61	Fallow Idle Cropland	105221	23,401	9.88	3.22	1.14	75,466	26,565	48,901	38.7	13.6	25.1
Medina	2011	74	Pecans	26	6	9.82	5.75	1.21	33	7	26	69.0	14.5	54.5
Medina	2011	205	Triticale	29	6	9.79	4.57	1.19	29	8	22	54.8	14.3	40.5
Medina	2011	211	Olives	5	1	9.86	3.56	1.10	4	1	3	42.8	13.2	29.6
Medina	2011	225	Dbl Crop WinWht Corn	152	34	9.82	4.53	1.21	153	41	112	54.3	14.6	39.8
Medina	2011	236	Dbl Crop WinWht Sorghum	319	71	9.85	2.94	1.18	208	83	125	35.2	14.1	21.1
Medina	2011	238	Dbl Crop WinWht Cotton	692	154	9.79	3.21	1.21	493	186	308	38.5	14.5	24.0
Medina	2011	243	Cabbage	3	1	9.89	2.84	1.10	2	1	1	34.0	13.2	20.9
			Total		**108,675**				**406,197**	**128,187**	**278,010**	*47.0*	*14.1*	*33.0*
			No fallow/idle		**85,274**				**330,731**	**101,622**	**229,110**			

COUNTY	YEAR	CDL_NUM	CDL_NAME	PIXELS	ACRES	ETr (ft)	ET (ft)	PPT (ft)	ET (ac-ft)	PPT (ac-ft)	NET ET (ac-ft)	ET (in)	PPT (in)	NET ET (in)
Ochiltree	2010	1	Corn	96908	21,552	8.43	5.08	2.39	109,539	51,429	58,110	61.0	28.6	32.4
Ochiltree	2010	2	Cotton	125905	28,001	8.31	4.05	2.35	113,480	65,824	47,656	48.6	28.2	20.4
Ochiltree	2010	4	Sorghum	145972	32,463	8.19	3.97	2.26	128,864	73,216	55,647	47.6	27.1	20.6
Ochiltree	2010	5	Soybeans	7535	1,676	8.45	4.89	2.44	8,199	4,086	4,113	58.7	29.3	29.5
Ochiltree	2010	6	Sunflower	705	157	8.42	4.02	2.43	631	380	250	48.3	29.1	19.1
Ochiltree	2010	10	Peanuts	38	8	8.53	4.96	2.35	42	20	22	59.5	28.2	31.3
Ochiltree	2010	24	Winter Wheat	711867	158,315	8.23	3.80	2.28	602,032	360,598	241,434	45.6	27.3	18.3
Ochiltree	2010	26	Dbl Crop WinWht Soybeans	597	133	8.49	5.35	2.43	710	323	387	64.2	29.2	35.0
Ochiltree	2010	27	Rye	12	3	8.14	3.69	2.29	10	6	4	44.3	27.5	16.8
Ochiltree	2010	28	Oats	812	181	8.13	3.35	2.20	604	398	207	40.2	26.4	13.7
Ochiltree	2010	29	Millet	1	0	8.54	5.05	2.31	1	1	1	60.7	27.8	32.9
Ochiltree	2010	33	Safflower	181	40	8.13	3.57	2.22	144	90	54	42.9	26.7	16.2
Ochiltree	2010	36	Alfalfa	1842	410	8.36	5.76	2.41	2,360	986	1,375	69.1	28.9	40.3
Ochiltree	2010	61	Fallow Idle Cropland	203168	45,183	8.18	3.18	2.27	143,726	102,466	41,260	38.2	27.2	11.0
Ochiltree	2010	74	Pecans	15	3	8.37	5.31	2.32	18	8	10	63.7	27.9	35.8
Ochiltree	2010	205	Triticale	170	38	8.20	3.89	2.29	147	87	60	46.6	27.5	19.1
Ochiltree	2010	225	Dbl Crop WinWht Corn	334	74	8.37	5.01	2.59	372	193	180	60.1	31.1	29.0
Ochiltree	2010	236	Dbl Crop WinWht Sorghum	1649	367	8.28	4.75	2.33	1,743	855	888	57.0	28.0	29.1
Ochiltree	2010	238	Dbl Crop WinWht Cotton	1962	436	8.37	5.14	2.46	2,244	1,074	1,170	61.7	29.5	32.2
			Total		**289,040**				**1,114,865**	**662,037**	**452,828**	*53.6*	*28.2*	*25.4*
			No fallow/idle		**243,857**				**971,139**	**559,572**	**411,568**			
Ochiltree	2011	1	Corn	121474	27,015	10.22	6.15	0.76	166,224	20,604	145,620	73.8	9.2	64.7
Ochiltree	2011	2	Cotton	84723	18,842	10.15	4.50	0.77	84,814	14,523	70,292	54.0	9.2	44.8
Ochiltree	2011	4	Sorghum	256549	57,055	9.96	3.56	0.80	202,878	45,599	157,279	42.7	9.6	33.1
Ochiltree	2011	5	Soybeans	11449	2,546	10.26	5.66	0.76	14,401	1,941	12,461	67.9	9.1	58.7
Ochiltree	2011	10	Peanuts	1	0	9.92	5.48	0.79	1	0	1	65.8	9.5	56.3
Ochiltree	2011	24	Winter Wheat	621038	138,115	10.01	3.88	0.79	536,537	109,089	427,448	46.6	9.5	37.1
Ochiltree	2011	27	Rye	43	10	9.83	3.25	0.81	31	8	23	39.0	9.8	29.3
Ochiltree	2011	28	Oats	3	1	10.19	3.88	0.77	3	1	2	46.5	9.2	37.3
Ochiltree	2011	36	Alfalfa	3070	683	10.28	7.01	0.77	4,784	527	4,257	84.1	9.3	74.8
Ochiltree	2011	61	Fallow Idle Cropland	202546	45,045	9.95	3.42	0.80	153,856	36,260	117,597	41.0	9.7	31.3
Ochiltree	2011	74	Pecans	9	2	10.05	5.55	0.79	11	2	10	66.6	9.5	57.0
Ochiltree	2011	205	Triticale	1941	432	10.13	3.75	0.77	1,619	332	1,287	45.0	9.2	35.8
Ochiltree	2011	225	Dbl Crop WinWht Corn	1599	356	10.28	6.80	0.75	2,416	268	2,149	81.5	9.0	72.5
Ochiltree	2011	236	Dbl Crop WinWht Sorghum	5565	1,238	10.17	6.51	0.77	8,057	958	7,099	78.1	9.3	68.8
Ochiltree	2011	238	Dbl Crop WinWht Cotton	1256	279	10.25	5.91	0.78	1,650	217	1,433	70.9	9.3	61.5
			Total		**291,618**				**1,177,284**	**230,327**	**946,957**	*60.2*	*9.4*	*50.9*
			No fallow/idle		**246,573**				**1,023,427**	**194,068**	**829,360**			

COUNTY	YEAR	CDL_NUM	CDL_NAME	PIXELS	ACRES	ETr (ft)	ET (ft)	PPT (ft)	ET (ac-ft)	PPT (ac-ft)	NET ET (ac-ft)	ET (in)	PPT (in)	NET ET (in)
Wharton	2010	1	Corn	416044	92,526	6.97	3.70	3.48	342,734	321,908	20,826	44.5	41.7	2.7
Wharton	2010	2	Cotton	270276	60,108	6.98	3.02	3.49	181,360	209,480	(28,120)	36.2	41.8	0.0
Wharton	2010	3	Rice	211530	47,043	6.96	4.41	3.22	207,505	151,610	55,895	52.9	38.7	14.3
Wharton	2010	4	Sorghum	94433	21,001	6.93	3.54	3.50	74,390	73,448	942	42.5	42.0	0.5
Wharton	2010	5	Soybeans	54728	12,171	6.98	3.18	3.43	38,656	41,771	(3,115)	38.1	41.2	0.0
Wharton	2010	6	Sunflower	5	1	7.03	5.13	3.20	6	4	2	61.5	38.4	23.1
Wharton	2010	24	Winter Wheat	3370	749	6.97	3.89	3.45	2,916	2,585	331	46.7	41.4	5.3
Wharton	2010	28	Oats	377	84	6.93	3.96	3.14	332	263	69	47.5	37.7	9.8
Wharton	2010	49	Onions	1	0	6.88	4.26	4.36	1	1	(0)	51.1	52.3	0.0
Wharton	2010	57	Herbs	556	124	6.91	2.54	4.10	314	507	(193)	30.5	49.2	0.0
Wharton	2010	61	Fallow Idle Cropland	940882	209,247	6.97	4.32	3.33	904,251	696,710	207,542	51.9	40.0	11.9
Wharton	2010	74	Pecans	129	29	7.01	4.93	3.23	141	93	49	59.1	38.8	20.4
Wharton	2010	92	Aquaculture	6068	1,349	6.83	3.90	3.69	5,266	4,981	285	46.8	44.3	2.5
Wharton	2010	239	Dbl Crop Soybeans Cotton	869	193	6.96	2.36	3.30	456	638	(183)	28.3	39.6	0.0
			Total		**444,626**				**1,758,328**	**1,503,999**	**254,329**	*45.5*	*41.9*	*6.5*
			No fallow/idle		**235,379**				**854,077**	**807,289**	**46,788**			
Wharton	2011	1	Corn	354665	78,876	8.73	3.98	1.44	313,685	113,458	200,227	47.7	17.3	30.5
Wharton	2011	2	Cotton	422430	93,946	8.71	3.57	1.45	335,064	136,018	199,046	42.8	17.4	25.4
Wharton	2011	3	Rice	216696	48,192	8.84	6.36	1.42	306,634	68,273	238,362	76.4	17.0	59.4
Wharton	2011	4	Sorghum	50218	11,168	8.64	3.90	1.48	43,598	16,533	27,066	46.8	17.8	29.1
Wharton	2011	5	Soybeans	15484	3,444	8.78	3.86	1.42	13,282	4,897	8,385	46.3	17.1	29.2
Wharton	2011	24	Winter Wheat	25823	5,743	8.82	4.52	1.41	25,947	8,103	17,844	54.2	16.9	37.3
Wharton	2011	26	Dbl Crop WinWht Soybeans	972	216	8.83	4.69	1.44	1,014	312	702	56.3	17.3	39.0
Wharton	2011	27	Rye	546	121	8.53	4.96	1.58	602	192	411	59.5	18.9	40.6
Wharton	2011	28	Oats	569	127	8.89	4.44	1.43	562	182	380	53.3	17.2	36.1
Wharton	2011	44	Other Crops	27	6	8.83	4.97	1.43	30	9	21	59.6	17.2	42.4
Wharton	2011	57	Herbs	527	117	8.78	4.14	1.43	485	167	317	49.6	17.1	32.5
Wharton	2011	61	Fallow Idle Cropland	957931	213,039	8.82	4.95	1.43	1,053,701	305,203	748,498	59.4	17.2	42.2
Wharton	2011	74	Pecans	870	193	8.59	6.42	1.58	1,242	306	936	77.0	19.0	58.0
Wharton	2011	92	Aquaculture	9309	2,070	8.56	7.44	1.50	15,405	3,108	12,297	89.3	18.0	71.3
Wharton	2011	239	Dbl Crop Soybeans Cotton	227	50	8.59	3.67	1.45	185	73	112	44.0	17.4	26.6
			Total		**457,308**				**2,111,437**	**656,832**	**1,454,605**	*57.5*	*17.5*	*40.0*
			No fallow/idle		**244,270**				**1,057,736**	**351,629**	**706,107**			

Appendix I. Annual water balance data from ET Demands Model

COUNTY	Etd	Etd_name	Year	PMETo	ETact	ETpot	PPT	Irrigation	Runoff	DPerc	*NIWR*	CDL	*NIWR*
				in	in	in	in	in	in	in	in	acres	ac-ft
Brazos	3	Alfalfa Hay	2010	67.9	63.3	63.4	7.6	52.7	0.1	5.3	55.8	2	8
Brazos	4	Grass Hay	2010	67.9	44.2	44.9	7.6	36.6	0.0	4.5	37.4		-
Brazos	7	Field Corn	2010	67.9	33.3	35.2	7.6	24.8	0.2	1.8	25.9	7,074	15,252
Brazos	58	Cotton	2010	67.9	39.5	41.0	7.6	31.9	0.0	2.8	31.9	11,341	30,176
Brazos	60	Sorghum	2010	67.9	40.2	41.9	7.6	31.0	0.0	2.9	32.6	969	2,630
			2010 Total										48,066
Brazos	3	Alfalfa Hay	2011	83.6	81.6	81.6	5.0	76.0	0.0	7.3	76.6		-
Brazos	4	Grass Hay	2011	83.6	57.0	58.0	5.0	52.2	0.0	5.1	52.1	6	27
Brazos	7	Field Corn	2011	83.6	44.3	47.4	5.0	40.6	0.1	2.9	39.4	3,462	11,354
Brazos	58	Cotton	2011	83.6	52.3	54.3	5.0	46.4	0.0	4.2	47.4	18,833	74,353
Brazos	60	Sorghum	2011	83.6	50.2	53.1	5.0	45.5	0.0	3.7	45.2	1,308	4,931
			2011 Total										90,666
Cameron	4	Grass Hay	2010	68.3	40.2	41.6	8.2	32.4	0.0	3.1	32.0		-
Cameron	7	Field Corn	2010	68.3	31.1	33.5	8.2	23.3	0.0	1.8	22.9	16050	30,611
Cameron	58	Cotton	2010	68.3	34.8	36.8	8.2	26.9	0.0	3.2	27.1	64087	144,775
Cameron	60	Sorghum	2010	68.3	36.0	38.5	8.2	26.9	0.1	2.7	27.9	103119	239,576
			2010 Total										414,963
Cameron	4	Grass Hay	2011	75.0	42.3	44.5	3.7	37.0	0.0	3.7	38.6	73	233
Cameron	7	Field Corn	2011	75.0	32.6	35.8	3.7	27.9	0.0	2.6	28.8	7422	17,839
Cameron	58	Cotton	2011	75.0	36.3	39.1	3.7	31.7	0.0	3.3	32.7	86274	234,866
Cameron	60	Sorghum	2011	75.0	36.8	40.5	3.7	34.0	0.0	3.3	33.3	56085	155,506
			2011 Total										408,443
Carson	3	Alfalfa Hay	2010	72.7	65.3	66.2	7.5	59.7	0.0	5.2	57.8	445	2,143
Carson	4	Grass Hay	2010	72.7	59.4	60.0	7.5	51.6	0.0	4.2	51.9		-
Carson	7	Field Corn	2010	72.7	47.6	49.6	7.5	39.4	0.0	2.8	40.1	17,112	57,167
Carson	13	Winter Grain	2010	72.7	40.7	44.6	7.5	31.4	0.0	1.7	33.2	93,914	259,986
Carson	58	Cotton	2010	72.7	44.2	46.0	7.5	35.3	0.0	3.3	36.7	48,596	148,722
Carson	60	Sorghum	2010	72.7	47.8	49.7	7.5	40.6	0.0	3.3	40.3	11,922	40,057
			2010 Total										508,076
Carson	3	Alfalfa Hay	2011	84.8	76.3	77.3	2.2	71.4	0.0	6.7	74.1	245	1,512
Carson	4	Grass Hay	2011	84.8	69.6	70.9	2.2	68.3	0.0	5.8	67.4		-
Carson	7	Field Corn	2011	84.8	55.7	58.4	2.2	52.5	0.0	3.8	53.5	17,263	76,986
Carson	13	Winter Grain	2011	84.8	46.3	50.8	2.2	45.7	0.0	3.0	44.1	73,507	270,188
Carson	58	Cotton	2011	84.8	47.5	50.8	2.2	45.4	0.0	3.5	45.3	54,046	204,035
Carson	60	Sorghum	2011	84.8	52.5	56.0	2.2	48.9	0.0	4.1	50.3	35,273	147,782
			2011 Total										700,503
Dawson	3	Alfalfa Hay	2010	72.9	63.8	64.4	6.1	59.7	0.0	5.5	57.8	1,265	6,088
Dawson	4	Grass Hay	2010	72.9	54.2	55.2	6.1	48.2	0.0	4.1	48.1		-
Dawson	13	Winter Grain	2010	72.9	41.8	45.3	6.1	33.3	0.0	2.8	35.7	16,918	50,382
Dawson	58	Cotton	2010	72.9	42.8	44.7	6.1	36.4	0.0	3.5	36.7	359,205	1,100,012
Dawson	60	Sorghum	2010	72.9	43.7	46.1	6.1	38.1	0.0	3.2	37.7	1,555	4,881
			2010 Total										1,161,363
Dawson	3	Alfalfa Hay	2011	87.8	78.9	79.8	1.1	75.0	0.0	7.4	77.8	397	2,573
Dawson	4	Grass Hay	2011	87.8	66.4	68.2	1.1	65.5	0.0	5.9	65.3		-
Dawson	13	Winter Grain	2011	87.8	45.5	50.6	1.1	45.7	0.0	3.6	44.4	824	3,053
Dawson	58	Cotton	2011	87.8	59.0	61.1	1.1	56.7	0.0	5.4	57.9	366,047	1,765,391
Dawson	60	Sorghum	2011	87.8	50.0	53.8	1.1	48.7	0.0	4.6	48.9	632	2,576
			2011 Total										1,773,593

COUNTY	Etd	Etd_name	Year	PMETo	ETact	ETpot	PPT	Irrigation	Runoff	DPerc	*NIWR*	CDL	*NIWR*
				in	in	in	in	in	in	in	in	acres	ac-ft
Hale	3	Alfalfa Hay	2010	69.6	60.4	61.0	6.3	53.6	0.0	5.4	54.2	1,295	5,846
Hale	4	Grass Hay	2010	69.6	54.2	54.8	6.3	48.0	0.0	4.2	47.9		-
Hale	7	Field Corn	2010	69.6	42.6	44.5	6.3	36.4	0.0	2.6	36.2	37,758	113,974
Hale	13	Winter Grain	2010	69.6	39.3	42.3	6.3	30.8	0.0	2.4	33.0	56,210	154,496
Hale	58	Cotton	2010	69.6	39.2	41.4	6.3	31.2	0.0	2.9	32.9	288,167	790,552
Hale	60	Sorghum	2010	69.6	41.0	43.0	6.3	34.5	0.0	3.3	34.7	8,187	23,649
			2010 Total										1,088,518
Hale	3	Alfalfa Hay	2011	84.3	75.6	76.4	1.5	74.8	0.0	7.4	74.0	978	6,033
Hale	4	Grass Hay	2011	84.3	67.2	68.5	1.5	64.6	0.0	5.8	65.6		-
Hale	7	Field Corn	2011	84.3	53.7	56.3	1.5	50.8	0.0	4.4	52.1	28,871	125,440
Hale	13	Winter Grain	2011	84.3	44.3	49.1	1.5	43.4	0.0	3.4	42.8	14,338	51,139
Hale	58	Cotton	2011	84.3	45.1	48.5	1.5	44.3	0.0	3.3	43.6	363,937	1,321,347
Hale	60	Sorghum	2011	84.3	49.0	52.6	1.5	45.8	0.0	4.4	47.4	1,601	6,328
			2011 Total										1,510,286
Medina	4	Grass Hay	2010	67.9	42.9	44.2	6.7	34.2	0.0	3.2	36.2	3	8
Medina	7	Field Corn	2010	67.9	33.1	35.4	6.7	26.7	0.0	2.0	26.4	33,117	72,888
Medina	13	Winter Grain	2010	67.9	31.1	35.6	6.7	21.2	0.1	1.6	24.4	22,609	46,030
Medina	58	Cotton	2010	67.9	39.3	41.1	6.7	32.3	0.0	3.0	32.6	12,336	33,515
Medina	60	Sorghum	2010	67.9	40.2	42.3	6.7	31.5	0.0	3.3	33.7	19,444	54,598
			2010 Total										207,039
Medina	4	Grass Hay	2011	82.2	51.9	53.7	3.6	49.9	0.0	4.5	48.3	0	2
Medina	7	Field Corn	2011	82.2	40.8	43.9	3.6	37.3	0.0	2.9	37.2	24,597	76,309
Medina	13	Winter Grain	2011	82.2	31.6	38.3	3.6	28.4	0.0	2.2	28.1	10,467	24,477
Medina	58	Cotton	2011	82.2	46.2	48.9	3.6	42.0	0.0	3.9	42.6	35,256	125,230
Medina	60	Sorghum	2011	82.2	47.5	50.8	3.6	44.5	0.0	3.8	43.9	9,857	36,087
			2011 Total										262,105
Ochiltree	3	Alfalfa Hay	2010	67.8	59.1	59.7	7.4	48.0	0.2	4.8	51.9	410	1,773
Ochiltree	4	Grass Hay	2010	67.8	55.0	55.6	7.4	47.7	0.0	4.1	47.7		-
Ochiltree	7	Field Corn	2010	67.8	46.2	47.7	7.4	37.6	0.2	2.6	38.9	21,552	69,942
Ochiltree	13	Winter Grain	2010	67.8	37.1	39.5	7.4	29.2	0.2	2.4	30.0	158,315	395,234
Ochiltree	58	Cotton	2010	67.8	41.8	43.1	7.4	33.6	0.1	3.2	34.6	28,001	80,707
Ochiltree	60	Sorghum	2010	67.8	46.7	48.4	7.4	40.7	0.1	3.7	39.6	32,463	107,126
			2010 Total										654,782
Ochiltree	3	Alfalfa Hay	2011	78.6	71.1	71.9	2.4	69.8	0.0	6.2	68.7	683	3,911
Ochiltree	4	Grass Hay	2011	78.6	64.0	65.2	2.4	61.8	0.0	5.4	61.6		-
Ochiltree	7	Field Corn	2011	78.6	52.7	55.1	2.4	49.7	0.0	3.3	50.3	27,015	113,263
Ochiltree	13	Winter Grain	2011	78.6	43.3	46.8	2.4	40.3	0.0	3.5	40.8	138,115	470,121
Ochiltree	58	Cotton	2011	78.6	43.9	46.6	2.4	41.3	0.0	3.3	41.4	18,842	65,077
Ochiltree	60	Sorghum	2011	78.6	47.6	50.8	2.4	43.3	0.0	4.3	45.2	57,055	215,047
			2011 Total										867,420
Wharton	4	Grass Hay	2010	60.2	39.6	40.0	8.9	28.7	0.0	3.3	31.1		-
Wharton	7	Field Corn	2010	60.2	29.0	30.5	8.9	17.8	0.1	1.6	20.1	92,526	155,158
Wharton	58	Cotton	2010	60.2	33.8	35.0	8.9	23.0	0.0	2.5	25.1	60,108	125,515
Wharton	60	Sorghum	2010	60.2	33.9	35.1	8.9	24.7	0.0	2.7	25.2	21,001	44,105
			2010 Total										324,778
Wharton	4	Grass Hay	2011	75.0	47.7	49.1	4.2	44.0	0.0	4.0	43.5		-
Wharton	7	Field Corn	2011	75.0	37.6	39.9	4.2	34.5	0.0	2.5	33.4	78,876	219,788
Wharton	58	Cotton	2011	75.0	43.8	45.8	4.2	40.4	0.0	3.3	39.6	93,946	309,688
Wharton	60	Sorghum	2011	75.0	41.7	44.4	4.2	37.8	0.0	3.8	37.7	11,168	35,068
			2011 Total										564,545

Appendix J. Major crop percentages by county and year extracted from the CDL.

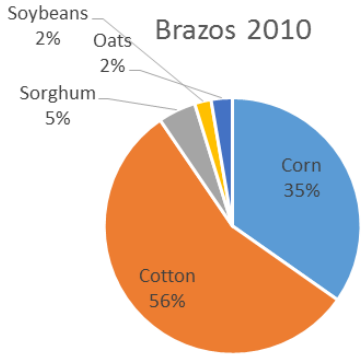

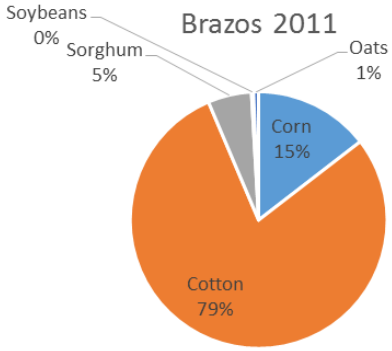

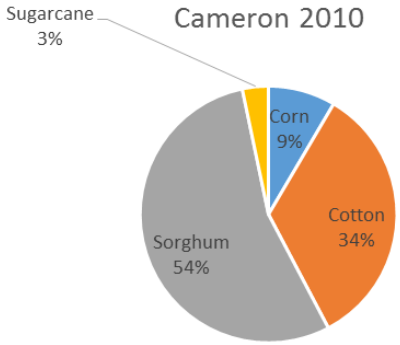

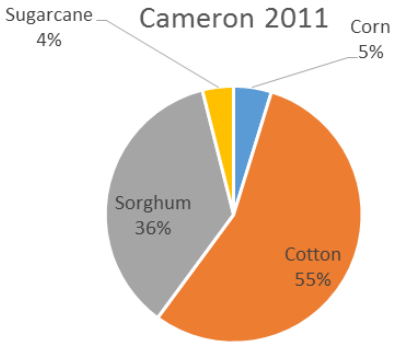

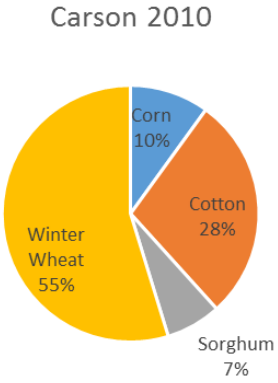

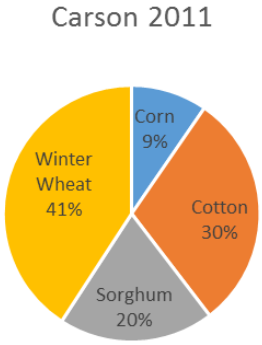

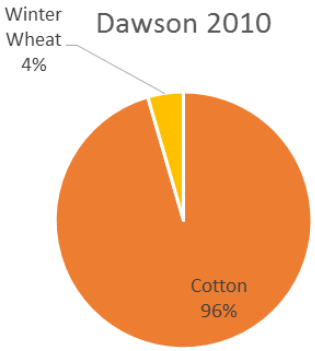

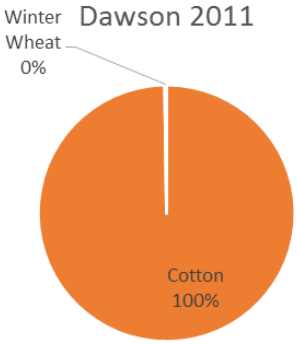

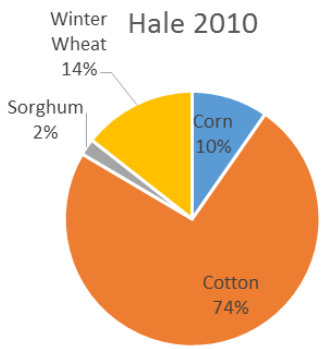
Hale 2010
Winter Wheat 14%
Sorghum 2%
Corn 10%
Cotton 74%

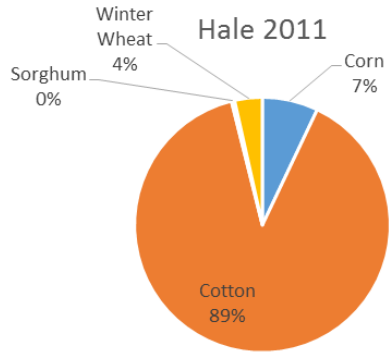
Hale 2011
Winter Wheat 4%
Sorghum 0%
Corn 7%
Cotton 89%

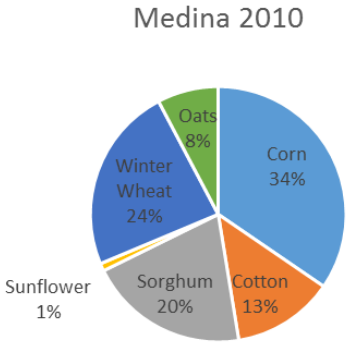
Medina 2010
Oats 8%
Corn 34%
Winter Wheat 24%
Sunflower 1%
Sorghum 20%
Cotton 13%

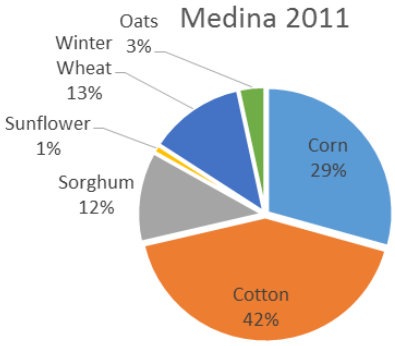
Medina 2011
Oats 3%
Winter Wheat 13%
Sunflower 1%
Corn 29%
Sorghum 12%
Cotton 42%

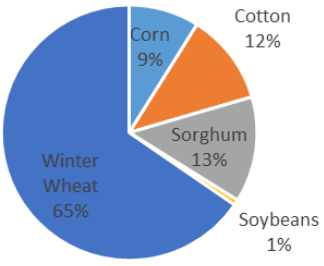
Ochiltree 2010
Corn 9%
Cotton 12%
Sorghum 13%
Winter Wheat 65%
Soybeans 1%

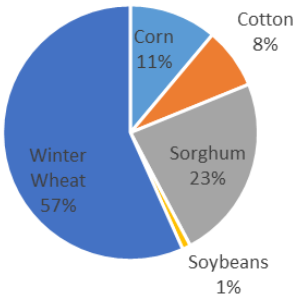
Ochiltree 2011
Corn 11%
Cotton 8%
Winter Wheat 57%
Sorghum 23%
Soybeans 1%

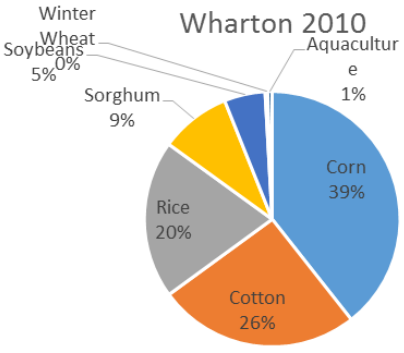
Wharton 2010
Winter Wheat 0%
Soybeans 5%
Aquaculture 1%
Sorghum 9%
Corn 39%
Rice 20%
Cotton 26%

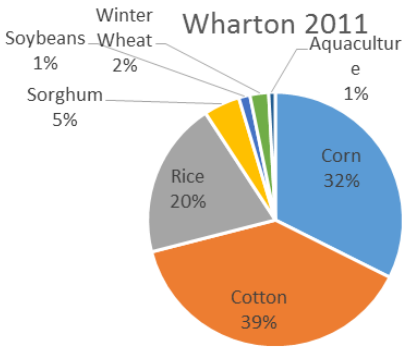
Wharton 2011
Soybeans 1%
Winter Wheat 2%
Aquaculture 1%
Sorghum 5%
Corn 32%
Rice 20%
Cotton 39%

Appendix K. TWDB staff comments on the February 24, 2017

page 1, paragraph 2 (and elsewhere throughout)

"…compare these results to the TWDB's Historical Water Use Survey–the current methodology used annually at the county-level." This statement, and other similar statements and/or references to the HWUS throughout the draft report, inaccurately describes the annual process by which TWDB staff estimate agricultural irrigation water use for every county in Texas. The first revised scope of work (Task 6, Milestone 2) of the contract states that "the final goal of this project is to identify tools with the ability to improve upon the current estimation methodology used by the Texas Water Development Board in developing annual irrigation water use estimates…" It is therefore essential that the current methodology be understood and described accurately within this report. Please consult the online description of the methodology and/or confer with TWDB staff to correct all references to the Historical Water Use Survey and related errors throughout.

See also page 4, section 2.2; page 49, paragraphs 1 and 2; page 51, section 6.3; page 52, section 6.4; page 67, paragraph 2; and all associated tables and figures that incorrectly reference the Historical Water Use Survey.

Response: There was considerable confusion between the nomenclature of Historical Water Use Estimates, Historical Water Use Surveys (HWUS) and Irrigation Water Use Estimates (IWUE). Any reference to HWUS was replaced with IWUE which were extracted for 2010 and 2011 from

http://www2.twdb.texas.gov/ReportServerExt/Pages/ReportViewer.aspx?%2fWU%2fSumFinal_CountyReport&rs:Command=Render

Furthermore, the methodology to produce IWUE (Section 2.2) was edited to currently 2015 reported data – all reference to MODIS methodology was removed as it was not fully adopted by TWDB.

page 56, paragraph 4

Task 5 (Implementation of most feasible ET algorithms at select sites) in the first revised scope of work states "for each county, we will compute an annual water use estimate of 2010 (wet) and 2011 (dry)." The report directly contradicts this statement on page 56: "Lastly, this pilot study was to assess feasibility and not an actual water-use assessment in the select counties." Please correct or remove this error.

Response: error removed and sentence edited.

page 58, Table 14

The Texas Alliance for Water Conservation (TAWC) is not a groundwater conservation district (GCD).

Response: table 14 heading changed to account for TAWC as a non-GCD source of data.

page 71, paragraph 3

"In summary, we fully believe the state of Texas has the need, even the obligation to implement a statewide irrigation water use program and satellite ET is the only method available." As is noted above, this sentence misinterprets the TWDB's existing agricultural irrigation water use estimation program and misrepresents the goal of this project which is to investigate the feasibility of using remote sensing to augment the TWDB's current methodology.

Response: sentence edited to read: "In summary, we fully believe the state of Texas has the need and abilities implement remote sensing into their state-wide irrigation water use estimation program."